STRUCTURAL, STRATIGRAPHIC EVOLUTION AND RESERVOIR CHARACTERISTICS OF ABU- SUFYAN SUB-BASIN, MUGLAD RIFT BASIN, SUDAN

BY

MOHAMED ABDELGADER AHMED YASSIN

A Dissertation Presented to the

DEANSHIP OF GRADUATE STUDIES

KING FAHD UNIVERSITY OF PETROLEUM & MINERALS

DHAHRAN, SAUDI ARABIA

In Partial Fulfillment of the

Requirements for the Degree of

DOCTOR OF PHILOSOPHY

In

GEOLOGY

MAY 2017

KING FAHD UNIVERSITY OF PETROLEUM & MINERALS
DHAHRAN- 31261, SAUDI ARABIA

DEANSHIP OF GRADUATE STUDIES

This thesis, written by **MOHAMED ABDELGADER AHMED YASSIN** under the direction his thesis advisor and approved by his thesis committee, has been presented and accepted by the Dean of Graduate Studies, in partial fulfillment of the requirements for the degree of **DOCTOR OF PHILOSOPHY IN GEOLOGY.**

Dr. Mustafa M. Hariri
(Advisor)

Dr. Abdulaziz Al-Shaibani
Department Chairman

Dr. Osman M. Abdullatif
(Co-Advisor)

Dr. Salam A. Zummo
Dean of Graduate Studies

Dr. Mohammad H. Makkawi
(Member)

7/6/17
Date

Prof. G. Bertotti
(Member)

Prof. Michael A. Kaminski
(Member)

To my father and mother, to my little family and to my country I dedicate this work

ACKNOWLEDGMENTS

I would like to express my sincere gratitude to King Fahd University of Petroleum & Minerals for giving me the opportunity to pursue Ph.D. study and supporting me to accomplish my Ph.D. degree. I would like to express my sincere gratitude to the Geosciences Department, College of Petroleum Engineering & Geosciences (CPG) and KFUPM for providing facilities and support. My thanks and appreciations go to the Sudapet Company and Sudan Ministry of Petroleum for providing the data used in this study and permitting publishing this work. Without any doubt, the first person to thank is Dr. Mustafa M. Hariri, my supervisor, who has been a great support, help, revision and correction. Thanks also are due to the committee members, Dr. Osman M. Abdullatif, Dr. Mohammad H. Makkawi, Prof. G. Bertotti, and Prof. Michael A. Kaminski for their guidance, help and reviewing this work. I am greatly indebted to the chairman of the Geosciences Department, Dr. Abdulaziz Al-Shaibani for his support and assistance during my studies at KFUPM. Thanks to Prof. Gabor Korvin who was a part of my committee members and leave the university. Likewise, I would like to thank geosciences Department faculty and staff. I extend thanks to my colleagues in the department for their support. I would also like to express my sincere appreciation to my colleagues at Sudapet, Yousif, Raina, Nouralla, Gebril, and Awadelkareem. Sincere thanks to my friends Hatim Dafallah and Mohamed Ibrahim. Thanks for the Sudanese community at KFUPM for their support. I appreciate Schlumberger Company for the Petrel software licenses that donated to the college. Finally, this work would not be possible without the support, patience, help, and prayers of my father, mother, wife, son, brothers, grandmother and all family to whom I am particularly grateful.

TABLE OF CONTENTS

LIST OF TABLES

.

LIST OF FIGURES

ABSTRACT (ENGLISH)

Full Name : Mohamed Abdelgader Ahmed Yassin

Thesis Title : **STRUCTURAL, STRATIGRAPHIC EVOLUTION AND RESERVOIR CHARACTERISTICS OF ABU-SUFYAN SUB-BASIN, MUGLAD RIFT BASIN, SUDAN**

Major Field : Geology

Date of Degree : May 2017

Sufyan Sub-basin is an East-West trending Sub-basin located in the northwestern part of the Muglad Basin, (Sudan) in the eastern extension of the West and Central Africa Rift System (WCARS). The exploration results of Sufyan Sub-basin showed that presence of hydrocarbon accumulations. Source rock for this hydrocarbon is believed to be the lacustrine shale of the Abu Gabra Formation and the fluvio-deltaic sandstone rock within Abu Gabra Formation represents the primary reservoir rocks. The trend of the Sufyan Sub-basin (E-W) is different from the general trend of Muglad Basin (NW-SE) and similar to Baggara basin in the west of Sudan and other basins in east Chad. The unique E-W trend of the boundary faults, the oblique faults within the Sub-basin were observed an en-echelon pattern, Sufyan Sub-basin relatively shallower than Muglad Basin, all these suggests that this Sub-basin originated by a mechanism different from Muglad Basin. Hydrocarbon exists within the sand layers that interbedded within the thick shale of the Abu Gabra Formation that deposited during the first rift cycle. The complex structural setting and depositional system are poorly understood in Sufyan Sub-basin which needs further detailed structure and sequence stratigraphic studies. This study integrates the kinematic structural models generated from the structural restoration with the depositional systems, stratigraphic sequences, and sand-body distribution in Sufyan sub-basin. Moreover, porosity and permeability of different lithofacies were analyzed under the sequence stratigraphic framework and 3D geological models were built for lithofacies, lithofacies associations, and porosity. Detailed sequence stratigraphic interpretation of the Sufyan Sub-basin was carried out using 22 wells, 2D, and 3D seismic data. Fault polygons maps for six horizons, four isopach maps, five cross-sections, and two associated kinematic models are presented in this study. These data revealed that the Early Cretaceous clastic sedimentation is controlled mainly by tectonic subsidence. Hydrocarbon reservoirs of the Sufyan Sub-basin basin are concentrated underwater distributary channels, distal bar, and sheet sands dominated in the delta front on structural highs produced by strike-slip movements of NW-SE-striking faults. Structural interpretation of Sufyan Sub-basin based

on 2D seismic data highlights the style of strike-slip related structure. Negative flower structures, en-echelon faults, and rhombic geometry all suggest a significant component of a pull-apart transtensional movement in Sufyan Sub-basin. Sedimentologic interpretation in this study was performed based on core cuttings, well logs, and seismic data. By using seismic sections across the wells, the spatial distribution of facies was achieved. Conceptual depositional models were constructed and interpreted based on facies interpretation. Tectono-Sequence Stratigraphic framework for the study area was proposed through the integration of sedimentologic interpretation, depositional systems, and tectonic evolution history. Four types of depositional systems have been recognized in the studied succession. These are braided delta, fan delta, sublacustrine fan, and lacustrine systems. Abu Gabra Formation categorized as a 2^{nd} order sequence and divided into five 3^{rd} order sequences. Depositional and post-depositional processes believed to be highly influenced the reservoir heterogeneity, quality, and architecture. Three dimensional geostatistical models characterizing the structural variation, lithofacies heterogeneity, reservoir architectures, and porosity distribution were established. The lithofacies heterogeneity together with the complex structural and stratigraphic settings have resulted in a complex reservoir geometries and highly variation in porosity distribution. This study expected to enhance the understanding of the control of tectonic evolution and structural models on depositional systems and sequence stratigraphic patterns. This study also explains the tectonic history of fault basins and discuss the control of faults initiation and reactivation over the filling process moreover the development and spatial distribution of various depositional systems in fault basins. The generated 3D models could use as a predictive tool for reservoir geometries and reservoir quality.

ملخص الرسالة

الاسم الكامل: محمد عبد القادر أحمد يس

عنوان الرسالة: التطور الهيكلي، الطبقى، و خصائص الخزانات فى حوض سفيان الفرعى، حوض مجلد، السودان

التخصص: جيولوجيا

تاريخ الدرجة العلمية: مايو 2017

حوض سفيان الفرعي هو حوض فرعي يتجه نحو الشرق والغرب يقع في الجزء الشمالي الغربي من حوض المجلد (السودان) في امتداد شرق غرب ووسط أفريقيا. أظهرت نتائج الاستكشاف في حوض سفيان الفرعي تواجد كميات اقتصادية من الهيدروكربون. ويعتقد أن صخور المصدر لهذا الهيدروكربون هى صخور تكوين أبو جبرة. وتشكل صخور الحجر الرملي (الدلتا) في تكوين أبو جبرة الخزان الرئيسي. يختلف اتجاه حوض سفيان الفرعي عن االتجاه العام لحوض المجلد (شمال غرب-جنوب شرق) ويشبه حوض بقارة في غرب السودان واألحواض الاخرى في شرق تشاد. ويشير الاتجاه الفريد (شرق-غرب) أن هذا الحوض الفرعي نشأ عن آلية مختلفة عن حوض المجلد الذي تكون نتجة للحركة التمددية فى الأصل. ويوجد الهيدروكربون في طبقات الرمال التي تتداخل داخل الصخر السميك في تكوين العصر الطباشيري المبكر (تكوين أبو جبرة) الذي تكون خلال دورة الصدع الأولى. تعقيد البنية الهيكلية ونظام الترسب غير مفهوم جيدا في منطقة الدراسة ويحتاج إلى مزيد من الدراسة. لا توجد دراسة تفصيلية تدمج النماذج الهيكلية الحركية المتحصل عليها من أعادة الهيكلة مع الأنظمة الترسيبية، والتسلسل الطبقي، وتوزيع الرمال في حوض سفيان الفرعي. باستخدام حوض المجلد في السودان كمثال على الاحواض المتصدعة، فإن الغرض من هذا العمل هو دراسة البنية التركيبية والنظم الترسيبية والتسلسل الطبقي وتوزيع الرمال في حوض سفيان الفرعي. تم تنفيذ التفسير التفصيلي للتسلسل الطبقي لحوض سفيان الفرعي باستخدام 22 بئرا، بيانات زلزالية ثنائية الابعاد، وثلاثية الابعاد. تم تضمين خطوط الزلازل لتوضيح التباين فى البنية الهيكلية والطبقية عبر الحوض. خرائط الصدوع، أربعة خرائط سمك، خمسة مقاطع عرضية، واثنين من النماذج الحركية استخدمت في هذه الدراسة. تكشف هذه البيانات عن أن الترسيب العصبي الطباشيري المبكر يسيطر علية الهبوط التكتوني. وتتركز الخزانات الهيدروكربونية في حوض حوض سفيان الفرعي فى ترسبات قنوات التوزيع التحت مائية والشريط القاصي والرمال الصخرية التي ترسبت فى الدلتا المتقدمة على ارتفاعات بنائية تنتجها حركات انزلاق الاضطرابات الناجمة عن الصدوع. التفسير الهيكلي لحوض سفيان الفرعي استنادا إلى البيانات الزلزالية الثنائية سلط الضوء على أسلوب هيكل الانزلاق ذات الصلة. وتشكل البنى السالبة، والصدوع المتشابكة، والهندسة المعينية كلها عنصرا تدل على الحركة الجانبية الافقية المكونة لحوض سفيان الفرعي. وقد أدخلت سيناريوهات بديلة أخرى لتاريخ التطور وآلية تشكيل الحوض مثل نموذج التمدد المنحرف. تم تنفيذ التفسير الرسوبي في هذه الدراسة على أساس قطع صخرية من الابار، سجلات الابار، والبيانات الزلزالية. وباستخدام المقاطع الزلزالية عبر الآبار، تم تحقيق التوزيع المكاني للرسوبيات. تم بناء النماذج الترسيبية وتفسيرها بناء على تفسير السحنات الصخرية. على اساس التكتونية الطبقية اقترح الإطار الطبقي لمنطقة الدراسة من خلال دمج التفسير الرسوبي، والنظم الترسيبية، وتاريخ التطور التكتوني. وقد تم تحديد أربعة أنواع من أنظمة الترسيب في الاجزاء المدروسة. هذه هي دلتا نهرية، مروحة دلتا، مروحة تحت مائية بحرية، ونظم بحيرية. صنف تكوين أبو جبرة على شكل تسلسل ترتيب ثنائى وتنقسم إلى خمسة تسلسل من الترتيب الثلاثى. من المتوقع أن تعزز هذه الدراسة فهم سيطرة التطور التكتوني والنماذج الهيكلية على أنظمة الترسيب وتسلسل الأنماط الطبقية. وتفسر هذه الدراسة أيضا التاريخ التكتوني للأحواض المتصدعة وتناقش سيطرة بدء الصدوع وإعادة تنشيطها على عملية التعبئة بالإضافة إلى التطوير والتوزيع المكاني لأنظمة الترسيب المختلفة في الاحواض المتصدعة.

CHAPTER 1

INTRODUCTION

1.1 Introduction

Tectonic evolution, structure, sediment supply and prevailing climate are the main factors that controlling the spatial distribution and temporal evolution of the depositional systems and sequence architectures in continental rift basins (Prosser, 1993). Tectonic movements are of extreme importance for the sequence boundaries formation and the sediments characters of sequences in continental rift basins (Hongwen et al., 2008). Tectonic create accommodation space; structure evolution modifies this accommodation space, and the prevailing climate determines whether this accommodation space can be filled by water or sediments (Prosser, 1993). Tectonic can raise or lower the accommodation zone or the transfer zone which separates the half grabens faulted blocks and hence the base level. Tectonic could also introduce a new sediment supply points, whereas tilting of basin floor fault blocks can cause a relocation of the shorelines and depocenters (Prosser, 1993).

The purpose of this work is to study structure, depositional systems, stratigraphic sequences, and sand bodies distribution in Sufyan sub-basin. This work expected to improve the understanding of the control of tectonic evolution and structural models on the depositional systems and sequence stratigraphic patterns. This study will also explain the tectonic evolution history and discuss the control of faults initiation and reactivation over the filling process.

The results of this study will help in constraining and correlating rocks of complicated strata in the study area and other areas with similar conditions. Integrating the kinematic structural models that generated from the structural restoration with the depositional systems, stratigraphic sequences, and sand-body distribution led to better hydrocarbon exploration in Abu Gabra Formation.

Such study might also provide an answer for very important questions need to be addressed, such as is there any thick and continues sand body within the syn-rift source rock to target it as a stratigraphic trap?

1.2 Problem statement

Sufyan Sub-basin has experienced a complex tectonic evolution, and abundance of hard and soft linkage between faults was developed that controlled the distribution of both the depositional system and sequence. Moreover, hydrocarbon exists in the sand layers that interbedded within the thick shale of Abu Gabra Formation that deposited during the first rift cycle. The complexity of the structure and depositional system are poorly understood in the study area which needs further detailed structure and sequence stratigraphic studies. No detailed study that integrates the kinematic structural models generated from the structural restoration with the depositional systems, stratigraphic sequences, and sand bodies distribution in Sufyan sub-basin.

1.3 Objectives

The main objective is to study the tectonic evolution and structural models and its control on the depositional systems and sequence stratigraphic patterns in Sufyan sub-basin.

The following tasks will be achieved during this study:

- Analyze the tectonic evolution and structural style of Sufyan sub-basin.
- Identify the possible causes of the unique trend of Sufyan Sub-basin, and the possible relationship with the Central African Shear Zone (CASZ).
- Identify the forming mechanism model for Sufyan Sub-basin.
- Characterize the sedimentary facies associations, depositional environment and establish sequence stratigraphic framework.
- Construct models link between the structure and their stratigraphic units under the regional tectonic framework.
- Generate 3D Geostatistical model including the structural, faices, and properties models.
- Data Integration and Interpretation (heterogeneity, sand bodies, reservoir delineation).

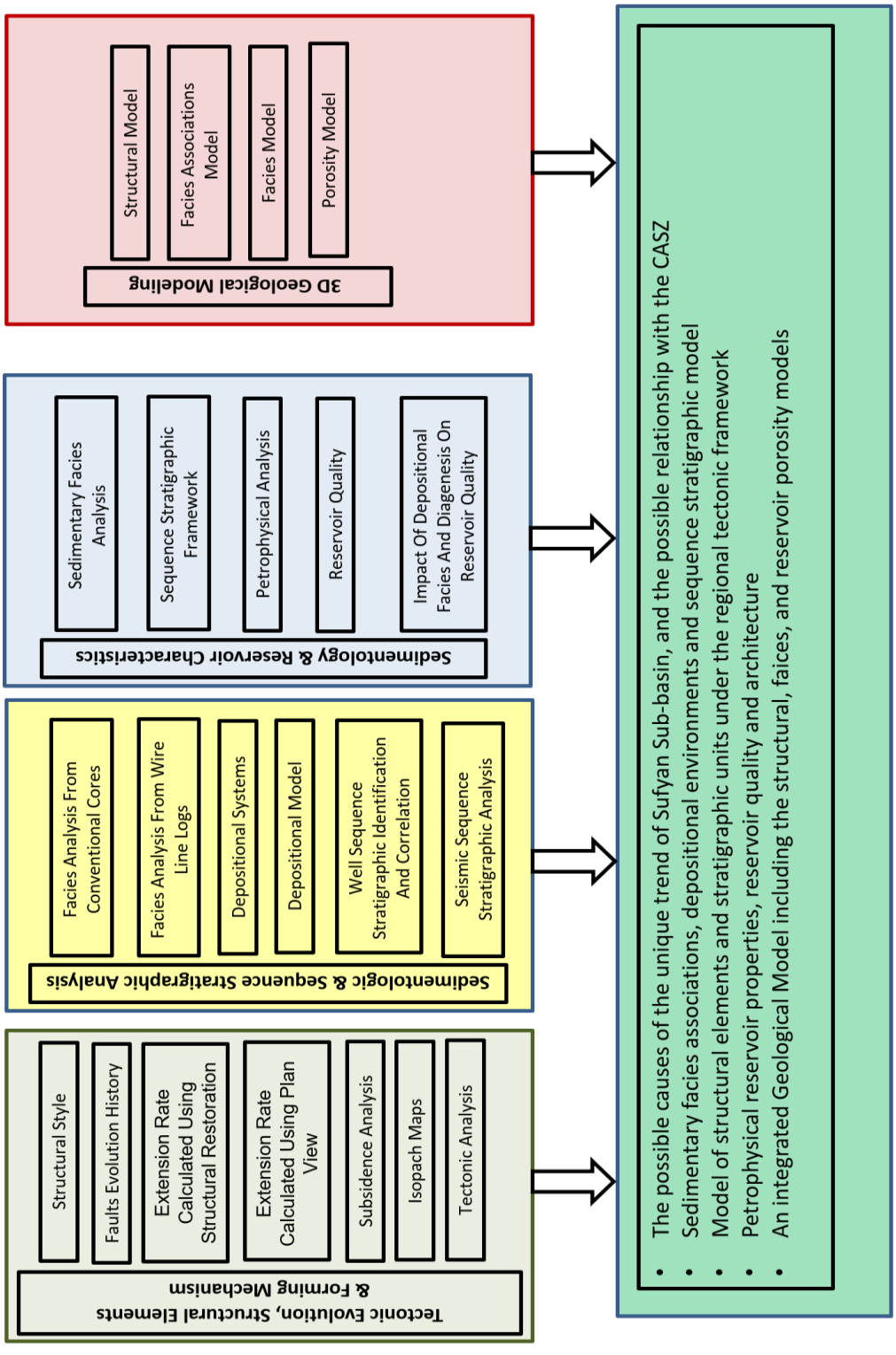

Figure 1-1: Workflow and the main objectives

1.4 Study Area

The Sufyan Sub-basin is situated in the northwestern part of Muglad basin with E-W orientation of the major boundary faults (Figure 1-2). Muglad Basin is the biggest sedimentary basin in Sudan with a total area of about 160,000 km^2 (with a width of about 200 km and a length of about 800 Km). Many hydrocarbon fields were discovered in Muglad Basin with various sizes such as Heglig and Unity oilfields (Makeen et al., 2015c).

Muglad Basin represents a major part of the West and Central African Rift Systems (WCARS) (Figure 1-2). Muglad rift basin is trending NW-SE and terminates on the northwestern side by the Central African Shear Zone (CASZ) (Fairhead, 1988; Schull, 1988) (Figure 1-3). The formation of the Muglad Basin is believed to be a rift structure that is related to the opening of the Atlantic Ocean since the Early Cretaceous by the right-lateral movement along the CASZ (Genik, 1993). The basin is divided into eight sub-basins which are South Kaikang, North Kaikang, Unity, Bamboo, Fula, East Nugara, West Nugara, and Sufyan (Lirong et al., 2013) (Figure 1-3).

Theses sub-basins are occupied by Cretaceous - Tertiary non-marine sediments (Schull, 1988). Sufyan sub-basin is a relatively independent structural unit in the Muglad rift Basin. It is 70km long and 40km wide with a total area of about 2,800km^2. The 2D and 3D seismic data coverage for the whole area is about 3718 Km and 698 Km^2 respectively. The sub-basin is bounded by Tomat Uplift with boundary fault in the south and Babausa Uplift to the north and east and connected with Nugara depression in the south-east (Figure 1-3). Sufyan Sub-basin exploration results have proved the existence of profitable accumulations of hydrocarbon.

Figure 1-2: Location map of the Muglad Basin including Sufyan Sub-basin. Modified from Makeen et al., (2015a).

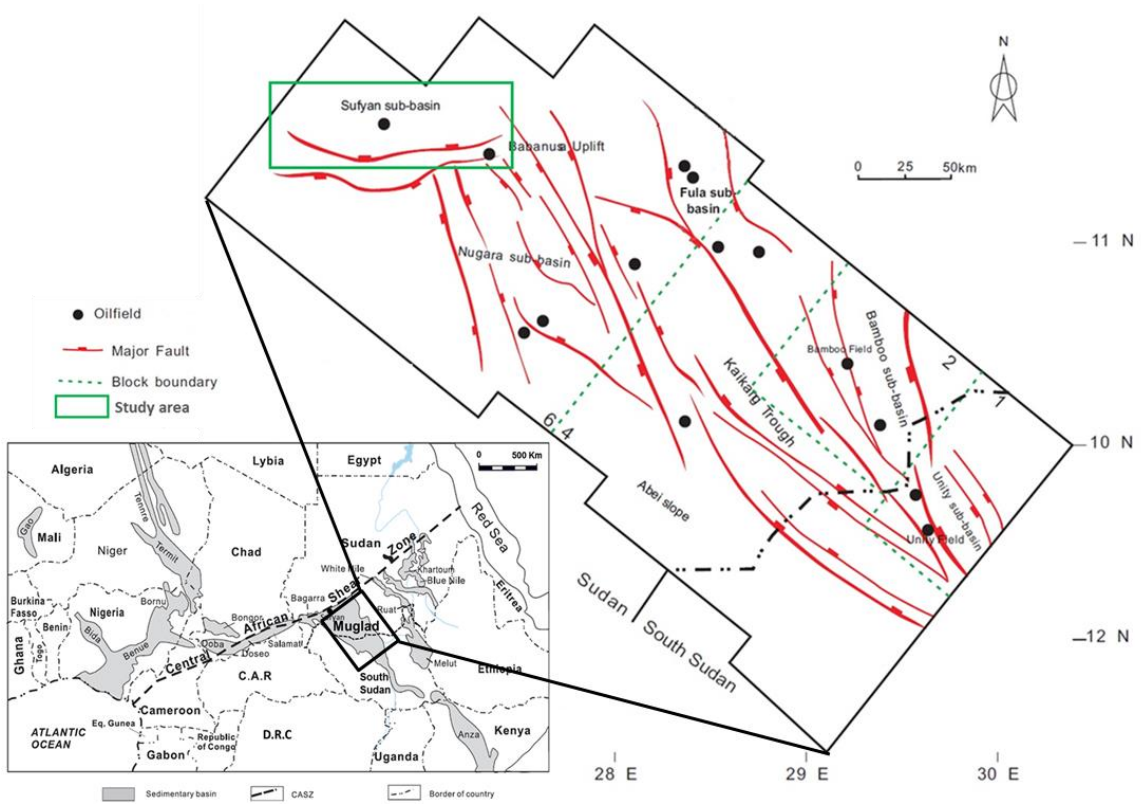

Figure 1-3: the Main map shows Muglad Basin structural units (interpreted from a different source of data and show only the regional faults), with the location of Sufyan Sub-basin and the major discovered oilfields. The other map shows the location of Muglad Basin with relation to the West and Central Africa Rift System (WARS) (modified from Lirong et al., 2013; Makeen et al., 2016).

Source rock for this hydrocarbon is believed to be the lacustrine shale of the Abu Gabra Formation. The thin sandstones beds within Abu Gabra Formation represent the primary reservoir with cap seals of interbedded shales within the formation and faults as lateral seals. The main traps are mainly structural, of medium and small size. The structural traps style in the sub-basin is the tilted fault blocks associated with en echelon faults.

CHAPTER 2

GEOLOGIC AND TECTONIC SETTING

2.1 Introduction

Muglad rift basin represents a major part of the West and Central African Rift Systems (WCARS) (Figure 2-1) and is mainly composed of discrete half and full grabens (Genik, 1993). The origin of the WCARS is believed to be related to the opening of the Atlantic Ocean (Figure 2-2) (Binks and Fairhead, 1992; Fairhead and Binks, 1991; Guiraud and Maurin, 1992).

The West and Central Africa is composed of three major Cratons; West African, Arabian-Nubian, and Congo Cratons (Figure 2-2), which were amalgamated trough the Pan-African orogenic belts (Bosworth, 1992). All the Mesozoic-Cenozoic rifts occur between the Cratons. Africa is divided to three main sub-plates; NW Africa, NE Africa and, S Africa (Figure 2-2) (Fairhead et al., 2013; Genik, 1993). Geology and structure of WCARS basins were developed as a result of the African sub-plate motion's changes through time (Fairhead et al., 2013; Genik, 1993). Basins of WCARS share similar common evolution history as they developed in a similar tectonic setting. However, individual basins show unique histories and structure due to it their location and orientation in relation to the tectonic events. While one basin is subjected to extensional regime another basin with different orientation might be subjected to strike-slip movement and this result in the relative sub-plate movements (Fairhead et al., 2013).

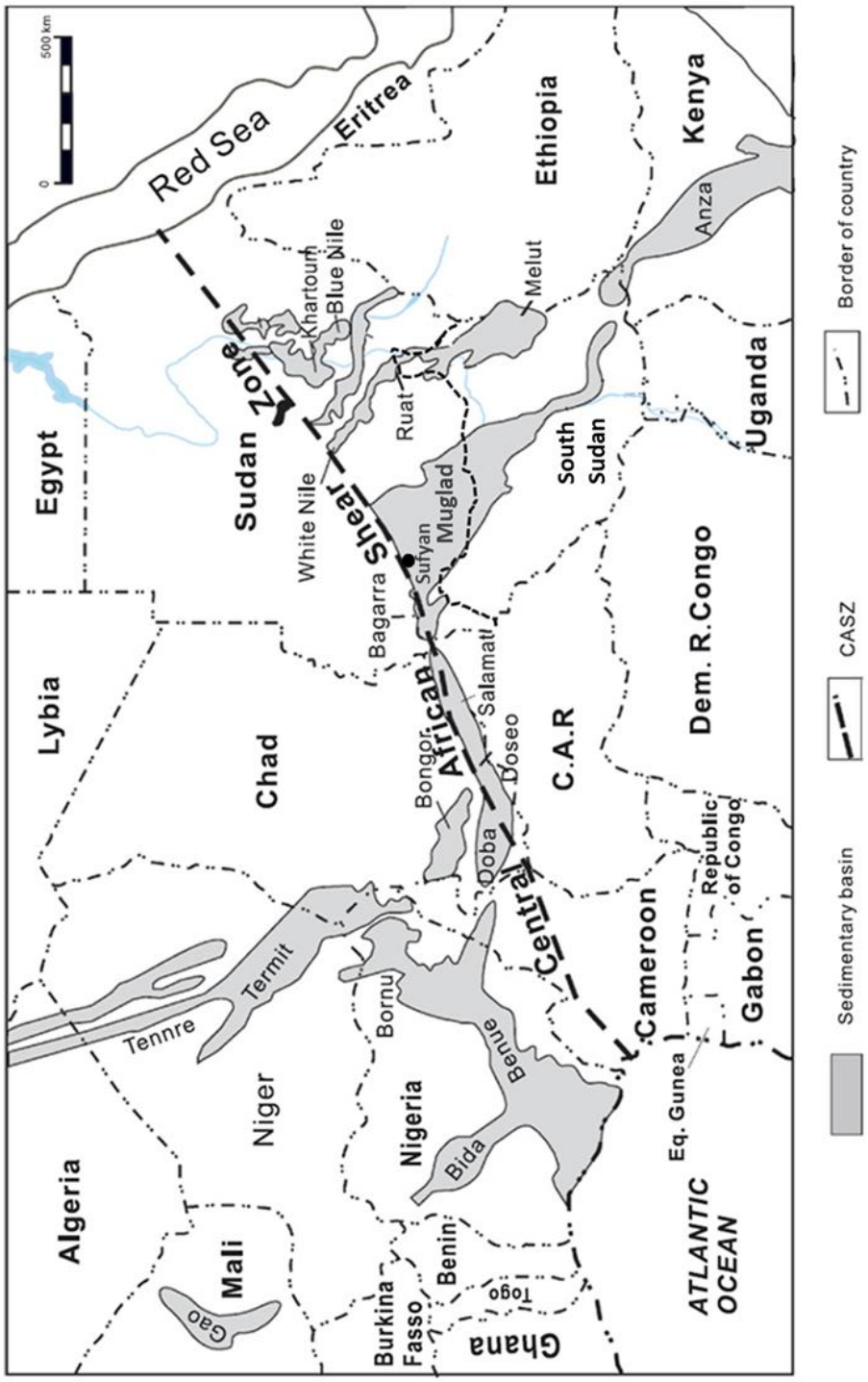

Figure 2-1: Map shows the location of Muglad Basin with relation to the West and Central Africa Rift System (WARS) (after Genik, 1993).

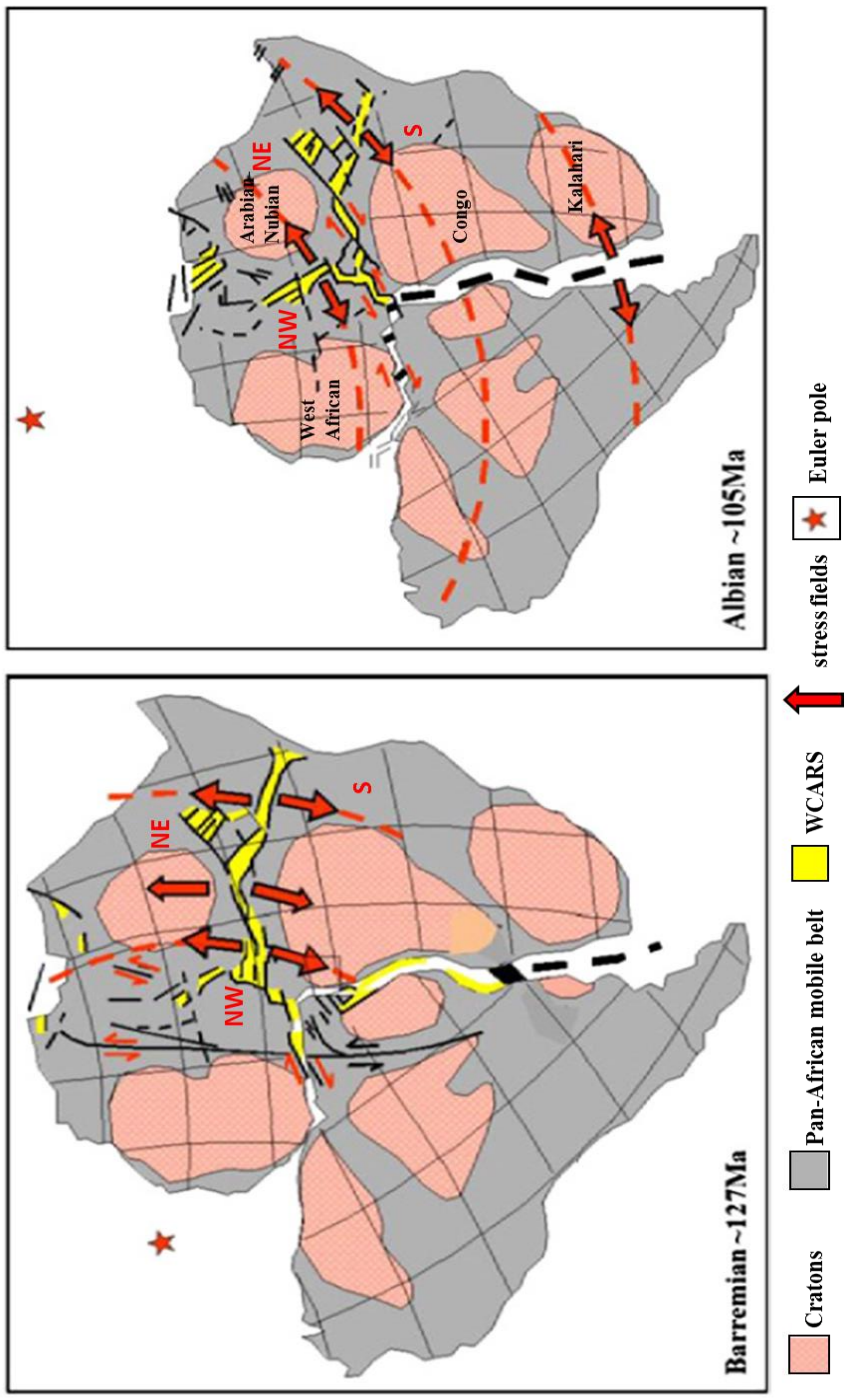

Figure 2-2: The varying stress field of Africa has resulted in major changes to the WCARS evolution. A) The early extensional phase of the WCARS during the Early Cretaceous. B) By the Albian (~105 Ma) the plate motions have changed within Africa as a result of the advanced stage of plate separation from South America (Fairhead et al., 2013).

Basins in the WCARS are settled in three main directions, NE-SW, ENE-WSW, and NW-SE (Figure 2-1and Figure 2-2). The greatest noticeable basin among the NE-SW direction is the Benue Trough in Nigeria. The ENE-WSW striking groups of basins are distributed parallel to the CASZ, such as Doba, Doseo, Salamat basins in eastern Chad and Bagarra Basin in western Sudan (Figure 2-3) (Genik, 1993). The NW-SE striking groups of basins are extensively distributed in the East and West Africa (Figure 2-1) (Guiraud and Maurin, 1992), such as Muglad Basin in Sudan and Termit Basin in Niger. All these ENE-WSW basins are interpreted as a pull-apart structure in origin as proved by their basin geometry, intra-basin flower structures, and tectonic situation (Genik, 1993).

El Hassan and El Nadi (2015) indicated that the Baggara Basin in Sudan situated in the eastern part of the WCARS in Sudan (Figure 2-3). However, they mentioned that compressional structures are generally hard to identify.

Although Sufyan Sub-basin is a part of Muglad Basin (Figure 2-3), the trend of the Sufyan Sub-basin (E-W) similar to orientation of Baggara basin in west of Sudan and other basins in east Chad The first phase of subsidence was fairly active and widespread, characterized by early stage of rifting and late stage of thermal contracted sagging (Genik, 1993). Fairhead et al. (2013) divided this phase to two stages, Neocomian to early Aptian (~130 Ma) (Figure 2-2) opening of the South Atlantic with North to South extension (Fairhead et al., 2013).

2.2 Tectonic Setting

The WCARS basins experienced multi-phase subsidence from the Cretaceous to recent due to the change of the regional crustal stress and stress regimes (Figure 2-2).

During the middle-late Aptian and Albian (~105 Ma), dextral transform movement along the Equatorial Atlantic ocean was developed (Figure 2-3). Muglad Basin subsided as a result of the crustal extension (NE-SW extension direction).

The Santonian (~ 85 Ma) compressional event has been reported in most of the region and has been attributed to the effect of collision of the African and Eurasian plates along the Alpine orogenic belt. The shortening direction was NNW–SSE to N-S (El Hassan and El Nadi, 2015; Fairhead et al., 2013; Genik, 1993; Guiraud et al., 2005; Guiraud and Bosworth, 1997). During this phase, a number of basins uplifted and exposed to erosion.

The compression event is well documented in the ENE-WSW oriented basins (Salamat, Doba, Doseo, and Baggara) due to their favorable orientation with respect to the compressional stresses (Figure 2-3). As a result of this compression event, negative and positive flower structures and numerous hydrocarbon traps have developed. The NW-SE trending Muglad sub-basins escaped from the inversion, due to their axes which are sub-parallel to compressional stress direction (McHargue et al., 1992).

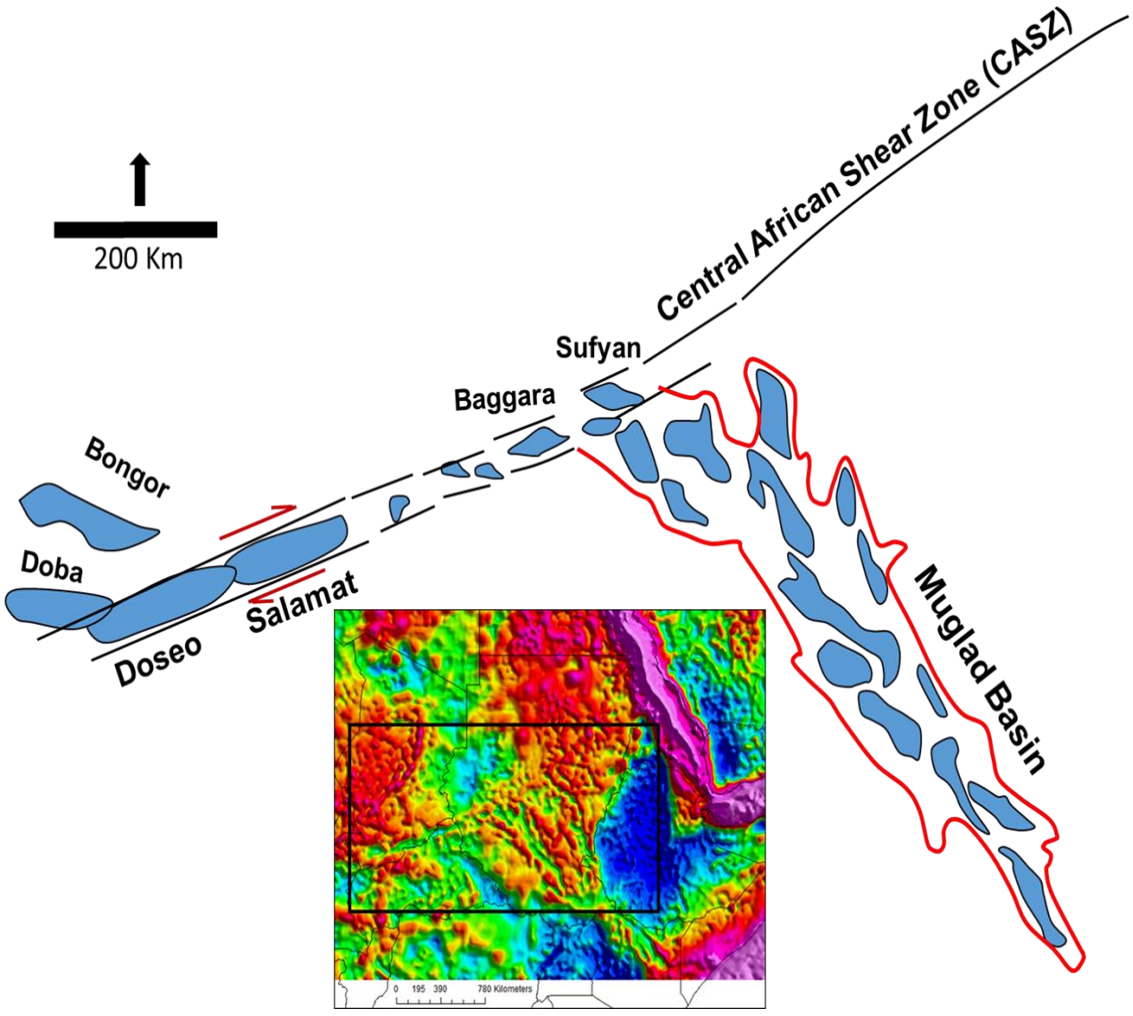

Figure 2-3: Generalized map (upper) interpreted from Bouguer gravity map (lower) showing part of the West and Central Africa Rift System and the relationship between Muglad Basin, Sufyan Sub-basin, Baggara Basin, Chad basins and the CASZ. The light blue polygons surrounded by the red boundary represent Muglad Basin and the different Sub-basins (upper). The black line represents the CASZ; other light blue polygons represent basins in west Sudan and Chad. Processed satellite-derived gravity data with digital 2 km grids resolution of Bouguer anomaly images were used during in this study.

The second phase of subsidence from 100 to 85 Ma is characterized by NE-SW extension (Fairhead et al., 2013) (Figure 2-4). During this phase, extension resulting from the derivative NE-SW tensile force and sharp change of plate motion direction occurred.

The second phase continued until the Middle Eocene (~40 Ma), when the most intense collision occurred along the Alpine orogenic belt. This event resulted in the closure of the Tethyan Ocean and exerted a strong influence on basin development in the Africa interior. Most of the Mesozoic rift basins ended during the Middle Eocene, except for the NW-SE-trending Tenere and Sudanese rifts (McHargue et al., 1992). The third phase of subsidence occurred between the Middle Eocene to Palaeocene (65 to 38 Ma) (Fairhead et al., 2013). The extension direction of this rift in Tenere and central Sudan is NE-SW, while in Benue Trough and Chad basins ESE-WNW to E-W extensional direction is indicated (Fairhead et al., 2013). During this phase, transtensional tectonism related to the development of East African Rift (EAR) occurred. During the Early Late Eocene, a major compressional event is identified along the Tethyan African–Arabian margin. The shortening event direction is N160°E (Fairhead et al., 2013).

2.3 Stratigraphy and Rift Cycles

Stratigraphic sequences are divided into different formations in Muglad basin, although the thickness varies from sub-basin to other (Figure 2-4). Several unconformities exist in Muglad basin, which separates Abu Gabra Formation from Bentiu Formation, Bentiu Formation from Darfur Group, Amal Formation from Nayil and Tendi formations, and Tendi from Adok and Zeraf formations (Figure 2-4).

However, most of the unconformities can only be observed on the basin margins (Genik, 1993). In the Muglad rift Basin, three rift cycles are recognized and dated as Early Cretaceous (about 140-95 Ma), Late Cretaceous (95-65 Ma), and Paleogene (65-30 Ma) (McHargue et al., 1992) (Figure 2-4). Each tectonic cycle seems to consist of rift-initiation phase, active rifting phase, and thermal sag phase (McHargue et al., 1992) (Figure 2-4). Every tectonic cycle is composed of basal sandstone unit, followed by a coarsening upward cycle (grading from lacustrine shale to marginal lacustrine mudstone and sandstone into fluvial mudstone and sandstone, and being covered by alluvial and fluvial sandstone). Stratigraphically, each rift correlated depositional cycle starts about near the margins of the rift with basal sand overlaid by a shale-dominated interval, which reflects basin deepening. Each of these shaly intervals occurs as a base of coarsening upwards section grading from the lacustrine shale into fluvial and lacustrine sandstone and mudstone when fully developed. The later, in turn, is capped with the fluvial sandstones that are regionally extensive (McHargue et al., 1992). The sediments of the three rifting episodes in the Muglad Basin reach a thickness of about 5400, 4200 and 5400 meters, respectively. After the Oligocene time, only sand dominated sediments of about 750 meters were deposited in the basin (McHargue et al., 1992). In Muglad basin, the stratigraphy can be seen as a result of rhythmic high sediment influx rate into depressions during episodes of cyclic alteration and subsidence patterns. The lithofacies association can be interpreted in light of different subsidence rate for various sub-basins. When subsidence was enormous during the time of active rifting, shale-dominated sediments were deposited. While during the time of low subsidence most likely during thermal sag phases, sand dominated sequence accumulated (Figure 2-4).

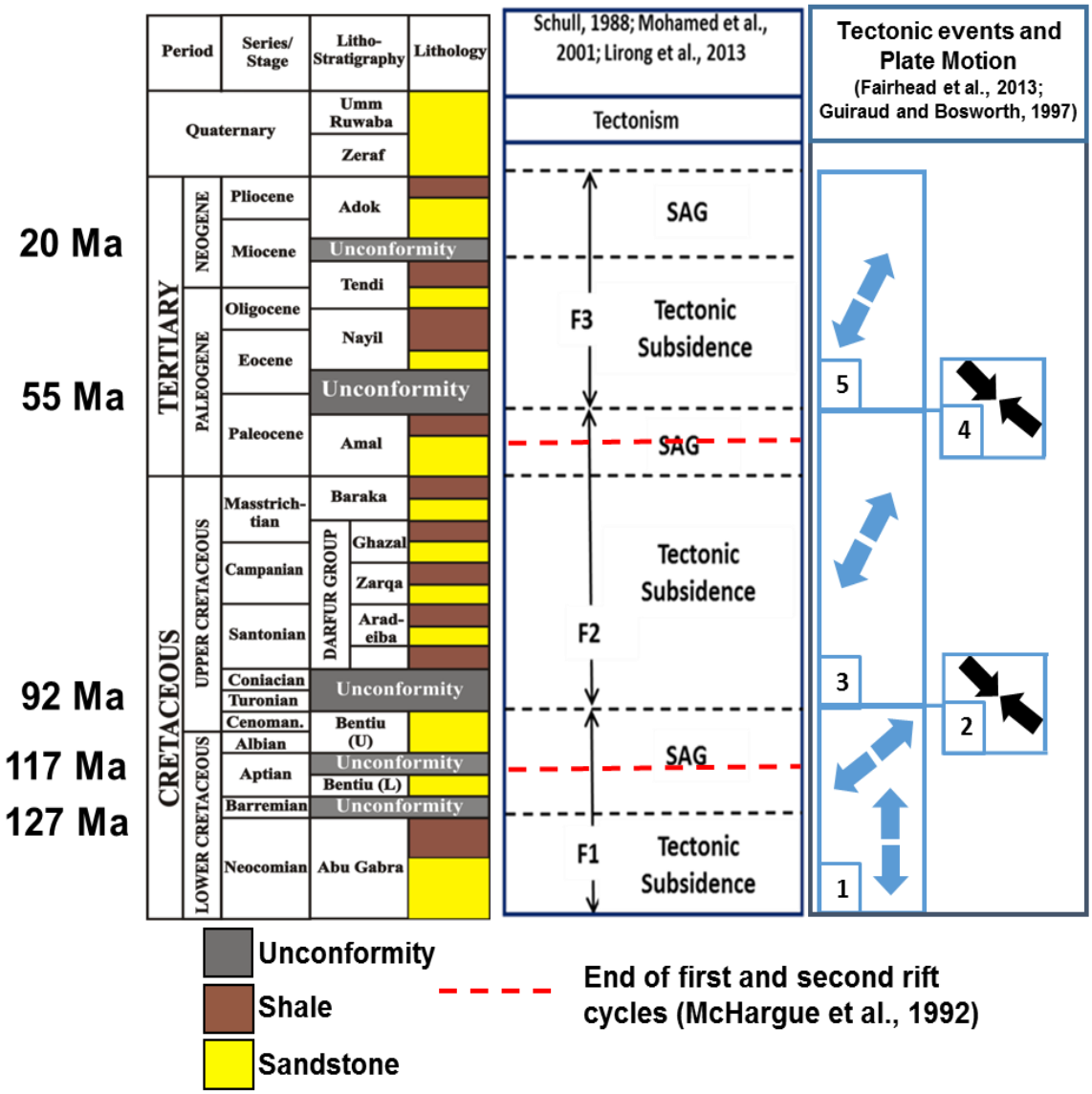

Figure 2-4: Stratigraphic and tectonic events charts for the Muglad Basin, Sudan, (after (Fairhead et al., 2013; Guiraud and Bosworth, 1997; Lirong et al., 2013; McHargue et al., 1992; Mohamed et al., 2001; Schull, 1988). The regional tectonic and stratigraphic contexts are summarized from previous work. Tectonic processes in surrounding regions are as follow 1- Drifting of S. Atlantic Ocean at Ca. 123 Ma (Combined strike-slip along CASZ and normal extension mechanism (regional crustal stretching along Muglad Basin). 2- Africa-Europe collision during 80-85 Ma. 3- Extension resulting from the derivative NE-SW tensile force and sharp change of plate motion direction. (NE-SW extension was developed as a result of NW-SE crustal compression). 4- Major stage of Africa-Europe collision; complete closing of Tethyan Ocean at Ca. 40 Ma. 5- Transtensional tectonism related to the development of East African Rift (EAR).

Throughout each tectonic cycle, a broad area reflects an influence of the initial subsidence, although the subsidence rate was slow. This pattern may explain the existence of regional unconformity overlaid by the basal sand-dominated unit. This unit is sandiest at the margins of the rift and often shaly towards the depocenter (McHargue et al., 1992).

The first depositional cycle has been penetrated only at the basin margins, hence the geographic representation of this unit remains uncertain. On the contrary, the basal sand unit of the second depositional cycle (Upper Bentiu), and the third depositional cycle (Upper Amal) interfingers towards the axis of the rift with suspended-load fluvial and shaly lacustrine accumulations (Figure 2-4). This modality is thought to be applicable for the sand unit of the first depositional cycle.

Following the accumulation of few hundred meters of the sand-dominated basal unit by the initial extension the phase of active rifting initiated. This initiation is marked by a rapid subsidence of the hanging wall close to the main sub-basin boundary-faults. During this rifting phase, the topographic relief postulated to be at maximum while the sediment accumulation rate was high, yet unable to keep pace with the rapid fault-activated subsidence. At that time, the basin was characterized by close/sluggish drainage system linking a series of lakes. Each fault-bounded sub-basin behaved as a trap for the sediment where a thick shale-dominated section has been developed. Periods and areas of rapid subsidence were dominated by shales, either due to the sediments accumulation in long-lived outspread lakes or due to rapid descending of the deposited sediments beneath the erosional base and quick burial. In both cases, sediments were suffered a little and/or winnowing after accumulation and the predominant shaly composition indicated the

introduction of mostly fine clastics into the basin. Each of the three tectonic phases witnessed incoming coarse clastics form outside of the basin. This is supported by the presence of thick sandstone accumulations along the margins of the rift and their insignificance among the sediments accumulated near the intra-basinal highs during the main tectonic phases.

The syn-rift sediments of the first tectonic cycle (Abu Gabra Formation) were associated with the extensive lacustrine shale where the water of these lacustrine was stratified enough to prevent the accumulation and subsequent preservation of organic reach kerogen shales representing the source rock of the oil in the Muglad basin (Schull, 1988). The second tectonic cycle syn-rift deposits (Lower Darfour Group) and the third tectonic syn-rift deposits (Nayil and Tendi Formations) again comprised mostly of lacustrine shales and fluvial overbank deposits (Figure 2-4). These shales do not represent petroleum sources where they have been penetrated, while the sand deposited within these sequences represent premium reservoirs in the southern parts of the Muglad Basin.

Towards the end of each tectonic cycle, the subsidence was altered gradually by a relatively slower rate of thermal down-warping basin-wide. The sediment influx during this stage took over the sub-basinal topography. Hence, the slow rate of subsidence allowed the continuous reworking by the bedload streams, which penetrates the mud transported downstream outside the basin by the drainage system. The rest of the sediments were preserved as sheets of amalgamated fluvial sand throughout the whole basin (Lower Bentiu, Lower Amal, and Adok Formation).

The distribution and thicknesses of sediments accumulated during each rifting phase of each tectonic cycle indicate that more influence of subsidence can be observed during the first tectonic rifting cycle than other cycles (Figure 2-5).

Similar to the subsidence related to the tectonic rifting, the thermal rifting through the sag phase following the first tectonic cycle was greater than the other subsequent two cycles. Moreover, the thermal sag subsidence was positioned above the proceeding subsidence of the below rifting phase for each tectonic cycle. Muglad basin received sediments from the surrounding uplifted regions. Nuba Mountains served as an important source of sediments (provenance) to Muglad basin during the Cretaceous. During the Tertiary, most of the sediments supply probably came from the north region, where the upwelling of deep hot material resulted in the formation of Darfur Dome which began to be subject to erosion (Genik, 1993) (Figure 2-6).

2.3.1 The first rift cycle

This cycle contains primarily the organic-rich lacustrine claystones and shales of Abu Gabra Formation (Figure 2-4). It is interbedded with fine-grained sands and silts. The Abu Gabra claystones and shales are the primary source rock in Muglad Basin and the interbedded sands are the main reservoir in the north-western Muglad Basin. The thickness of Abu Gabra Formation is up to 4 km and it forms the major sedimentary section of the first rifting phase. These lacustrine deposits overlain by Bentiu Sandstone (sag phase), consist mostly of stacked channel and bar deposits of braided and meandering streams (McHargue et al., 1992). Bentiu sandstones are the primary reservoir rocks in Muglad Basin marks the end of the first cycle (Figure 2-4).

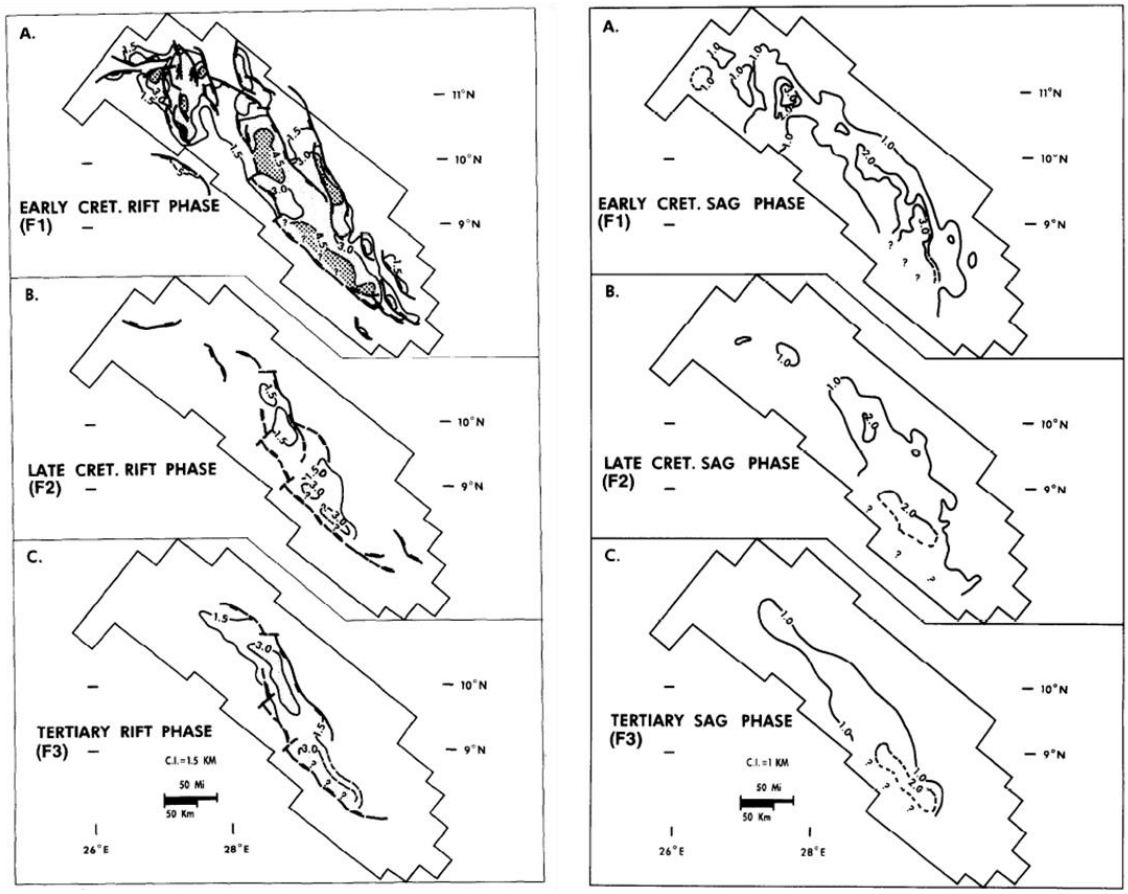

Figure 2-5: Isopach maps in Muglad Basin. Left: Isopach maps of sediments deposited during the rift phase of each tectonic cycle. Right: Isopach maps of sediments deposited during the sag phase of each tectonic cycle (McHargue et al., 1992).

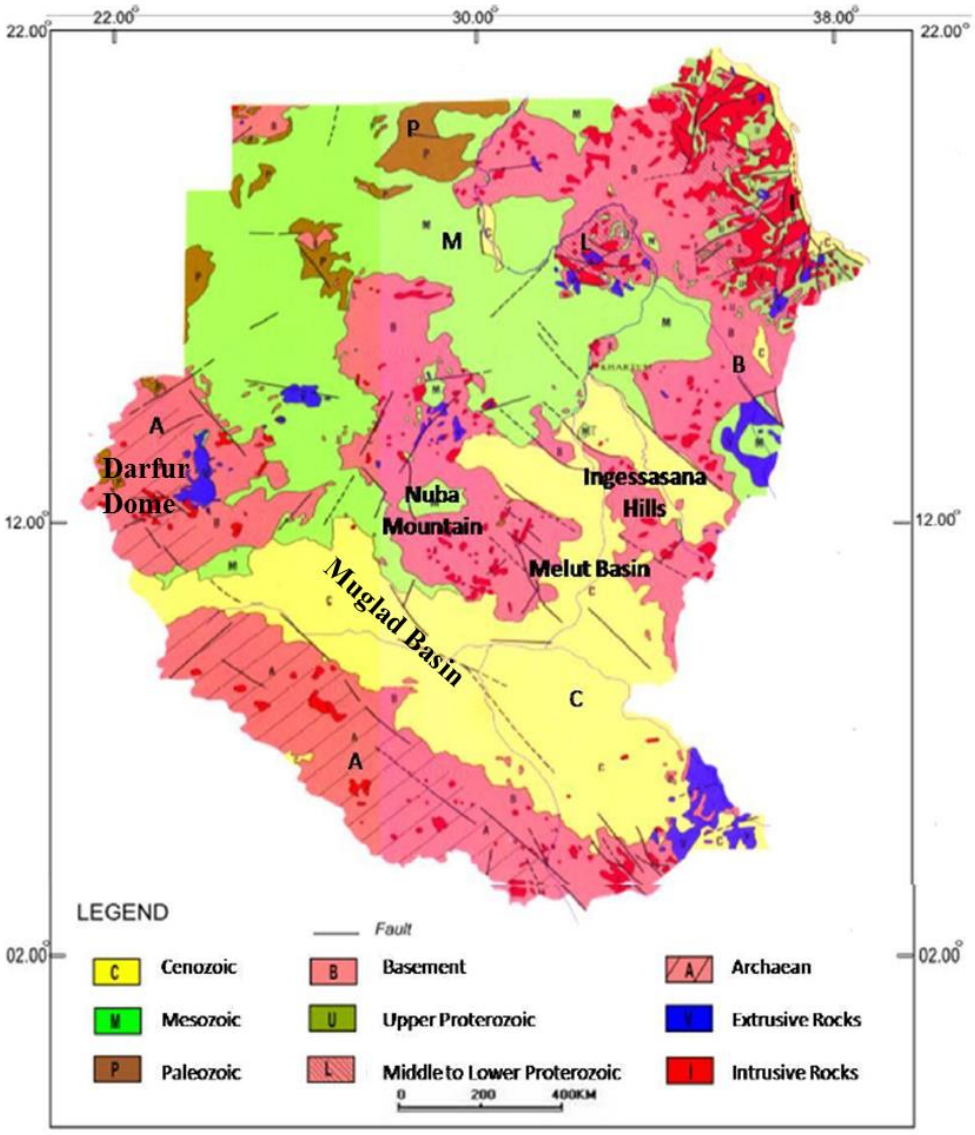

Figure 2-6: Geological map of the Sudan and South Soudan, showing the variety of geology with a combination of metamorphic, igneous and sedimentary rocks. It shows also Muglad basin location (after GRAS, 2005).

Bentiu Formation marked by short deposition duration, but the vertical section is thick especially in the deep areas and this due to the high sedimentation rate (Mohamed et al., 2001).

2.3.2 The second rift cycle

This cycle began with deposition of the Darfur Group, a coarsening-upward interval consisting primarily of interbedded marginal lacustrine and fluvial-deltaic sandstone and claystones. It consists of Aradeiba, Zarqa and Ghazal formations and includes the major hydrocarbon seals (Aradeiba Formation) (Figure 2-4). Aradeiba and Zarqa formations are dominated by claystone, shale, and siltstone. The Aradeiba and Zarga Formations are interbedded with the floodplain and lacustrine claystones, shales, and siltstones (seal) and several fluvial/deltaic channel sands (reservoir), followed by the deposition of increasingly coarser grained sediments of Ghazal and Baraka formations (Schull, 1988). The Darfur Group overlain by the Paleocene Amal Formation (thick Sandstone represents the sag phase of the second rift cycle). In the northwestern part of the Muglad Basin the syn-rift sediments of the Darfur group were relatively eroded and the remaining section is thin (Figure 2-7) (Schull, 1988).

2.3.3 The third rift cycle

During this cycle, Kordofan group (Nayil, Tendi, and Adok formations) was deposited. The third rift cycle was initiated by deposition of the thick Eocene Nayil shale that grades upward into an increasingly sandy interval of upper Nayil and younger Tertiary units. The Nayil and Tendi formations form the syn-rift sedimentary section of Cycle 3 and consist

mainly of shales with sandstone interbeds (Mohamed et al., 1999). The top of the Adok formation is marked by a major erosional unconformity.

2.4 Structural Style of Muglad Rift Basin

The Central African Shear Zone (CASZ) was reactivated fault zone inherited from the Pan-African orogeny (Caby, 2003) (Figure 2-8). It separates the NW-SE trending rift basins of West Africa from the Central Africa, and play important role in initiation and development of the E-W trending basins as well as the Sudanese rift basins. CASZ has been demonstrated right lateral movement (dextral) in Cretaceous (Genik, 1993). Structural studies on the Muglad rift basin by Schull (1988), Mann (1989) and McHargue et al. (1992) emphasized that the Muglad rift basin is a half-graben formed as a result of extensional forces in early Cretaceous.

The Muglad basin is considered as an extensional fault basin which consists of horsts and graben development and the formation of extremely complex fault system (Mann, 1989). In the central and southern Muglad basin, an apparently older north-northwest trend also exists (Schull, 1988). Mann (1989) studied the thick-skin and thin-skin detachment faults in rift-related basins in Sudan. His extensive work resulted in a model that illustrates the relationship between thick-skin (including basement) and thin-skin (excluding basement) detachment faults in half-graben rift-basins developed in Sudan. According to Mann (1989), the Muglad rift basin developed due to low-angle listric normal faulting and originated within the deep crust or mantle (thick-skin) (Figure 2-9).

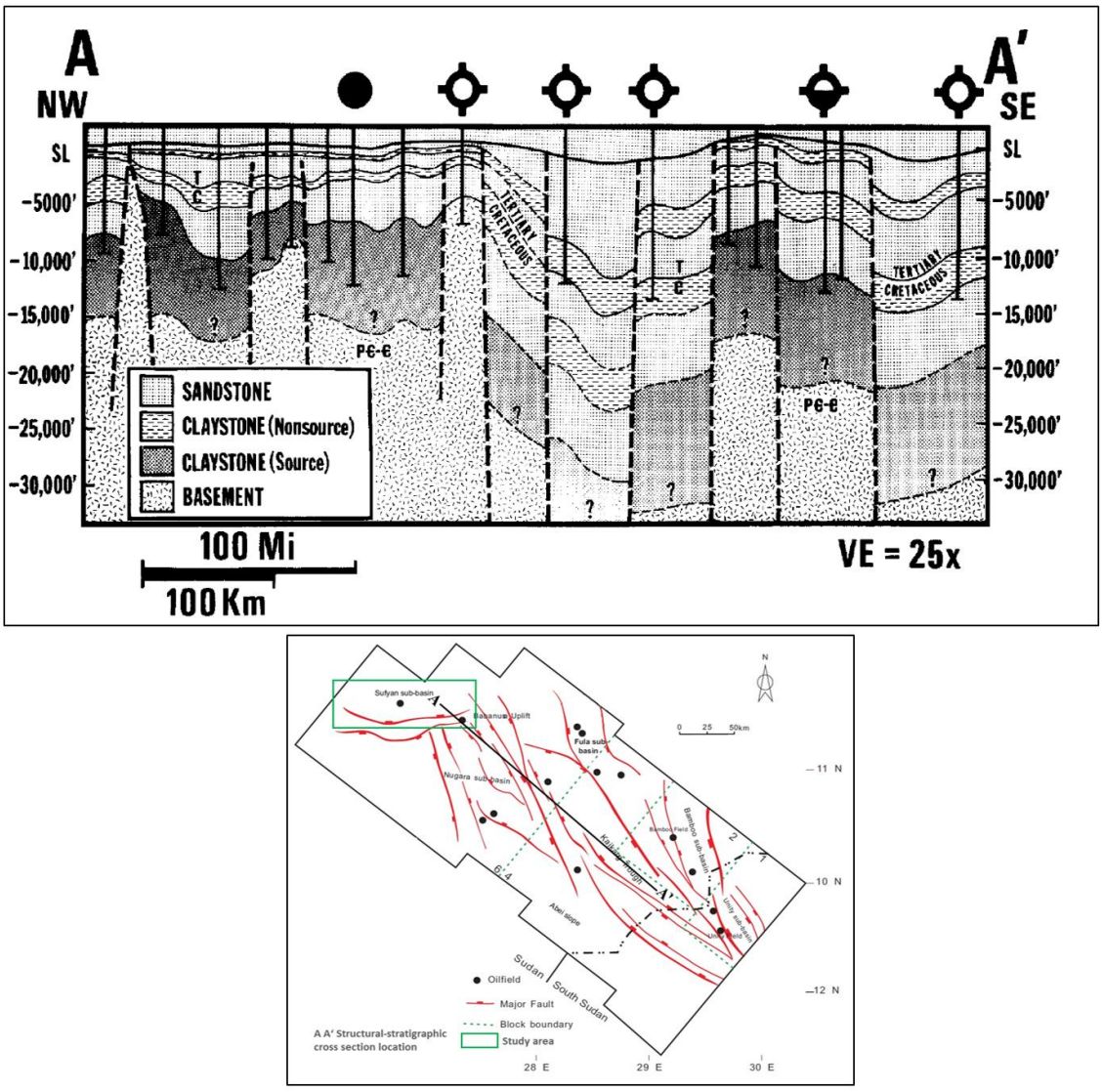

Figure 2-7: Generalized Muglad basin structural-stratigraphic cross-section (up). The location of this cross-section (down) after Schull (1988).

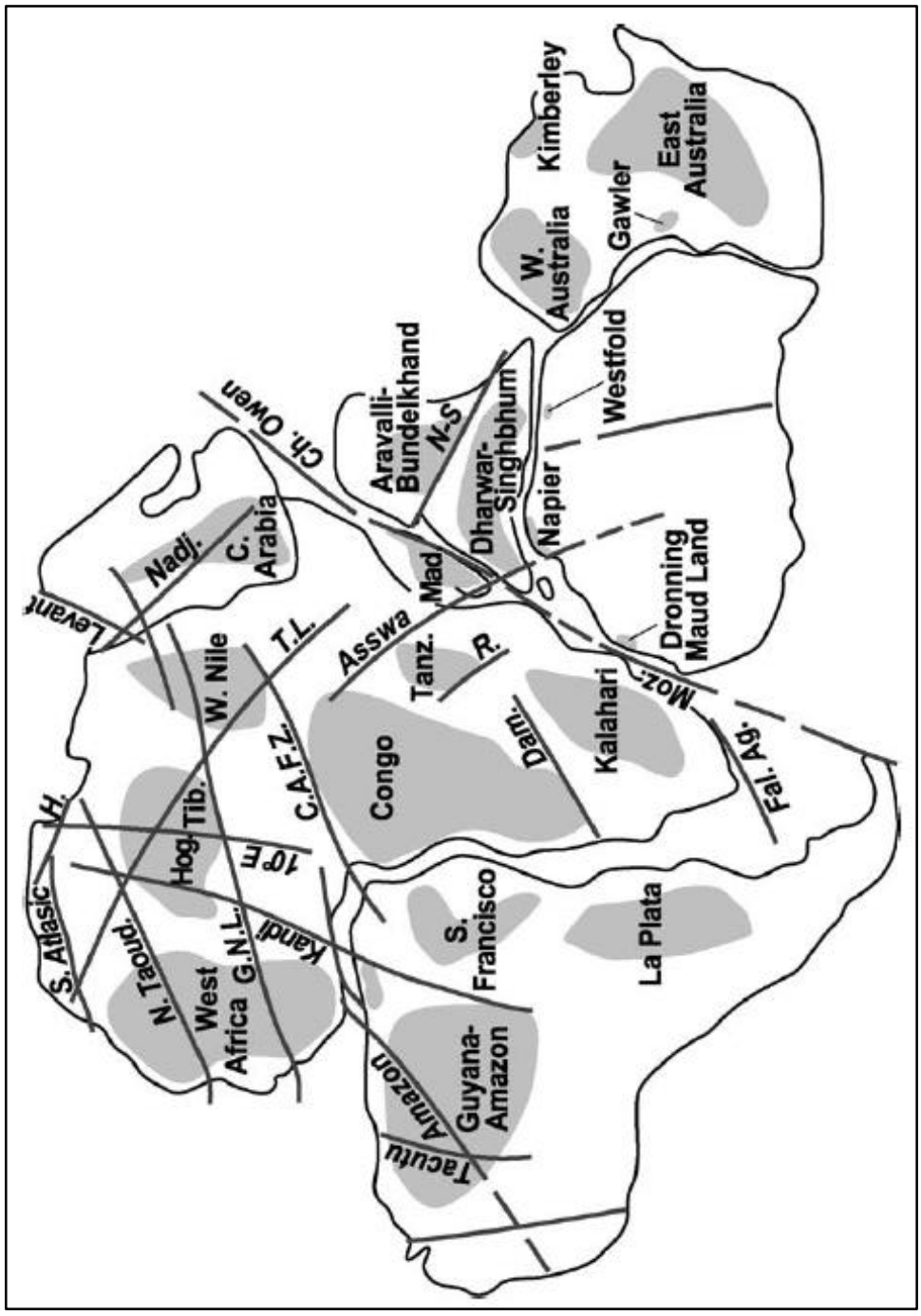

Figure 2-8: Major fault zones of the Gondwana. Apparent Archean and Paleoproterozoic cratons in gray. CAFZ, Central African Fault Zone or Central African Shear Zone (CASZ) (after Caby, 2003).

The extension of the upper crust by simple shear is believed to have involved the development of planer and listric faults (domino and rigid body rotation) (McHargue et al., 1992). The dominant structural controls in the Muglad Basin are the dip-slip normal faults. The complicated fault system in the Muglad Basin exhibits a wide range in geometry displacement and growth history. The complex history of extension resulted in prominent productive and prospective structures, which were categorized as rotated fault blocks, reverse and drape folds. The rotated fault blocks represent the common and important traps across the basin. The drape folds were formed on the upthrow side of the deep-seated normal faults. They have been found in areas where the faults were formed during the early rifting phase. In some areas, a downthrown rollover anticlines were formed as result of rotation along listric faults (Figure 2-9) (Mann, 1989).

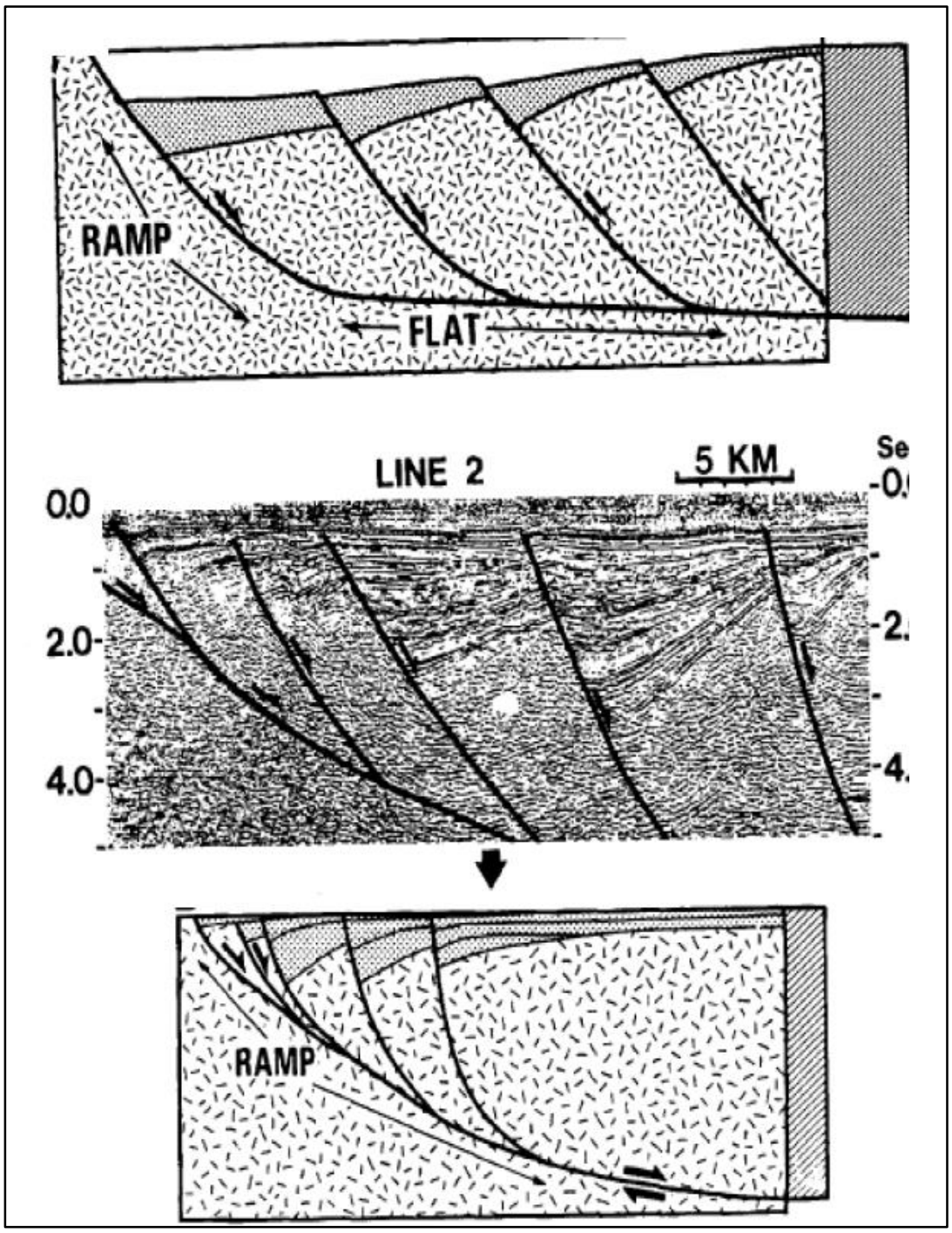

Figure 2-9: shows the Structure style of the Muglad rift basin showing the thick skin fault (After Mann, 1989).

CHAPTER 3

DATA AND METHODS

3.1 Available dataset

The available data in this study consists of seismic data, structural and two-way time (TWT) maps, gravity data, and well data (cores and well logs). Most of Sufyan Sub-basin is covered by 2D seismic data and the prospective areas are covered by 3D seismic data.

3.1.1 Seismic data

The seismic database used in the present study includes post-stack time migrated 2D and 3D reflection seismic surveys. Most surveys consist of dip lines oriented NE-SW and strike lines oriented NW-SE. The total length of the 2D seismic data is about 4500 km with a grid of about 1×1.5 km and the 3D seismic data is about 669 Km^2.

3.1.2 Gravity data

Processed satellite-derived gravity data with digital 2 km grids resolution of Bouguer anomaly images were used during this study. Compiled Bouguer Gravity Grid (density 2.00g/cc) includes three land surveys and an airborne survey with grid cell size of 1km also was used.

3.1.3 Well data

Wireline logs from 22 wells distributed in the study area. Those includes gamma ray, acoustic (sonic), density, and neutron logs. Six conventional cores from two wells were used from the as the basis of this investigation.

3.2 Methods

3.2.1 Structural restoration

Six horizons were interpreted, Top Amal Formation, Darfur Group, Bentiu Formation, Top Upper Abu Gabra Formation, Top Middle and Lower Abu Gabra formations, and Top Basement. Top Amal horizon shows strong amplitude and good continuity which is easily identified and regionally traced. The general seismic reflection feature of Darfur Group shows stronger amplitude, higher frequency and better continuity than Amal Formation. Top Bentiu Formation in the seismic sections shows a package of high frequency, strong amplitude, and medium continuity. Top Upper Abu Gabra Formation in the seismic sections shows a package of low frequency, weak amplitude, and poor continuity. Top Middle and Lower Abu Gabra Formation in the seismic sections show a package of low-moderate frequency, fair-strong amplitude, and fair continuity. Top Basement continues and is easily traced in the basin marginal area but becomes poor with weaker amplitude and lower frequency in the basin internal area.

Fault polygons maps for six horizons, four isopach maps, five 2D seismic cross-sections, and two associated kinematic models are presented. Interpretation of plan view maps and restored 2D seismic cross-sections were used to understand the evolution history of Sufyan Sub-basin. These include strike-slip and dip-slip components. Because of material

movement out of the plane of section (strike-slip), a method that restores stratigraphic surfaces in plan view (Rouby et al., 1993) was applied.

The total amounts of extension using plan view were applied using the fault polygon map of top Basement that was interpreted from seismic data.

In different parts of the Sub-basin, fault heaves were added together to identify the total extension. The sum of faults heaves was divided by the length before the extension to identify the percentage of extension.

The 2D structural restoration was conducted using 2D Move software provided by Midland Valley Company. The aim of structural restoration is to remove the faults' effects and to identify the extensional rates during the evolution history of the Sub-basin. The horizons and faults that interpreted from the 2D seismic sections represent the main input data for the structural restoration. The Sub-basin evolution history was explained from the restoration final results. The geo-seismic section was restored to its paleo-structure in several stages, prior to deformation time to recent time.

The workflow of structural restoration started by importing the depth-converted seismic section into the 2DMove software. Decompaction correction was applied. Faults effects were removed using the Inclined Shear algorithm (White et al., 1986), then by flattening the reconstructed horizon using a restore algorithm. Finally, by back stripping the shallowest horizons and repeating the steps for all the horizons starting from the shallowest to deepest. The depth to detachment is not imaged by reflection seismic data, so that is

calculated using area balanced method (Davison, 1986; Dula, 1991; Gibbs, 1983; McHargue et al., 1992).

For fault reconstruction, inclined shear algorithm was applied. Extension percentage and stretch factors were estimated using the relationship between the line length before reconstruction (length undeformed) and after the reconstruction (length deformed). Generally, lengthening increases by Increases in fault throw or/and decreases in fault dip angle.

$$e = \Delta I / I_o$$

$$ß = 1 + e$$

Where:

e: Extension

ΔI: the difference of length before restoration and after restoration.

Io: Length after restoration

ß: Stretch

3.2.2 Sedimentology and reservoir characteristics

The methods used in this study include subsurface facies analysis from core and wireline logs. Gamma ray log, acoustic log, density log, and neutron log were used during this study. The regional seismic line was used to illustrate the structure and stratigraphy across the Sub-basin. Sedimentologic interpretation aimed to determine the sedimentary facies and facies associations based on core and well logs. Sedimentary facies and facies associations

were integrated with the seismic data through the synthetic seismograms and seismic facies analysis were conducted to determine the spatial distribution of depositional systems. Conceptual depositional models were constructed and interpreted based on facies interpretation in Abu Gabra Formation. The sequence stratigraphic principles used in this study based on the classical concepts introduced by Posamentier and Allen (1999), Vail et al., (1977), and particularly by Van Wagoner et al., (1990). Petrographic thin sections, Scanning electron microscopy (SEM) and X-ray diffractometry (XRD) techniques were carried out to identify the detrital components and the authigenic components including the clay minerals and diagenetic features.

3.2.3 Sequence stratigraphy

Sedimentologic interpretation aimed to determine the sedimentary facies and facies associations based on core and well logs. Sedimentary facies and facies associations were integrated with the seismic data through the synthetic seismograms and seismic facies analysis were conducted to determine the spatial distribution of depositional systems. Seismic facies analysis mainly based on Sangree and Widmier (1979) methodology for non-marine environments.

Conceptual depositional models were constructed and interpreted based on facies interpretation in Abu Gabra Formation. Second order super-sequences, second-order sequences, and third order sequences were identified using well logs data. The sequence stratigraphic principles used in this study based on the classical concepts introduced by Posamentier and Allen (1999), Vail et al., (1977), and particularly by Van Wagoner et al., (1990).

According to the toplaps, downlaps, onlaps, and truncations of seismic reflection, sequence boundaries were identified.

Using well logs, Galloway, W.E (1989) stated that the identification of sequence boundary of different order cycles would be more difficult because of their varied facies expression and different log responses depending on the paleogeography of the area. In this case, it will be defined by the abrupt contrast in facies tract above and below the sequence boundary as well as a change in the degree of fluvial sandstone amalgamation (Shanley and McCabe, 1994).

Using well logs, we need first to subdivide the stratigraphic succession through the identification of the maximum flooding surface (MFS) and sequence boundaries (SB). Time significant surface such as (maximum flooding surface, sequence boundary, transgressive surface and flooding surface) are used in sequence stratigraphy for correlation of strata with much great confidence and subdividing the sedimentary package into cyclic patterns. The easiest surface to identify is the maximum flooding surface which associates with a condensed organic-rich layer which is typically characterized by hot gamma-ray responses. Typically sequence boundary exists temporally and spatially between two maximum flooding surfaces.

3.2.4 3D Geostatistical modeling

The methods used in this study include subsurface facies analysis from core and wireline logs. Gamma ray log, acoustic log, density log, and neutron log were used during this study. Sedimentologic interpretation aimed to determine the sedimentary facies and facies associations based on core and well logs. Sedimentary facies and facies associations were

integrated with the seismic data through the synthetic seismograms and seismic facies analysis were conducted to determine the spatial distribution of depositional systems. Conceptual depositional models were constructed and interpreted based on facies interpretation in Abu Gabra Formation. The sequence stratigraphic principles used in this study based on the classical concepts introduced by Posamentier and Allen (1999), Vail et al., (1977), and particularly by Van Wagoner et al., (1990).

The three-dimensional (3D) geostatistical modeling was carried out in petrel®, PC-based modeling software. The 3D Petrel model comprises mainly the structural framework of the area (including both faults and horizons) and the property model (populated for shale volume and porosity as extracted from the petrophysical analysis). The model represents a detailed configuration of the zonation for upper Abu Gabra Formation. 3D geocelluar model is required as a grid model to populate all reservoir properties spatially. It is involving multi-steps of constructing a structural model (faults and horizons), pillar gridding, zone, and layering. Detailed description for the 3D geocelluar model construction steps is presented and illustrated with figures and snapshots extracted from the Petrel model.

The petrophysical reservoir properties such as porosity and volume of shale were also calculated using wireline logs (i.e., GR, RHOB, and NPHI) and core data. Cutoffs for facies, porosity, and shale volume were assigned and used for facies classification. Major parasequence sets boundaries separating stratigraphic units in the studied wells were selected to construct the surfaces and zones of the model framework. 3D structure grid was built using seismic interpretation and stratigraphic parasequence sets boundaries. The

distribution of the facies associations and lithofacies was performed separately within each zone using sequential indicator simulation (SIS). The porosity and volume of shale modeling were done using Sequential Gaussian Simulation (SGS) algorithm. Porosity model was guided by facies model to qualify sand bodies delineation, reservoir heterogeneity, and spatial continuity. Geostatistical analysis was performed for facies and petrophysical reservoir properties, it includes multivariate geostatistical analysis, variogram modeling, and data trend analysis. Multi-realizations of high-resolution facies associations, Lithofacies, and porosity models were generated.

CHAPTER 4

STRUCTURAL AND TECTONIC ANALYSIS

4.1 Introduction

The trend of the Sufyan Sub-basin (E-W) is different from the Muglad Basin general strike (NW-SE) and similar to Baggara basin in the west of Sudan and other basins in east Chad (Figure 4-1). The unique E-W trend, suggests that this Sub-basin originated by a mechanism different from Muglad Basin that is considered more extensional in origin. The Sufyan Sub-basin is believed to be highly affected by the Central African Shear Zone (CASZ).

This chapter discusses the tectonic evolution and structural elements of Sufyan Sub-basin. It provides evidence for describing Sufyan as a transtensional pull-apart Sub-basin and discusses implications for hydrocarbon exploration. Other alternative scenarios for evolution history and the forming mechanism are identified such as the oblique extension model.

4.1.1 Continental rift systems

Continental rift systems are likely to follow zigzagging routes, which are formed due to the weakness zones in the basement rocks (Daly et al., 1989; Dixon et al., 1987; McConnell, 1972; Morley et al., 2004; Smith and Mosley, 1993).

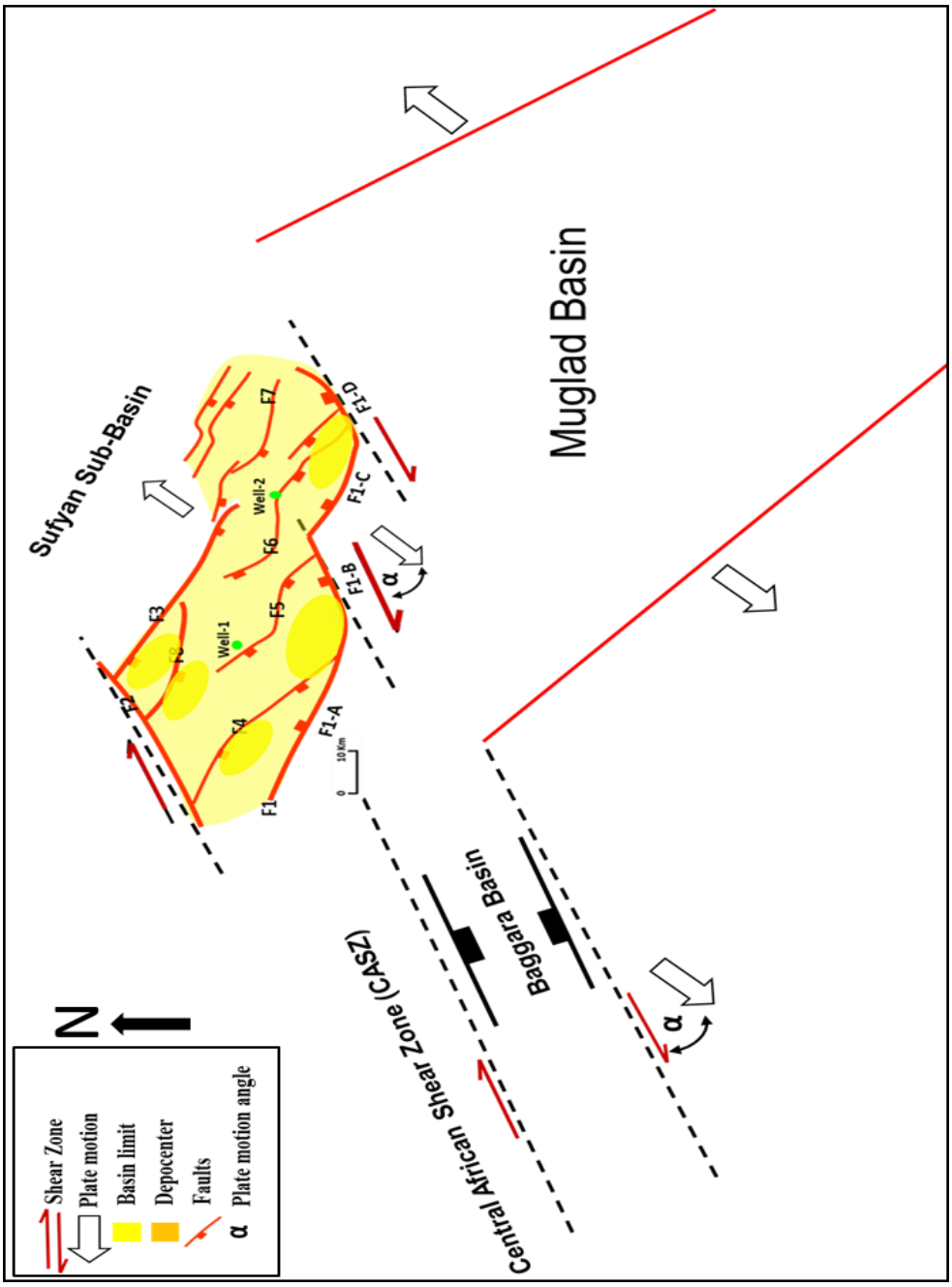

Figure 4-1: Conceptual model for the pull-apart systems in the study area interpreted from gravity and seismic data. The dotted lines represent the CASZ and its branches. Sufyan Sub-basin is a pull-apart basin affected by both CASZ (transtensional) and Muglad Basin (extension). Baggara Basin is a pull-apart basin affected only by the CASZ (strike-slip movement).

The oblique rift during extension can yield geometries similar to those formed during the strike-slip and transtensional movement (Morley et al., 2004). Understanding the variation between the two structural styles and their related stress regimes is important (Morley et al., 2004). The intermediate principal stress is represented by the vertical principal stress in the transtensional movement (Sanderson and Marchini, 1984), while the maximum principal stress represented by the vertical principal stress is in the oblique extension.

4.1.2 Muglad Basin

Muglad Basin is the greatest sedimentary basin in Sudan and South Soudan with a total area of about 160,000 km^2 (with a width of about 200 km and a length of about 800 Km). The formation of the Muglad Basin is believed to be a rift structure that is related to the opening of the Atlantic Ocean since the Early Cretaceous period by the right-lateral movement along the CASZ (Genik, 1993). The basin is divided into eight Sub-basins which are South Kaikang, North Kaikang, Unity, Bamboo, Fula, East Nugara, West Nugara, and Sufyan (Lirong et al., 2013; Makeen et al., 2016). These Sub-basins are occupied by Cretaceous - Tertiary non-marine sediments (Schull, 1988).

4.1.3 Sufyan Sub-basin

Sufyan Sub-basin is bounded by Tomat Uplift with boundary fault in the south and Babausa Uplift to the north and east, and connected with Nugara depression in the south east. Sufyan Sub-basin exploration results have shown the occurrence of accumulations of hydrocarbon. Source rock for this hydrocarbon is believed to be the lacustrine shale of the Abu Gabra Formation (Qiao et al., 2016). The TOC of Abu Gabra source rock in the area of study ranges from 1.45 to 5.15 wt % with an average of 2.84 wt % (Qiao et al., 2016). Samples

with TOC more than 1.0 wt % and 2.0 wt % account for 96.92 % and 60.45 % of the total, respectively, and are evaluated together as good to excellent source rock (Qiao et al., 2016). The sandstone rock within Abu Gabra Formation represents the primary reservoir. The main trap style in the Sub-basin is the tilted fault blocks related to en echelon faults.

4.2 Structural Elements of Sufyan Sub-basin

Sufyan Sub-basin is bounded by three major faults, the southern fault (F1) (Figure 4-2) dipping toward the north, the northern fault (F3) (Figure 4-2) dipping toward the south, and the northwest fault (F2) (Figure 4-2) dipping toward the northwest. Six major transtensional oblique faults were also observed in an en-echelon pattern (F3, F4, F5, F6, F7, and F8) (Figure 4-2). Those faults are trending mainly NW-SE (Figure 4-2). Both types of faults are thick-skin faults (basement involved) and extend to the shallow horizons. Other faults are small and minor faults but are very important because they control and form the structural hydrocarbon traps in the study area. Interpretation of reflection seismic data of the Sub-basin reveals graben geometry with two depocenters that are controlled by the southern boundary Fault.

The strike-slip faults in Sufyan Sub-basin are always occurring with steep and straight fault surfaces. Most the faults have a trend of NE and NNE. The Fault No.2 (F2) is the typical example (Figure 4-2).

The strike-slip faults in Sufyan Sub-basin are always occurring with steep and straight fault surfaces. Most the faults have a trend of NE and NNE. The Fault No.2 (F2) is the typical example (Figure 4-2).

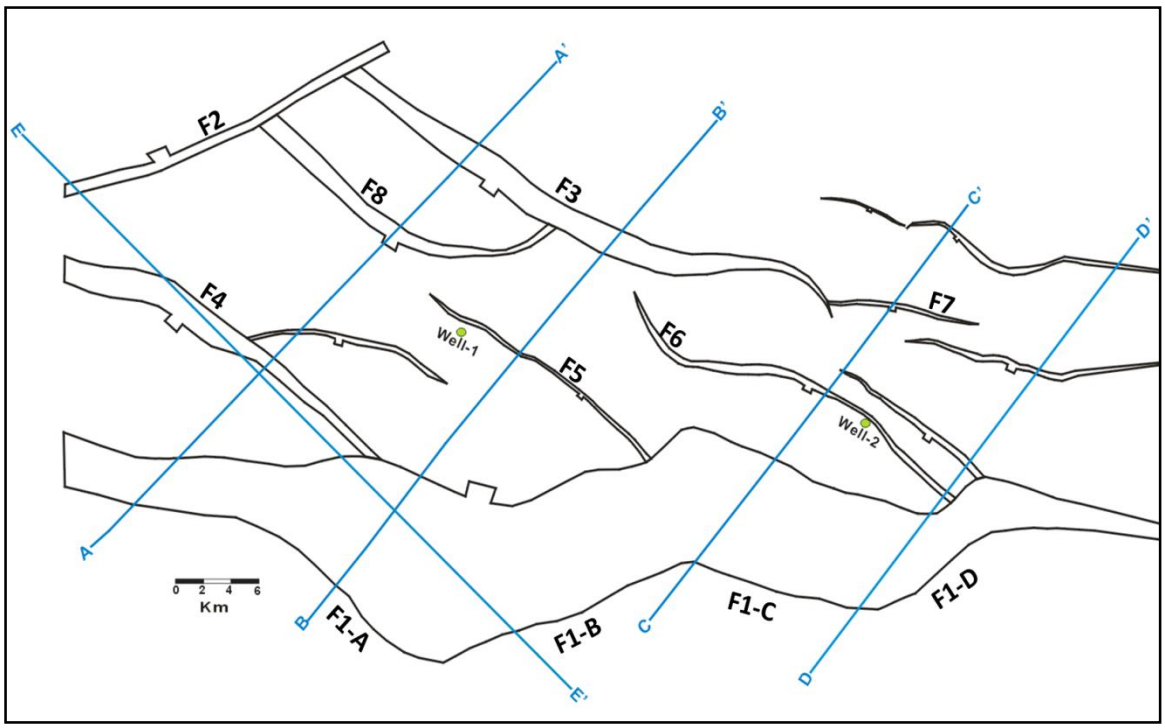

Figure 4-2: Structural map of top Basement, interpreted from 2D seismic data shows faults (boundary faults F1, F2, and F3) (major faults F4, F5, F6, F7, and F8), location of wells (Well-1 and Well-2) and regional seismic lines (AA', BB', CC', DD', and EE`). F2 represented as a part of the CASZ.

The southern boundary fault has zigzagging map patterns, involving ENW-ESE segments (F1-A and F1-C) and NE-SW segments (F1-B and F1-D) (Figure 4-2). Figure 4-3 and Figure 4-4 shows the different dip angles of the southern (F1) boundary fault in different locations. Different fault styles, such as listric fault (the upper section is the high angle and the lower section is flat) and high-angle (the dip angle is more than 40 degrees).

The western segment of the southern boundary fault (F1) (Figure 4-3) show relatively weak activity in the Early Cretaceous period during the deposition of Abu Gabra Formation and it was relatively enhanced in its activity during the deposition of Bentiu Formation. The strike of the western segment of F1 (F1A) is WNW-ESE and the dip azimuth is NNE with dip angle ranging from 45 to 70 degree and fault throw about 1700 m. The middle part dip angle ranging from 20 to 60 degree and fault throw about 2400. The eastern segment dip angle ranging from 40 to 60 degree and fault throw about 2000 m.

Sufyan Sub-basin has the structural characteristics of differences from west to east directions (Figure 4-2). It can be divided into western, middle, and eastern parts. Each of them has their own characteristics. There are three tilted fault blocks (Figure 4-3) in the western part of the Sufyan Sub-basin controlled by the north boundary fault (F3), south boundary fault (F1), major fault 4 (F4), and major fault 8 (F8). The geometry of the Sub-basin in the western part is described as a tilt block (Figure 4-3).

In the middle part, an asymmetrical graben with one depocenter controlled by the south boundary fault (F1) and the major fault 5 (F5) (Figure 4-4), and another one controlled by an old antithetic fault and the northern boundary fault (F3) (Figure 4-4). In the middle part, the southern fault (F1) became very huge (Figure 4-4B).

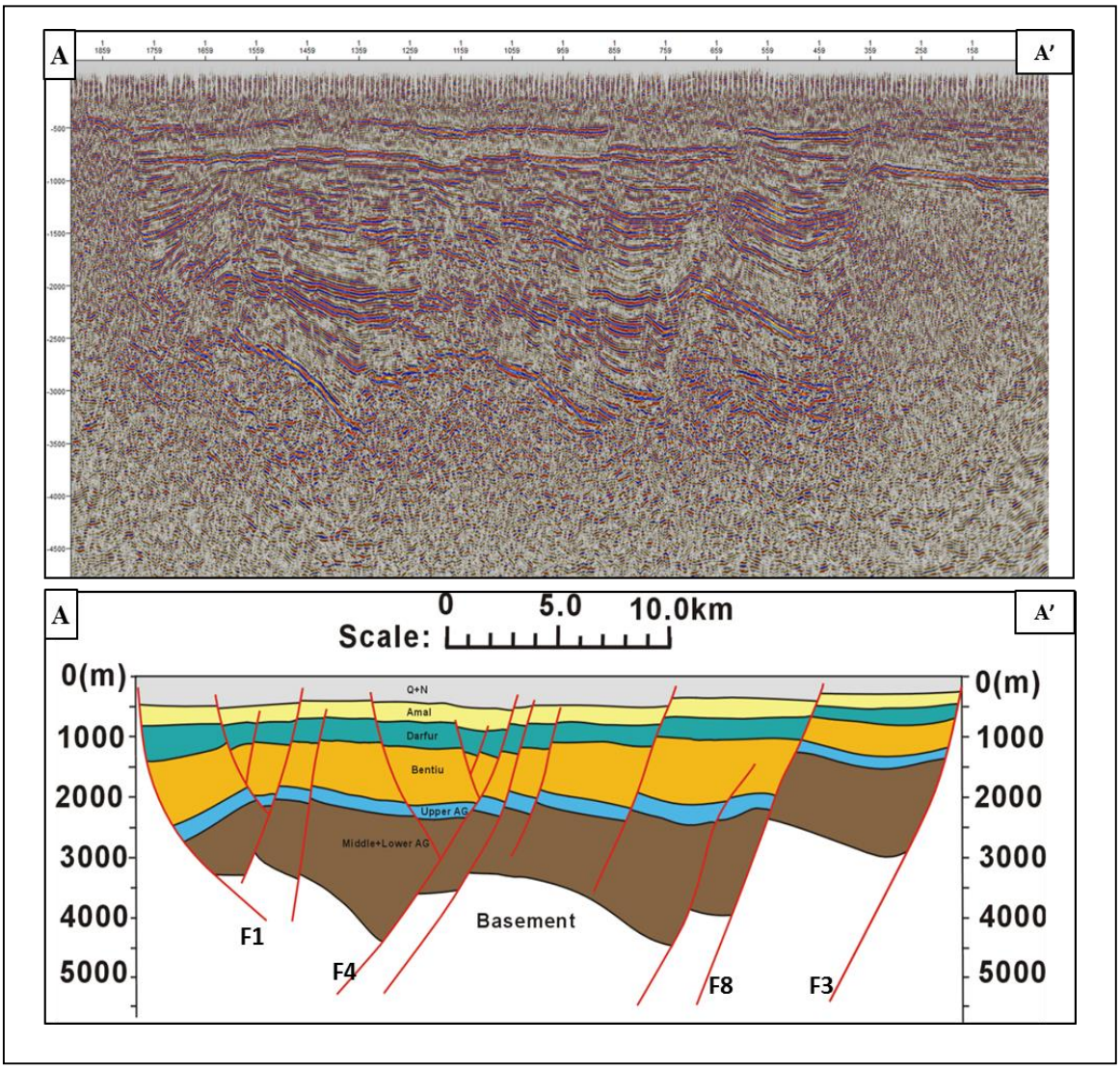

Figure 4-3: A-A` Regional seismic line (Upper) and Geoseismic section (lower) (locations of the line in Figure 4-2). Horizons from top to bottom are top of; Amal Formation, Darfur Group, Bentiu Formation, Upper Abu Gabra Formation, Middle and Lower Abu Gabra formations, and basement.

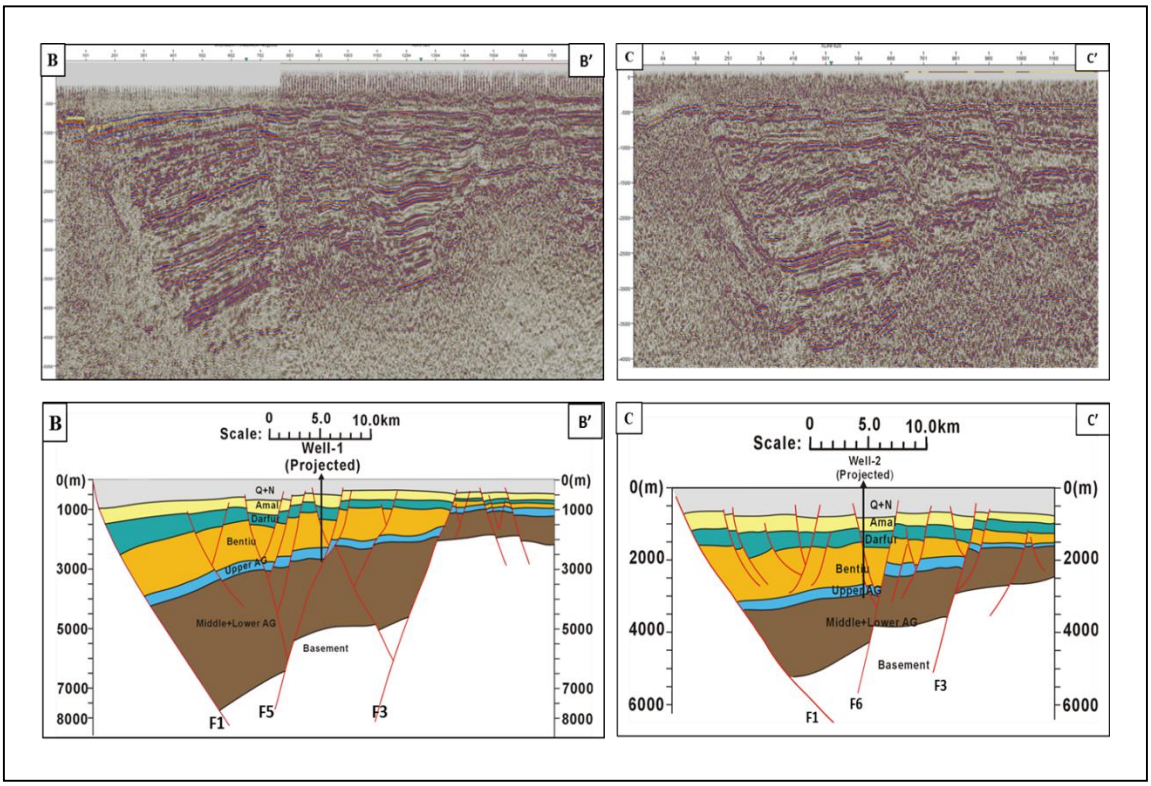

Figure 4-4: B-B` Regional seismic line and Geoseismic section. C-C` Regional seismic line and Geoseismic section (right) (locations of the lines in Figure 4-2). Horizons from top to bottom are top of; Amal Formation, Darfur Group, Bentiu Formation, Upper Abu Gabra Formation, Middle and Lower Abu Gabra formations, and basement.

In the eastern part, only one depocenter was developed controlled by the southern boundary fault (F1), the northern boundary fault, and major fault 6 (F6) (Figure 4-5). The geometry of the Sub-basin in the western part is described as half graben (Figure 4-5).

4.3 Evolution History of Sufyan Sub-basin

Interpretation of restored 2D seismic cross-sections (Figure 4-6 and Figure 4-7), plan view map (Figure 4-11), isopach maps (Figure 4-8), and subsidence analysis (Figure 4-9, Figure 4-10, Figure 4-12) were used to analyze the evolution history of Sufyan Sub-basin which include strike-slip and dip-slip components. Methods that restore stratigraphic surfaces in plan view (Rouby et al., 1993) applied because of movement out of the plane of sections (strike-slip).

4.3.1 Vertical evolution history

The Sub-basin evolution history was described using two methods. In the first method, two regional seismic lines were restored with 2D Move software using inclined shear algorithm. Those two regional lines were balanced and restored at top Amal Formation, top Darfur group, top Bentiu Formation, top Upper Abu Gabra Formation, top Middle and Lower Abu Gabra formations, and top basement levels. For extension percentage calculation using the 2D structural restoration, regional line length before reconstruction (length undeformed) and after the reconstruction (length deformed) were identified.

The second method is the plan view restoration using a fault polygon map of top Basement. In different parts of the Sub-basin (western, middle, and eastern), fault heaves were added together to identify the total extension. The sum of faults heaves was divided by the length before the extension to identify the percentage of extension.

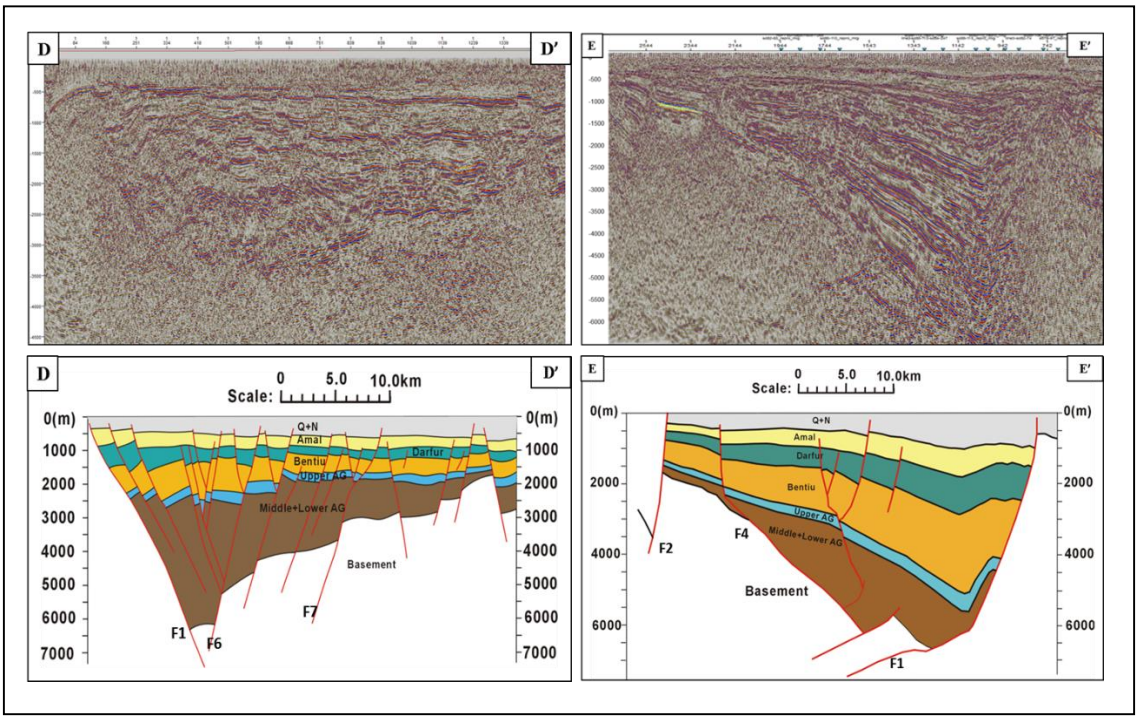

Figure 4-5: D-D` Regional seismic line and Geoseismic section. E-E` Regional seismic line and Geoseismic section (right) (locations of the lines in Figure 4-2). Horizons from top to bottom are top of; Amal Formation, Darfur Group, Bentiu Formation, Upper Abu Gabra Formation, Middle and Lower Abu Gabra formations, and basement.

The total amount of extension and stretch factors were estimated for Sufyan Sub-basin. Sufyan Sub-basin has the structural characteristics of different blocks from west to east direction and deferent belts in N-S direction. It can be divided into western, middle, and eastern blocks. Each of them has their own characteristics.

4.3.1.1 Western part

The west regional cross-section A-A' (Figure 4-6) is based on the depth-migrated seismic line shown in Figure 4-3. It is about 36.44 Km long and trending SW-NE traversing the western part of Sufyan Sub-basin.

The A-A' cross-section was balanced and restored using the inclined shear method at top of Amal Formation, Darfur group, Bentiu Formation, Upper Abu Gabra Formation, Middle and Lower Abu Gabra formations, and basement (Figure 4-6) levels.

The calculated extensional strains are a minimum value since the section balancing did not account for minor compressional strain during later basin inversion.

This interpretation and corresponding restorations yield a total extensional percent at the top of the basement of about 38.3% and the stretch factors ß =1.38 (Table 4-1).

4.3.1.2 Middle Part

Using the basement structural map and by applying the method of adding the fault heaves together, total extensions were identified. The total extension percentage ranges from 41.39% to 48.39% and the stretch factors ß ranges from 1.41 to 1.49 (Table 4-1).

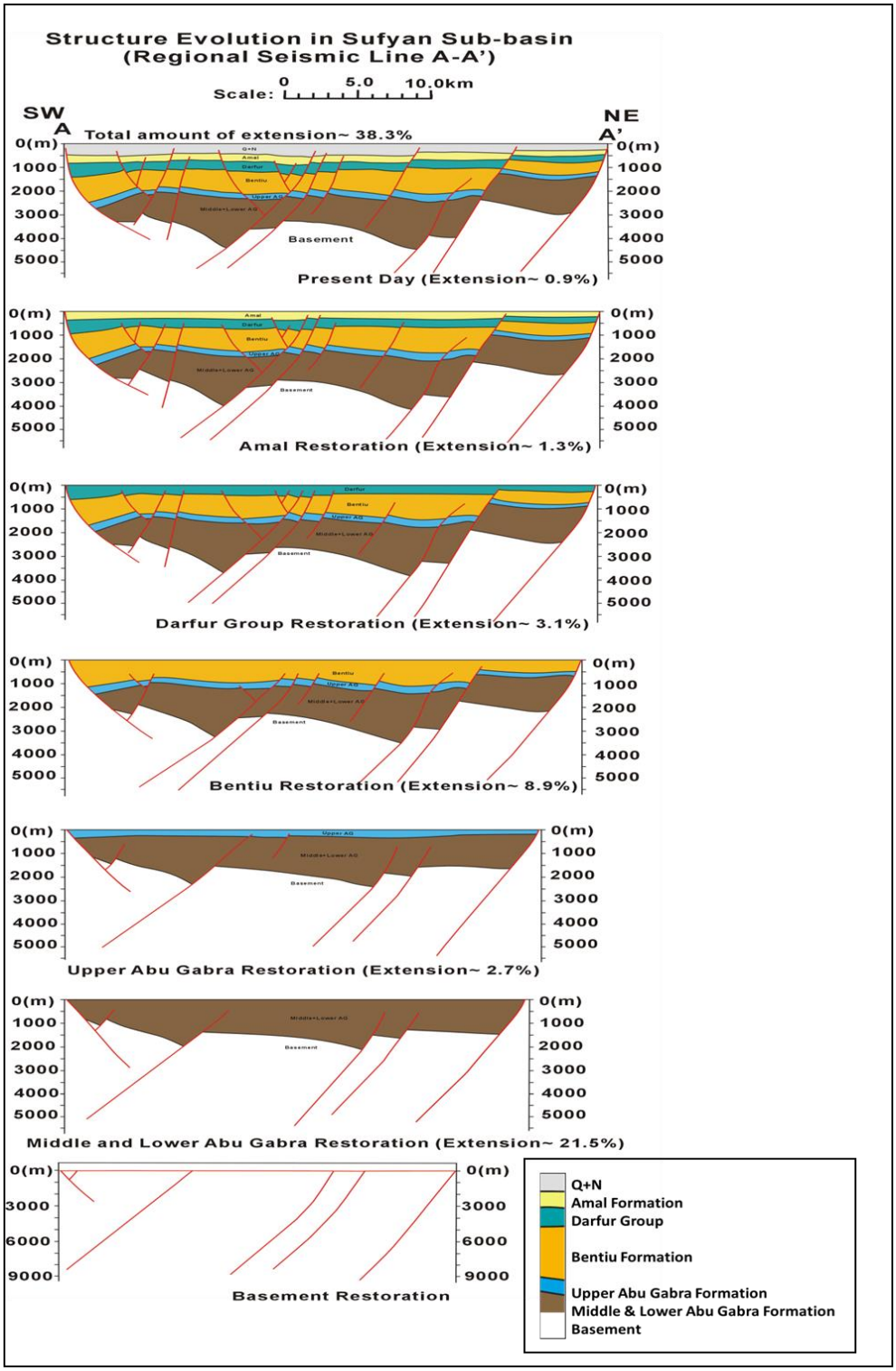

Figure 4-6: Shows the sequential restoration/decompaction of regional line A-A' (location of this line in Figure 4-2).

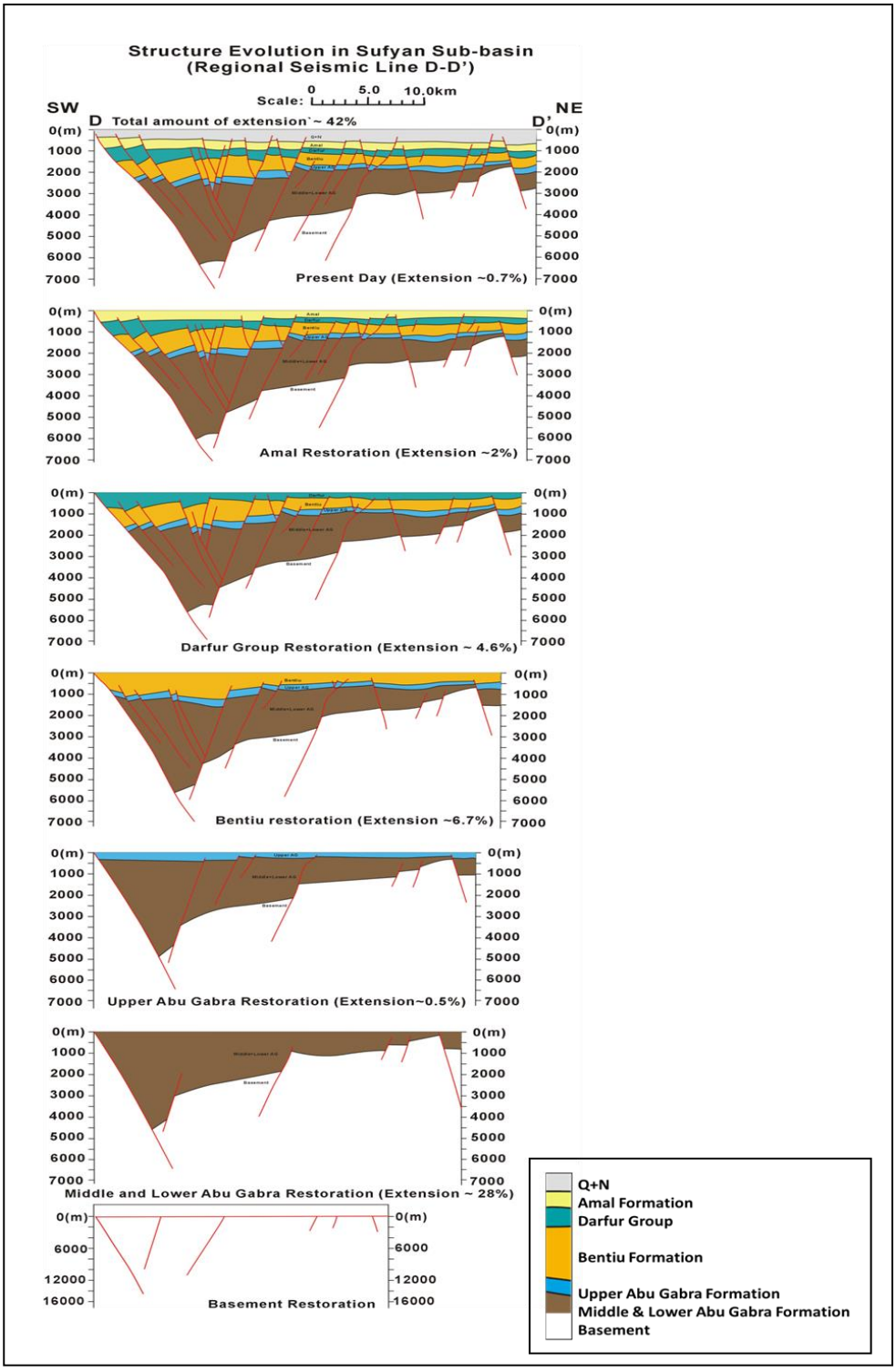

Figure 4-7: Shows the results of the structural restoration of regional lines D-D' (location of this line in Figure 4-2).

Table 4-1: show the total amounts of extension using plan view (Upper). The total amounts of extension using 2D structural restoration (Lower).

Total amount of extension using plan view					
	Sum of faults heave	Length before extension	Sum of faults heave/Length before extension	The percentage of extension	ß factor
A	9.52	26.5	0.36	35.92	1.36
B	8.97	21.67	0.41	41.39	1.41
C	8.02	16.5	0.49	48.61	1.49
D	6.8	18.06	0.38	37.65	1.38

Total amount of extension using 2D structural restoration						
	Length undeformed (Before extension)	Length deformed (After extension)	Length deformed- Length undeformed	(Length deformed-Length undeformed)/ Length undeformed	The percentage of extension	ß factor
A	25.46	35.22	9.76	0.38	38.33	1.38
D	16.18	23.07	6.89	0.43	42.58	1.43

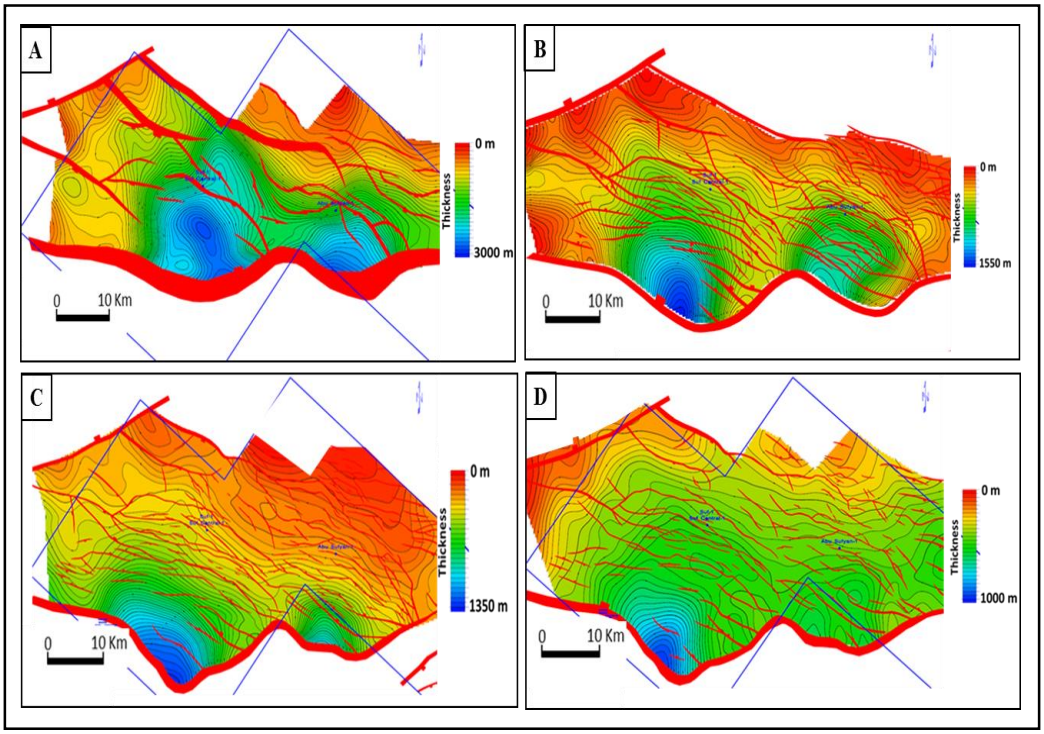

Figure 4-8: Isopach maps of sediments deposited during the rift-sag phases of two tectonic cycles in Sufyan Sub-basin. (A) Early Cretaceous Period First Rift Phase (Abu Gabra Formation). (B) Early Cretaceous Period First Sag Phase (Bentiu Formation). (C) Late Cretaceous Period Second Rift Phase (Darfur Group). (D) Late Cretaceous Period Second Sag Phase (Amal Formation).

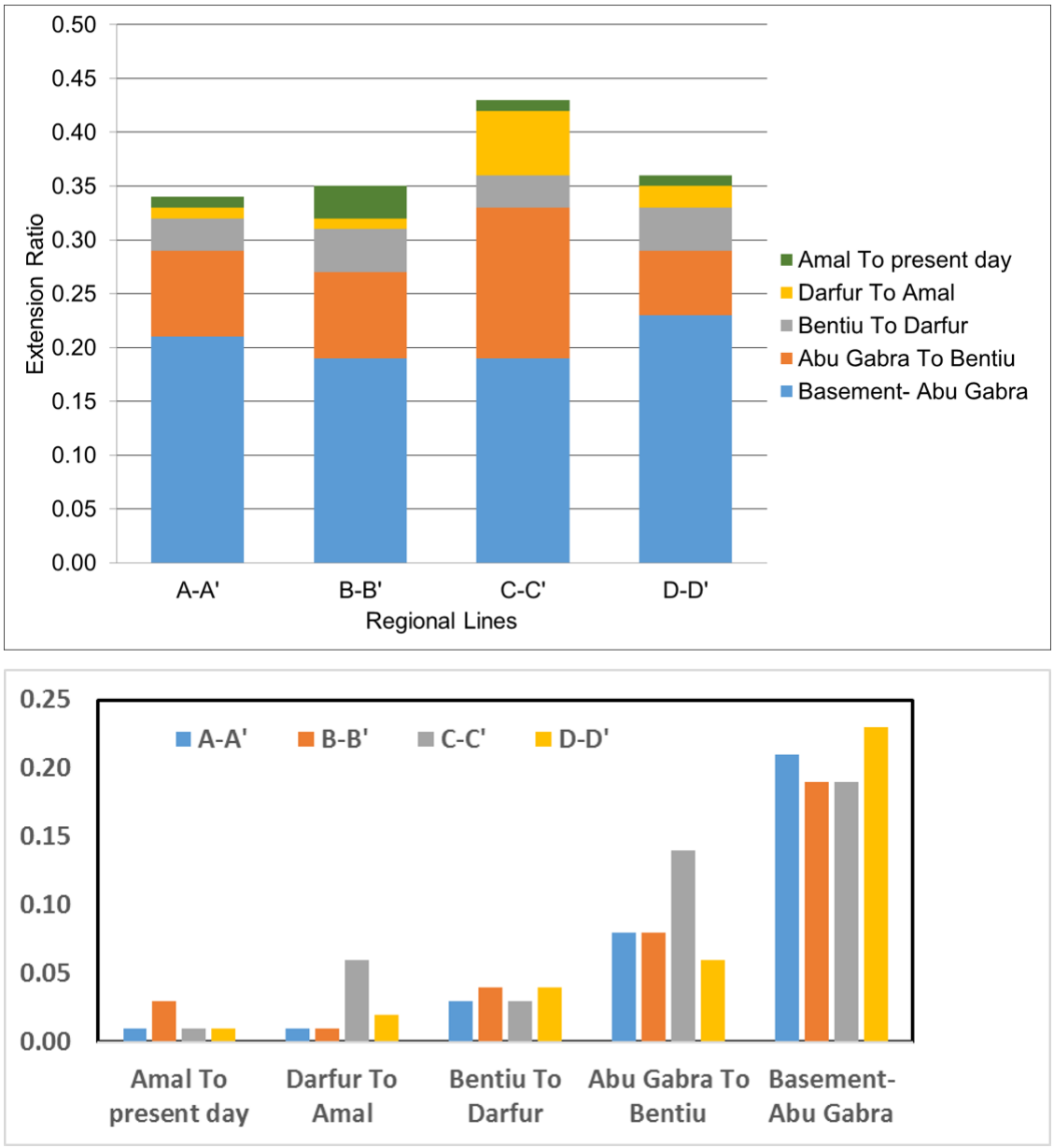

Figure 4-9: Extension ratio variation spatially and temporally. The extension ratio is high during the first rift cycle and starts to decrease with time (for the regional seismic line location see Figure 4-2).

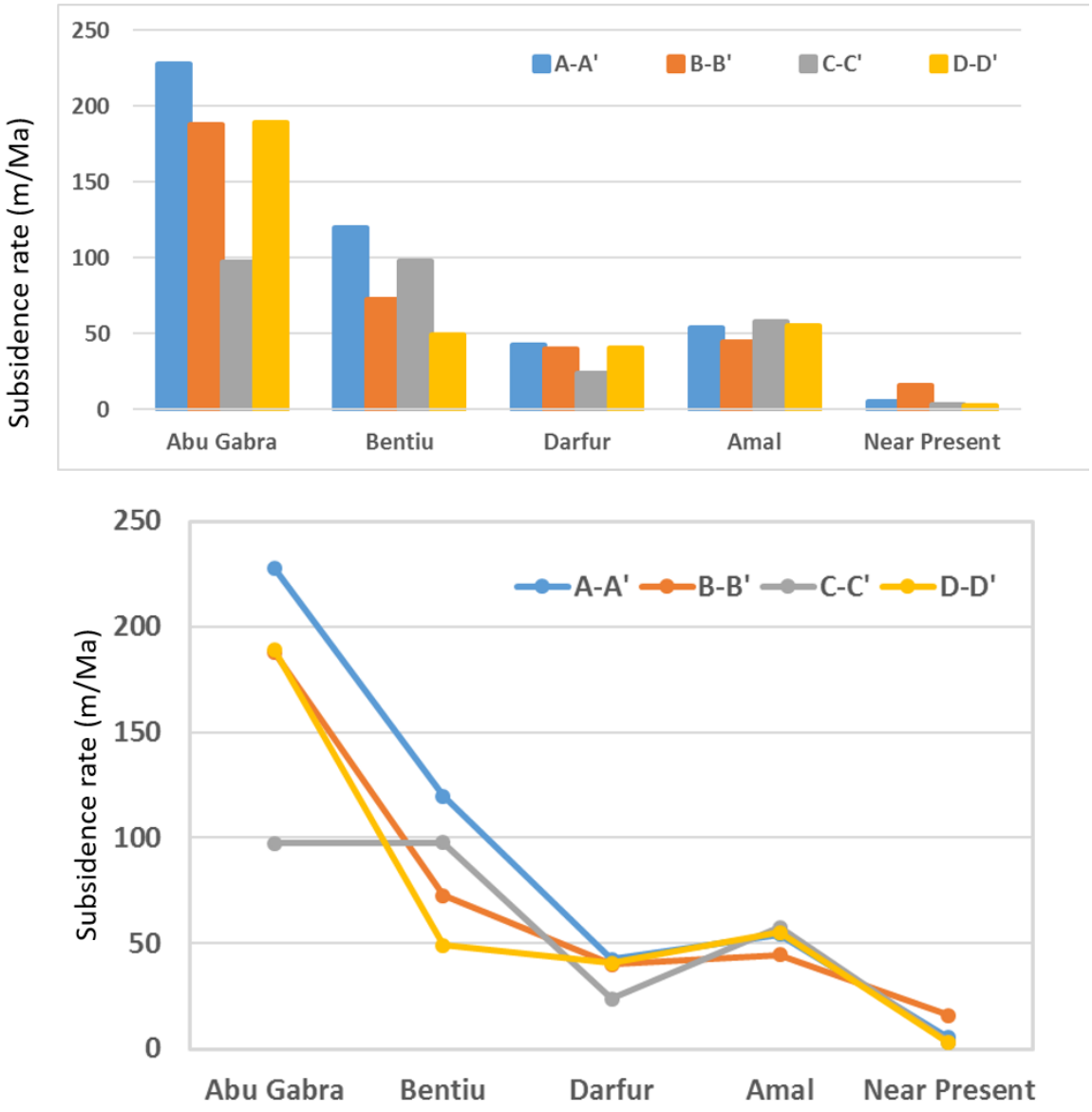

Figure 4-10: Subside rate (m/Ma) variation spatially and temporally (for the regional seismic line location see Figure 4-2). The subsidence rate is high during the first rift cycle and start to decrease with time

4.3.1.3 Eastern Part

The east regional cross-section D-D' (Figure 4-7) is based on the depth-migrated seismic line shown in Figure 4-5D. It is about 23.87 Km long and trending SW-NE traversing the eastern part of Sufyan Sub-basin.

The D-D' cross-section was balanced and restored using the inclined shear method at top of Amal Formation, Darfur group, Bentiu Formation, Upper Abu Gabra Formation, Middle and Lower Abu Gabra formations, and basement levels (Figure 4-7).

This interpretation and corresponding restorations yield a total extensional at the top of the basement of about 42.6% and the stretch factors ß =1.42.

4.3.2 Plan view evolution history

4.3.2.1 First rift cycle

During the Early Cretaceous period, the first Rift-Sag cycle was developed. The first rift cycle in Sufyan Sub-basin consists of tectonic subsidence (Figure 4-12) and Sag phases (Figure 4-11 a and b). The extension during this cycle is not equal along the Sub-basin (Figure **4-9**). The extension during the tectonic subsidence in the western part is about 21.5% (Figure 4-6) (which represent 89.2% of the total extension of the sub-basin) and in the eastern part is about 28% (Figure 4-7) (which represent 82.82% of the total extension of the sub-basin) (Table 4-1). During this phase, the boundaries and major faults were initiated (**Figure 4-11**a).

The Early Cretaceous period first rift isopach is strongly affected by the tectonic events. Thicknesses during this phase changed gradually over tens of kilometers (from 0 to 3000

m) (Figure 4-8A); sudden changes can be related to the occurrence of faults. The south boundary fault (F1) is characterized by strong differences in thicknesses during this phase. The strata display thickening towards the fault. The stratigraphic thickening in the southern part was produced by fault movement during the deposition (syn-deposition). Using growth strata as indicators, the faults orientation and location can be determined during the Early Cretaceous rift phase can be determined. Certain segments of the South boundary fault (F1) were active during this episode (Figure 4-8A). Two depocenters controlled by the south boundary fault (F1) were developed during this phase (Figure 4-8A), between segments F1-A and F1-B and between segments F1-C and F1-D (Figure 4-8A). The thick strata indicate that at least two parts of the south boundary fault segment first developed in the Early Cretaceous period. Those depocenters are bounded by steep faults and resulted in about 21.5% extension (5.47 km), which likely occurred in oblique-extensional fashion based on the structural setting.

The extension during the sag phase is about 8.9% (Figure 4-6) in the western part and about 6.7% (Figure 4-7) in the eastern part (Table 4-1). During this phase, boundaries and major faults were re-activated.

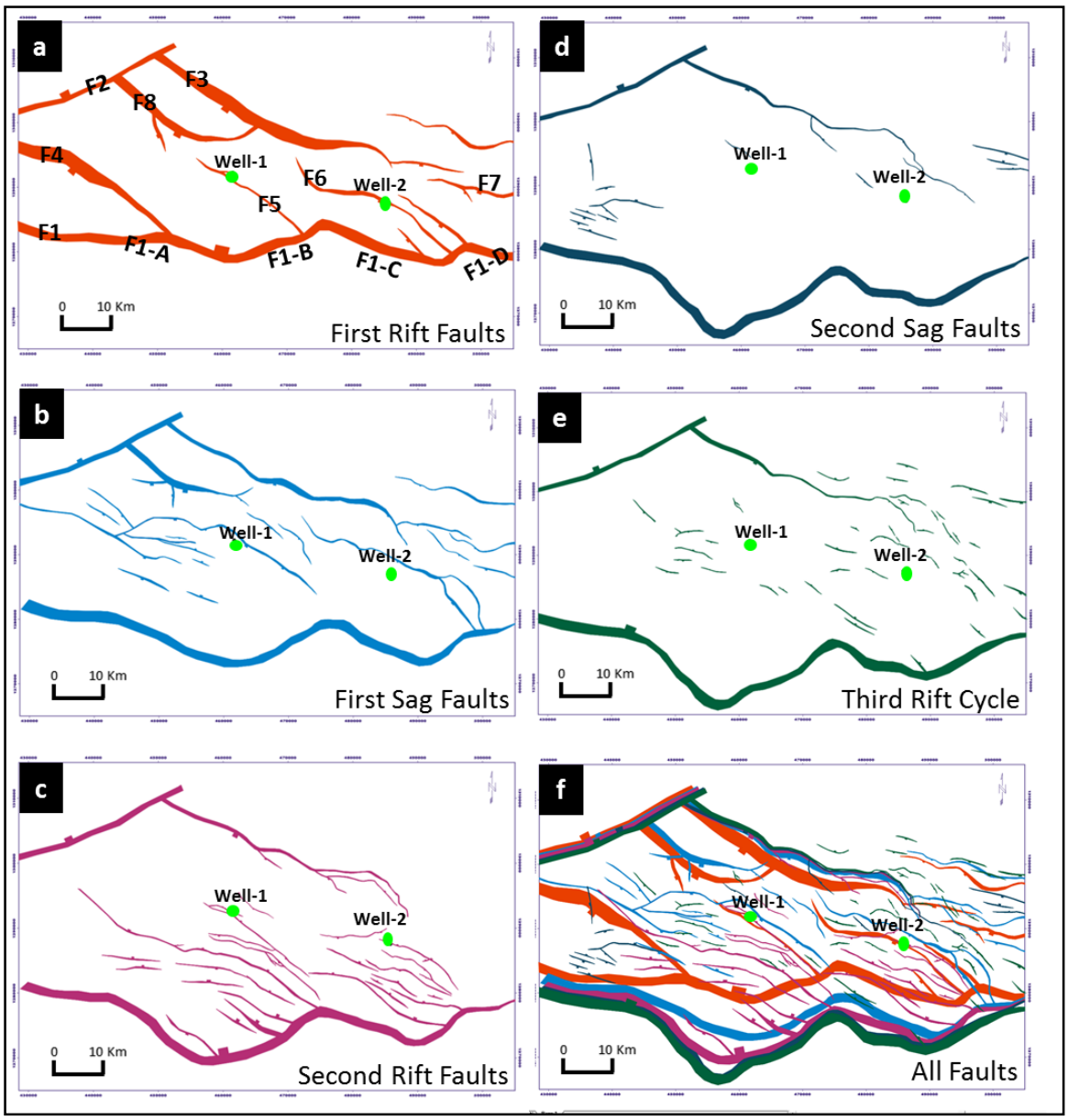

Figure 4-11: Plan view of fault polygons map interpreted from the 2D seismic data for each formation showing the spatial and temporal changes in Sufyan Sub-Basin geometry. To identify the fault timing (initiation and reactivation), structural restoration was applied. (a) Top fault polygons map shows the faults that initiated during the first tectonic subsidence (Early Cretaceous) (During the deposition of Abu Gabra Formation). (b) Faults that initiated and re-activated during the first sag phase (Early Cretaceous) (During the deposition of Bentiu Formation). (c) Faults that initiated and re-activated during the second rift phase (Late Cretaceous) (During the deposition of Darfur Group). (d) Faults that initiated and re-activated during the second sag phase (Late Cretaceous) (During the deposition of Amal Formation). (e) Faults that initiated and was re-activated during the third tectonic cycle (Tertiary) (During the deposition of Nayil, Tendi, and Adok formations). (f) All the faults that generated and reactivated during different time.

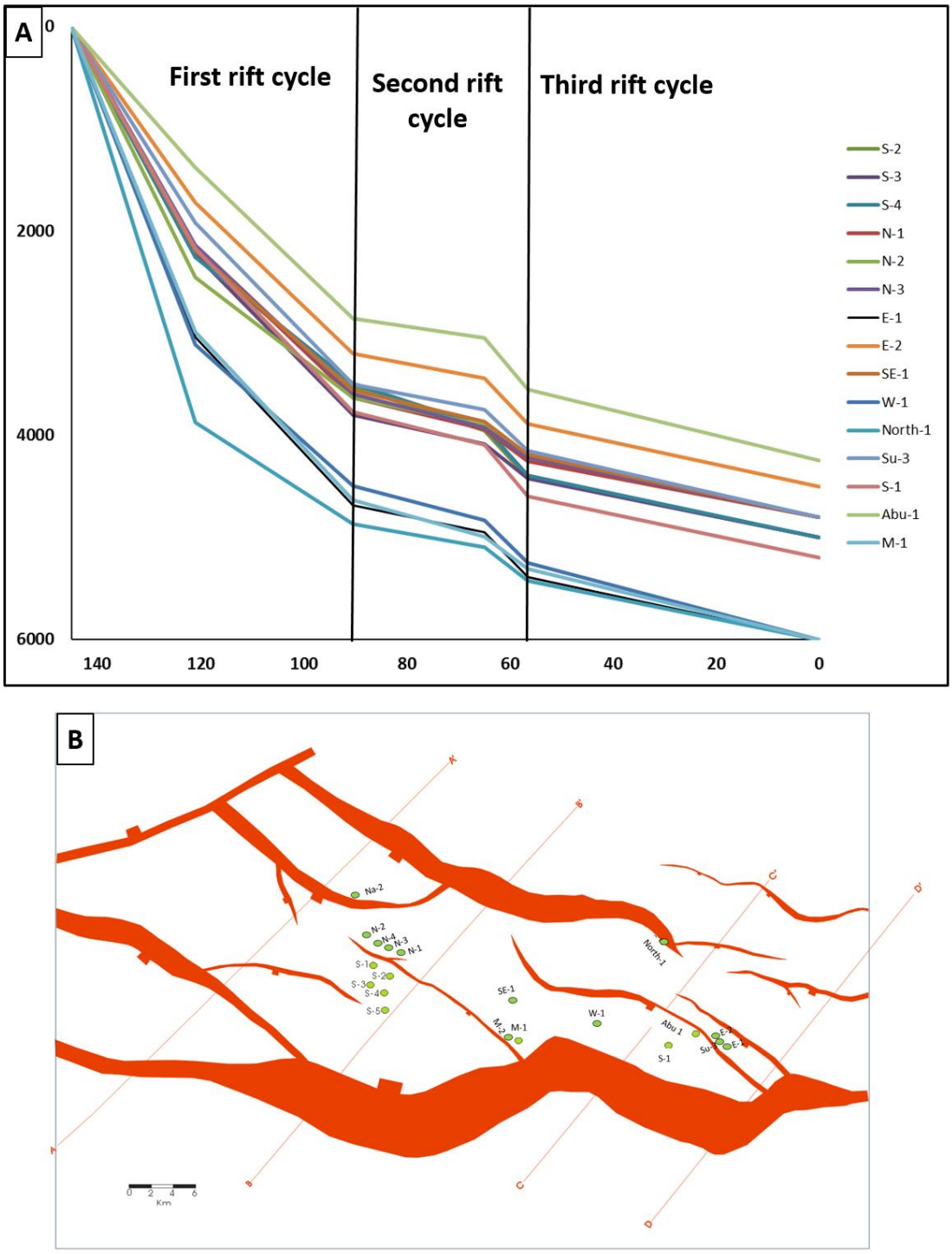

Figure 4-12: shows the backstripping tectonic subsidence rate of Sufyan Sub-basin (A). The subsidence analysis well locations (B).

The Early Cretaceous period first Sag thicknesses vary from 0 to 1550 m and graded over tens of kilometers (Figure 4-8B); sudden changes can be related to the presence of faults. The south boundary fault (F1) is characterized by strong differences in thicknesses during this phase. The stratigraphic thickening in the southern part was produced by fault movement during the deposition (syn-deposition). Certain segments of the south boundary fault (F1) were active during this episode (Figure 4-8B). One depocenter was developed during this phase (Figure 4-8B), controlled by the F1-A segment of the south boundary fault (Figure 4-8B).

Restorations and forward modeling of two regional lines propose that the first rift cycle faults represent 82-86% of total extension. Stretching factors across Sufyan Sub-basin vary between 1.36 and 1.49 (Table 4-1).

4.3.2.2 Second rift cycle

During the Late Cretaceous period, the second Rift-Sag cycle was developed. The second rift cycle in Sufyan Sub-basin consists of tectonic subsidence (Figure 4-12) and Sag phases (Figure 4-11 c and d).

The extension during the tectonic subsidence in the western part is about 3.1% (Figure 4-6) and in the eastern part is about 4.6% (Table 4-1; Figure 4-7). During this phase, many faults were initiated antithetically to the transtensional (oblique) faults (F4, F5, and F6). These faults are highly controlled by F1-B and F1-D segments of the southern boundary fault (F1).

The Late Cretaceous period second rift isopach is strongly affected by the tectonic events. Thicknesses during this phase changed gradually over tens of kilometers (from 0 to 1350 m) (Figure 4-8C); sudden changes can be related to the occurrence of faults. The south boundary fault (F1) is characterized by strong differences in thicknesses during this phase. The strata exhibits thickening towards the fault. Certain segments of the south boundary fault (F1) were active during this episode (Figure 4-8C). One depocenter was developed during this phase (Figure 4-8C), controlled by F1-A segment of the south boundary fault (Figure 4-8C).

The extension during the sag phase is about 1.3% (Figure 4-6) in the western part and about 2% (Table 4-1; Figure 4-7) in the eastern part. During this phase, shortening and compressional sense of movement are better shown in the map view (Figure 4-11).

The Late Cretaceous period first Sag thicknesses vary from 0 to 1000 m and change mostly gradually over tens of kilometers (Figure 4-8D); sudden changes can be related to the occurrence of faults. The south boundary fault (F1) is characterized by strong differences in thicknesses during this phase. The stratigraphic thickening in the southern part was produced by fault movement during the deposition (syn-deposition). Certain segments of the south boundary fault (F1) were active during this episode (Figure 4-8B). One depocenter was developed during this phase (Figure 4-8D), controlled by F1-A segment of the south boundary fault (Figure 4-8D).

4.3.2.3 Third rift cycle

The third rift cycle in Sufyan Sub-basin is associated with an extension of about 0.9% (Figure 4-6, Figure 4-11, Figure 4-12) in the western part and about 0.7% (Table 4-1;

Figure 4-7). In this cycle, many small faults are initiated and the preexisting faults were reactivated (Figure 4-11 e).

4.3.2.4 Faults Initiation and re-activation

The F1 southern boundary fault is the largest fault in the Sub-basin trending WNW-ESE. According to its movement, it can be divided into four segments (F1-A, F1-B, F1-C, and F1-D) (Figure 4-2). This fault was initiated during the first rift cycle (during the deposition of Abu Gabra Formation) and reactivated again during the deposition of all other formations.

The F3 northern boundary fault (trending WNW- ESE) and the F2 northwestern boundary fault (trending of NE-SW) (Figure 4-2) were initiated during the first rift cycle and reactivated during the deposition of all other formations.

F4, F5, F6, F7, and F8; are transtensional (oblique) faults (en-echelon pattern in the maps) (Figure 4-2) trending NW-SE located in the area between F1 and F3. These faults were initiated during the first rift cycle and reactivated again during the deposition of all other formations.

4.4 Sufyan Sub-basin forming mechanism

One of the greatest structural challenges in the interpretation of rifts is defining whether the rift system developed under strike-slip stress regime or an oblique extensional regime (Morley et al., 2004).

The activation of rift obliquely to basement lineaments yield geometries fairly similar to those formed during strike-slip movement (especially, transtensional) (Morley et al., 2004).

By analysis of regional context from the satellite Bouguer gravity data (Figure 4-1), five 2D seismic lines (Figure 4-6), four isopach maps (Figure 4-8), structural maps interpreted from 2D seismic data (Figure 4-11), and two kinematic models we determine that the both oblique rifting and strike-slip (transtensional) movements have played significant roles in Sufyan Sub-basin evolution history.

4.4.1 Model of transtensional movement

The regional relationship and fault systems orientation indicated that the possible origin of Sufyan Sub-basin is a pull-apart that resulted from a dextral oblique shear movement of the CASZ. The Sub-basin origin is possibly transtensional movement rather than pure strike-slip movement. This suggestion is based on the following observations and characteristics:

- The general trend of Sufyan Sub-basin that is similar to Baggara basin in Sudan and other basins in eastern Chad (Bongor, Doseo and Dobo Basins) located in the Central African Shear Zone (CASZ).
- Close similarities between Sufyan Sub-basin in Sudan and Doseo Basin in Chad are also shown in the seismic sections and structural maps. There are high similarities between the two basins in terms of basin direction and internal structure.
- In the southern part of Sufyan Sub-basin, flower structures (associated with a pull-apart structure) are associated with southern strike-slip fault segments (F1-B and F1-D) (Figure 4-4 and Figure 4-5D). Flower structures are limited at the area of large fault orientation changes (bending) (F1-B and F1-D) contrasting the major faults' lateral movement. The flower structures are a result of the major southern fault segment's

collapse. Flower structures were also documented in the WCARS by Genik (1993); Guiraud et al. (2005); Guiraud and Bosworth (1997).

- Structural maps and restoration indicated that Sufyan Sub-basin evolved from a narrow graben to a wider rhombic Sub-basin due to oblique slip faults (Figure 4-11). This characteristic is a very notable issue in pull-apart basin structures (Dooley and McClay, 1997).
- Scaled analog sandbox models have demonstrated usefulness for simulating the evolution of the pull-apart basins (Figure 4-13A) (Wu et al., 2009). Sufyan Sub-basin shows similarity with the pull-apart sandbox model in terms of geometry and vertical sections.
- Sufyan sub-basin could be separated to two pull apart basins, typically with a sigmoidal to rhombohedral shapes (Figure 4-14A and B).
- Fairhead et al. (2013) indicated that such geometry is possibly due to the poly-phase development of the basin where each phase is exposed to different amounts of transtension (Wu et al., 2009). The evolution history of Sufyan Sub-basin determined from the structural restoration proved that it is a multi-rift development with different amounts of transtension during each phase.

Branches of CASZ interpreted from the Bouguer gravity data extended to northern part of Muglad Basin. Two of the CASZ branched and possibly affected the northwest strike-slip fault (F2) and the strike-slip segments (F1-B and F1-D) of the southern boundary faults (Figure 4-1).

4.4.2 Model of oblique extension and transtension

Sufyan Sub-basin experienced multi-phase subsidence from the Cretaceous to recent time in response to the change of regional crustal stress. At least three basin-forming mechanisms were combined to form the sub-basin.

The widespread distribution of the first phase was characterized by the early stage of rifting and a late stage of thermal contracted sagging (Genik, 1993). During this phase, combined strike-slip movement along CASZ and normal extension mechanism (regional crustal stretching) along Muglad Basin occurred.

The south boundary fault (F-1) sense of movement (N-S extension) (Figure 4-14C) during the Early Cretaceous period first rift phase (Figure 4-8A) and the two depocenters (Figure 4-8A) controlled by the south boundary fault, support the interpretation that formed by pure extension.

The sense of movement (NE-SW extension) (Figure 4-8B) of the south boundary fault (F-1) during the Early Cretaceous period first sag phase (Figure 4-8B) and the one depocenter controlled by F1-A, support the interpretation that F1 formed by oblique extension and this interpretation is compatible with the oblique restricted bend model proposed by Morley (1995) (Figure 4-13B and C).

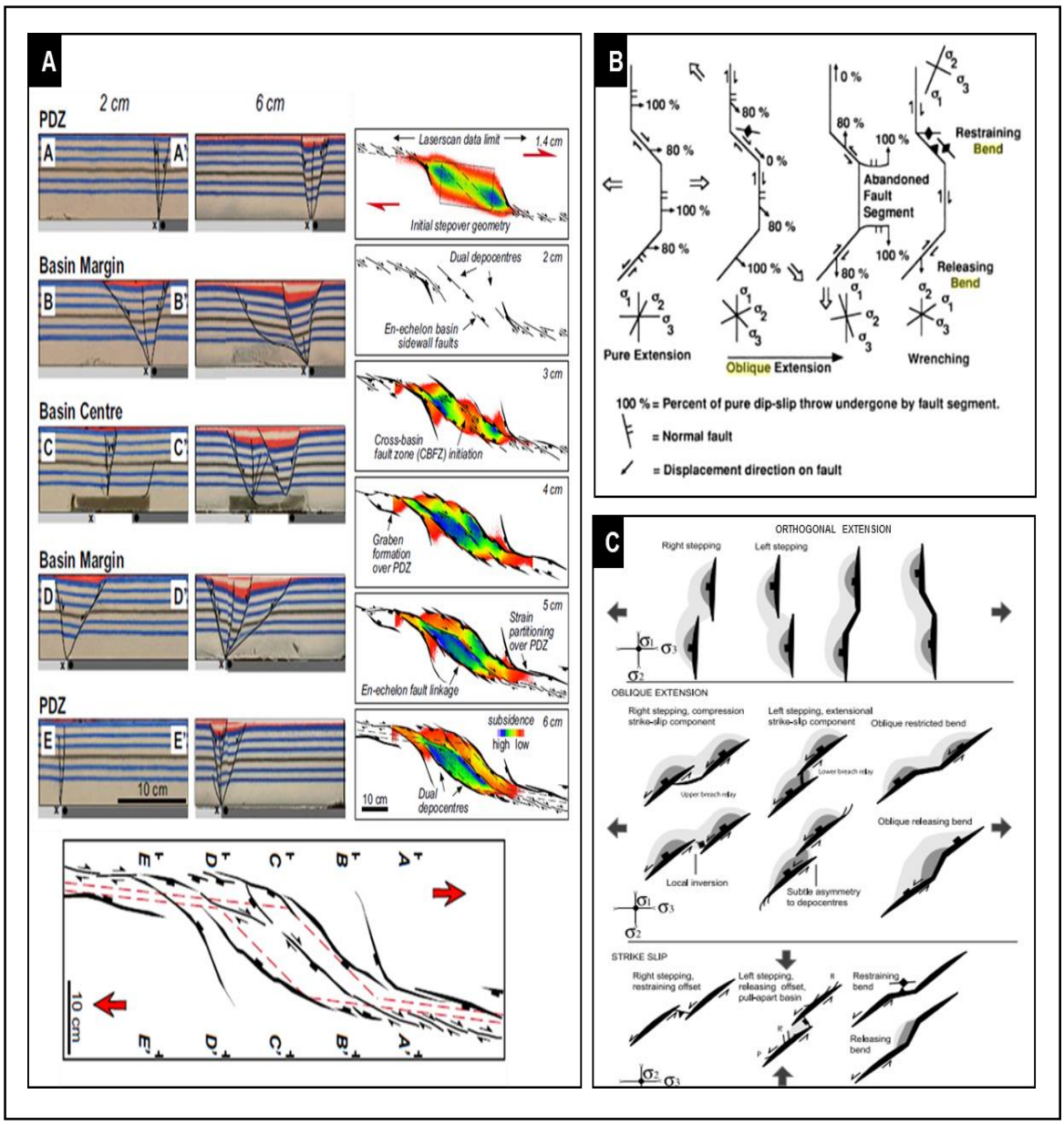

Figure 4-13: Analogue modeling (A) 4D evolution of a pull-apart basin in transtension including vertical sections, faults development during the subsidence, and fault map showing section locations (Wu et al., 2009). (B) Examples, of how faults change their sense of motion and subsidence rates as a result of changing the extension direction or changing to pure strike-slip (Morley, 1995). (C) Fault geometries developed under extension, oblique slip and strike-slip with their related depocenters (Morley et al., 2004).

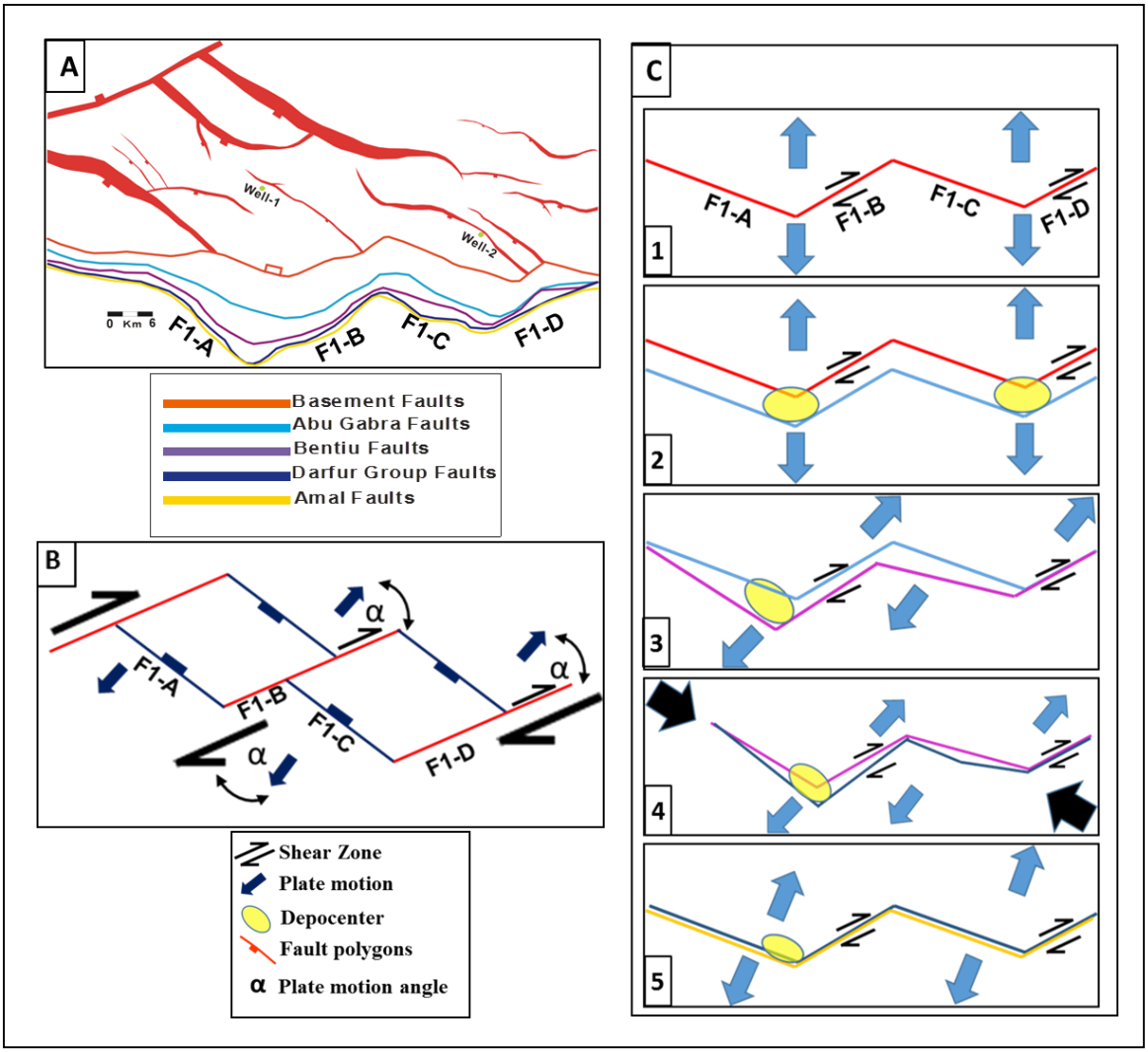

Figure 4-14: Different models that can explain the structural evolution of Sufyan Sub-basin. (A) The fault polygon maps of top Basement, Abu Gabra Formation, Bentiu Formation, Darfur Group, and Amal Formation overlapped together to show the change of the Sub-basin geometry with time (temporal evolution) as a result of the oblique extension and transtension movement. (B) A conceptual model for the dextral pull-apart systems in the study area. Sufyan Sub-basin is a pull-apart basin affected by both CASZ (transtensional movement) and Muglad Basin (extension). Sufyan sub-basin could be separated to two pull apart basins with a sigmoidal to rhombohedral shapes (C) Different models that can explain the zigzag plan view geometry of the south boundary fault (F1) which evolve during multiphase rifting.

The sense of movement of the south boundary fault (F-1) (NE-SW extension, as a result of NW-SE crustal compression) (Figure 4-8C) during the Late Cretaceous period second rift phase, the bend in F1-C (Figure 4-14C), and the one depocenter controlled by F1-A, support the interpretation that F1 formed by strike-slip movement (transtension) and it is compatible with the wrenching restraining bend model proposed by Morley (1995) (Figure 4-13B and C). The sense of movement (NE-SW extension) of the south boundary fault (F-1) (Figure 4-14B) during the Late Cretaceous period second sag phase and the limited depocenter controlled by F1-A, support the interpretation that it form by oblique extension.

Most of the E-W trending Mesozoic rift basins ended formation during the Middle Eocene, except for the NW-SE-trending Tenere and Sudanese rifts (McHargue et al., 1992). The third rift cycle is very limited in Sufyan Sub-basin.

Although Sufyan Sub-basin is part of Muglad Basin (Figure 4-1), the sub-bain has E-W trend and shows similarities with the ENE-WSW groups of basins in the WCARS such as Baggara Basin (Figure 4-1). Sufyan Sub-basin shows unique evolution history due to its location within the CASZ (E-W to ENE-WSW orientations) in relation to the tectonic events. The Central African Shear Zone (CASZ) was a reactivated fault zone inherited from the Pan-African orogeny. The regional stress regimes were mainly N-S and NE-SW, which reactivated the basement lineaments of the CASZ obliquely.

We conclude that Sufyan Sub-basin is a dextral pull-apart basin affected by both CASZ (transtensional) and Muglad Basin (extension) (Figure 4-14).

4.5 Implication on Hydrocarbon Exploration

Pull-apart basins have the appearance of asymmetric graben or half-graben structure, with similarities to oblique-extensional structures in rift basins (Dooley and McClay, 1997). Hydrocarbon structural traps in pull-apart basins are similar to those in extensional basins, but with more complex structure and smaller size. In a pull-apart basin, we expect to have many soft-linked structures (relay ramps) (Dooley and McClay, 1997). Source rock for this hydrocarbon is believed to be the lacustrine shale of the Abu Gabra Formation. The sandstone rock within Abu Gabra Formation represents the primary reservoir.

Based on the drilling data and geochemistry studies of well-1 and well-2 (Figure 4-2), the upper part of Middle Abu Gabra Formation is the main source rock in Sufyan Sub-basin. The strong structural activity controlled the petroleum migration, accumulation, and preservation. The main oil supply was from Abu Gabra Formation source rock, specially the two depocenters in the western and eastern segments of the south boundary fault (Figure 4-8A). Vertical migration along the faults was dominant while lateral migration distance was limited and is mainly adjusted within blocks. A lot of secondary faults were developed in the Tertiary period.

Faulting has been fairly active since the Tertiary period and caused oil and gas escaping. Compared with other parts of the Muglad Basin, Sufyan Sub-basin is faulted much stronger since the third period of fault-depression with significant activities and a long time of faulting and occurrence of much more new small faults. Most of these new faults are placed in the center of the Sufyan Sub-basin, especially at the eastern part of the middle segment and western part of the east segment of the south boundary fault (F1) (Figure 4-11D).

The inversion tectonic affected Sufyan Sub-basin during the second and third rift cycles. This is clear from the transtensional movement of the south boundary fault (F1). Figure 4-5E shows anticline developed by the transtensional movement of F1 during the second rift cycle, the anticline shows erosional features.

The lateral movement of the southern boundary fault (F1) (Figure 4-2) released the compressional stress during the late Santonian period and hence no big four-way dip closure traps developed. The area favorable for hydrocarbon accumulation is the middle structural zone, northwest, and northeast of the middle depocenters. Types of structural traps in Sufyan Sub-basin are faulted anticline, tilted fault blocks, and faulted nose structure in the middle zone which was developed during the first and second rift cycles. The middle structural zone formed during the Early Cretaceous period and distributed in a favorable path for hydrocarbon migration.

The highly prospective areas identified in Sufyan Sub-basin based on this study are:

- The areas of flower structures (but these are relatively small prospects).
- The areas that are near the two depocenters that are controlled by F1-B and F1-D segments of the southern boundary fault (F1), in between the major transtensional (oblique) faults (Figure 4-2).

CHAPTER 5

DEPOSITIONAL SYSTEMS, SEQUENCE STRATIGRAPHIC PATTERN, AND THEIR CONTROLS

5.1 Introduction

Sequence stratigraphy has been extensively applied in basin studies within the perspective of passive margin settings, where accommodation may be mainly due to the sea level fluctuations (Posamentier and Allen, 1993; Vail et al., 1977). During the last two decades, sequence stratigraphy has been developed rapidly (Catuneanu et al., 2011; Weimer and Posamentier, 1993). Conventional sequence stratigraphy has been developed mainly for passive-margin basins, which are relatively stable in term of tectonic activity and the accommodation space is mainly depend on the sea level changes (Alejandro, E., Paul, 2006; Douglas, 1995; Galloway, W.E., 1989; Van Wagoner et al., 1990; Weimer and Posamentier, 1993; Emery and K.J. Myers, 1996; Posamentier and Allen, 1993; Catuneanu, 2006, 2002, Catuneanu et al., 2011, 2009, 2005). Tectonic history, structural evolution and prevailing climate of rift basins are the main factors that control the stratigraphy and facies pattern (Prosser, 1993; Williams, 1993). In continental basins, tectonic movements are of extreme importance for the sequence boundaries formation and the sediments characters of sequences (Martins-Neto and Catuneanu, 2010; Schlische and Olsen, 1990). Tectonic create accommodation space; structure evolution modifies this accommodation space, and the prevailing climate determines whether this accommodation

space can be filled by water or sediments (Prosser, 1993). During the evolution history of the rift basin, tectonic including the rift cycles and different subsidence rate play a significant role in controlling the accommodation space and depositional systems. (Leeder and Gawthorpe, 1987; Shanley and McCabe, 1994; Ravnås et al., 2000; Lin et al., 2001). The changing of the sequence stratigraphic model with the tectonic setting yet not completely understood and suitable model for rift basins still not fully developed (Martins-Neto and Catuneanu, 2010). The tectono-sequence stratigraphic analysis has become a main international theme for petroleum system and basin analysis (Gawthorpe and Leeder, 2000; Hou et al., 2012; Wu et al., 2015; Zhou et al., 2014). Understanding of physiography and stratigraphy of the rift basins has pointed that most of the rift basins consist mainly of three tectonostratigraphic phases (Prosser, 1993). These are (1) rift initiation; (2) rift climax; and post-rifting (Prosser, 1993). Each of these phases has distinct stratigraphic and sedimentologic characteristics depending on the regional and local structural controls. Sediments which deposited in the syn-rift phase are highly affected by the tectonic pulses and structural evolution (Prosser, 1993).

The Sufyan Sub-basin is located in the northwestern part of Muglad Basin and trending E-W. Muglad Basin is the largest sedimentary basin in Sudan with a total area of about 160,000 km^2 (with a width of about 200 km and a length of about 800 km).

According to previous studies in Muglad basin and Sufyan Sub-basin (Mann, 1989; McHargue et al., 1992; Wu et al., 2015; Yassin et al., 2016), the tectonic settings are very complex in Sufyan Sub-basin.

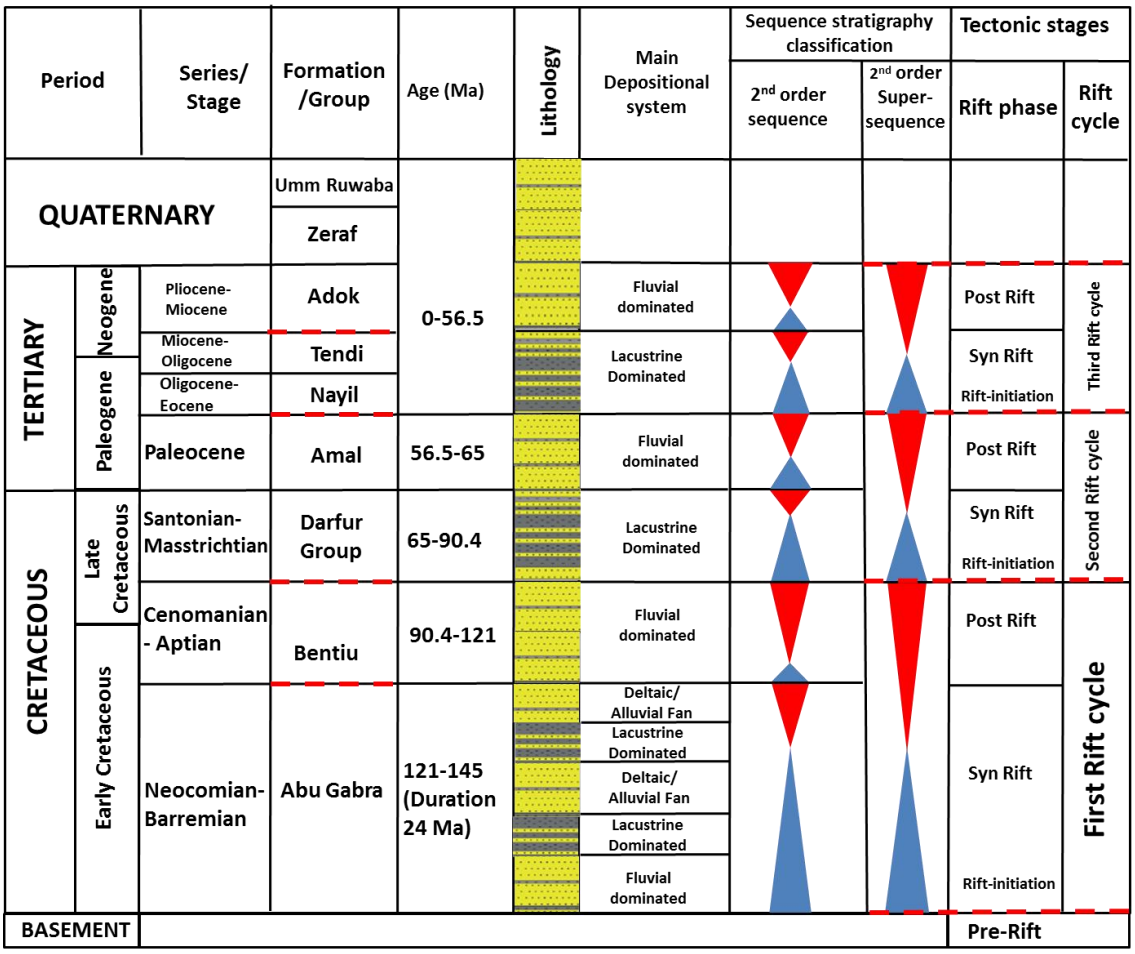

Figure 5-1: Stratigraphic and tectonic events charts for the Muglad Basin, Sudan, modified after (Fairhead et al., 2013; Guiraud and Bosworth, 1997; Lirong et al., 2013; McHargue et al., 1992; Mohamed et al., 2001; Schull, 1988).

Three syn-rift and post-rift cycles were influenced Muglad basin and its related sub-basins (Figure 5-1) (McHargue et al., 1992), hence tectonics played a significant role in controlling the depositional systems and sequences.

This chapter discusses the tectonic evolution and its controls on the depositional systems, and sequence stratigraphy of Sufyan Sub-basin for better hydrocarbon exploration and development.

5.1.1 Sufyan Sub-basin

Sufyan Sub-basin is an independent structural unit in the Muglad Basin. It is 70 km long and 40 Km wide with a total area of about 2800 km^2. Sufyan Sub-basin exploration results have shown the occurrence of accumulations of hydrocarbon.

In Sufyan Sub-basin, three rift cycles are recognized and dated as Early, Late Cretaceous, and Paleogene age (Figure 5-1). Each tectonic cycle seems to contain rift-initiation phase, active rifting phase, and thermal sag phase (McHargue et al., 1992). Every tectonic cycle is represented by a basal sandstone unit, followed by a coarsening upward cycle (grading from lacustrine shale to marginal lacustrine mudstone and sandstone into fluvial mudstone and sandstone, and being covered by alluvial and fluvial sandstone).

During the first rift phase (high subsidence rate), Abu Gabra Formation was formed (Figure 5-2B). Based on seismic and well data, Abu Gabra Formation divided into five 3^{rd} order sequences (SQ-A, SQ-B, SQ-C, SQ-D, and SQ-E) from bottom to top, representing five tectonostratigraphic stages (Figure 5-3).

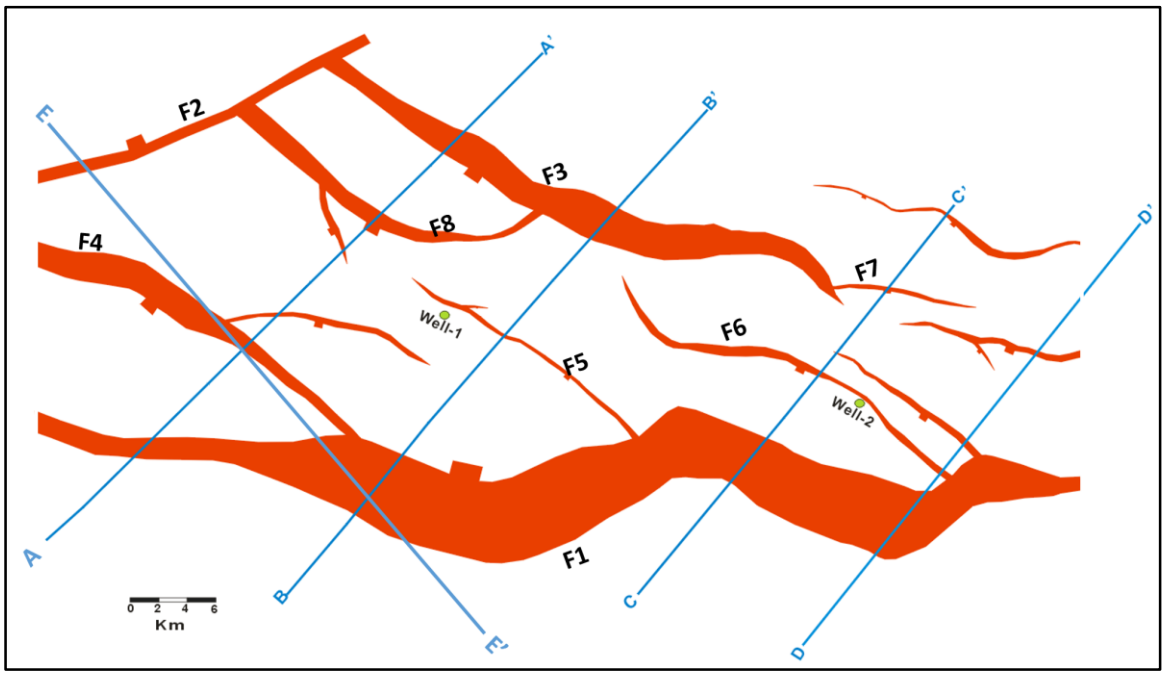

Figure 5-2: Structural map of top Basement, interpreted from 2D seismic data shows faults (boundary faults F1, F2, and F3) (major faults F4, F5, F6, F7, and F8), location of wells (Well-1 and Well-2) and regional seismic lines (AA', BB', CC', DD', and EE'). F2 represented as a part of the CASZ (A).

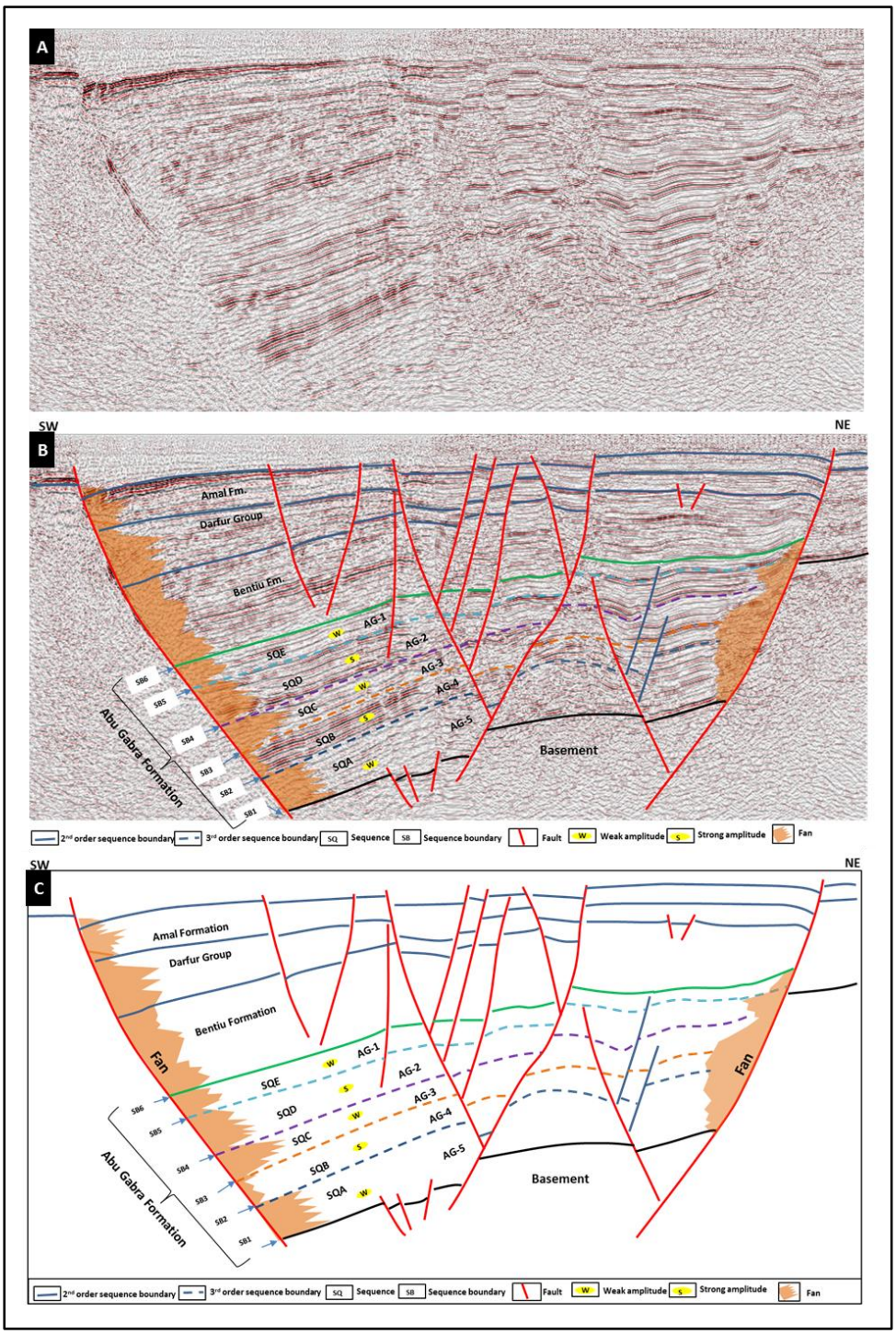

Figure 5-3: The seismic profile BB' and its interpretation (see location in Figure 5-2). (A) The seismic profile BB' without interpretation. (B) The seismic profile BB' with its interpretation. (C) Interpretation of the above seismic profile.

5.2 Subsurface facies analysis from conventional core

Based on core description, seven lithofacies were identified in Abu Gabra Formation (Table 5-1; Figure 5-4). It is mainly composed of continental-derived clastics. These include bedded conglomeratic sandstone, planar cross-bedded sandstone, trough cross-bedding sandstone, massive sandstone, ripples cross-laminated sandstone, massive to blocky mudstone and siltstone, and mudstone and shale.

Lf1: Conglomeratic sandstone

Description

This lithofacies consist of conglomeratic sandstone with pebbly sand and fine to coarse sandstone. Subangular to subrounded clast were identified, sorting is poor.

Interpretation

The moderate to poor sorting suggests short transportation distances. These elements attributed to distributary channel deposits in the fan delta.

Lf2: Planar cross-bedded sandstone

Description

This lithofacies consist of fine, very coarse to pebbly sandstone. It describes as a light grey planar cross-bedded sandstone facies, with medium grain size. The grains are varying from rounded to sub-rounded with moderately to well sorting.

Table 5-1: Lithofacies in Abu Gabra Formation interpreting using conventional cores

Code	Lithofacies	Lithology	Sedimentary structures/Description	Interpretation
Lf1	conglomeratic sandstone	Conglomerate, pebbly Sand, fine to very coarse sandstone	Planar cross-beds	Distributary channel deposits primary in fan delta front or braided delta plain.
Lf2	Planar cross-bedded sandstone	Fine, very coarse to pebbly sandstone	Light gray planar cross-bedded sandstone facies, with medium grain size. The grains are vary from rounded to sub-rounded with moderately to well sorting.	Transverse and linguoid bedforms (2-D dunes) in a fluvial channel (braided channel or pint bar) or distributary channels deposited mainly in braided delta plain as well in crevasse splays.
Lf3	Trough cross-bedded sandstone	Fine, very coarse to pebbly sandstone	Light and gray trough cross-bedded sandstone facies, with fine grain size. The grains are rounded to sub-rounded with poor sorting.	Sinuous-crested and linguoid (3-D Dunes). Migrating 3-D dunes in a braided channel bar. Dunes (fluvial channel or delta distributary channel or delta mouth bar).
Lf4	Massive sandstone	Very fine to coarse sandstone	Massive or faint lamination. Light grey massive sandstone facies, with fine to coarse grain size. The grains are rounded to sub-rounded with moderately sorting.	Underwater distributary channels deposits primary in braided delta.
Lf5	Ripples cross-laminated sandstone	Very fine to coarse sandstone	Light gray ripples laminated sandstone facies, with very fine grain size. The grains varies from rounded to sub-rounded with moderately sorting with flaser bedding.	Ripples (top fluvial bar or delta mouth bar or floodplain or levee or crevasse splay distal bar)
Lf6	Massive to blocky mudstone and siltstone	Mudstone and siltstone	Massive, desiccation cracks. Dark grey moderately laminated to massive mudstone with some root casts.	Overbank or flood deposits or prodelta deposits or interdistributary bay.
Lf7	Mudstone, shale, and siltstone	Mudstone, shale, very fine sandstone, and siltstone	Black shale, dark gray to greenish gray mudstone, and horizontally laminated bedding siltstone and very fine sandstone.	Prodelta or lacustrine deposits

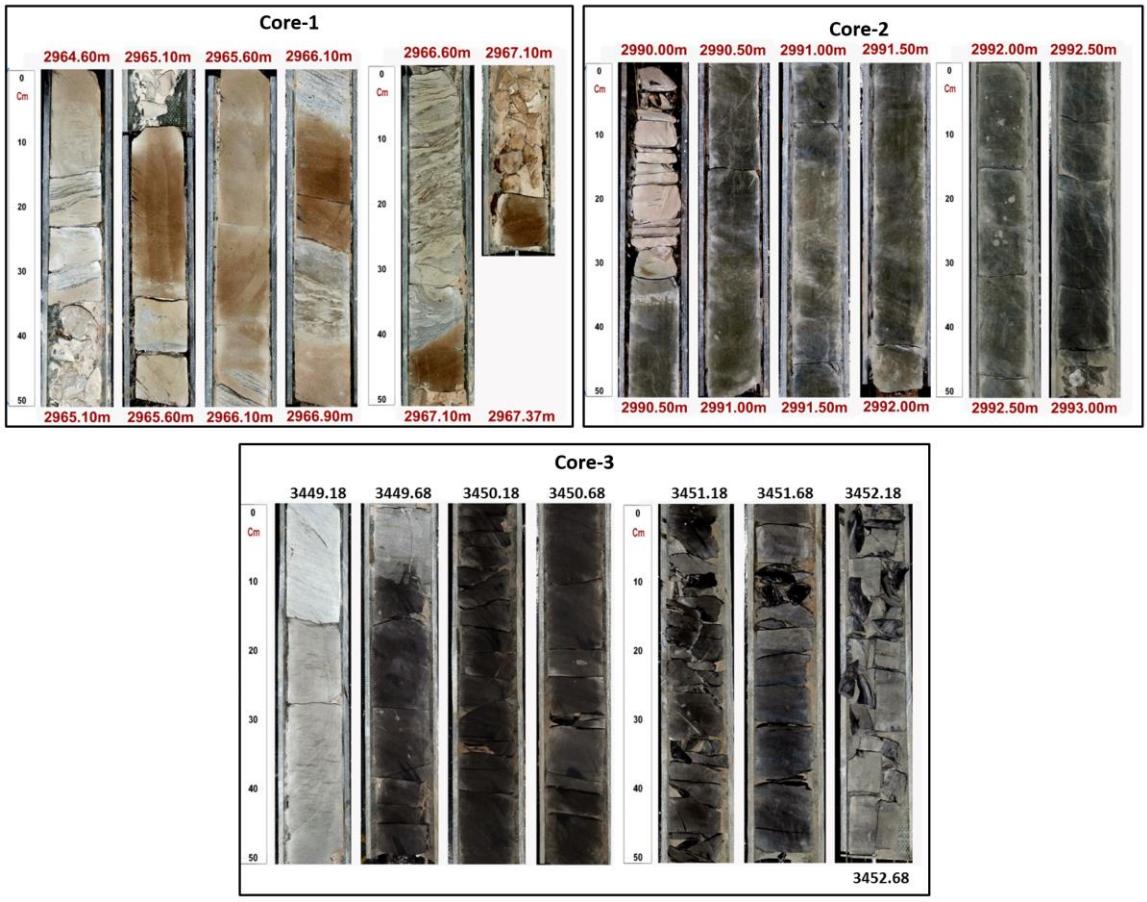

Figure 5-4: Core photos of representative facies. Showing lithofacies 1, 2, 3, 4, and 7

Interpretation

The planar cross-bedded sandstone facies is indicating for braided distributary channel deposits. The coarse-to-medium grained sandstone deposits indicated a fluvial system.

Lf3: Trough cross-bedded sandstone

Description

This lithofacies consist of fine, very coarse to pebbly sandstone. It describes as a light and grey with fine grain size sandstone. The grains are rounded to sub-rounded with poor sorting.

Interpretation

The coarse-to-medium grained sandstone deposits indicated a fluvial system. The trough cross-bedded sandstone represents a meandering channel and point bar deposits. It could be interpreted as a fluvial channel or delta distributary channel or delta mouth bar.

Lf4: Massive sandstone

Description

This lithofacies consist of very fine to coarse sandstone. Massive or faint lamination. It describes as a light grey massive sandstone facies, with fine to coarse grain size. The grains are rounded to sub-rounded with moderately sorting.

Interpretation

The well sorted fine-grained sandstone suggests long transportation distances with high energy current. It could be interpreted as underwater distributary channels deposits in the braided delta.

Lf5: Ripples cross-laminated sandstone

Description

This lithofacies consist of very fine to coarse sand. It describes as light grey ripples laminated sandstone facies, with very fine grain size. The grains vary from rounded to sub-rounded with moderately sorting with flaser bedding. Usually, they occupy the top part of coarser and sandy facies with an overall fining-up vertical trend.

Interpretation

Interbedded sandstone and siltstone relatively indicating for low current energy. It usually overlies the coarse-grained sandstone facies on top of the fining-up sequence. The lithofacies of this group could be interpreted as a top fluvial bar or delta mouth bar or floodplain or levee or distal bar.

Lf6: Massive to blocky mudstone and siltstone

Description

This lithofacies consist of mudstone and siltstone. It describes as a massive mudstone with desiccation cracks to blocky mudstone and siltstone. The mudstone is mainly dark grey moderately laminated to massive with some root casts.

Interpretation

This lithofacies are mainly deposited in overbank or floodplain in the fluvial system. The siltstone, claystone lithofacies may indicate a prodelta to shallow lacustrine deposits or interdistributary bay.

Lf7: Mudstone and shale

Description

This lithofacies consists of mudstone, shale, very fine sandstone, and siltstone (Figure 5-5). It describes as black shale, dark grey to greenish-grey mudstone, and horizontally laminated bedding siltstone and very fine sandstone.

Interpretation

The very fine lithofacies deposits indicate that it is mainly deposited in Prodelta, semi-deep to deep lacustrine. This facies represents the low energy deposits.

5.3 Depositional systems

Four types of the depositional system were recognized in Sufyan Sub-basin based on the interpretation of seismic, core, and well log data. Those depositional systems are fan delta, braided delta, lacustrine system, and sublacustrine fans. No wells penetrated the deepest strata in the Sub-basin; those deposits were interpreted using seismic facies and analogs from nearby Sub-basins. The published sedimentary models of continental rift basins, suggests that alluvial fans and fluvial deposits existing in some deeper parts representing the rift initiation phase (Gawthorpe and Leeder, 2000; Prosser, 1993; Wu et al., 2015).

Formation	Depositional system	Sub-environment	Microfacies	Abbreviation	Gamma ray geometry		
					Curve Shape	Lithofacies	Curve Samples
Abu Gabra	Braided Delta	Fluvial dominated delta plain **(LfA-7)**	Floodplain	FP	Linear shaped	Lf6, Lf5	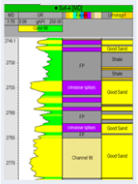
			Crevasse splays	CS	Funnel shaped	Lf6, Lf4, Lf2, Lf5	
			Channel fill	CF	Box or bell shaped	Lf6, Lf2, Lf3, Lf5	
		Delta plain **(LfA-6)**	Distributary channel	DC	Box or bell shaped	Lf2, Lf3, Lf6	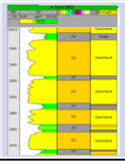

Formation	Depositional system	Sub-environment	Microfacies	Abbreviation	Gamma ray geometry		
					Curve Shape	Lithofacies	Curve Samples
Abu Gabra	Braided Delta	Proximal delta Front **(LfA-5)**	Underwater Distributary Channel	UW DC	Box or bell shaped	Lf3, Lf4, Lf6	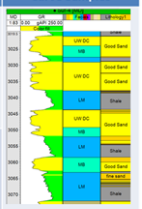
			Mouth Bar	MB	Funnel shaped	Lf5, Lf3	
		Distal delta Front **(LfA-4)**	Interdistributary Bay	IDB	Linear shaped	Lf5, Lf6	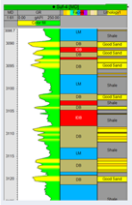
			Distal Bar	DB	Funnel shaped	Lf7, Lf5, Lf4	

Formation	Depositional system	Sub-environment	Microfacies	Abbreviation	Gamma ray geometry		
					Curve Shape	Lithofacies	Curve Samples
Abu Gabra	Lacustrine/ Prodelta	Prodelta/ Shallow Lacustrine **(LfA-3)**	Sheet Sand	SS	Interfinger	Lf5, Lf6, Lf4	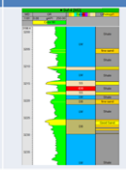
		Sub-lacustrine fan **(LFA-2)**	Sub-lacustrine distributary channel	SLDC	bell shaped	Lf3, Lf4, Lf6	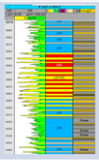
		Semi-Deep lacustrine **(LfA-1)**	Lacustrine mudstone	LM	Linear shaped	Lf7	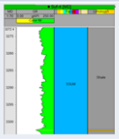

Figure 5-5: Showing different depositional systems in Abu Gabra Formation interpreted using core and well log data. Sub-environment, microfacies, lithofacies and gamma ray geometry are described in detail.

Gamma ray log motives of different sedimentary facies were captured according to their electric properties, which were identified by the shape of log curves, amplitude, and connect relation (Figure 5-5). Log motives from wireline logs were calibrated with core and mud log data. The purpose of this analysis is to study the sediments vertical change of succession, rhythm, the energy of the deposition, and corresponding sedimentary facies of a particular environment or sub-environment based on logging curve combination attributes.

In the study area, two types of deltas were found, namely fan deltas and braided deltas (Figure 5-6). Fan deltas are conglomeratic dominated deltas developed where the fan is deposited immediately into the water from the nearby lands (Dunne et al., 1988; McPherson et al., 1987). Usually, fan delta located on the hanging wall side of the basin boundary fault (antithetic fault) in the steep scarp slope. Braided deltas are coarse grained rich deltas (Dunne et al., 1988; McPherson et al., 1987). Usually, braided delta deposited in the gentle slope such as the ramp slope side of the antithetic faults. Fan deltas and braided deltas can be distinguishing in the subaerial components of this depositional system; the subaqueous components of both are similar (Dunne et al., 1988; McPherson et al., 1987).

5.3.1 Fan-delta

Fan-delta deposits are mostly linked with the steep slope of the southern boundary fault in the Sufyan Sub-basin. The aerial extent of fan delta deposits is small when correlating it with the braided delta.

On the seismic, wedge-shaped is recognized close to the steep fault slope and it’s the major characteristic of the fan delta front deposits (Figure 5-3). The fan delta deposited in the

margin of southern boundary fault and shows oblique progradation, medium amplitude, medium continuity, and low frequency of seismic reflection configurations which represent fan delta. Chaotic reflection configurations are discontinuous, discordant reflections suggesting a disordered arrangement of reflection surfaces. They are interpreted either as strata deposited in a variable, relatively high-energy setting, which indicate the sedimentary is slope fan.

The grain size of the fan delta (conglomeratic sandstone) generally coarser than the braided delta grains (Table 5-1).

In Sufyan Sub-basin, fan delta show vertical progradation cycles, start from shallow lacustrine mudstone and shale (Lf7) (Figure 5-5) to delta front (Figure 5-6), fine-to-medium-grained sandstone (Lf3, Lf4, Lf5, and Lf6) to delta plain (Figure 5-6), coarse-grained trough cross-bedded sandstone (Lf2) and conglomerate (Lf1).

Prodelta deposits (Figure 5-6) are mainly consists of mudstone (Lf7) interbedded with sheet sand (Lf6 and Lf7) and it is difficult to be distinguished from lacustrine deposits.

The underwater part of the fan delta (fan delta front) is consists of sub-environments such as:

- Underwater distributary channel deposits (Figure 5-6) that contain Lf4, Lf3, and Lf6.
- Inter-distributary bays deposits (Figure 5-6) that mainly composed of Lf6.
- Mouth bar deposits that contain Lf5 and Lf3. On the gamma ray logs, mouth bar deposits show funnel-shaped (coarsening upward).

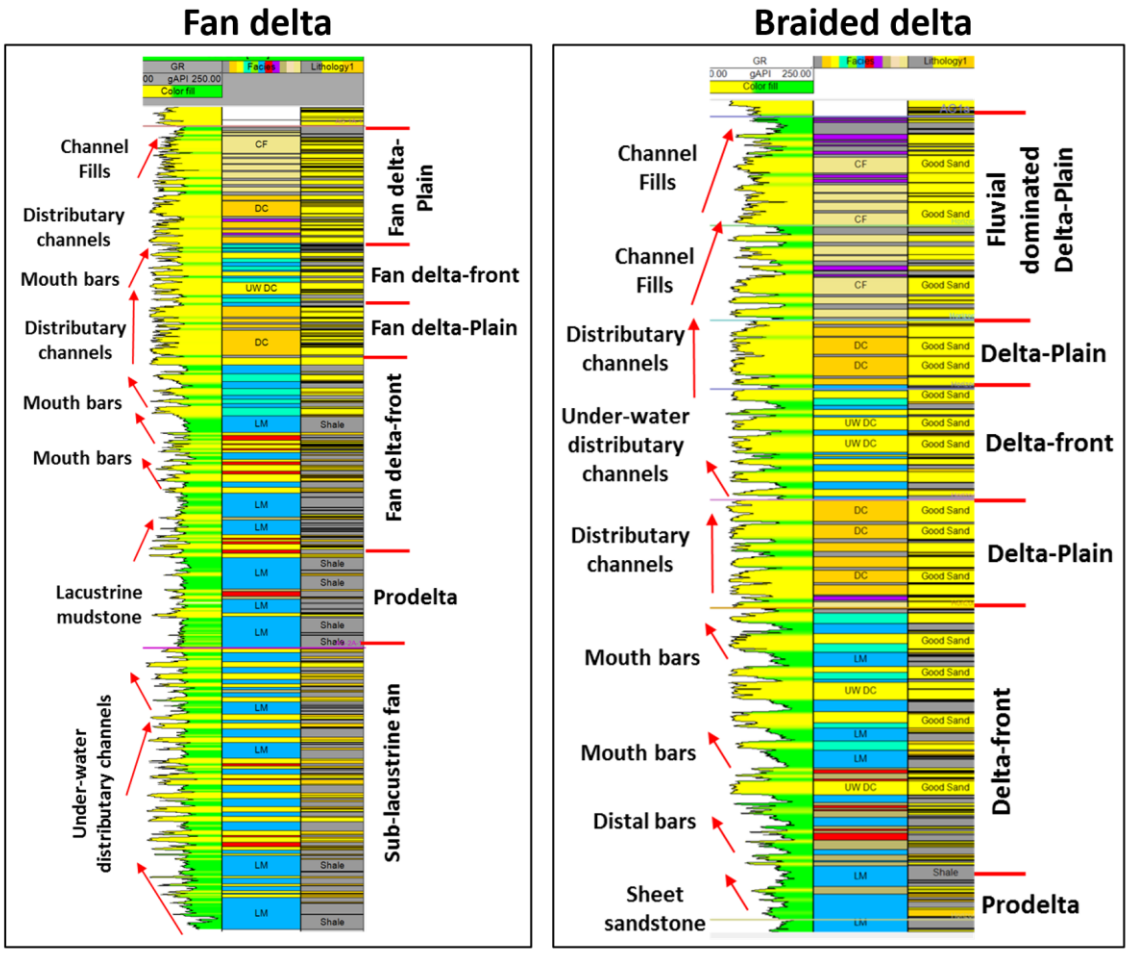

Figure 5-6: Vertical successions of fan-delta (left) and braided delta (right). Deposited in Sufyan Sub-basin. Well log is the gamma ray (GR). The yellow color is sandstone dominated and green is mudstone dominated.

5.3.2 Braided delta

Braided delta deposits in Sufyan Sub-basin are developed mainly on the ramp slope side of the southern boundary fault. By combining the core data and logging curve, two, four, and one micro-facies were identified in the delta plain (Figure 5-6), delta front (Figure 5-6), and prodelta (Figure 5-6) respectively. Braided delta show sub-parallel external forms in seismic sections. The reflection configurations of the braided delta in seismic are characterized by medium amplitude, medium continuity, and high frequency.

5.3.2.1 Fluvial dominated delta plain

Fluvial facies association represent about 20% in the studied succession. It comprises three sedimentary facies associations (architecture elements); each one is characterized by its sedimentary features and specific depositional setting.

Channel fills

Consists of light grey, medium to coarse-grained, unconsolidated to poorly consolidated, sub-rounded to sub-angular sandstones. Fluvial channel fills is dominant in the uppermost part of Abu Gabra Formation and consists of are planar (Lf2) to trough (Lf3) cross-bedded sandstone overlain by the ripples cross-laminated sandstone (Lf5) and underlain by the massive to blocky mudstone and siltstone (Lf6) (Figure 5-5).

Argillaceous matrix and clay cement are common. The sandstone bodies range in thickness between 2 and 10 m and are occasionally vertically stacked up to 25 m thick. The relatively coarse-grained sediments represent high energy and relatively high sediment supply exceeding the available accommodation space leading to high degree of amalgamation

(sheet-like deposits). The logging curve showed bell or box shape on the gamma-ray log (Figure 5-5). Sand thickness ranging from 3 to 10 m.

Floodplain fines

Comprises reddish brown, massive, parallel laminated, rooted mudstone and shale. It consists mainly by ripples cross-laminated sandstone (Lf5) and Massive to blocky mudstone and siltstone (Lf6) (Figure 5-5). They range in thickness between 2 and 15 m. These facies are dominant in the uppermost Abu Gabra Formation (Figs. 3 and 5). The high preservation of fine-grained material and upward-fining trend suggest increasing rates of base-level rise that eventually led to flooding of the area during humid climate (Miall, 1996). Increasing the base-level rise will increase the fine-grained sediments preservation upward of each story.

Crevasse splay

This lithofacies association contains Lf6, Lf4, Lf2, and Lf5 from bottom to top (Figure 5-5). The massive sandstone (Lf4) and the planar cross-bedded sandstone (Lf2) overlain by the massive to blocky mudstone and siltstone (Lf6) and underlain by ripples cross-laminated sandstone (Lf5). This lithofacies association is interpreted as Crevasse splay deposited in delta plain, showing funnel-shaped (coarsening upward) on the gamma-ray log (Figure 5-5).

This facies thickness usually varies from 2 to 5 m and its fine to very fine grained. The internal structure of crevasse splays is mixed, indicating their origin by numerous flood events, and fast sedimentation rates.

5.3.2.2 Delta Plain

From top to bottom, delta plain deposits are relatively thin (about 20 m) and composed of several distributary channels and floodplains (Figure 5-5). The distributary channels facies association consists of light grey sandstone facies, with medium grain size. The grains are varying from rounded to sub-rounded with moderately to well sorting. The sandstone bodies are trough to planar cross-bedded (Lf2, Lf3). The base is occasionally paved by coarse intraclasts and the top is dominated by Massive to blocky mudstone and siltstone (Lf6) (Table 5-1). The delta plain showing bell-shaped (fining upward) on the gamma-ray log (Figure 5-5). Sand sheets thickness ranging from 3 to 7 m.

5.3.2.3 Delta front

In Sufyan Sub-basin, delta front has developed and can be additional categorize four types of sedimentary sub-environments (Figure 5-5): interdistributary bays, mouth bars, underwater distributary channels, and distal bar.

Underwater distributary channels

The lithofacies of this sub-environment is medium to fine trough cross-bedding sandstones (Lf3) (scour surface) with fining-upward grains which changed into massive sandstone (Lf4) in the upper (Figure 5-5). The sandstone is mainly transparent to translucent, sub-rounded to rounded, moderately sorted. The top consisted of grey and dark grey mudstone of parallel bedding (Lf6). The log curve showed bell or box shape with obvious high variation (Figure 5-5). Sand body thickness ranging from 1 to 4 m.

Interdistributary bays

The lithofacies of this sun-environment is consists of massive mudstone with desiccation cracks to blocky mudstone and siltstone (Lf6) and ripples cross-laminated sandstone (Lf5) (Figure 5-5).

The mudstone is mainly dark grey moderately laminated to massive with some root casts. The log curve showed line shape and amplitude was flat with high GR and medium-low resistivity (Figure 5-5).

Mouth bars

This sub-environment consists of fine, very coarse to pebbly sandstone. It describes as a light and grey with fine grain size sandstone. The grains are rounded to sub-rounded with poor sorting (Lf3). This sub-environment also consists of ripples cross-laminated sandstone (Lf5) (Figure 5-5). It describes as a light grey ripples laminated sandstone facies, with very fine grain size. The grains vary from rounded to sub-rounded with moderately sorting with flaser bedding. Usually, Lf3 occupy the top part of finer lithofacies Lf5 with an overall coarsening-upward trend. The thinly interbedded, medium grained sandstones (Lf3), and the ripples cross-laminated sandstone (Lf5) are interpreted as mouth bar deposits, displaying funnel-shaped (fining upward) on the gamma-ray (Figure 5-5). Sand thickness ranging from 1 to 5 m.

Distal bar

This sub-environment contains Lf7, Lf5, and Lf4 from the bottom to top (Figure 5-5). This sub-environment contains ripples cross-laminated sandstone (Lf5). It consists of very fine

to coarse sand and describes as a light grey ripples laminated sandstone facies, with very fine grain size. The grains vary from rounded to sub-rounded with moderately sorting with flaser bedding. Lf5 underlain by the massive to blocky mudstone and siltstone (Lf6). This lithofacies consist of mudstone and siltstone. It describes as a massive mudstone with desiccation cracks to blocky mudstone and siltstone. The mudstone is mainly dark grey moderately laminated to massive with some root casts. The ripples cross-laminated sandstone and the massive to blocky mudstone and siltstone are interpreted as distal bar deposits, showing funnel-shaped (fining upward) on the gamma ray log. Sand thickness ranging from 0.5 to 1.5 m (Figure 5-5).

The zone of the distal bars and underwater distributary channels in seismic data are characterized by parallel high amplitude, good continuity, and medium frequency (Figure 5-5).

5.3.2.4 Prodelta

Sheet sand

This sub-environment contains Lf5, Lf6, and Lf4 from bottom to top (Figure 5-5). The massive to blocky mudstone and siltstone (Lf6) overlain by the massive sandstone (Lf4) and underlain by the ripples cross-laminated sandstone (Lf5). This lithofacies association is interpreted as sheet sand deposited in prodelta, showing interfinger shaped on a gamma-ray log (Figure 5-5). Sand sheets thickness ranging from 0.5 to 1.5 m.

5.3.3 Lacustrine system

This sub-environment contains mainly mudstone and shale (Lf7). This lithofacies consists of mudstone, shale (Figure 5-5). It describes as black shale, dark grey to greenish grey mudstone moderately hard, flaky, and occasionally blocky. The very fine lithofacies deposits indicate that it is mainly deposited in Prodelta, semi-deep to deep lacustrine. This facies represents the low energy deposits. The logging curve linear shaped on the gamma-ray log (High gamma ray) (Figure 5-5).

5.3.4 Sublacustrine fan

Sublacustrine fan deposits develop as a catastrophic event when suddenly injects sediment into the deep lake/sea floor (Kneller and Branney, 1995; Mulder and Syvitski, 1995).

The lithofacies of this sub-environment is medium to fine trough cross-bedding sandstones (Lf3) (scour surface) with fining-upward grains which changed into massive sandstone (Lf4) in the upper. The sandstone is mainly transparent to translucent, subrounded to angular, poorly sorted. The top consisted of grey and dark grey mudstone of parallel bedding (Lf6). The log curve showed bell or box shape with obvious high variation (Figure 5-5). The causes of formation of the Sublacustrine fan in Sufyan Sub-basin are mainly due to the progradation of the braided delta front or fan delta front to the deeper water, leading to the fine to coarse-grained sandstone that interbedded with thick deep lacustrine mudstone. The gamma ray logs change sharply and quickly showing interfingering shape (Figure 5-5). The thickness of sand bodies in the Sublacustrine fan deposits ranges from 3 to 5 m and they are dominantly distributed in the huge bedding of grey to black mudstone.

5.4 Sequence stratigraphy

First order sequence is a sequence that was deposited in about 200-400 million years (Catuneanu, 2006; Miall, 2013; Vail et al., 1977). Second order sequence is a sequence that was deposited in about 10-100 million years(Catuneanu, 2006; Miall, 2013; Vail et al., 1977). Third order sequence is a sequence that was deposited in about 1-10 million years (Catuneanu, 2006; Miall, 2013; Vail et al., 1977).

The tectono-sequence stratigraphic evolution history of rift basins can be divided into several scales: the large scale (rift cycles) and it is corresponding to 2nd order super-sequence, the intermediate scale (rift phases) and it is corresponding to 2nd order sequences, and the small scale (rift stages) and it is corresponding to the 3rd order sequences (Ravnås et al., 2000; Zhou et al., 2014). The intermediate scale of the tectono-sequence stratigraphic evolution history of rift basins as described by Prosser (1993) are subdivided into four phases: rift initiation, rift climax, immediate post-rift, and late post-rift. The time of maximum rate of displacement of a fault can be termed the rift climax (Prosser, 1993). The small scale (rift stage) is corresponding to the 3rd order sequences and it is composed of early syn-rift, rift climax, and late syn-rift described by Zhou et al (2014). These rift stages are comparable with Prosser (1993) rift phases. The early syn-rift stage is equivalent to the rift initiation phase, rift climax stage is equivalent to rift climax stage, and the late syn-rift is equivalent to of the immediate post-rift of Prosser (1993).

The large scale in Sufyan Sub-basin (rift cycles) is equivalent to 2nd order super-sequence and it is composed of three rift cycles (Figure 5-1).

The intermediate scale in Sufyan Sub-basin (rift phases) is corresponding to 2nd order sequence (Figure 5-1), each rift cycle consists of rift-initiation phase, syn-rift phase, and post-rift phase.

The small scale in Abu Gabra Formation is equivalent to 3rd order sequence and it is composed of five stages of basin evolution, which are early syn-rift/rift initiation stage, rift climax-1 stage, late syn-rift-1stage, rift climax-2 stage, and late syn-rift-2 stage (Figure 5-7).

5.4.1 Second order super-sequences

In Sufyan Sub-basin, three rift cycles are recognized and dated as Early Cretaceous (about 140-95 Ma), Late Cretaceous (95-65 Ma), and Paleogene (65-30 Ma) age. Each rift cycle seems to be 2nd order super-sequence (Figure 5-1) and each tectonic cycle consists of sediments that deposited during the rift-initiation phase, syn-rift phase, and post-rift phase and each one is corresponding to 2nd order sequence (Figure 5-1).

A basal sandstone unit, followed by a coarsening upward cycle (grading from lacustrine shale to fluvio-deltaic mudstone/sandstone and capped by fluvial sandstone), represents every tectonic cycle. The first depositional cycle penetrated only at the basin margins; hence, the geographic representation of this unit remains uncertain. On the contrary, the basal sand unit of the second depositional cycle (Upper Bentiu formation), and the third depositional cycle (Upper Amal formation) interfingers towards the axis of the rift with suspended-load fluvial and shaly lacustrine accumulations. This modality thought to be applicable for the sand unit of the first depositional cycle.

The main control in these sequences is tectonic activities that Associated with Africa and South America's separation. In Sufyan Sub-basin, Abu Gabra Formation deposited during the rift phase of the first rift cycle (Figure 5-1) and contains fluvial dominated basal sand in the deeper part (rift initiation) followed by the lacustrine shale, claystone, and sandstone (syn-rift). These lacustrine deposits overlain by the sandstone of Bentiu Formation deposited during the post-rift and consists mostly of stacked channel and bar deposits of braided and meandering streams. In this work, we will study the Abu Gabra Formation in detail.

5.4.2 Second order sequences

These sequences are at formations' scales and sequence boundaries were placed at the formations' tops. The main control on these types of sequences along with the tectonic is climate. The first sequence in Sufyan Sub-basin is the Abu Gabra Formation and it is mainly containing fluvial dominated basal sand in the deeper part (rift initiation) followed by the lacustrine shale, claystone, and sandstone of Abu Gabra Formation (syn-rift) (Figure 5-7). Abu Gabra Formation began in the Early Cretaceous Neocomian and ended in the Barremian with a duration time of 24 million years. Abu Gabra Formation deposited during the first syn-rift phase (the highest period of subsidence) (Figure 5-3) (Wu et al., 2015). In Sufyan Sub-basin, Abu Gabra Formation varying in faulting pulses and high/low subsidence (Yassin et al., 2016). It is categorized as a 2^{nd} order sequences with 24 Ma and consists of rift initiation and syn-rift phases. Based on analysis of tectonic evolution, biostratigraphy, seismic, well logs and core data, Abu Gabra Formation could be divided further into two sub-rift phases (syn-rift-1 and syn-rift-2) (Figure 5-7).

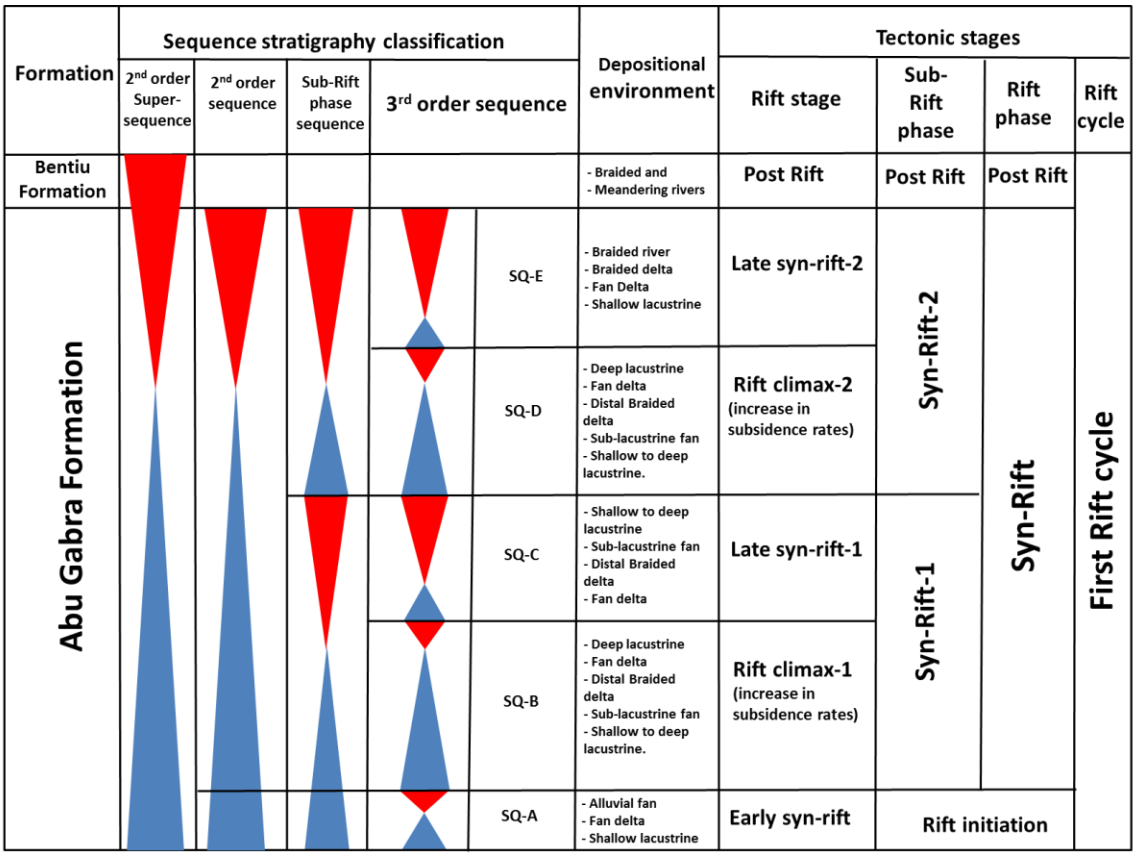

Figure 5-7: Depositional systems and sequence stratigraphic framework of the Lower Cretaceous (Abu Gabra Formation) for the Sufyan Sub-basin, Muglad Basin.

The vertical variation in the depositional sequences, seismic amplitudes (Low and high), and tectonic subsidence of Abu Gabra Formation support this subdivision. System tracts within this sequence could be described in terms of seismic reflection configuration and from strata relationship of gamma logs.

5.4.3 Third order sequence

Third order cycle is a sequence that was deposited in approximately 1-10 million years (Catuneanu, 2006). This sequence comprises systems tracts and their essential parasequences. Within the major coarsening upward second order cycle deepening trend of Abu Gabra Formation, other minor sequences can be established. These small-scale sequences could be recognized from the lake level oscillations recorded, and fluvial graded profile adjustment. Thus, third-order sequences have been defined on the basis of major basin-wide lacustrine flooding episodes in Abu Gabra formation and fluvial type's variation. These cyclic patterns were caused by different allogenic and autogenic controls (Miall, 2010). The end product of which gives the hierarchal arrangement of the stratigraphic column. There are five 3rd order sequences within the two 2nd order sequences (sub-rift phases) of Abu Gabra Formation (Figure 5-7).

The motif of gamma-ray logs of the study area is characterized by upward-coarsening and upward-fining Parasequence sets. Each Parasequence set and Parasequence is 10's meters thick. The upward coarsening Parasequence set, Parasequence, bed set thicknesses, sandstones coarsening upward, and the sandstone/claystone ratio varies considerably from one system tract to another.

Well, data is very important to study the 3rd order sequences and the higher sequence orders. In this study, SQ-A and SQ-B were not penetrated by wells and were interpreted only from seismic data. Only SQC, SQD, and SQE were penetrated by the available wells. In the following section, SQ-A, SQ-B, SQ-C, SQ-D, and SQ-E will be analyzing in detail.

5.4.3.1 Sequence- A (SQ-A)

SQ-A corresponds to the lower part of Abu Gabra Formation (AG-5) (Figure 5-3). This sequence was penetrated only at the Muglad basin margins, hence the geographic representation of this unit remains uncertain . On the contrary, the basal sand unit of the second rift cycle (Upper Bentiu formation), and the third rift cycle (Upper Amal formation) interfingers towards the axis of the rift with suspended-load fluvial and shaly lacustrine accumulations. This sequence composed of an alluvial fan, shallow lacustrine, and fan-delta deposits and contains two system tracts, transgressive system tract (TST) and highstand system tract (HST) (Figure 5-7). In Sufyan Sub-basin, SQ-A was not penetrated by well data. The nearest wells that penetrated this sequence are located in Fula Sub-basin. From seismic data, SQ-A in Sufyan Sub-basin is equivalent to SQ-A in Fula Sub-basin. According to the well data in Fula Sub-basin, the lithofacies is mostly sandstone interbedded with red to brown mudstone, which reflects the redox environment. On the seismic data, SQ-A shows unconformable contact with the basement. Fan deltas locally deposited in the margin of southern boundary fault and show wedge-shaped, medium amplitude, medium continuity, and medium frequency of seismic reflection configurations (Figure 5-3). Chaotic reflection configurations were recognized. They are interpreted as strata deposited in relatively high-energy depositional setting such as slope fan.

5.4.3.2 Sequence-B (SQ-B)

This sequence corresponds to the middle part of Abu Gabra Formation (AG-4) (Figure 5-3). In this sequences, the depositional system in Sufyan Sub-basin converts from fluvial dominated (SQ-A) to lacustrine dominated (SQ-B). As a result, thick claystone was accumulating. This sequence reaches up to hundreds of meters thick and has been recognized basin-wide.

At the sub-basin center, deep lacustrine mud deposits were developed while braided deltas and fan deltas occurred in the sub-basin margin. This sequence consists of two system tracts, transgressive system tract (TST) and highstand system tract (HST) (Figure 5-7). The transgressive system tract (TST) is dominant and characterized by very thick claystone. The seismic configuration described as parallel high amplitude, good continuity, and medium frequency, which interpreted as deep to shallow lacustrine.

5.4.3.3 Sequence-C (SQ-C)

This sequence corresponds to the middle part of Abu Gabra Formation (AG-3) (Figure 5-3, Figure 5-7, Figure 5-8). This sequence reaches up to hundreds of meters thick and has been recognized basin-wide (Figure 5-9). This sequence contains transgressive system tract (TST) and highstand system tract (HST) (Figure 5-7 and Figure 5-8). The highstand system tract (HST) is dominant and characterized by thick sandstone. This sandstone is deposited in braided and Fan deltas as a result of the decrease of the accommodation space.

In this sequence, the depositional system in Sufyan Sub-basin converts from lacustrine dominated to shallow lacustrine, braided, and fan deltas dominated (Figure 5-10). At the sub-basin center, shallow to semi-deep lacustrine mud deposits were developed while

braided deltas and fan deltas occurred in the sub-basin margin. In Sufyan Sub-basin, fan delta mainly develops in the steep slope of the basin (southern area) while delta develops in the gentle slope (northern and northwestern areas). The lacustrine level was dropped while the braided deltas and fan deltas were expanding and occurred in the sub-basin margin. The vertical-facies associations within both the upward-coarsening and upward fining parasequences are interpreted to be a record of a gradual decrease in or an increase of water depth of the lacustrine system.

Parasequence within this sequence changes from being fining upward in lower part which represent the transgressive system tract (TST) to be coarsening upward in the upper sequence which represent the highstand system tract (HST).

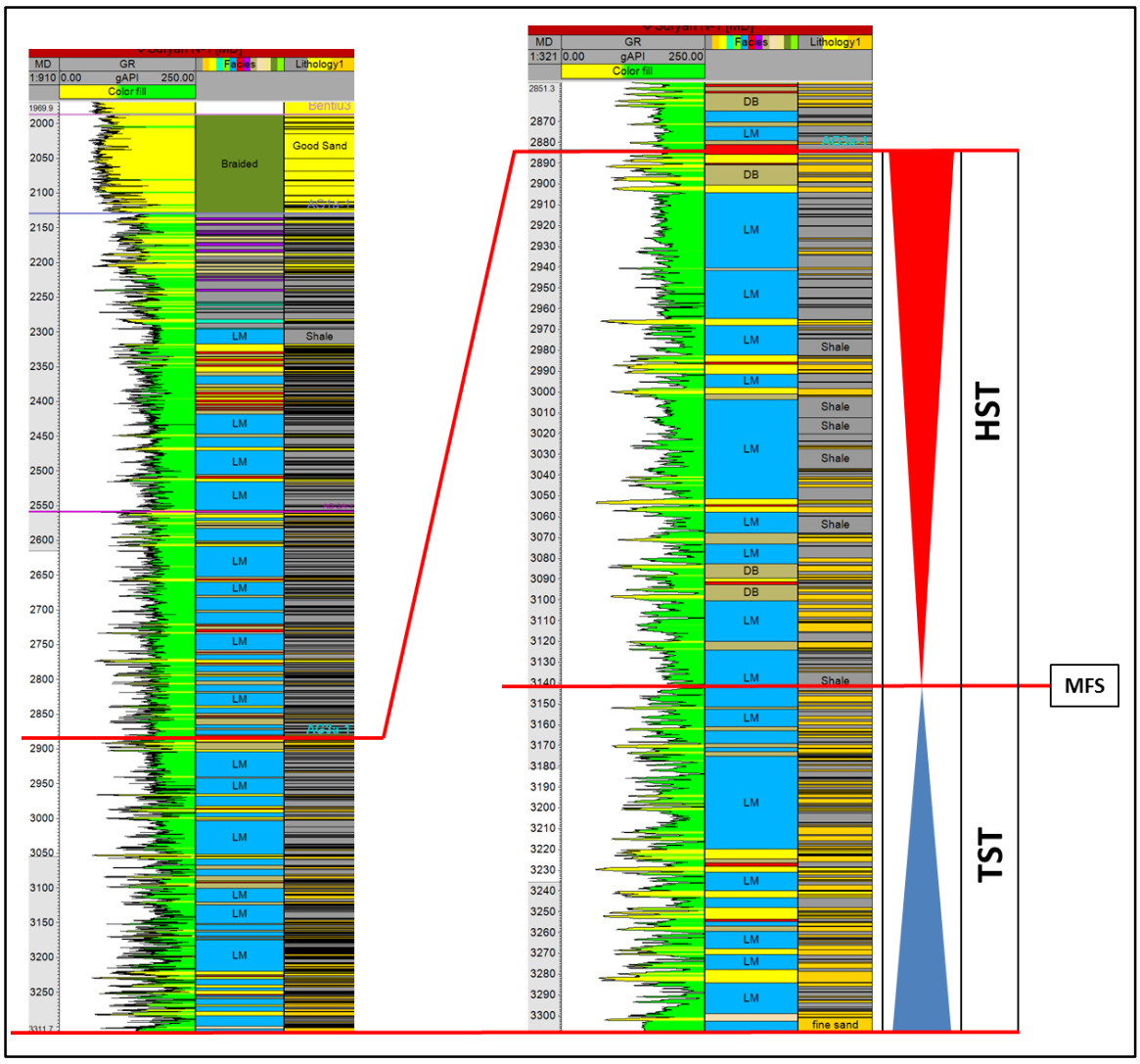

Figure 5-8: Braided delta, third order sequence of the lower part (SQ-C) (late syn-rift-1) of syn-rift-1 (Abu Gabra Formation); given the code AG-3. System tract of this sequence is the transgresive and highstand system tract (TST and HST).

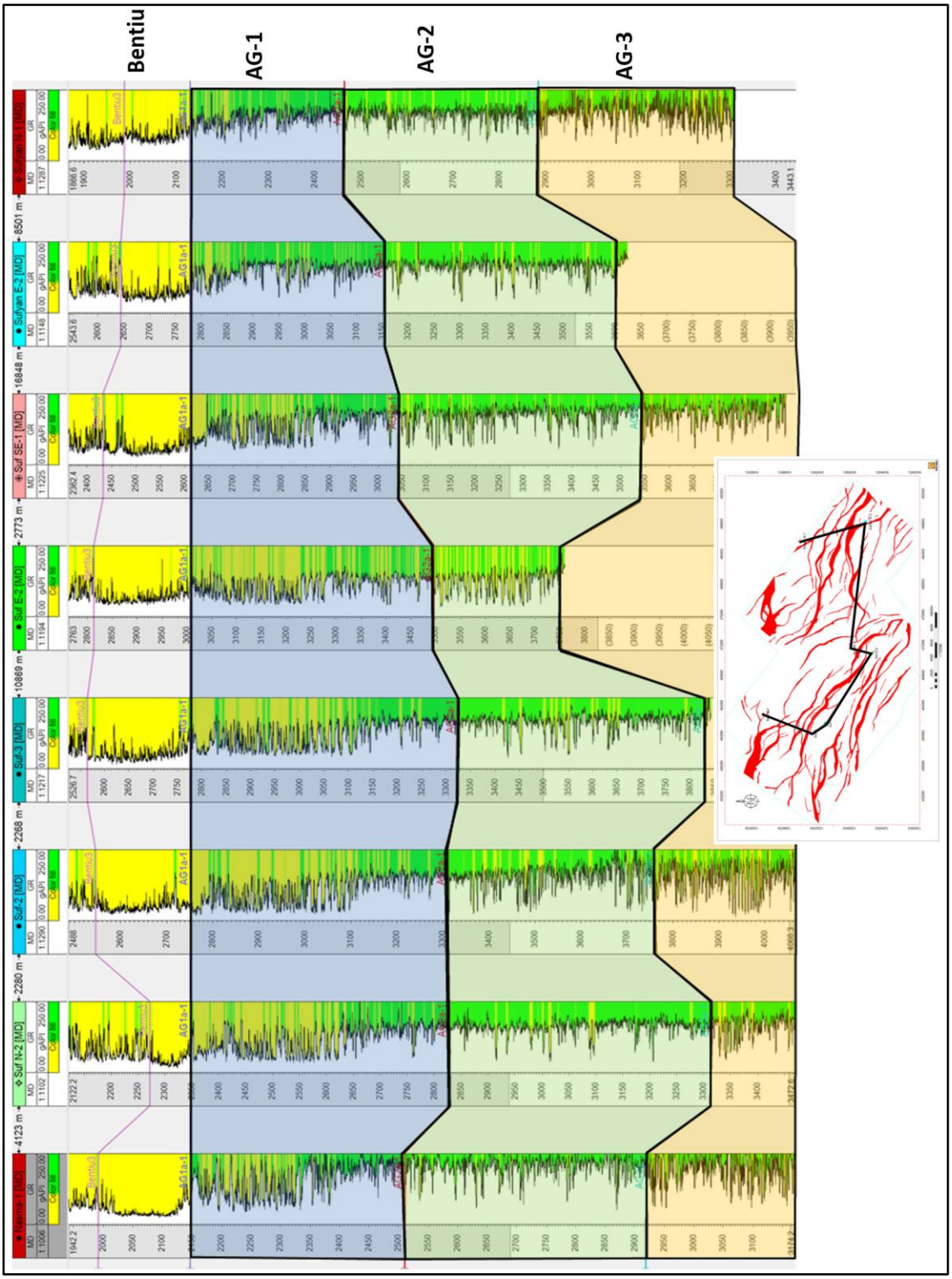

Figure 5-9: Correlation profile cross the study area between Bentiu Formation, AG-1, AG-2, and AG-3.

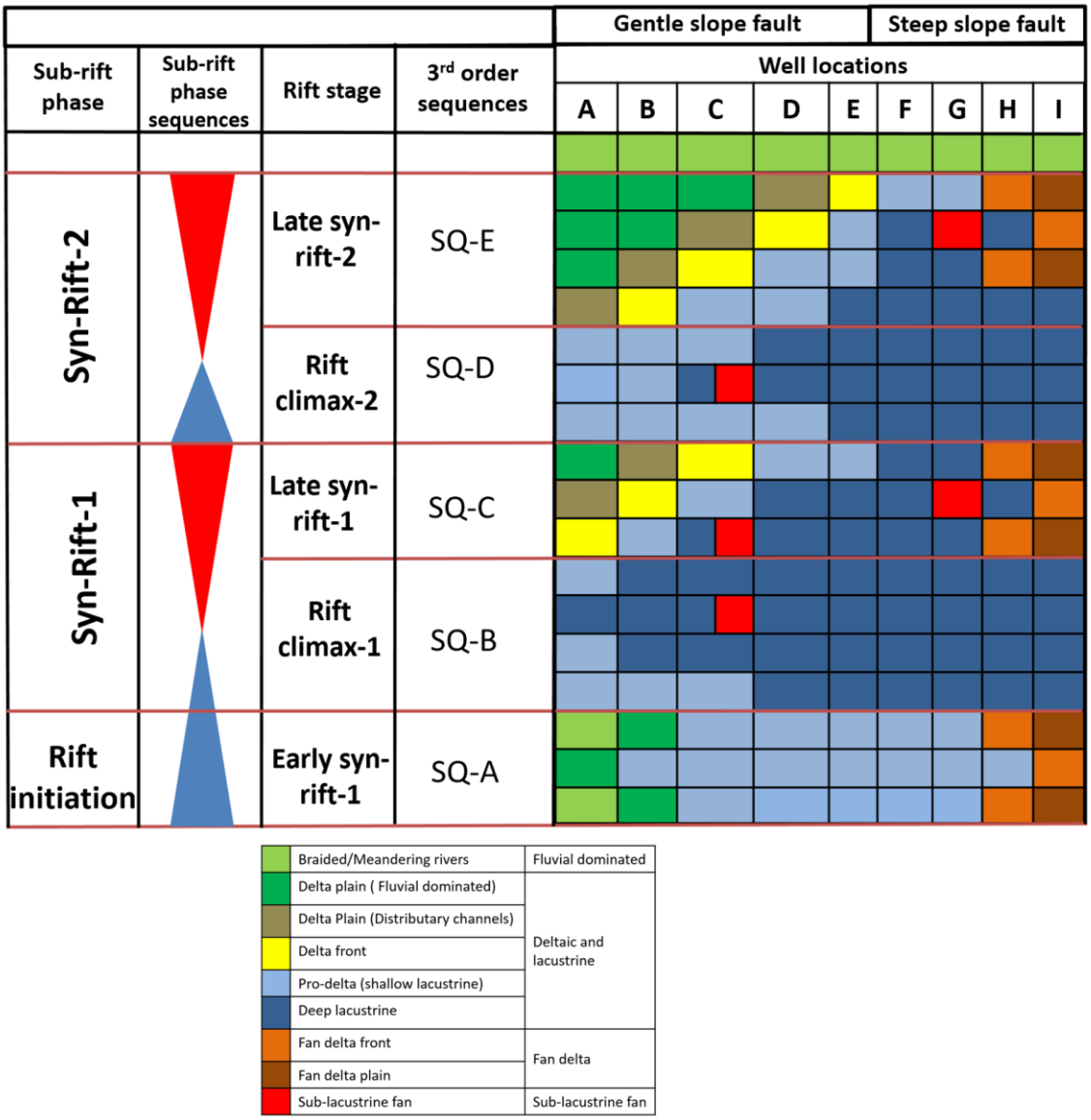

Figure 5-10: Tectonostratigraphic model. Depositional systems and systems tracts in lacustrine sequence framework of the Abu Gabra Formation, Sufyan Sub-basin. During the early syn-rift stage of the basin development (SQ-A), sequences dominated by LST alluvial fan, fluvial, fan delta deposits; during rift climax stage (SQ-B and SQ-D), sequences dominated by the TST lacustrine and sublacustrine fan deposits; during the late syn-rift stage (SQ-C and SQ-E), sequences dominated by HST braided delta and fan delta deposits. Gentle slope fault dominated by braided delta deposits. Steep slope fault dominated by fan delta deposits.

5.4.3.4 Sequence-D (SQ-D)

This sequence corresponds to the upper part of Abu Gabra Formation (AG-2) (Figure 5-3, Figure 5-7, Figure 5-11). In this sequence, the depositional system in Sufyan Sub-basin converts from fluvio-deltaic (SQ-C) to lacustrine dominated (SQ-D) (Figure 5-10). As a result, a thick claystone accumulates (Figure 5-11). This sequence reaches up to hundreds of meters thick and has been recognized basin-wide (Figure 5-9). The thick mudstone of this sequence categorized as a major source rock interval in Sufyan Sub-basin. At the sub-basin center, deep lacustrine mud deposits were developed while braided deltas and fan deltas (Figure 5-10) occurred in the sub-basin margin. Sublacustrine fan deposits were recognized in this sequence (Figure 5-5). This sequence contains transgressive system tract (TST) and highstand system tract (HST) (Figure 5-11). The transgressive system tract (TST) is dominant (Figure 5-11) and characterized by very thick claystone. The seismic configuration described as parallel high amplitude, good continuity, and medium frequency which interpreted as deep to shallow lacustrine.

5.4.3.5 Sequence-E (SQ-E)

This sequence corresponds to the uppermost part of the Abu Gabra Formation (AG-1) (Figure 5-3, Figure 5-7, Figure 5-12). In this sequence, the depositional system in Sufyan Sub-basin convert from lacustrine dominated (SQ-D) to shallow lacustrine, braided, and fan deltas dominated (SQ-E) (Figure 5-10). This sequence reaches up to hundreds of meters thick and has been recognized basin-wide (Figure 5-9). At the sub-basin center, deep lacustrine mud deposits were developed while braided deltas and fan deltas occurred in the sub-basin margin. In Sufyan Sub-basin, fan delta mainly develops in the steep slope of the

basin (southern area) while delta develops in the gentle slope (northern and northwestern areas). Fluvial environment and braided delta environment deposited at the ramp side of the major southern boundary fault and fan delta deposited at the cliff side of the major southern boundary fault, those environments are immediately followed by small shallow lakes in the middle. The lacustrine level was dropped while the braided deltas and fan deltas were expanding and occurred in the sub-basin margin. The vertical-facies associations within both the upward-coarsening and upward fining parasequences are interpreted to be a record of a gradual decrease in or an increase of water depth of the lacustrine system. The sequence reaches its maximum thickness at the basin edges where sedimentary load deposited when rivers enter the water body of the lake. Thickness starts thins basin-ward and grains size decreases. This sequence contains transgressive system tract (TST) and highstand system tract (HST) (Figure 5-12). The highstand system tract (HST) is dominant and characterized by thick sandstone.

The transgressive system tract (TST) interpreted to be the prodelta and shallow lacustrine where medium to coarse sandstone with a considerable amount of claystone is deposited. The highstand system tract (HST) interpreted to be the delta-front and delta-plain where considerable amounts of medium to coarse sandstone with a low amount of claystone is deposited. On the seismic section, this sequence is characterized by discontinuous parallel reflectors, with possible progradational and aggradational reflectors close to the footwall.

Parasequence within this sequence changes from being fining upward in lower part which represent the transgressive system tract (TST) to be coarsening upward in the upper sequence which represent the highstand system tract (HST).

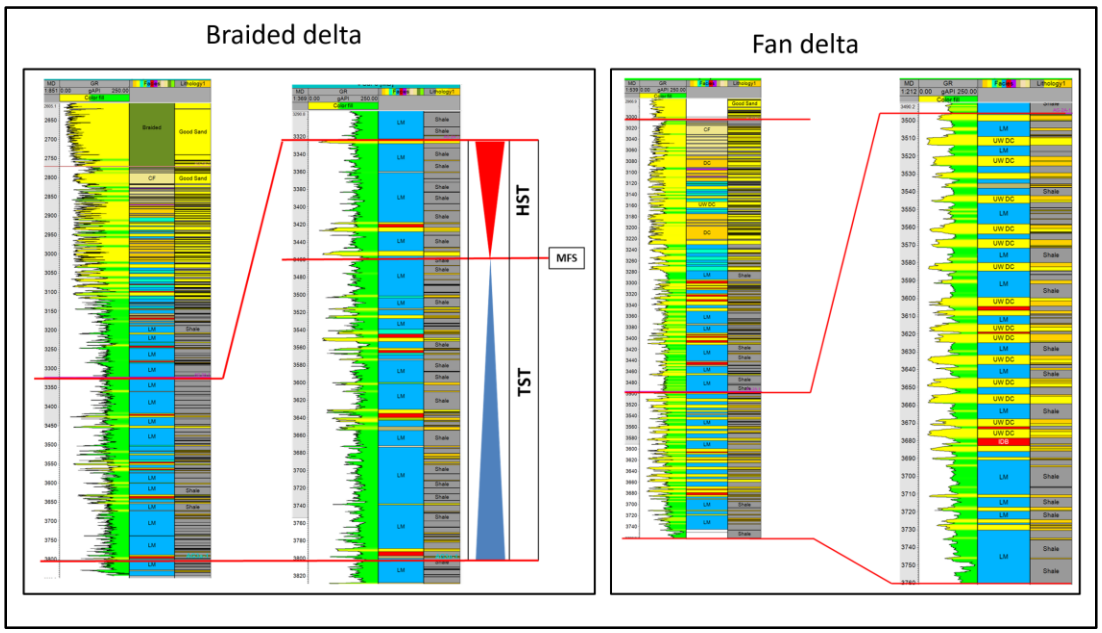

Figure 5-11: Braided delta (left) and fan delta (right), third order sequence of the middle part (rift climax-2) of syn-rift-2 (Abu Gabra Formation); given the code AG-2/SQ-D. System tract of this sequence is the transgresive and highstand system tract (TST and HST).

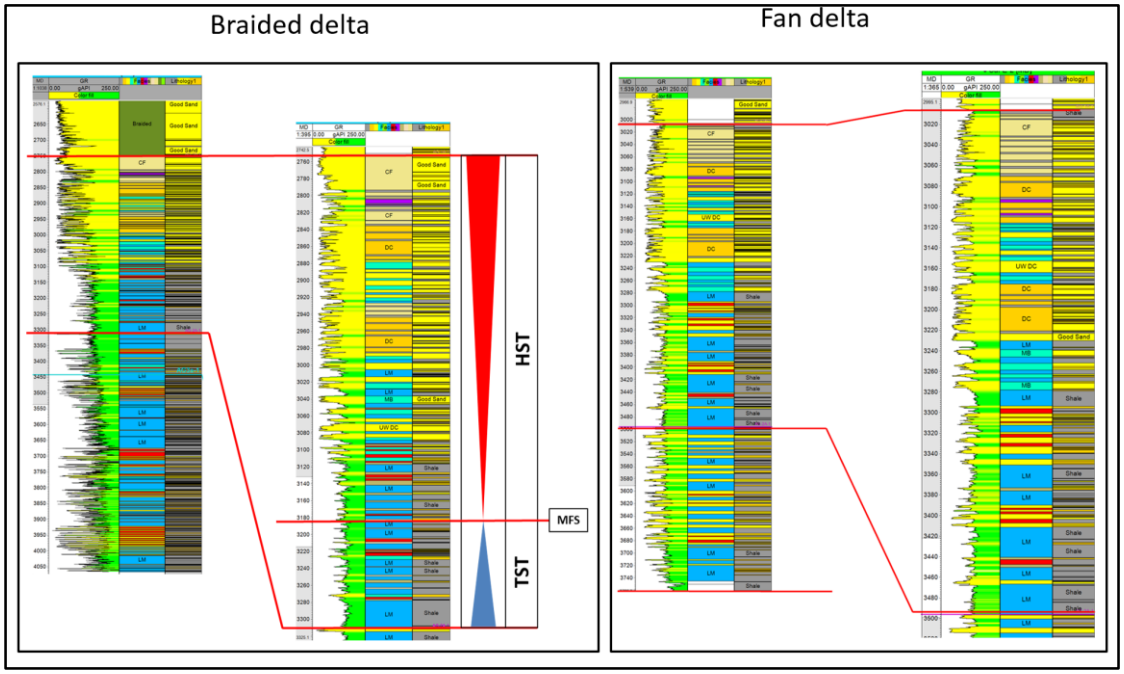

Figure 5-12: Braided delta (left) and fan delta (right), third order sequence of the upper part (late syn-rift-2) of syn-rift-2 (Abu Gabra Formation); given the code AG-1/SQ-E. System tract of this sequence is the transgresive and highstand system tract (TST and HST).

5.5 Tectono-stratigraphic model

Lacustrine basin fills generally show depositional systems that reflect over-filled, filled, and under-filled lakes (Carroll and Bohacs, 1999; Dong et al., 2011; Martins-Neto and Catuneanu, 2010; Zhou et al., 2014). Rift basins are characterized by phases of subsidence due to pulses of extension related to faults initiation and reactivation, usually the subsidence followed by tectonic inactivity period. During the rift initiation/early syn-rift and post-rift stages, no new accommodation is created and sediment supply slowly fills the existing space resulting to a transformation gradually from underfilled to a filled or even overfilled basin. Normally, sediment supply increases rapidly after a tectonic pulse, because of the basin subsidies in the area and uplifted in another area which causes higher areas susceptible to erosion.

Sufyan Sub-basin basin is mainly influenced by the central Africa shear zone right-lateral strike slip fault (Yassin et al., 2016), the sequence filling and distribution features are controlled by the stages of tectonic evolutions (Figure 5-1). The sequence filling and evolution processes are controlled by the tectonic movements in the study area, and different sequence filling in Abu Gabra Formation have been caused by the rifting stages (Figure 5-7). Through analyzing the systems tracts development on wells and seismic sections (Figure 5-2), further understandings on sequence filling features are realized. Abu Gabra formation was filled during the syn-rifting phase of the first rifting cycle, which corresponded to the development of sequences from SQ-A to SQ-E.

The tectonic evolution, Sedimentologic model, and sequence stratigraphy of the study area indicate that sedimentation took place during the early Cretaceous in five stages (early syn-

rift/rift initiation stage, rift climax-1 stage, late syn-rift-1stage, rift climax-2 stage, and late syn-rift-2 stage) (Figure 5-7) and marked by five different lithological units. Each of these stages has their own idealized seismic attributes and reflection configurations. These reflection configurations and attributes can be integrated with wells data to interpret seismic facies associations of the study area. The following section will focus on the tectonostratigraphic model of Abu Gabra Formation in Sufyan Sub-basin.

5.5.1 Early syn-rift

During this stage (Figure 5-7), SQ-A (AG-5) was deposited (Figure 5-13). The sedimentary environments vary from place to place throughout the study area. Thickness changes across the half-graben from south to north, which suggests that sedimentation was principally controlled mainly by tectonic subsidence (Figure 5-13). The first increase of fault movement causes a depression in the crust's surface to which gravity-driven sedimentary systems developed (WILLIAMS, 1993). The rift initiation/early syn-rift stage was penetrated only at the basin margins; hence the geographic representation of this unit remains uncertain. Early syn-rift deposits are mostly controlled by fault differential movement; the thicknesses of filled stratum vary obviously. SQ-A is developed during the rift initiation of the first cycle and dominated by fan, fan-delta, and shallow lacustrine deposits (Figure 5-13). Interpretation of this stage shows an overall wedge shaped. Reflector packages involve a system where sedimentation kept pace with the subsidence. Fan deltas locally deposited in the margin of southern boundary fault and show wedge-shaped (Figure 5-13A).

5.5.2 Rift climax-1

During this stage (Figure 5-7), SQ-B (AG-4) was deposited (Figure 5-13). This period of the basin history is characterized high tectonic subsidence (Figure 5-7) with respect to the sedimentation rate and therefore considerable expansion of the lake. The deposition during this stage is controlled by fault differential movement during the high tectonic subsidence and therefore the considerable expansion of the lake (Figure 5-13) occurred. The time of maximum rate of displacement of a fault can be termed the rift climax (Prosser, 1993). On the seismic section, the rift climax systems tract is characterized by an increase in the amount of aggradations, together with the development of divergent forms related to continuing tilting of the hanging wall during deposition (Prosser, 1993). In Sufyan Sub-basin, rift climax on seismic data is characterized by chaotic zone close to the depocenter, aggradation, and downlap is clear in the southern boundary fault (Figure 5-3). At the sub-basin center, deep lacustrine mud deposits were developed while braided deltas and fan deltas occurred in the sub-basin margin. The rift climax corresponds to the lacustrine system and characterized by deep lacustrine sediment (Figure 5-7). The rift climax-1 is interpreted to be the transgressive system tract of the 2nd order sequences for the sub-rift-1 which began at the top of the lowstand system tract (LST) of the rift initiation/early syn-rift-1 after the first flooding surface until it reaches the time of the maximum flooding surface (Figure 5-7). This surface corresponding to the thick horizon of claystone. This claystone is deposited in a deep lacustrine as a result of the increase of the accommodation space associated with the high subsidence. Rift climax represents of Abu Gabra formation is dominated by deep lacustrine and sub-lacustrine fan environments (Figure 5-7).

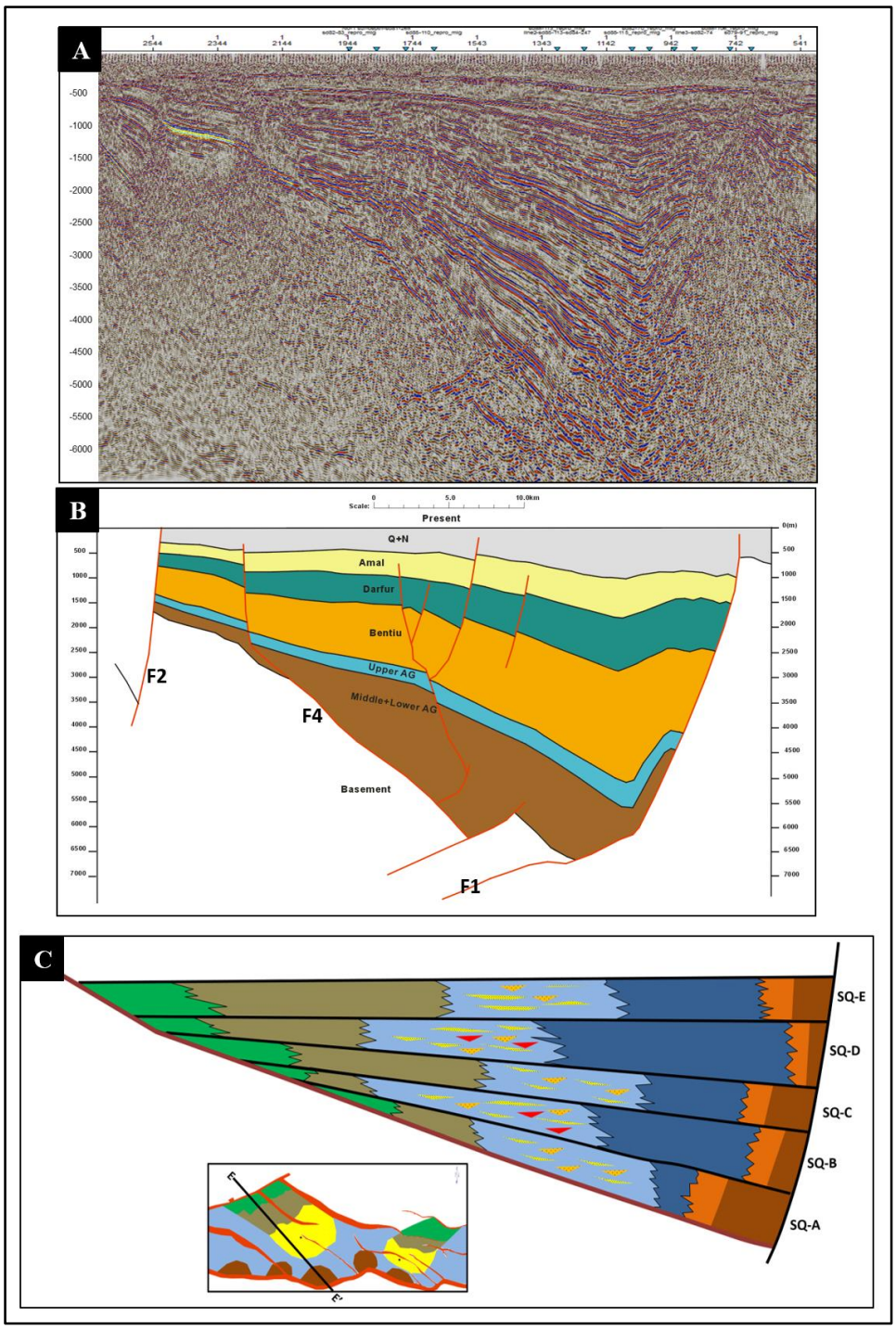

Figure 5-13: The seismic profile E-E' with its interpretation (for the location see Figure 5-2) (A) The seismic line without interpretation. (B) The seismic interpretation. (C) Schematic diagram from the detail interpretation of Abu Gabra Formation showing the distribution of depositional systems.

5.5.3 Late syn-rift-1

During this stage (Figure 5-7), SQ-C (AG-3) was deposited (Figure 5-13). This period of the basin history is characterized low or no tectonic subsidence and therefore the lake level was dropped. At the sub-basin center, deep lacustrine mud deposits were developed while shallow lacustrine, braided deltas, and fan deltas occurred in the sub-basin margin (Figure 5-13).

This sequence contains transgressive system tract (TST) and highstand system tract (HST) (Figure 5-7). The highstand system tract (HST) is dominant and characterized by thick sandstone. This sandstone is deposited in braided and Fan deltas as a result of the decrease of the accommodation space.

5.5.4 Rift climax-2

During this stage (Figure 5-7), SQ-D (AG-2) was deposited (Figure 5-13). This period is characterized by high tectonic subsidence and therefore considerable expansion of the lake and the maximum flooding occurred.

At the sub-basin center, deep lacustrine mud deposits were developed while braided deltas and fan deltas occurred in the sub-basin margin. Sub-lacustrine fan deposits were developed during this stage near to the intra-basinal fault zones where the subsidence rate and accumulation space are increased (Figure 5-10).

The transition from the late syn-rift-1 to rift climax-2 stage is recorded at all wells in the study area. That is the abrupt change from sedimentation in fluvio-deltaic dominated unit to a shallow lacustrine and later to a deeper lacustrine environment (Figure 5-13). This

change seems to be the result of increased subsidence with respect to the sedimentation rate in the central area. The strata of this stage thin landward and thicken basinward having a wedge shape (Figure 5-13). This geometry results in pinching out of deep lacustrine at the ramp side of the basin. The deep lake is characterized by maintaining thermal stratification of the water column and a permanent anoxic bottom. These conditions allowed the production and preservation of source rich lacustrine stratified unit around this central zone.

The strata which deposited during this stage is contained two system tracts, transgressive system tract (TST) and highstand system tract (HST) (Figure 5-7). The transgressive system tract (TST) is dominant and characterized by very thick claystone. This claystone is deposited in a deep lacustrine as a result of the increase of the accommodation space associated with the high subsidence.

5.5.5 Late syn-rift-2

During this stage (Figure 5-7), SQ-E (AG-1) was deposited (Figure 5-13). This period is characterized by low or no tectonic subsidence and therefore the lake level was dropped. At the sub-basin center, deep lacustrine mud deposits were developed while braided deltas and fan deltas occurred in the sub-basin margin.

During this stage, fan delta mainly develops in the steep slope fault zone in the southern area (Figure 5-10, Figure 5-13, Figure 5-14) while delta develops in the gentle slope fault zone (northern and northwestern areas) (Figure 5-10, Figure 5-13, Figure 5-14). Fluvial environment and braided delta environment deposited at the ramp side of the major southern boundary fault and fan delta deposited at the cliff side of the major southern

boundary fault, those environments are immediately followed by small shallow lakes in the middle (Figure 5-13). The transition from the rift climax-2 to late syn-rift-2 stage was gradual, and it is characterized by shallow lacustrine and fluvio-deltaic environments (Figure 5-13). Facies types of this unit vary largely from one place to another depending on the location of delta lobes. At the proximal part, facies are dominated by coarse to very coarse grained sandstone with considerable amounts of gravels. The distal part is characterized by clay facies. Here the main control for accommodating water depth change is the tectonic activities and the main control for water supply is the climate.

The strata which deposited during this stage is contained two system tracts, transgressive system tract (TST) and highstand system tract (HST) (Figure 5-7). The highstand system tract (HST) is dominant and characterized by thick sandstone. This sandstone is deposited in braided and Fan deltas as a result of the decrease of the accommodation space.

5.6 Controls on depositional systems and sequences

Tectonic history, structural evolution and prevailing climate of rift basins are the main factors that control the stratigraphy and facies pattern (Prosser, 1993). In continental basins, tectonic movements are of extreme importance for the sequence boundaries formation and the sediments characters of sequences (Morley, 1995; Morley et al., 2004, 1990; Ravnås et al., 2000). Tectonic create accommodation space; structure evolution modifies this accommodation space, and the prevailing climate determines whether this accommodation space can be filled by water or sediments. The main controlling factors are tectonic and climate. These factors affect depositional processes either directly or indirectly.

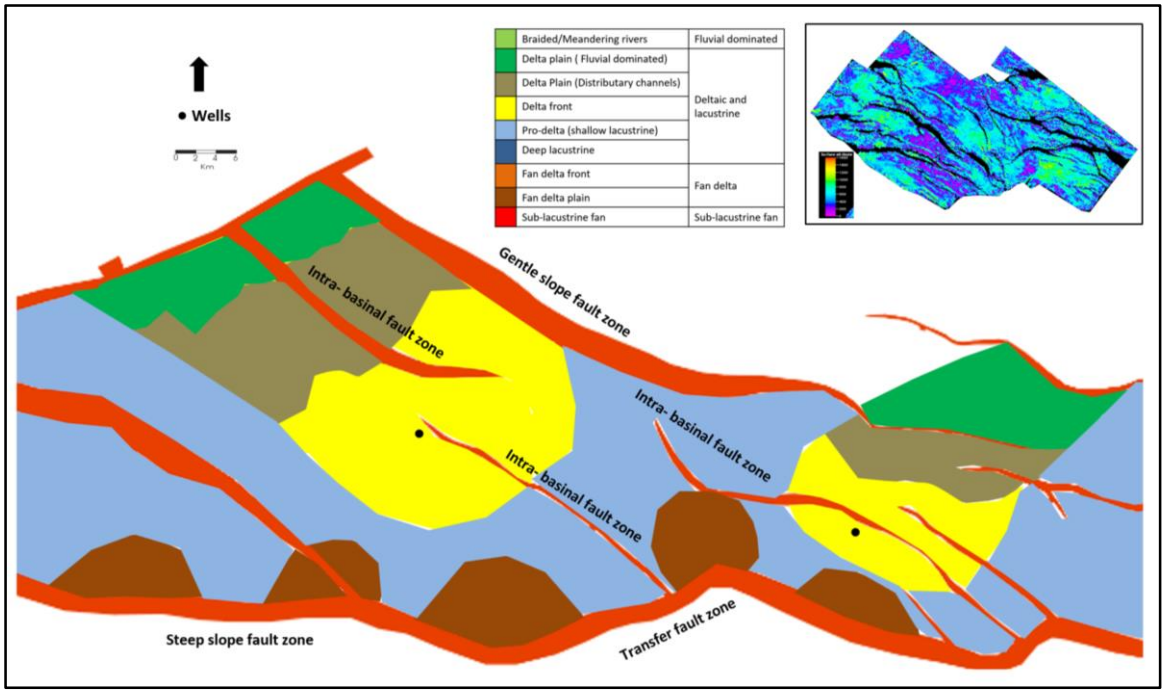

Figure 5-14: Diagram showing depositional systems superimposed over the structural map of the late syn-rift-2 stage of Sufyan Sub-basin. This diagram mainly based on well data, seismic facies, and seismic attributes (Root Mean Square =RMS) (see RMS map above right corner).

5.6.1 Structural elements of Sufyan Sub-basin

Sufyan Sub-basin is bounded by three major faults, the southern fault (F1) dipping toward the north, the northern fault (F3) dipping towards the south, and the northwest fault (Figure 5-2) dipping toward the northwest (Yassin et al., 2016). Six major transtensional oblique faults were also observed in an en-echelon pattern (F3, F4, F5, F6, F7, and F8). Those faults are trending mainly NW-SE (Figure 5-2). Both types of faults are thick-skin faults (basement involved) and extend to the shallow horizons. Other faults are small and minor faults but are very important because they control and form the structural hydrocarbon traps in the study area.

Interpretation of seismic reflection data of the Sub-basin reveals grabens and half grabens geometries with two depocenters that are controlled by the southern boundary Fault. Sufyan Sub-basin has the structural characteristics of differences from west to east directions. It can be divided into western, middle, and eastern parts. Each of them has their own characteristics. In the western part, symmetrical graben were developed controlled by Fault-4 (F4) and fault-8 (F8) (Figure 5-15) (Yassin et al., 2016). In the middle part, an asymmetrical half-graben with one depocenter controlled by the south boundary fault (F1) (Figure 5-16). In the eastern part, an asymmetrical half-graben with one depocenter was developed controlled by the southern boundary fault (F1) (Figure 5-17) (Yassin et al., 2016). Sufyan Sub-basin is a dextral pull-apart basin affected by both CASZ (transtensional) and Muglad Basin (extension). It could be divided to two pull apart Sub-basins (East and west) with a sigmoidal to rhombohedral shapes (Yassin et al., 2016). Each one of those two pull apart Sub-basins has one depocenters that are controlled by the

southern boundary Fault. In the western pull apart, F1-B segment of the southern boundary fault believed to the major control of the sub-basin topography and control the distribution of the braided delta (Figure 5-18).

5.6.2 Tectonic

Depositional systems and sand bodies distribution within each sequence are control mainly by the high and low areas (accommodation space) due to the variation in the subsidence rates along the major boundary faults (Gawthorpe and Leeder, 2000; Leeder and Gawthorpe, 1987; Morley et al., 2004, 1990; Zhou et al., 2014). The following section will focus on the controlling factors on the basin fill. The study area is located on the north margin of Muglad Basin, the sequence filling started from Cretaceous; the super-sequence is controlled by the tectonic stress of three great rifting cycles since Cretaceous (Figure 5-19, Table 5-2). In the early period of Lower Cretaceous, due to the effect of middle Africa shear zone right-lateral strike-slip stress field, Sufyan Sub-basin began to form.

The accommodation space resulted from the initiation and reactivation of the major faults. The sequence thickness varying between the filling of hanging wall and footwall varies obviously; therefore, despite the integral “north is relatively thin and south relatively thick” (Figure 5-13). The sediment supply of the study area is furnished by the north Muglad uplifting, and the effects of near source area and braided river entering lake are very obvious; the relatively intensive rifting movement created large accommodation space, and the lacustrine system was developed. The sediment supply was sufficient, which resulted in the large sequence filling thickness. The sequence filling within the study area are mainly dominated by lake surface fluctuation and sediment supply.

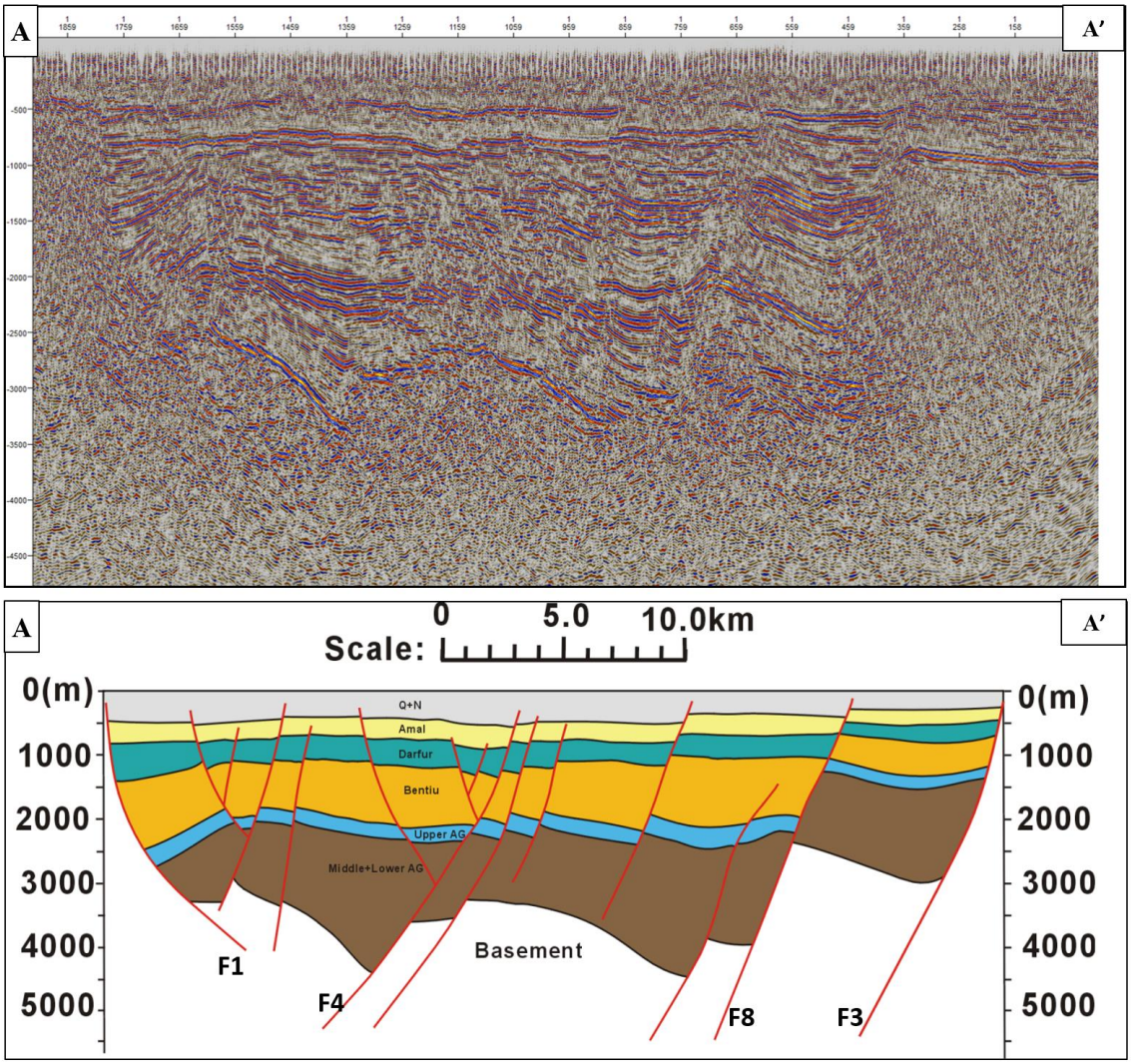

Figure 5-15: A-A' Regional seismic line and Geoseismic section (locations of the lines in Figure 1-5). Horizons from top to bottom are top of; Amal Formation, Darfur Group, Bentiu Formation, Upper Abu Gabra Formation, Middle and Lower Abu Gabra formations, and basement.

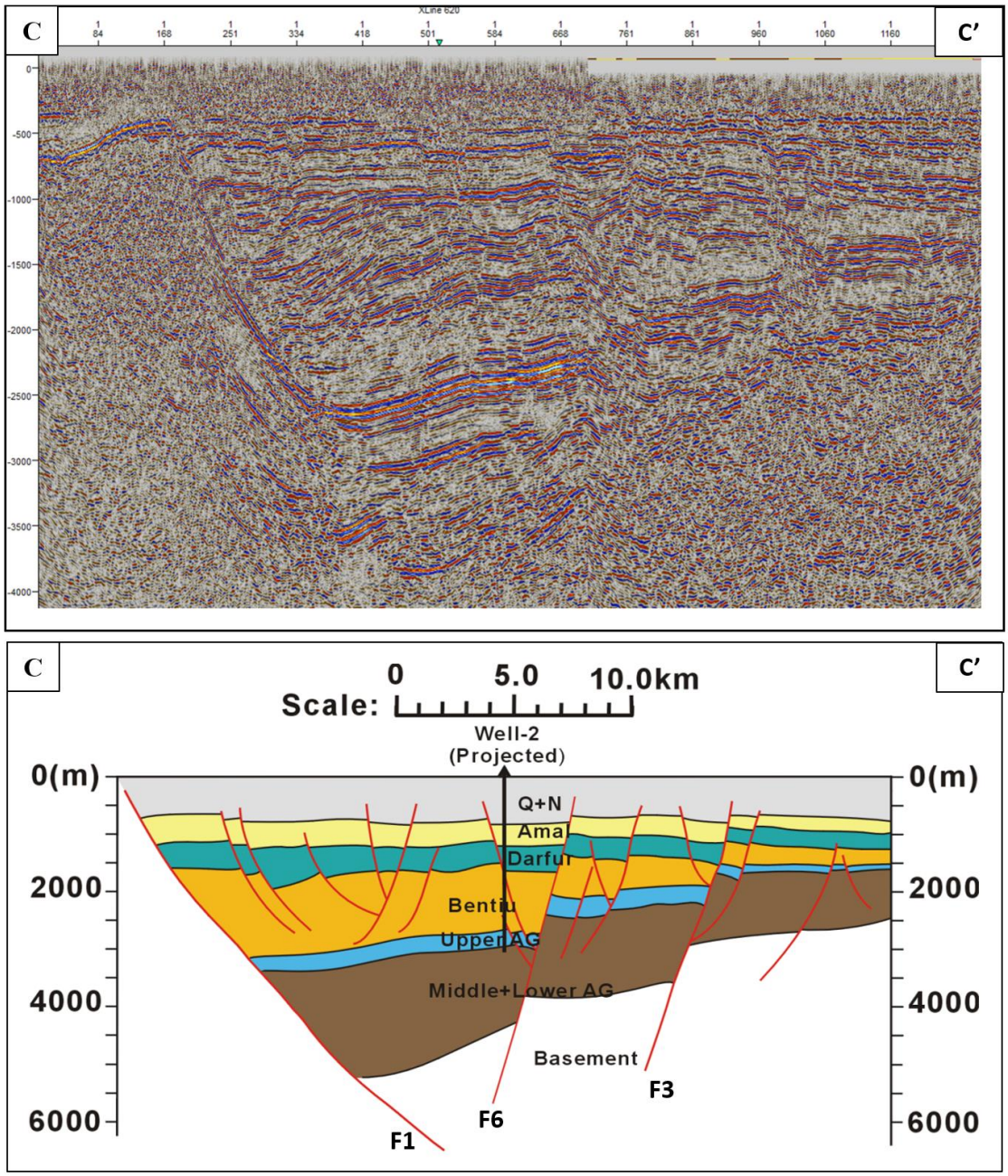

Figure 5-16: C-C' Regional seismic line and Geoseismic section (locations of the lines in Figure 1-5). Horizons from top to bottom are top of; Amal Formation, Darfur Group, Bentiu Formation, Upper Abu Gabra Formation, Middle and Lower Abu Gabra formations, and basement.

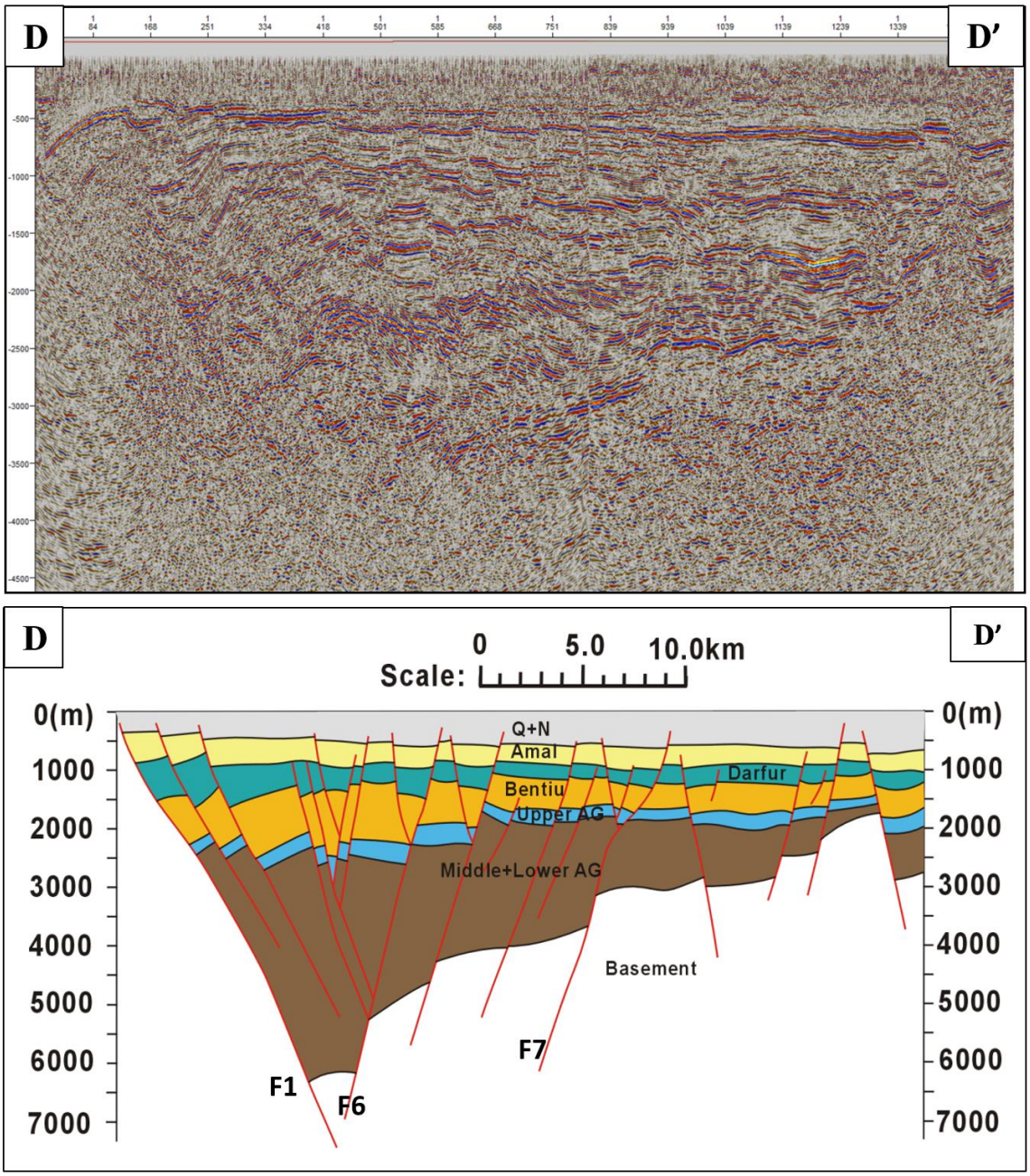

Figure 5-17: D-D' Regional seismic line and Geoseismic section. Horizons from top to bottom are top of; Amal Formation, Darfur Group, Bentiu Formation, Upper Abu Gabra Formation, Middle and Lower Abu Gabra formations, and basement.

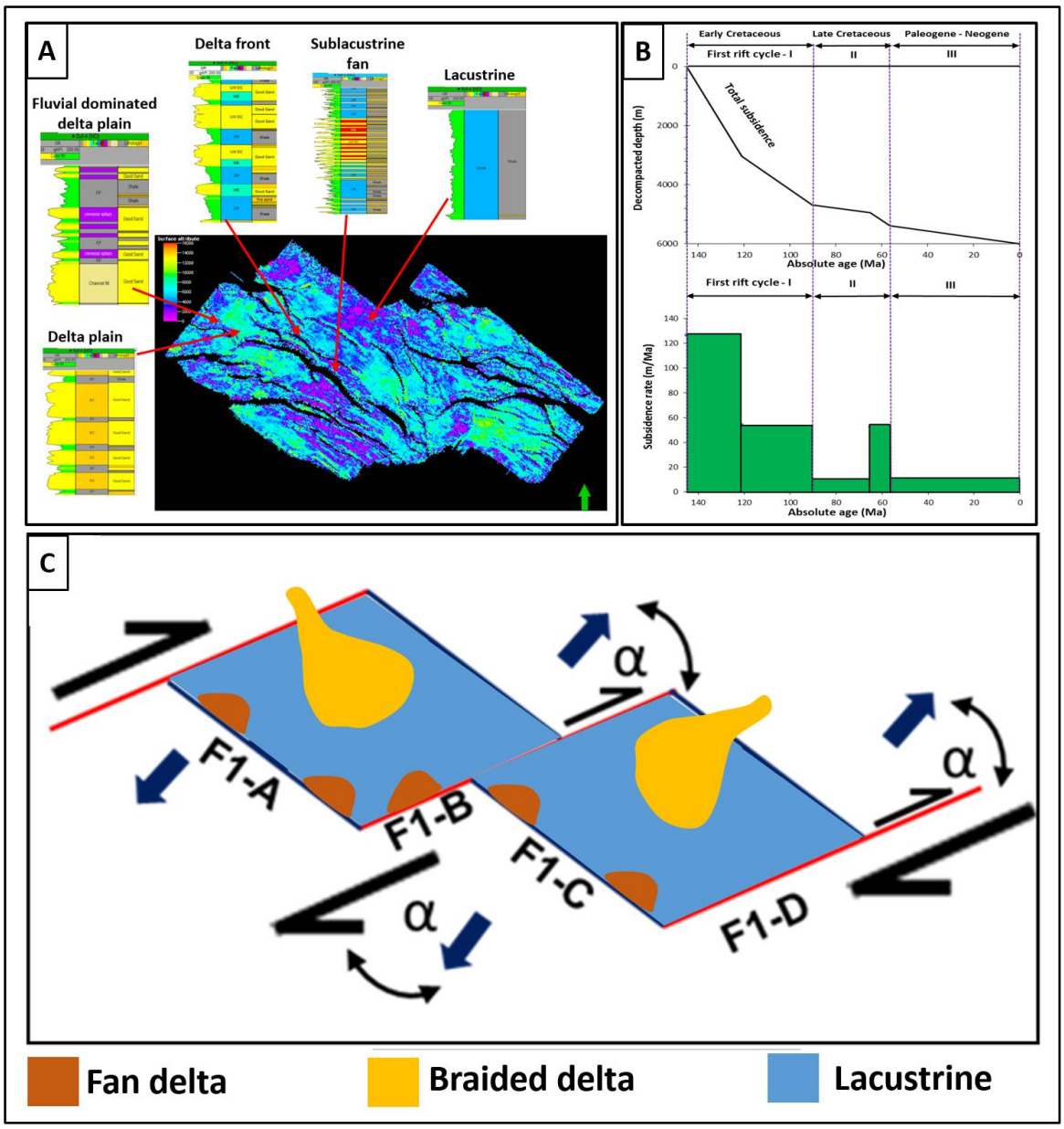

Figure 5-18: Model that can explain the structural evolution of Sufyan Sub-basin and its control on deposition. (A) seismic attributes (Root Mean Square =RMS) showing the outer configuration of the delta, gamma ray logs showing the vertical stacking pattern of the delta sub-environment. (B) shows the backstripping tectonic subsidence rate of the study area. (C) A conceptual model for the dextral pull-apart systems in the study area. Sufyan sub-basin could be separated to two pull apart basins with a sigmoidal to rhombohedral shapes.

Table 5-2: Show the total amounts of extension using 2D structural restoration (Yassin et al., 2016)

Extension (m/ma)					
Location	Abu Gabra	Bentiu	Darfur	Amal	Near Present
227.917	227.917	119.608	42.520	54.118	5.487
187.917	187.917	72.549	40.157	44.706	15.929
97.500	97.500	97.712	23.622	57.647	3.363
189.167	189.167	49.020	40.551	55.294	2.832

During the first and second syn-rift phases, faulting action enlarged the accommodation space of the depression rapidly (Figure 5-20); the basin was in under-compensation status, the lake basin began to transgress to the margins, and both SQ-B and SQ-D appeared as retrogressive vertical superimposition. During SQ-A, C, and E development, the effect of the rift subsidence weakened, and the rift-depression conversion transition basin was developed. During these periods, the accommodation space was reduced, and the progressive strata superimposition pattern was developed.

5.6.2.1 Subsidence history

Using the backstripping process (Allen and Allen, 2013), Sufyan Sub-basin subsidence history has been simulated quantitatively (Figure 5-21). The Sufyan Sub-basin experienced multi-phase subsidence from the Cretaceous to recent periods in response to the changes of regional crustal stress. At least three rift cycles were observed from the subsidence curve (Figure 5-21). The first rift cycle (Figure 5-21) from 145 to 90.4 Ma shows the heights rate of subsidence, it is characterized by early stage of rifting (subsidence rate: 126.58 m/Ma) and late stage of rifting (post-rift) (subsidence rate: 53.93 m/Ma). During this phase, combined strike-slip movement along CASZ and normal extension mechanism (regional crustal stretching) along Muglad Basin occurred. During the first syn-rift phase (during the deposition of Abu Gabra Formation), five sub rift phase occurred, those are: Early syn-rift (AG-5) (relatively low subsidence rate) (Figure 5-21), rift climax-1 (AG-4) (relatively high subsidence rate) (Figure 5-21), late syn-rift-1 (AG-3) (relatively low subsidence rate) (Figure 5-21), rift climax-2 (AG-2) (relatively high subsidence rate) (Figure 5-21), and late syn-rift-2 (AG-1) (relatively low subsidence rate) (Figure 5-21).

5.6.2.2 Influence of rifting on accommodation space and basin geometry

In Muglad Basin, the lacustrine system evolved in response to active rift extensional force that prevailed during the early rifting phase in the rift-basins of southern Sudan (Schull, 1988). Sufyan Sub-basin is asymmetrical half grabens with steep boundary fault on the south and gentle slope ramped margin on the north (Figure 5-13 and Figure 5-19). Variations in basin geometry produced by differences in the subsidence and sedimentation rates. The water and sediment capacity changed as a result of variation in basin volume. The first rifting phase of Sufyan Sub-basin (145 to 121 Ma) was characterized by the highest displacement among the other two rifting phases (Figure 5-21). Therefore, during the first rift phase, thick lacustrine systems developed with a wide range of facies variation. In Sufyan Sub-basin, Abu Gabra Formation was developed during the first rift phase and divided into two sub-rift phases (syn-rift-1 and syn-rift-2) (Figure 5-7). Abu Gabra Formation has five stages of basin evolution, which are early syn-rift/rift initiation, rift climax-1, late syn-rift-1, rift climax-2, and late syn-rift-2 (Figure 5-20and Figure 5-21).

At the early syn-rift/rift initiation stage, the system began with a wide fluvial deposition that was overlain by an abrupt changed deep lacustrine (rift climax stage), overlain by shallowing upward fluvio-deltaic environment (late syn-rift stage). The concentration and distribution of these facies vary from one place to another within the lacustrine system, because the geometry of the basin developed asymmetrically through time.

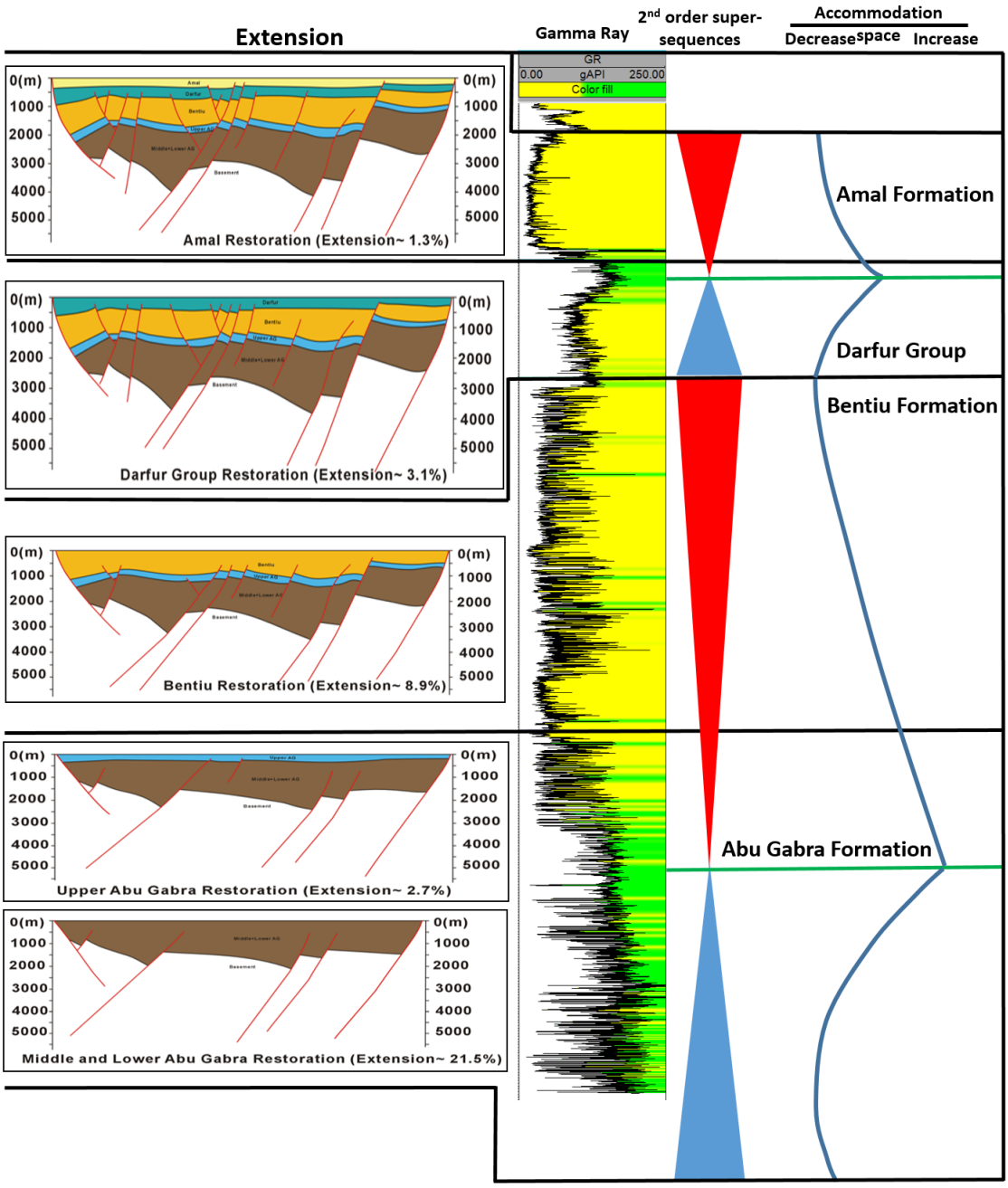

Figure 5-19: The control of tectonic evolution on sequence stratigraphic patterns. Gamma ray log shows second order super sequences and structural restoration shows the extension variation with the time. These sequences are rifting phase cycles.

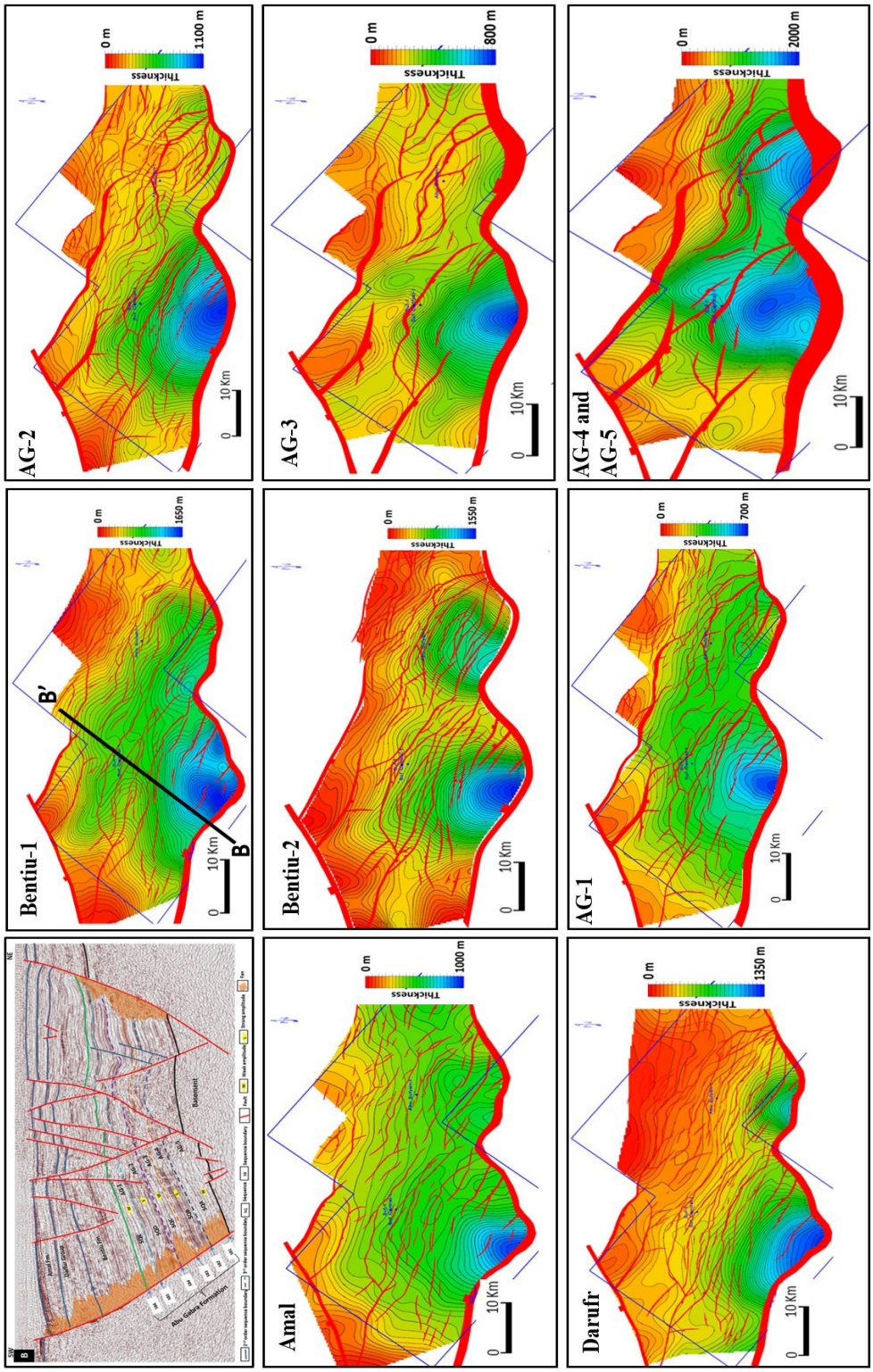

Figure 5-20: Isopach maps of sediments deposited during the rift-sag phases of tectonic cycles in Sufyan Sub-basin.

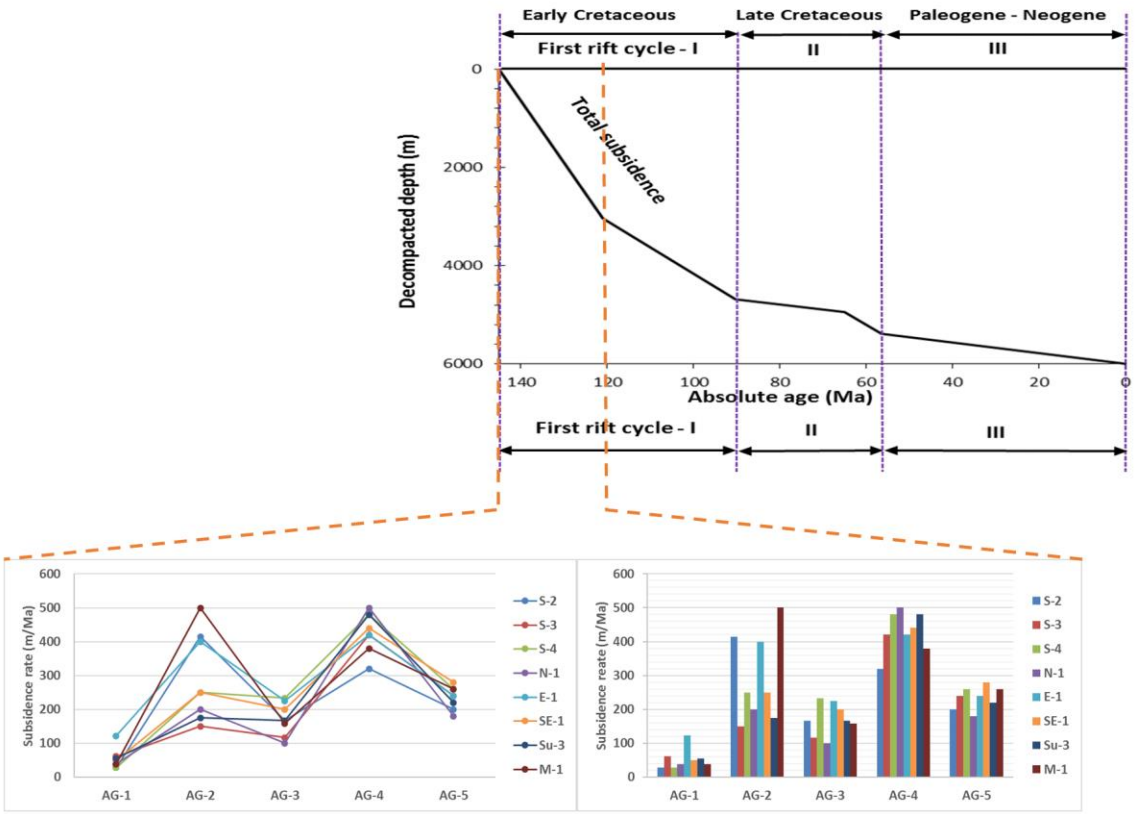

Figure 5-21: shows the backstripping tectonic subsidence rate of Sufyan Sub-basin and the subsidence rate during the first rift stage (during the deposition of Abu Gabra Formation) (see wells location in Figure 5-2).

The variation of stratigraphic sequences within rift cycle (Figure 5-19, **Table 5-2**) and within rift phase indicate that the subsidence took place in pulses rate and not as one event. Seismically, the sedimentary record of the syn-rift and rift climax stages could be differentiated (Figure 5-13).

Many supporting pieces of evidence could be recognized from the seismic and well data stratigraphic column of Sufyan Sub-basin that can confirm this period of tectonic activities and relaxation (Figure 5-19 and Figure 5-13). The syn-rifting and rift initiation sediments of Abu Gabra Formation keep pace of thick skin faulting and slide with the basement complex forming a wedge shape.

This gives an indication of how rapidly subsidence took place and to which extend this subsidence goes deep. Rift climax shows a period of maximum displacement.

5.6.3 Climate

The effect of climate in the rift basin is considered to be very important together with tectonic. Both the sedimentary process and base level fluctuation will be affected (Ayhan and Nemec, 2005; Juhász et al., 1997). In the higher order, first and second order cycle climate input is clearly noticed in facies transition from deep lacustrine to fluvio-deltaic to the fluvial environment.

Here water supply of the lake mass is largely controlled by humidity and aridity periods. The transition from a lacustrine to the fluvio-deltaic unit is mainly due to tectonic and climatic control. Facies association variation represents the expression of climate change.

Fluvial longitudinal graded profile depends on the net of sediment that enters the fluvial system which depends on rain and humidity in the deranged area. This, in turn, will determine fluvial types and their facies association in small-scale high-resolution third and high-frequency sequences, climate plays major roles in parasequences stacking pattern, which is controlled largely by Milankovitch cycle. This cycle reflects variation in orbital parameters of earth, caused by gravitational effects of other bodies in the solar system. This gravitational effect will control, directly or indirectly sedimentation processes in episodic periods. In the Muglad Basin, these cycles translated to small scale fining upward and coarsening upward within the major trend of coarsening upward of third order cycles.

CHAPTER 6

SEDIMENTOLOGY AND RESERVOIR CHARACTERISTICS

6.1 Introduction

The Sufyan Sub-basin is situated in the northwestern part of Muglad Basin (Figure 6-1). Three rift cycles are recognized in Sufyan Sub-basin and dated as Early, Late Cretaceous, and Paleogene age (Figure 6-2). Each tectonic cycle seems to contain rift-initiation, active rifting, and thermal sag phases (McHargue et al., 1992). The main source rock for this hydrocarbon in Muglad Basin is believed to be the lacustrine shale of the Abu Gabra Formation (Makeen et al., 2015a, 2015b, 2015c, 2015d, 2013; Mohamed et al., 1999). The latest studies of Abu Gabra Formation in Muglad Basin have focused mainly on source rocks rock characterization and evaluation (Lirong et al., 2013; Makeen et al., 2015a,b,c), sedimentology and tectonostratigraphy (Wu et al., 2015), tectono-stratigraphic evolution and structural analysis (Yassin et al., 2016) without carefully investigating the reservoir quality of the sandstone beds within the area. The detailed reservoir heterogeneities investigations of the Abu Gabra Formation sandstones remain rare and limited. This chapter focuses on the depositional facies, sequence stratigraphy, and the diagenetic processes and investigates its controls on reservoir quality.

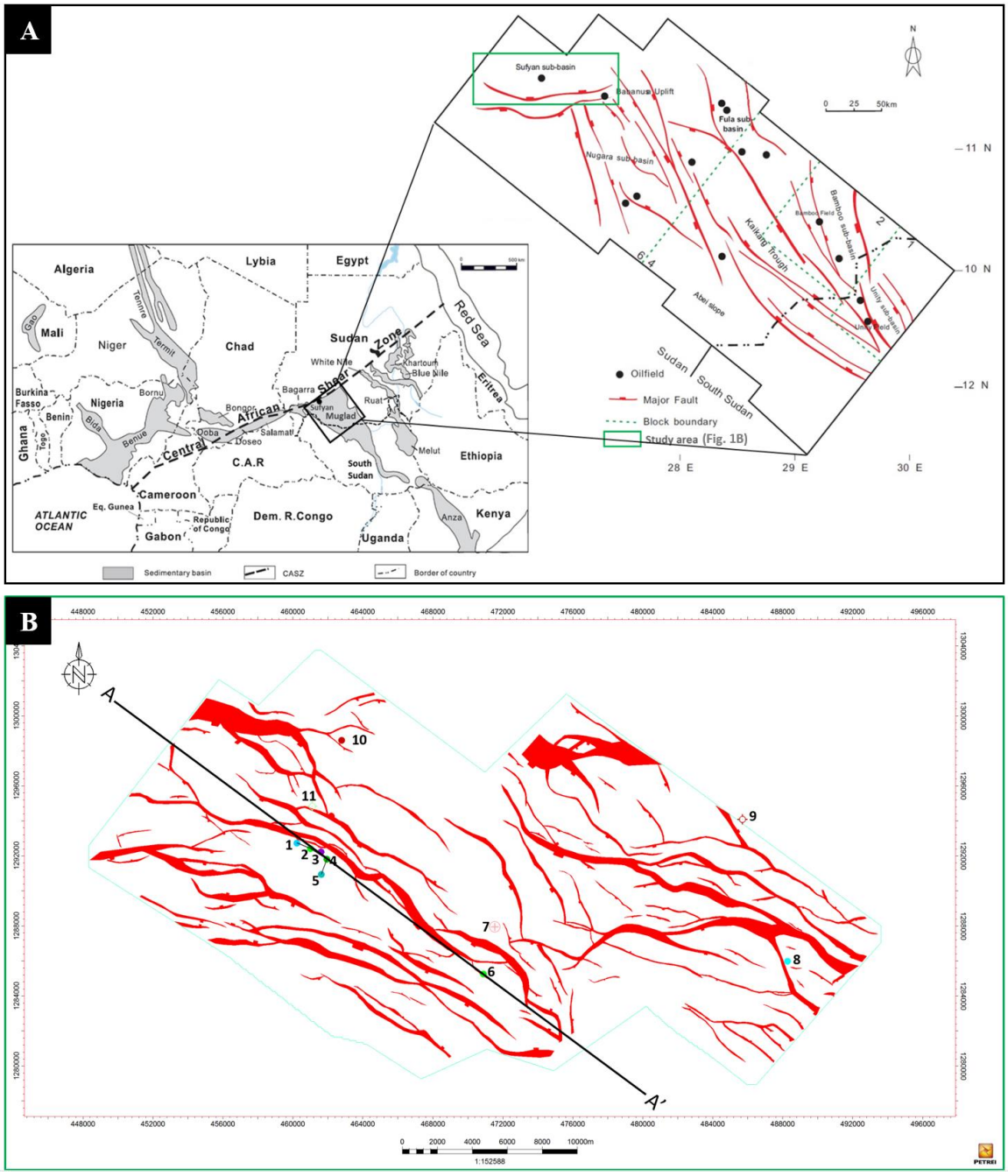

Figure 6-1: Location Map of the study area. (A) Main map shows Muglad Basin structural units interpreted from seismic and gravity data (from different source of data and show only the regional faults), with location of Sufyan Sub-basin and the major discovered oilfields. The other map shows the location of Muglad Basin with relation to the West and Central Africa Rift System (WARS) (modified from Lirong et al., 2013; Makeen et al., 2016; Yassin et al., 2016). (B) Structural map of top Abu Gabra Formation, interpreted from 3D seismic data shows faults, location of wells (from 1 to 11) and regional seismic line AA'.

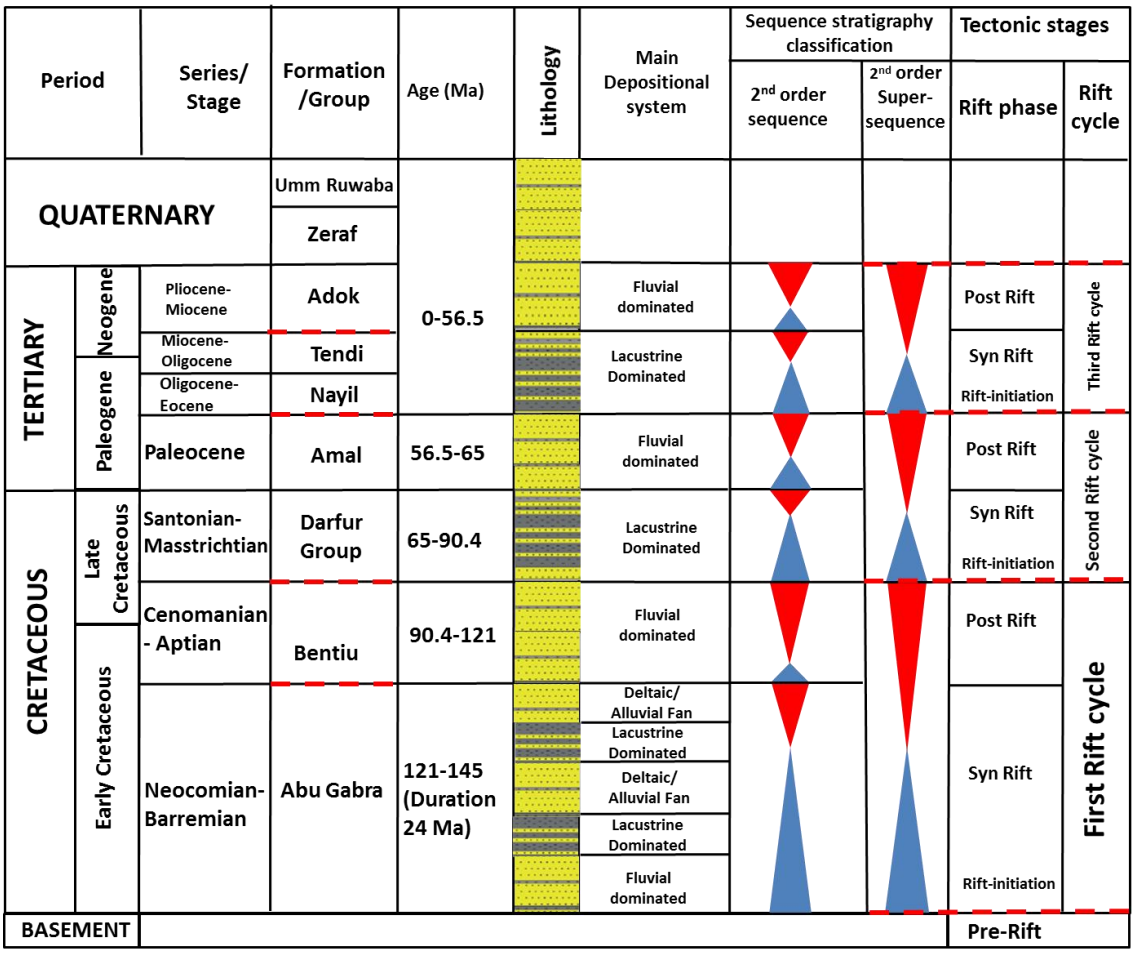

Figure 6-2: Stratigraphic and tectonic events charts for the Muglad Basin, Sudan, modified after (Fairhead et al., 2013; Guiraud and Bosworth, 1997; Lirong et al., 2013; McHargue et al., 1992; Mohamed et al., 2001; Schull, 1988).

Many researchers focused on the study of the reservoir quality under the sequence stratigraphic framework (e.g., Taylor et al., 2000; Ketzer et al., 2002, 2003; Al-Ramadan et al., 2005; El-ghali et al., 2006, 2009a), the depositional facies (e.g., Lima and Ros, 2003; Zhang et al., 2008; El-Ghali et al., 2009a), and the diagenetic processes (e.g., Schmid et al., 2004; Dutton and Loucks, 2010; Morad et al., 2010; Feng et al., 2013). Diagenetic processes might reduce porosity and permeability compaction and cementation but also could enhance porosity and permeability by dissolution (Gier et al., 2008; Luo et al., 2009). Different macro-to micro-scales of sedimentological heterogeneities (depositional and diagenetic) influenced and impacted the reservoir quality and architecture (Mahgoub et al., 2016).

6.2 Sedimentary facies

Based on core description, seven lithofacies were recognized in Abu Gabra Formation (Figure 6-3). It is mainly composed of continental-derived clastics. These include bedded conglomeratic sandstone, planar cross-bedded sandstone, trough cross-bedding sandstone, massive sandstone, ripples cross-laminated sandstone, massive to blocky mudstone and siltstone, and mudstone and shale. The bedded conglomeratic sandstone (Lithofacies-1) consist of bedded conglomerate and conglomeratic sandstone with pebbly sand and fine to very coarse sandstone. Clasts are poorly sorted, and grains are sub-angular to sub-rounded. The short transportation distance was due to the poor sorting. These elements attributed to distributary channel deposits primary in fan delta front or braided delta plain. The planar cross-bedded sandstone (Lithofacies-2) consist of fine, very coarse to pebbly sandstone. It describes as a light grey planar cross-bedded sandstone facies, with medium grain size. The grains are varying from rounded to sub-rounded with moderately to well sorting. The

planar cross-bedded sandstone facies is indicating for braided distributary channel deposits. The coarse-to-medium grained sandstone deposits indicated a fluvial system. The trough cross-bedded sandstone (Lithofacies-3) consist of fine, very coarse to pebbly sandstone. It describes as a light and grey with fine grain size sandstone. The grains are rounded to sub-rounded with poor sorting. The coarse-to-medium grained sandstone deposits indicated a fluvial system. The trough cross-bedded sandstone represents a meandering channel and point bar deposits (Figure 6-3). It could be interpreted as a fluvial channel or delta distributary channel or delta mouth bar. The massive sandstone (Lithofacies-4) consist of very fine to coarse sandstone. Massive or faint lamination. It describes as a light grey massive sandstone facies, with fine to coarse grain size. The grains are rounded to sub-rounded with well to moderately sorting. Long transportation distance was proposed based on the sorting (well to moderate). It could be interpreted as underwater distributary channels deposits primary in the braided delta. The ripples cross-laminated sandstone (Lithofacies-5) consist of very fine to coarse sand (Figure 6-3). It describes as light grey ripples laminated sandstone facies, with very fine grain size. The grains vary from rounded to sub-rounded with moderately sorting with flaser bedding. Usually, they occupy the top part of coarser and sandy facies with an overall fining-up vertical trend. Interbedded sandstone and siltstone relatively indicating for low current energy. It usually overlies the coarse-grained sandstone facies on top of the fining-up sequence. The lithofacies of this group could be interpreted as a top fluvial bar or delta mouth bar or floodplain or levee or distal bar. The massive to blocky mudstone and siltstone (Lithofacies-6) consist of mudstone and siltstone. It describes as a massive mudstone with desiccation cracks to blocky mudstone and siltstone. The mudstone is mainly dark grey

moderately laminated to massive with some root casts. This lithofacies are mainly deposited in overbank or floodplain in the fluvial system. The siltstone, claystone lithofacies may indicate a prodelta to shallow lacustrine deposits or interdistributary bay. The mudstone and shale (Lithofacies-7) consist of mudstone, shale, very fine sandstone, and siltstone (Figure 6-3). It describes as black shale, dark grey to greenish-grey mudstone, and horizontally laminated bedding siltstone and very fine sandstone. The very fine lithofacies deposits indicate that it is mainly deposited in Prodelta, semi-deep to deep lacustrine. This facies represents the low energy deposits.

6.3 Depositional systems and lithofacies association

Four types of the depositional system (fan delta, braided delta, lacustrine system, and sublacustrine fan deposits) were recognized in Sufyan Sub-basin based on the analysis of seismic, core, and well log data. Gamma ray log motives of different sedimentary facies were captured according to their electric properties, which were identified by the shape of log curves, amplitude, and connect relation (Figure 6-4). Log motives from wireline logs were calibrated with core and mud log data. The purpose of this analysis is to study the sediments vertical change of succession, rhythm, the energy of the deposition, and corresponding sedimentary facies of a particular environment or sub-environment based on logging curve combination attributes. According to well-4 and well-2, seven electrofacies (lithofacies associations) in Abu Gabra Formation were identified. These lithofacies associations are distributed according to the location of the wells in the study area. These lithofacies associations were calibrated to the core and cutting description to give an accurate interpretation.

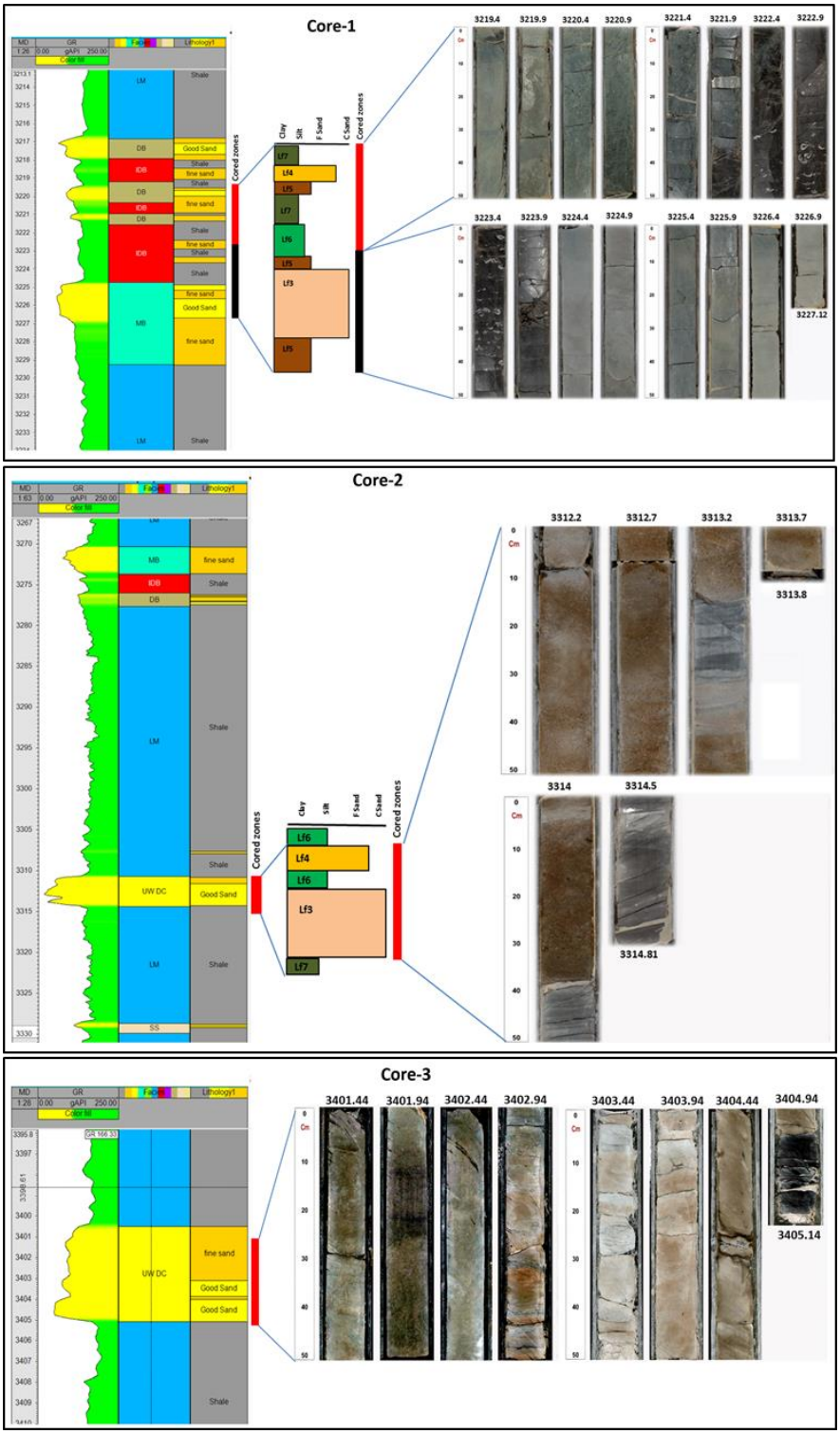

Figure 6-3: Core photos and gamma ray log of representative facies.

Each one of these lithofacies was assigned to the specific depositional environment to give a general idea about water depth and depositional system in which they accumulated.

6.3.1 Lithofacies Association-1 (LFA-1)

Description: This lithofacies association is characterized by high gamma ray values (serrated linear shape of gamma ray) with a predominance of claystone in the lithology (Figure 6-4). This lithofacies reaches more than 100 meters at the deepest part and the thickness is thinning landward to the ramp side of the fault.

Interpretation: This lithofacies association is interpreted to be semi-deep to deep lacustrine environment (Figure 6-4). Sand shale ratio of this association is 13 % and 87 % respectively (Figure 6-5).

6.3.2 Lithofacies Association-2 (LFA-2)

Description: This lithofacies association is characterized by high gamma ray values (serrated linear shape of gamma ray) with a predominance of claystone in the lithology interbedded with sandstone. This lithofacies reaches more than 75 meters at the deepest part and the thickness is thinning upward and reach 25 meters.

Interpretation: This lithofacies association is interpreted to be sub-lacustrine fan environment.

6.3.3 Lithofacies Association-3 (LFA-3)

Description: This lithofacies is characterized by irregular shapes of gamma ray that indicates sandstone interbedded with claystone (Figure 6-4).

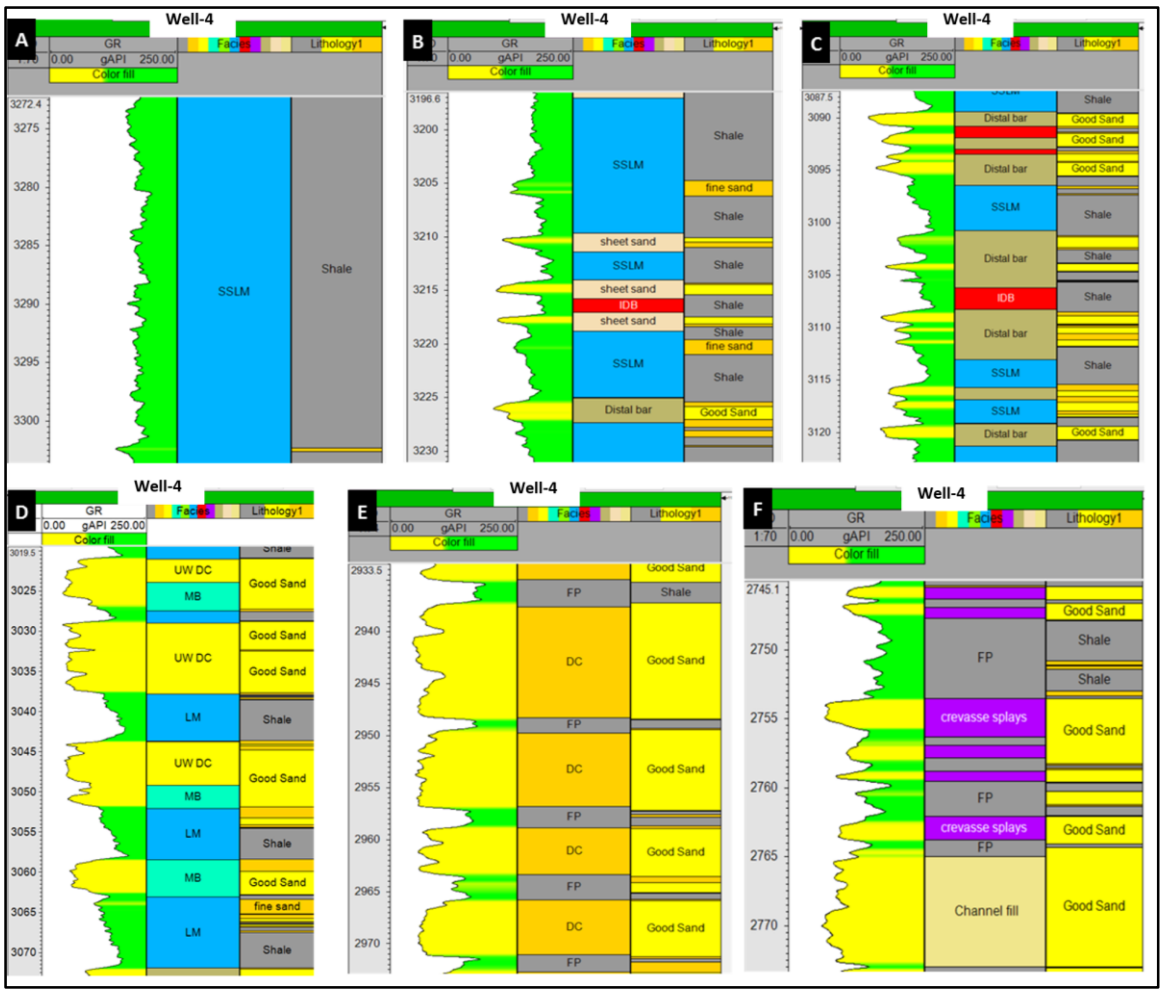

Figure 6-4: Showing different depositional systems in Abu Gabra Formation interpreted using core and well log data (gamma ray geometry are described in detail). (A) Lithofacies association of deep lacustrine. (B) Lithofacies association of prodelta. Including the distal bar, sheet sands, interdistributary bay, and shallow lacustrine mud deposits. (C) Lithofacies association of distal delta front. Coarsening-upward mudstone and sandstone representing shallow lacustrine mud, distal bars, and interdistributary bay deposits. (D) Lithofacies association of proximal delta front. Coarsening-upward mudstone and sandstone representing mouth bars, underwater distributary channels, distal bar, and shallow lacustrine mud. (E) Lithofacies association of delta plain. Including distributary channels and flood plains deposits. (F) Lithofacies association of fluvial-dominated delta plain. Fining-upward fluvial sandstone and mudstone representing channel fill, flood plain, and Crevasse splays.

The corresponding lithology from cutting description shows alternated fine-grained sandstone and mudstone. This lithofacies association reaches about 120 to 145 meters.

Interpretation: The depositional setting of this lithofacies association is interpreted to be prodelta or shallow lacustrine deposits. Vertically it is located at the top of the deep lacustrine lithofacies and laterally it extends all over the study area with more sandstone input landward (Figure 6-4). Sand shale ratio of this association is 27 % and 73 % respectively (Figure 6-5).

6.3.4 Lithofacies Association-4 (LFA-4)

Description: This lithofacies is characterized by stacked funnel shapes of coarsening-upward cycles (Figure 6-4). The corresponding vertical profile from a cutting description shows mudstone interbedded with sandstone and siltstone. This lithofacies association reaches more than 60 meters' thickness.

Interpretation: This lithofacies is interpreted as distal delta front environment. This lithofacies are usually formed when a fluvial stream enters a water body. Coarsening-upward mudstone and sandstone representing shallow lacustrine mud, distal bars, and interdistributary bay deposits. Vertically, this association located over the prodelta or the shallow lacustrine, deep lacustrine or a fluvial environment of Abu Gabra formation. Laterally this lithofacies represents a delta lobe body. This lobe spreads all over the study area; however, each unit of the delta occupied a certain place in the basin.

6.3.5 Lithofacies Association-5 (LFA-5)

Description: This lithofacies is characterized by stacked blocky shapes to funnel shapes of coarsening-upward cycles (Figure 6-4).

The corresponding vertical profile from a cutting description shows claystone and siltstone at the bottom of this cycle. This lithofacies association reaches more than 80 meters.

Interpretation: This lithofacies is interpreted as proximal delta front environment followed by fine-grained sandstone in the middle which is interpreted as middle delta. Proximal delta front is composed of coarse to very coarse grained sandstone at the top. It is always accompanied by more or less under water distributary channels and mouth bars. These lithofacies are usually formed when a fluvial stream enters a water body.

Vertically it is located over the distal delta front, shallow lacustrine, deep lacustrine of Abu Gabra formation (Figure 6-4). Sand shale ratio of this association is 64 % and 36 % respectively (Figure 6-5).

6.3.6 Lithofacies Association-6 (LFA-6)

Description: This lithofacies is characterized by blocky shapes of low gamma rays (Figure 6-4). The corresponding lithological profile from the core and cutting description displays a medium to coarse grained sandstone and minor amounts of gravel with a grain size ranging from 60 to 75 mm. This lithofacies reaches about 50 to 55 meters.

Interpretation: This lithofacies is interpreted as distributary channels sandstone deposited in the delta plain and marked down by scoured fill gravelly sandstone (Figure 6-4). Sand shale ratio of this association is 92 % and 8 % respectively (Figure 6-5).

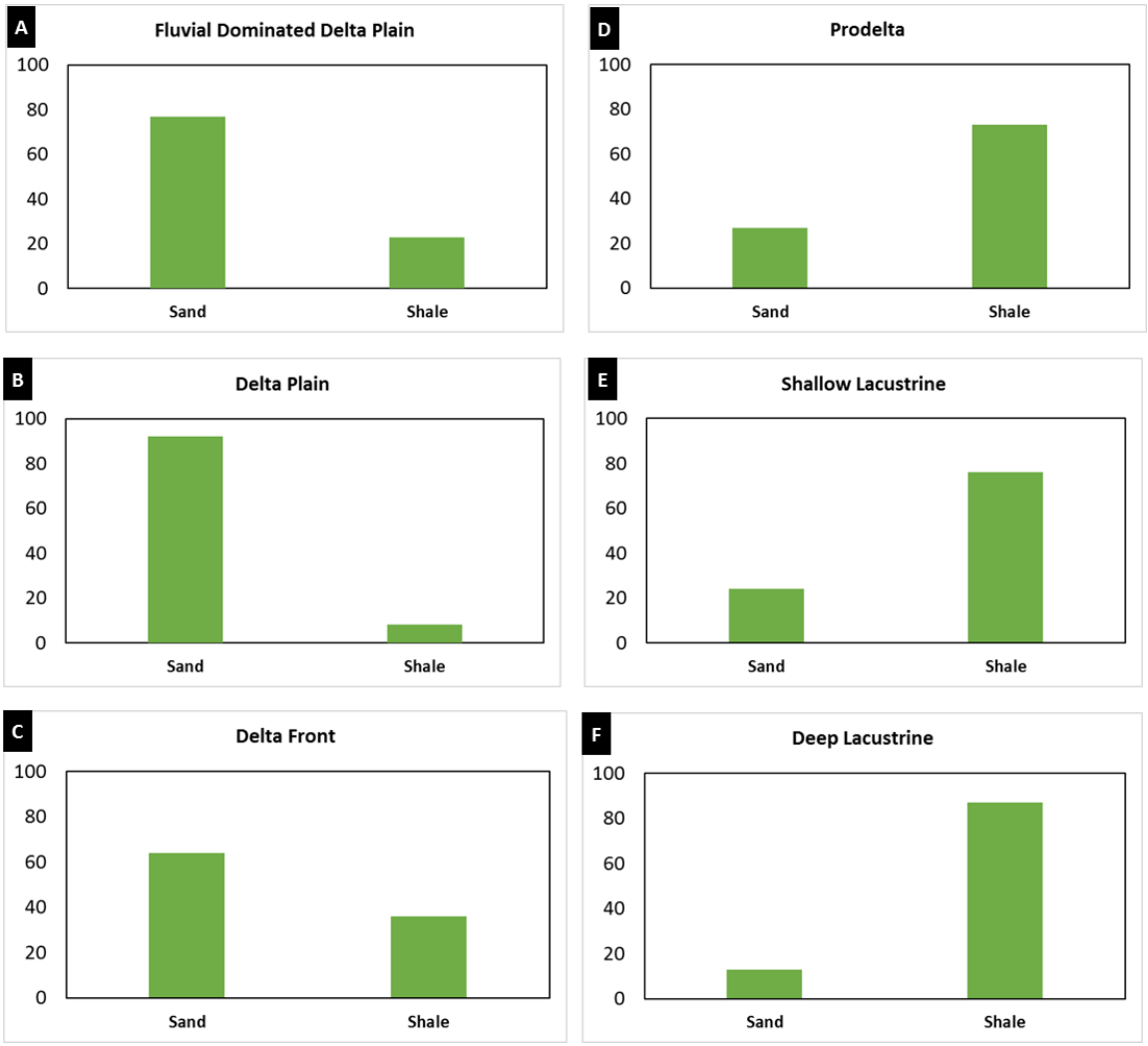

Figure 6-5: Sand and shale percentage in Abu Gabra Formation for different depositional systems. Calculated using well logs.

6.3.7 Lithofacies Association-7 (LFA-7)

Description: This lithofacies is characterized by stacked multi bell-shape gamma rays (Figure 6-4). The lithology description of this lithofacies shows multi fining upward. This lithofacies reaches about 45 to 55 meters.

Interpretation: This lithofacies is interpreted to be fluvial-dominated delta plain and composed of floodplains, crevasse splays, and channel fills deposits. The lithology of which is fine to coarse grained sandstone and over bank claystone. Sand shale ratio of this association is 77 % and 23 % respectively (Figure 6-5).

6.4 Facies distribution and reservoir heterogeneity

The above-mentioned facies associations were interpreted at each well based on different wireline logs and cored intervals. The spatial distributions and temporal evolution were carried out in order to identify the lateral and vertical facies variations and to produce a predictive model, represents sand bodies distribution and reservoir quality variation.

On the basin scale, the Abu Gabra Formation showed difference depositional systems, sandstone bodies thickness, geometry, and architecture. At the sub-basin center (Figure 6-6), deep and shallow lacustrine mud deposits were developed while braided deltas and fan deltas occurred in the sub-basin margin (Figure 6-7 and Figure 6-8). Fan-delta mainly develops in the steep slope fault zone in the southern area (Figure 6-6) while delta develops in the gentle slope fault zone (northwestern, northern, and eastern areas) (Figure 6-6 and Figure 6-8). Fluvial environment and braided delta environment deposited at the ramp side of the major southern boundary fault and fan delta deposited at the cliff side of the major

southern boundary fault, those environments are immediately followed by small shallow lakes in the middle (Figure 6-6).

In the study area, braided delta sandstones of the upper Abu Gabra Formation are well-developed in northwestern, northern, and eastern parts of the sub-basin (Figure 6-6). Fan delta sandstones of the upper Abu Gabra Formation are well-developed in the southern part of the sub-basin (Figure 6-8).

In the study area, fan delta and braided delta can be distinguishing in the subaqueous components of this depositional system; the subaerial components of both are similar. The sand bodies thickness in the fan delta front is thicker than the sand bodies in the braided delta front (Figure 6-8).

On the vertical scale succession covering the upper Abu Gabra formation, the depositional stratigraphic hierarchy as distinguished in the area begins with; muddy dominated (prodelta/shallow lacustrine shales and mudstones) with sand percentage 27% and shale percentage 73%. They pass upward to thin beds of delta-front sandstones with sand percentage 64% and shale percentage 36%. Then, the succession is converted to sand-dominated thick vertically-stacked and amalgamated delta plain with sand percentage 92% and shale percentage 8% (Figure 6-5). In this study, the quantification of the inter-well scale heterogeneities are strongly enhanced by the integration of the high-resolution seismic attributes (Figure 6-6), spatially and the high-resolution wireline logs (Figure 6-8), temporally.

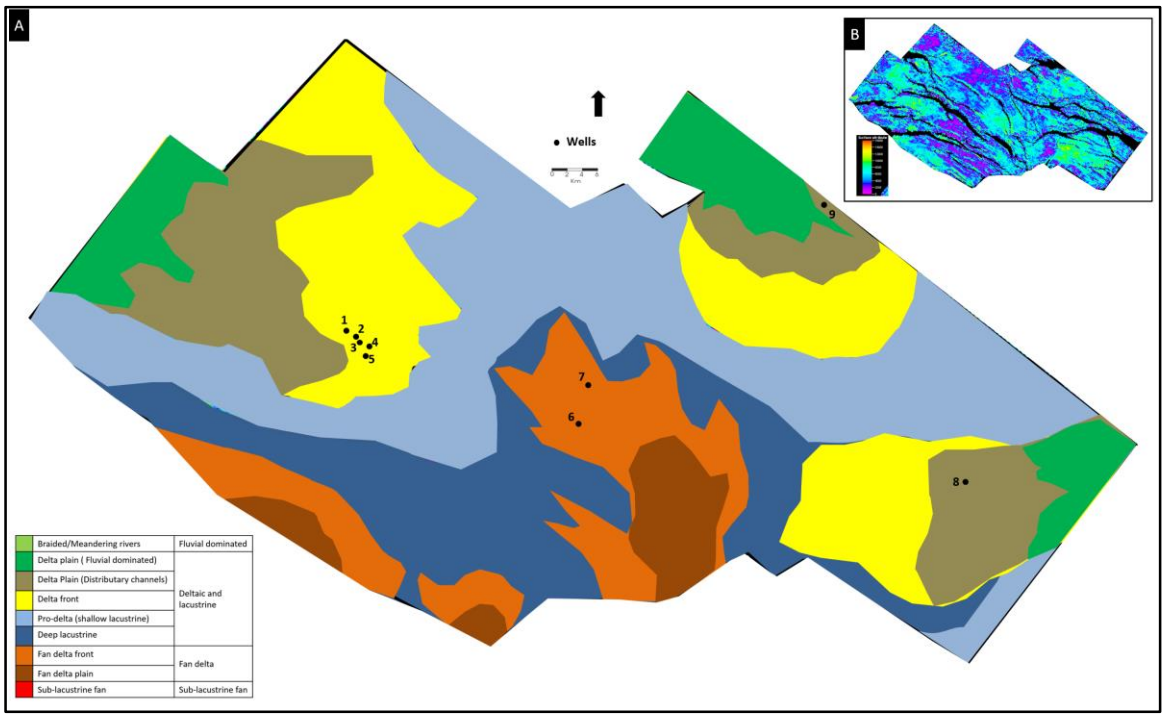

Figure 6-6: Schematic diagram showing depositional systems in the late syn-rift-2 stage of Abu Gabra Formation, Sufyan Sub-basin. This diagram mainly based on well data, seismic facies, and seismic attributes (Root Mean Square =RMS) (see RMS map above right corner).

The vertical evolution and lateral distribution pattern of sand bodies in the upper Abu Gabra Formation provide better insight about sandstone reservoir heterogeneity in macro to meso-scale (well log correlation) (Figure 6-9). Correlation profile crosses the braided delta (Figure 6-9), show the vertical and lateral variation.

6.5 Sequence stratigraphy

First order sequence is a sequence that was deposited in about 200-400 million years (Catuneanu, 2006; Catuneanu et al., 2011, 2009; Martins-Neto and Catuneanu, 2010). Second order sequence is a sequence that was deposited in about 10-100 million years (Catuneanu, 2006; Miall, 2013; Vail et al., 1977). Third order sequence is a sequence that was deposited in about 1-10 million years (Catuneanu, 2006; Miall, 2013; Vail et al., 1977).

6.5.1 Third order sequence

Within the major coarsening upward second order cycle deepening trend of Abu Gabra Formation, other minor sequences can be established. These small-scale sequences could be recognized from the lake level oscillations recorded, and fluvial graded profile adjustment. Thus, 3rd order sequences have been defined on the basis of major basin-wide lacustrine flooding episodes in Abu Gabra formation and fluvial type's variation. These cyclic patterns were caused by different allogenic and autogenic controls (Miall, 2010).

The end product of which gives the hierarchal arrangement of the stratigraphic column. There is five 3rd order sequences (from SQ-A to SQ-E) within the two 2nd order sequences (sub-rift phases) of Abu Gabra Formation (Figure 6-10 and Figure 6-11). The motif of gamma-ray logs of the study area is characterized by upward-coarsening and upward-fining Parasequence sets. Each Parasequence set and Parasequence is 10's meters thick.

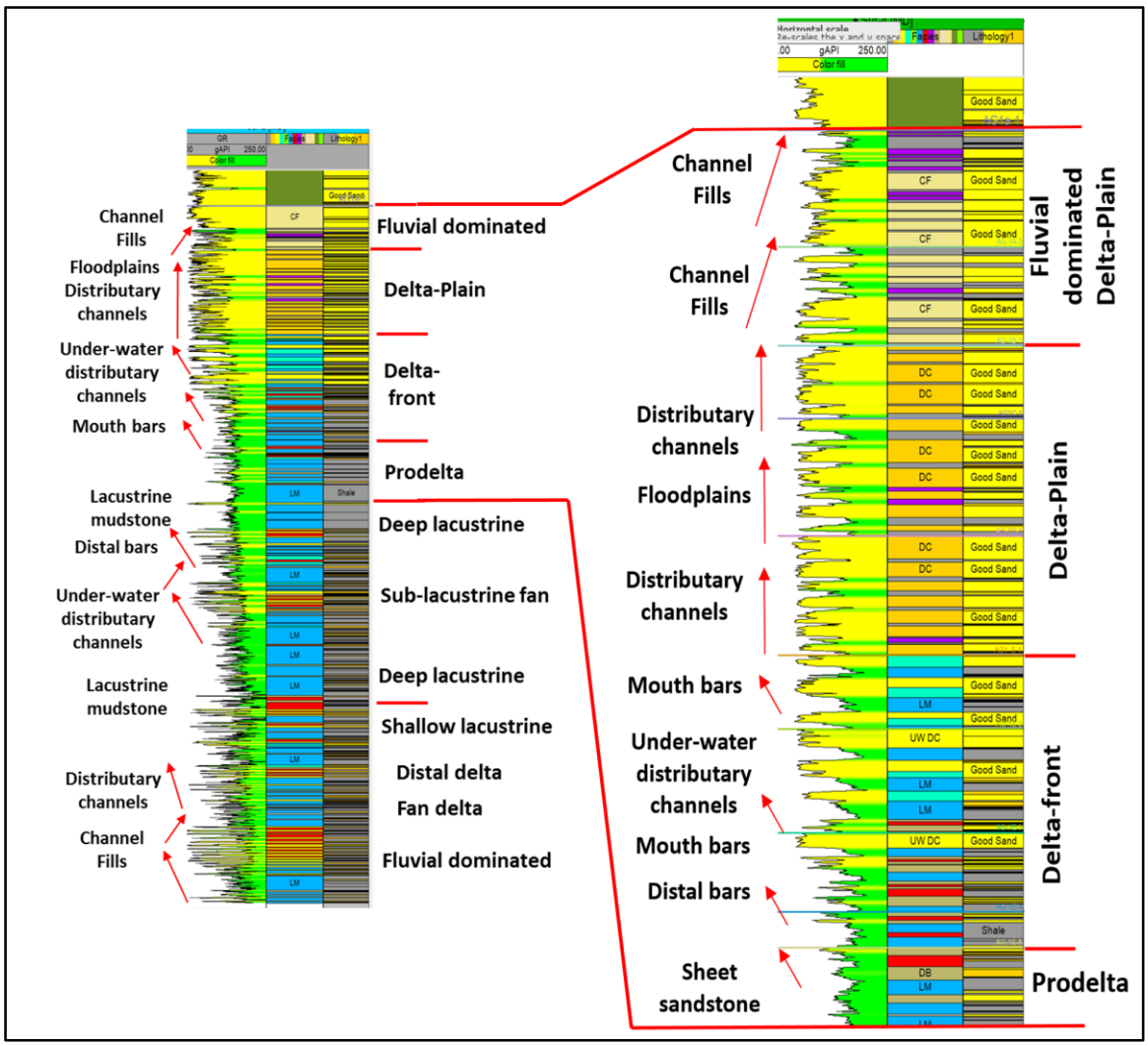

Figure 6-7: Vertical successions of braided delta which were deposited in Sufyan Sub-basin (for well location, see Figures. 1A and 5). Well log is the gamma ray (GR). Yellow color is sandstone dominated and green is mudstone dominated.

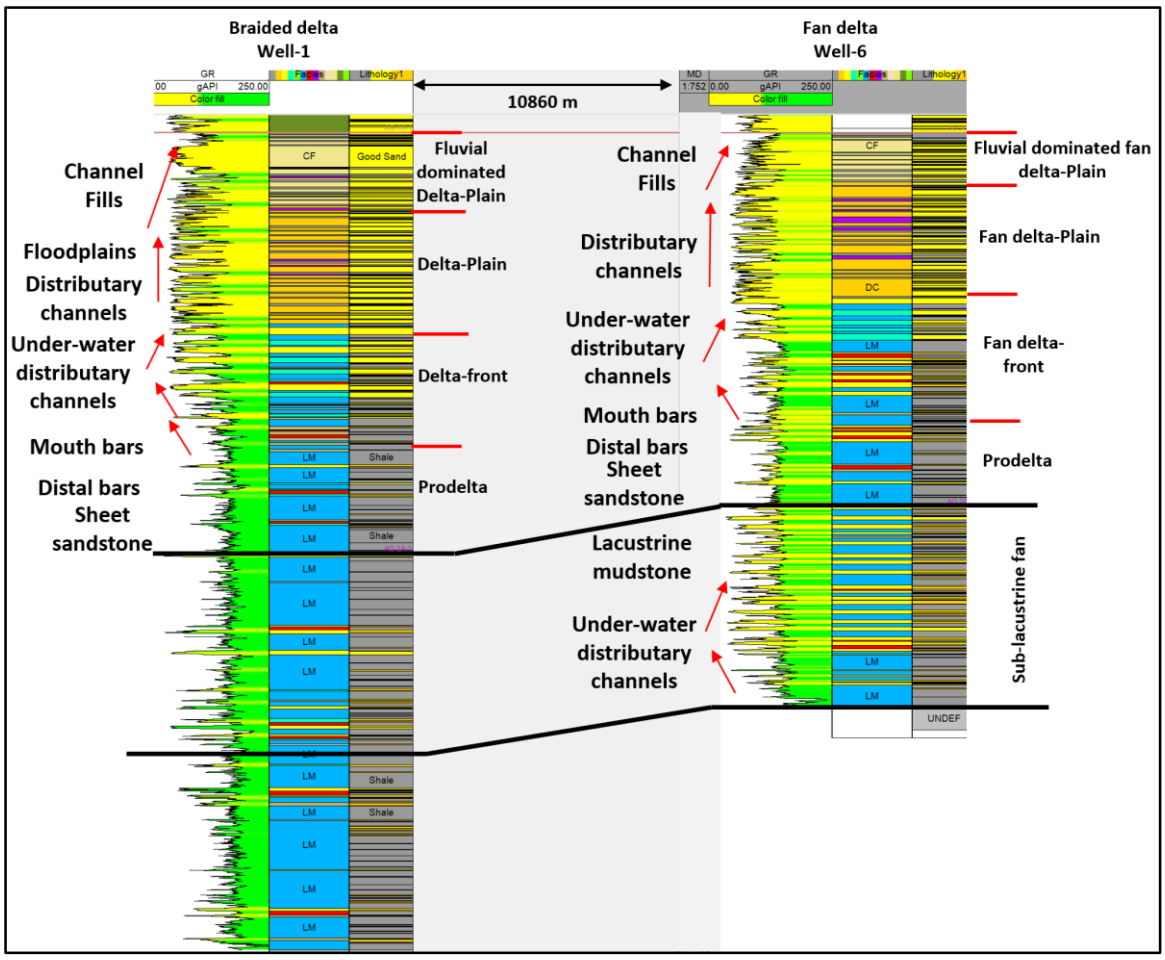

Figure 6-8: Vertical successions of fan-delta (left) and braided delta (right). Deposited in Sufyan Sub-basin (for well location, see Figures. 1A and 5). Well logs is the gamma ray (GR). Yellow color is sandstone dominated and green is mudstone dominated.

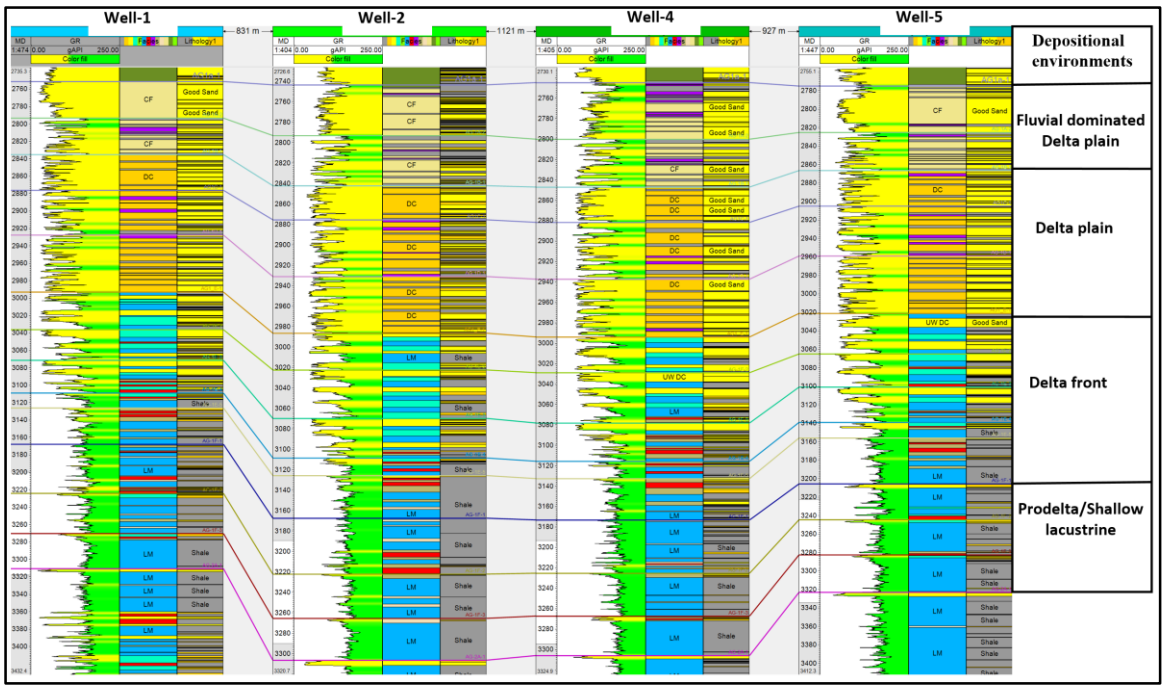

Figure 6-9: Correlation profile cross the study area with different interpreted depositional environments (for well location, see Figs. 1A and 5).

The upward coarsening Parasequence set, Parasequence, bed set thicknesses, sandstones coarsening upward, and the sandstone/claystone ratio varies considerably from one system tract to another. In the following section, SQ-E will be analyzed in detail. Sequence-E corresponds to the upper most part of the Abu Gabra Formation (AG-1) (Figure 6-10). In this sequence, the depositional system in Sufyan Sub-basin converts from lacustrine dominated (SQ-D) to shallow lacustrine, braided, and fan deltas dominated (SQ-E). This sequence reaches up to hundreds of meters thick and has been recognized basin-wide (Figure 6-6). At the sub-basin center, deep lacustrine mud deposits were developed while braided deltas and fan deltas occurred in the sub-basin margin (Figure 6-6). In Sufyan Sub-basin, fan delta mainly develops in the steep slope of the basin (southern area) while delta develops in the gentle slope (northern and northwestern areas) (Figure 6-6 and Figure 6-11). The lacustrine level was dropped while the braided deltas and fan deltas were expanding and occurred in the sub-basin margin. The vertical-facies associations within both the upward-coarsening and upward fining parasequences are interpreted to be a record of a gradual decrease in or an increase of water depth of the lacustrine system. The sequence reaches its maximum thickness at the basin edges where sedimentary load deposited when rivers enter the water body of the lake. Thickness starts thins basin-ward and grains size decreases. This sequence consists of transgressive system tract (TST), early highstand system tract (early HST), and late highstand system tract (late HST) (Figure 6-10). The late highstand system tract (late HST) is dominant and characterized by thick sandstone. The transgressive system tract (TST) interpreted to be the prodelta and shallow lacustrine where medium to coarse sandstone with a considerable amount of claystone is deposited. The early highstand system tract (early HST) interpreted to be deposited in the

delta-front, and the late highstand system tract (late HST) interpreted to be deposited in the delta-plain where considerable amounts of medium to coarse sandstone with a low amount of claystone is deposited.

On the seismic section, this sequence is characterized by discontinuous parallel reflectors, with possible progradational and aggradational reflectors close to the footwall. Parasequence within this sequence changes from being fining upward in lower part which represent the transgressive system tract (TST) to be coarsening upward in the upper sequence which represent the early highstand system tract (early HST) and late highstand system tract (late HST).

6.5.2 Parasequence sets, Parasequences, and bed sets

Parasequence set is define as a sequence of genetically related parasequences forming a unique stacking pattern and usually bounded by major flooding surface and their correlative surfaces (Van Wagoner et al., 1990).

In the study area, four parasequence sets interpreted in the 3rd order sequence (SQ-E). Each parasequence sets represent genetically related succession with distinctive stacking pattern and flooding surface as a boundary (Figure 6-12). Each parasequence set represents depositional sequence. Parasequence set-1: prodelta, Parasequence set-2: Delta front, Parasequence set-3: Delta plain, Parasequence set-4: Fluvial dominated delta plain (Figure 6-12).

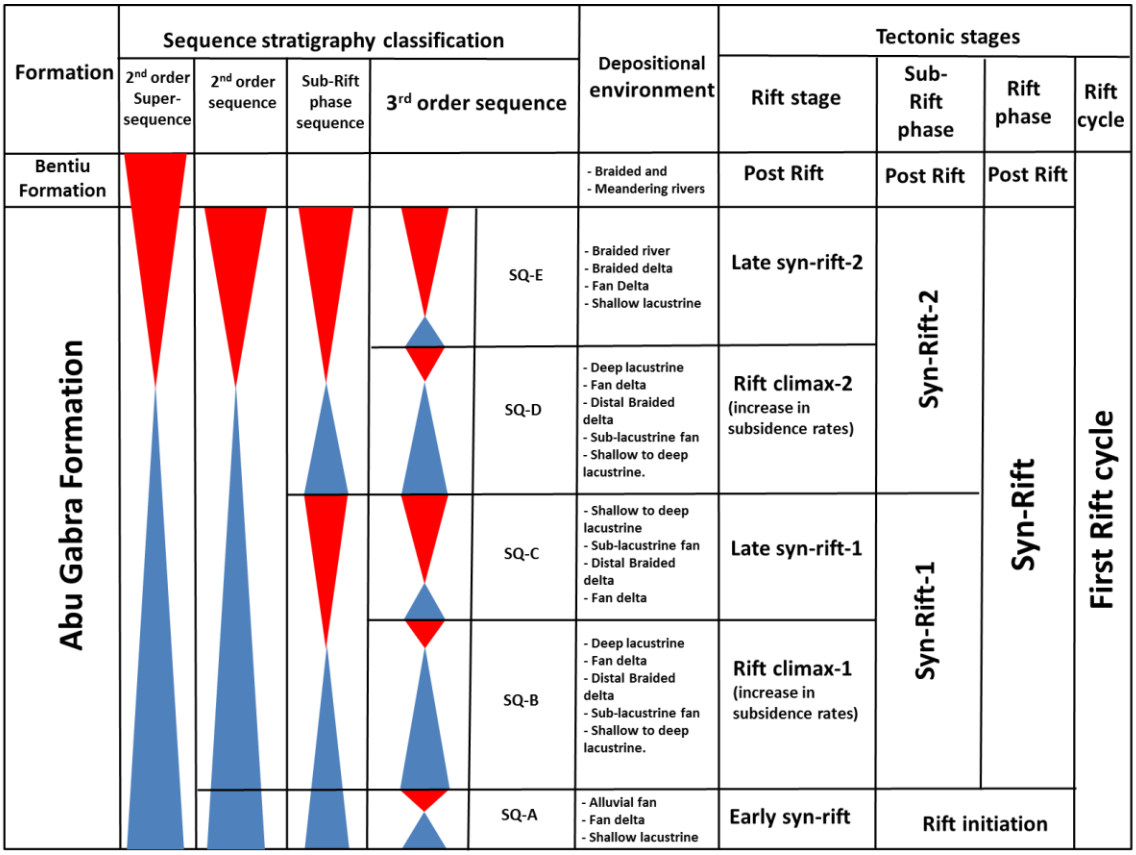

Figure 6-10: Depositional systems and sequence stratigraphic framework of the Lower Cretaceous (Abu Gabra Formation) for the Sufyan Sub-basin, Muglad Basin.

Parasequence set-2 divided into five parasequences (Figure 6-12), within each parasequence the sandstone bedsets thickening upward, sandstone/claystone ratio increases upward, and grain size increases upwards. The parasequence boundary of each one characterized by an abrupt change in lithology from sandstone below the boundary to mudstone above the boundary and abrupt decrease in bed thickness.

Parasequence set-2 (Figure 6-12) characterized by progradational Parasequence set (Figure 6-12). Within this parasequence set, the rate of deposition increase upward and the rate of accommodation space decrease upward and overall the rate of deposition is greater than the rate of accommodation.

For each braided delta and fan delta in the study area (Figure 6-6), parasequences could be correlated laterally (Figure 6-13) across the study area (for well location, see Figure 6-1B and Figure 6-6).

For wells 1, 2, 4, and 5 (Figure 6-13); parasequence 2-1 could be subdividing into four bed-sets. Sandstone beds thickening upward, sandstone/claystone ratio increases upward, and grain size increases upwards (Figure 6-13). Well-1 shows increase in sandstones beds correlated with the other wells. Parasequence 2-2 represent one bed-set with thick sandstone beds in well-2. Parasequence 2-3 could be subdividing into four bed-sets. Sandstone beds thickening upward, sandstone/claystone ratio increases upward, and grain size increases upwards (Figure 6-13). Parasequence 2-4 could be subdividing into four bed-sets (Figure 6-12). Parasequence 2-5 could be subdividing into three bed-sets (Figure 6-13).

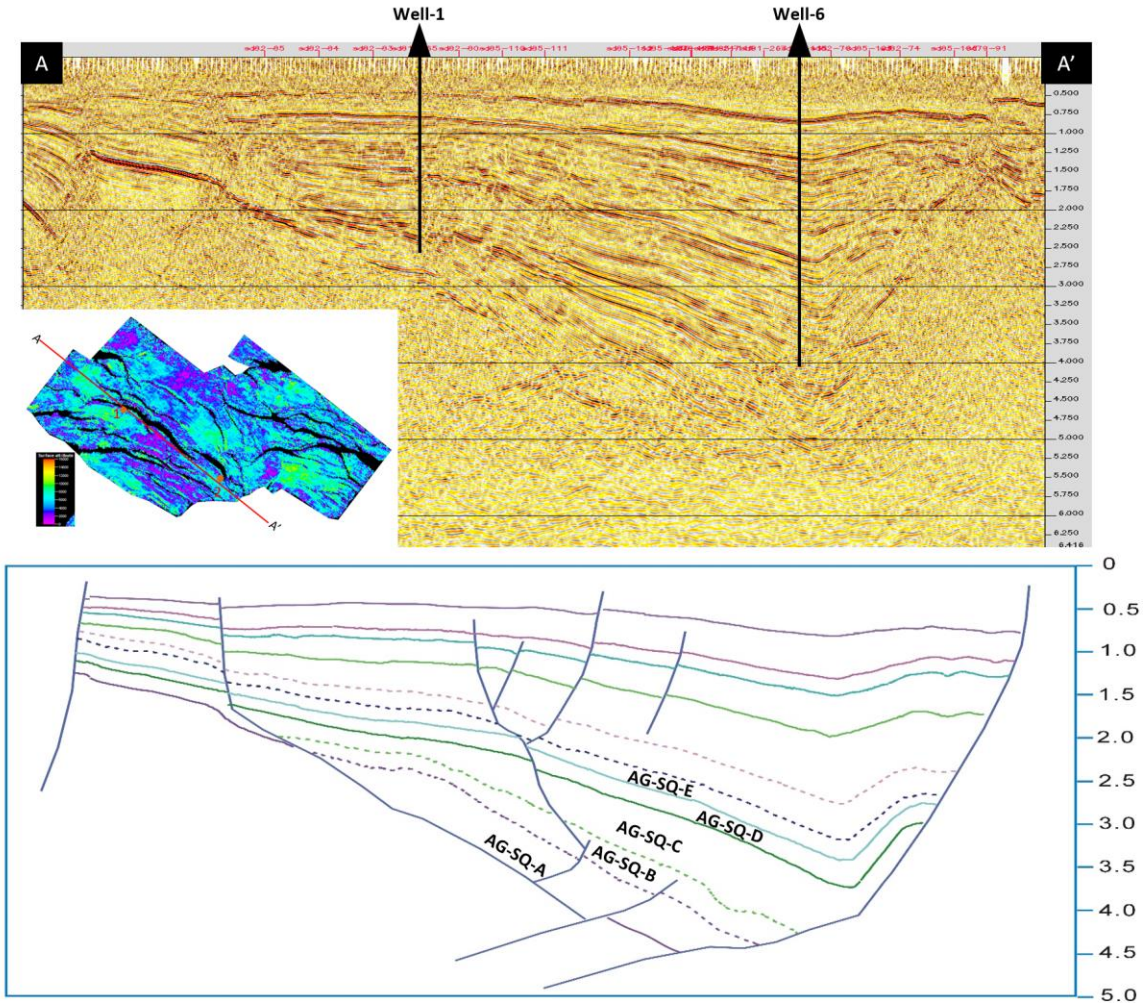

Figure 6-11: The seismic profile AA' and its interpretation (see location in Figure 6-1B). Seismic line (upper) and its interpretation (lower) with detail interpretation for the Abu Gabra Formation. In the middle, we can see the seismic attribute map (RMS: Root Mean Square). Well-1 drilled in the braided delta (ramp side of the major southern boundary fault), while well-6 drilled in the fan delta (wedge shape) close to the depocenters (cliff side of the major southern boundary fault) SQ=3rd order sequence.

The stratigraphic correlation of the upper Abu Gabra formation (SQ-E) introduced up to four parasequences sets depending on their presence in each well. This correlation is based on well logs (GR) and described cores from Abu Gabra Formation. Parasequence set-2 could be subdividing into five parasequences (Figure 6-12), parasequence set-3 could be subdividing into three parasequences (Figure 6-12), and parasequence set-4 could be subdividing into two parasequences (Figure 6-12). The stratigraphic zonation indicated that these parasequences sets and parasequences are completely present in the braided delta wells such as wells 1, 2, 4, and 5 (Figure 6-6 and Figure 6-8), which is located toward the northwest basin margin. For instance, in Well-6 (fan delta) the lowermost parasequences sets and parasequences show an increase in sandstone percentage (Figure 6-6 and Figure 6-8).

6.5.3 Tectono-sequence stratigraphy

The tectono-sequence stratigraphic evolution history of rift basins can be divided into several scales: the large scale (rift cycles) and it is corresponding to 2nd order super-sequence, the intermediate scale (rift phases) and it is corresponding to 2nd order sequences, and the small scale (rift stages) and it is corresponding to the 3rd order sequences (Ravnås et al., 2000; Zhou et al., 2014). The intermediate scale of the tectono-sequence stratigraphic evolution history of rift basins as described by Prosser (1993) are subdivided into four phases: rift initiation, rift climax, immediate post-rift, and late post-rift. The time of maximum rate of displacement of a fault can be termed the rift climax (Prosser, 1993). The large scale in Sufyan Sub-basin (rift cycles) is equivalent to 2nd order super-sequence and it is composed of three rift cycles (Figure 6-2). The intermediate scale in Sufyan Sub-basin

(rift phases) is corresponding to 2nd order sequence (Figure 6-2), each rift cycle consists of rift-initiation phase, syn-rift phase, and post-rift phase. The small scale in Abu Gabra Formation is equivalent to 3rd order sequence and it is composed of five stages of basin evolution, which are early syn-rift/rift initiation stage, rift climax-1 stage, late syn-rift-1stage, rift climax-2 stage, and late syn-rift-2 stage (Figure 6-10). The following section will focus on the tectono-sequence stratigraphy of the late syn-rift-2 stage, Upper Abu Gabra Formation (Sequence-E) in Sufyan Sub-basin.

The late syn-rift-2 stage

During this stage (Figure 6-10), SQ-E was deposited. This period is characterized by low or no tectonic subsidence and therefore the lake level was dropped. At the sub-basin center, deep lacustrine mud deposits were developed while braided deltas and fan deltas occurred in the sub-basin margin. During this stage, fan delta mainly develops in the steep slope fault zone in the southern area while delta develops in the gentle slope fault zone (northern and northwestern areas). Fluvial environment and braided delta environment deposited at the ramp side of the major southern boundary fault and fan delta deposited at the cliff side of the major southern boundary fault, those environments are immediately followed by small shallow lakes in the middle. The transition from the rift climax-2 to late syn-rift-2 stage was gradual, and it is characterized by shallow lacustrine and fluvio-deltaic environments. Facies types of this unit vary largely from one place to another depending on the location of delta lobes.

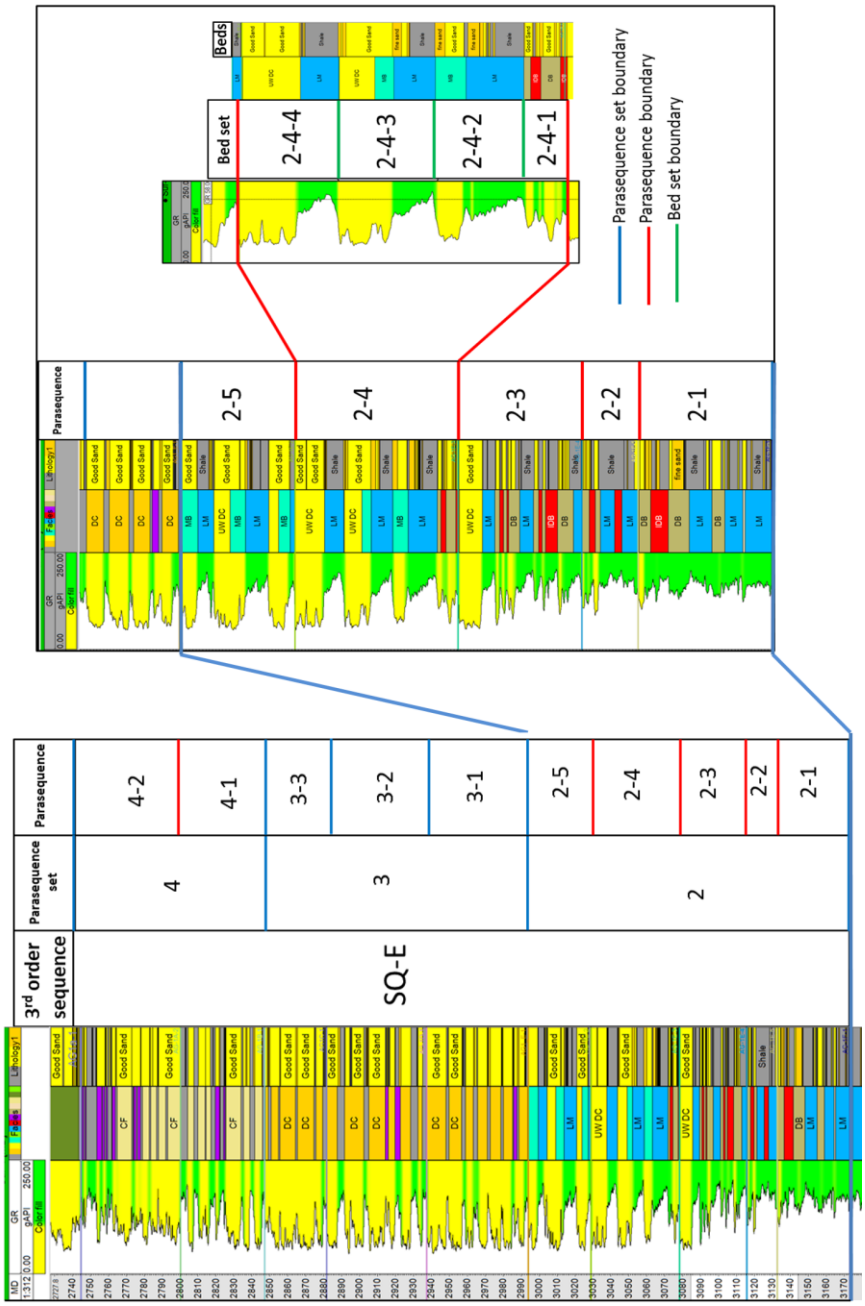

Figure 6-12: Well log (well-2) responses (GR) for a braided delta from the Early Cretaceous Abu Gabra Formation, Sufyan Sub-basin (for well location, see Figs. 1B and 5). Shows 3rd order sequence, parasequence sets, parasequences, bed set, and beds. The 3rd order sequence (SQ-E) composed of four parasequence sets, each one of them represent a depositional sequence. Parasequence set-1: prodelta, Parasequence set-2: Delta front, Parasequence set-3: Delta plain, Parasequence set-4: Fluvial dominated delta plain. Parasequence set-2, composed of five parasequences. Parasequence 2-4, composed of four-bed sets. Depth is in meters.

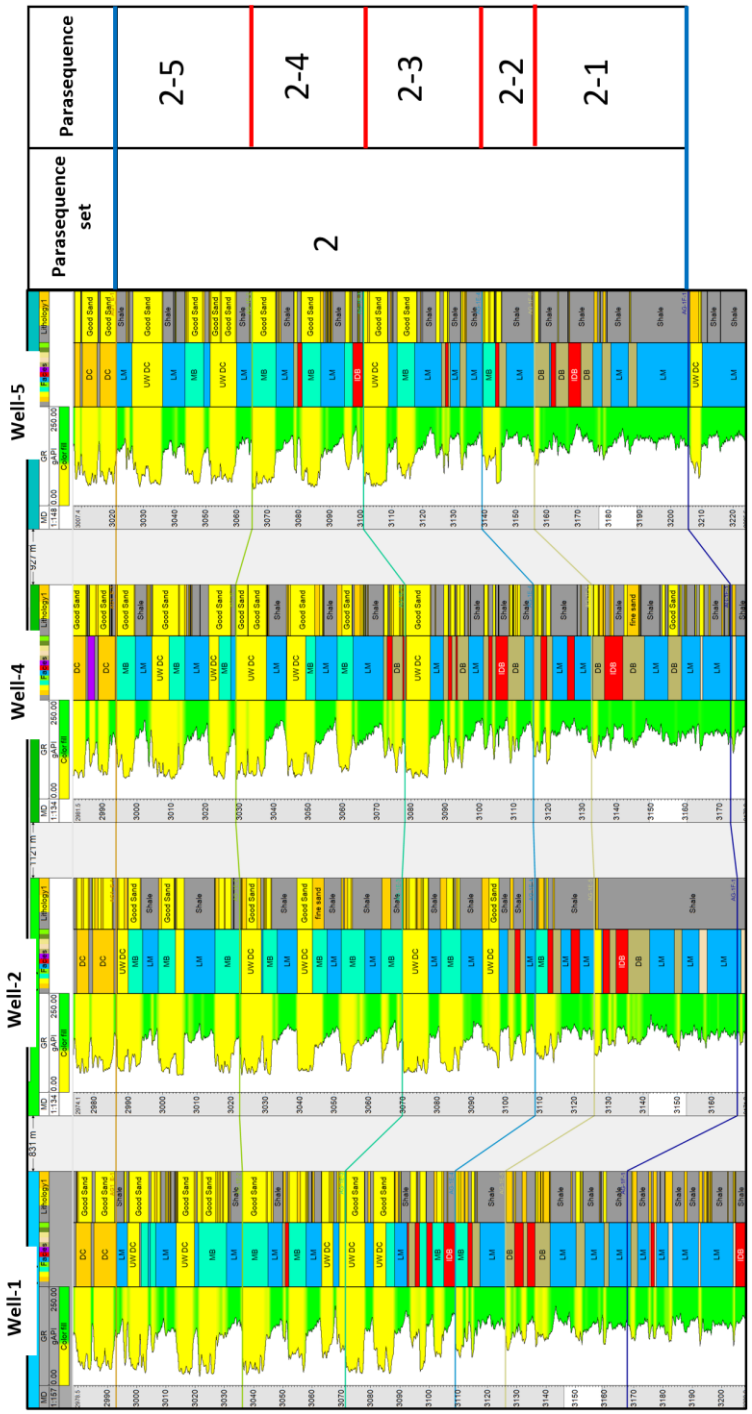

Figure 6-13: Parasequences correlation profile crosses the study area (for well location, see Figs. 1A and 5). The 3rd order sequence (SQ-E) composed of four parasequence sets, each one of them represent depositional sequence. Parasequence set-2, represent the delta front depositional sequences and composed of five parasequences.

At the proximal part, facies are dominated by coarse to very coarse grained sandstone with considerable amounts of gravels. The distal part is characterized by clay facies. Here the main control for accommodating water depth change is the tectonic activities and the main control for water supply is the climate.

The strata which deposited during this stage is consists of transgressive system tract (TST), early highstand system tract (early HST), and late highstand system tract (late HST) (Figure 6-10). The late highstand system tract (late HST) is dominant and characterized by thick sandstone (Figure 6-10). This sandstone is deposited in braided and Fan-delta plains as a result of the decrease of the accommodation space.

6.6 Petrography of sandstones

The point counting of thin-sections from the Abu Garba Formation reveal the presence of quartz, k-feldspar, plagioclase, Mica, and opaque minerals as detrital minerals. The authigenic minerals are mainly, clay cement, calcite cement, quartz overgrowth, and iron oxides cement.

6.6.1 Detrital composition

The Abu Gabra sandstones consist of Sub-feldspathic arenite to quartz arenite based on the sandstone classification of (Dott, 1964) (Figure 6-14). Detrital grains are dominated by quartz (45.8-70.6%) with an average of 54.94%, which is mostly monocrystalline quartz (17.4-62.8%) (Figure 6-15) with an average of about 36.92% and polycrystalline quartz (7.8-28.4%) with an average of about 18.02%. The content of feldspars mostly potassium feldspar (K-feldspar) (1.4-14.4%) with average about 10.08% from the whole volume and the plagioclase is relatively low (generally less than 5%). Few quantities of mica (0-2.4%)

and minor opaque minerals (0-1.8%) were found (Table 6-1). Feldspar is rarely found; it is less stable and alters to other minerals such as clays and micas during weathering and transportation. Detrital matrix clays have been recorded with much amount in all of the studies samples where their relative abundances vary between 9.8 and 4.6%. This amount has a patchy distribution and is pore filling (Table 6-1).

The quartz grains in the studied samples are sub-rounded to sub-angular and angular to sub-rounded. Furthermore, the sorting of the quartz grains in the studied sandstones samples moderately sorted to poorly sorted, moderately sorted and moderately sorted to well sorted. This could be attributed to the relatively shorter distance of transportation and to the relative less prolonged abrasion of the studied sandstones.

6.6.2 Authigenic Components/ Cements

Calcite cement was recorded on many samples at different depths with few amounts ranging between 0 to 6.8% with an average of 1.52% (Table 6-1). Siderite cement was not observed in most of the examined samples. Well-developed syntaxial quartz overgrowths (Figure 6-15) are recorded in all of the analyzed samples with few amounts ranging between 1% and 6.4% with an average of about 2.83%. Iron oxides are found in most of the examined samples and they were recorded as a cementing material. However, the iron oxides may reach maximum up to 3.4% (Table 6-1).

6.6.3 Clay minerals

The estimation of the clay mineral was performed mainly using the ethylene-glycol solvated XRD patterns as suggested by Schwertmann and Niederbudde 1993. The kaolinite was noted in all of the studied samples with different percentages ranging between 60.69%

– 98.10%. The favorable climatic conditions for the kaolinite development are basically tropical and subtropical climates. The authigenic kaolinite was formed due to the alteration of the K-feldspar in the organic-rich strata as occurred in studied samples at different depths. Furthermore, this detrital presence of the kaolinite has been confirmed by the relatively flatted kaolinite peaks in the XRD plates. The analysis of the clay mineral in the investigated samples shown traces of smectite minerals which range between 0.18% and 0.27%. Illite occurs as traces in all of the analyzed samples and varies between 1.18% and 1.55%. The chlorite was recorded in the all examined samples and ranging between 0.4 to 37.40%. Moreover, the high amount of chlorite in some of the studied clay minerals suggested that due to the source rock origin, which is rich in the ferromagnesian mineral.

6.6.4 Diagenetic processes

The detailed petrographic analysis of investigated core samples from Well-1 showed that the sedimentary succession was affected by several diagenetic processes, which have influenced its porosity and permeability. The identified diagenetic processes have either resulted in a decrease or in an increase of the porosity. Therefore, have diminished or improved the reservoir quality. Factors and processes which have reduced the porosity in Abu Gabra Formation sandstone are the kaolinite precipitation, the presence of detrital clays, carbonate cementation (calcite and siderite), iron oxides precipitation, compaction, and quartz overgrowths (Figure 6-16). Factors and processes which have increased the porosity in Abu Gabra Formation sandstone are included dissolution of feldspars and micas, partial dissolution of the calcite cement and clays, and chlorite coatings prevent quartz overgrowth.

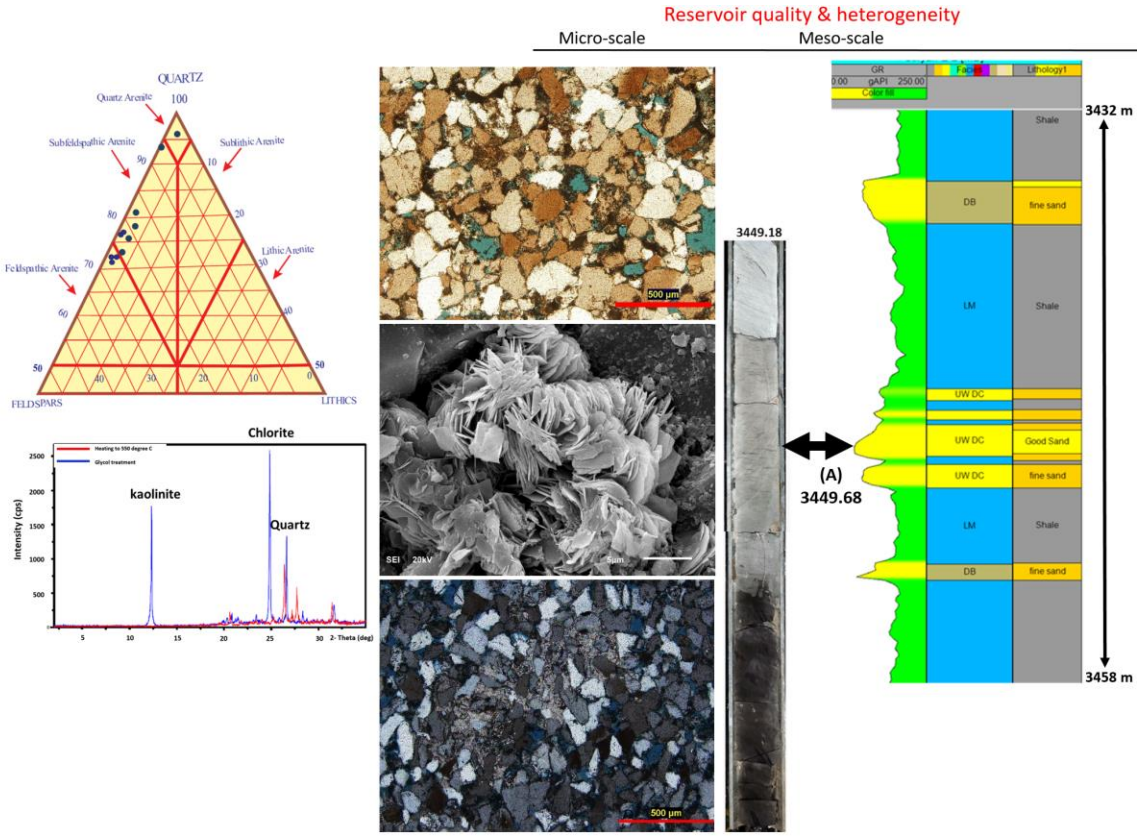

Figure 6-14: Reservoir quality and heterogeneity at a different scale. Showing facies analysis from core and well logs; sandstone classification (Dott, 1964), thin-sections, SEM, and X-ray diffraction analysis showing different clay types revealed in heating to 550 degree C and glycol treated diffractograms.

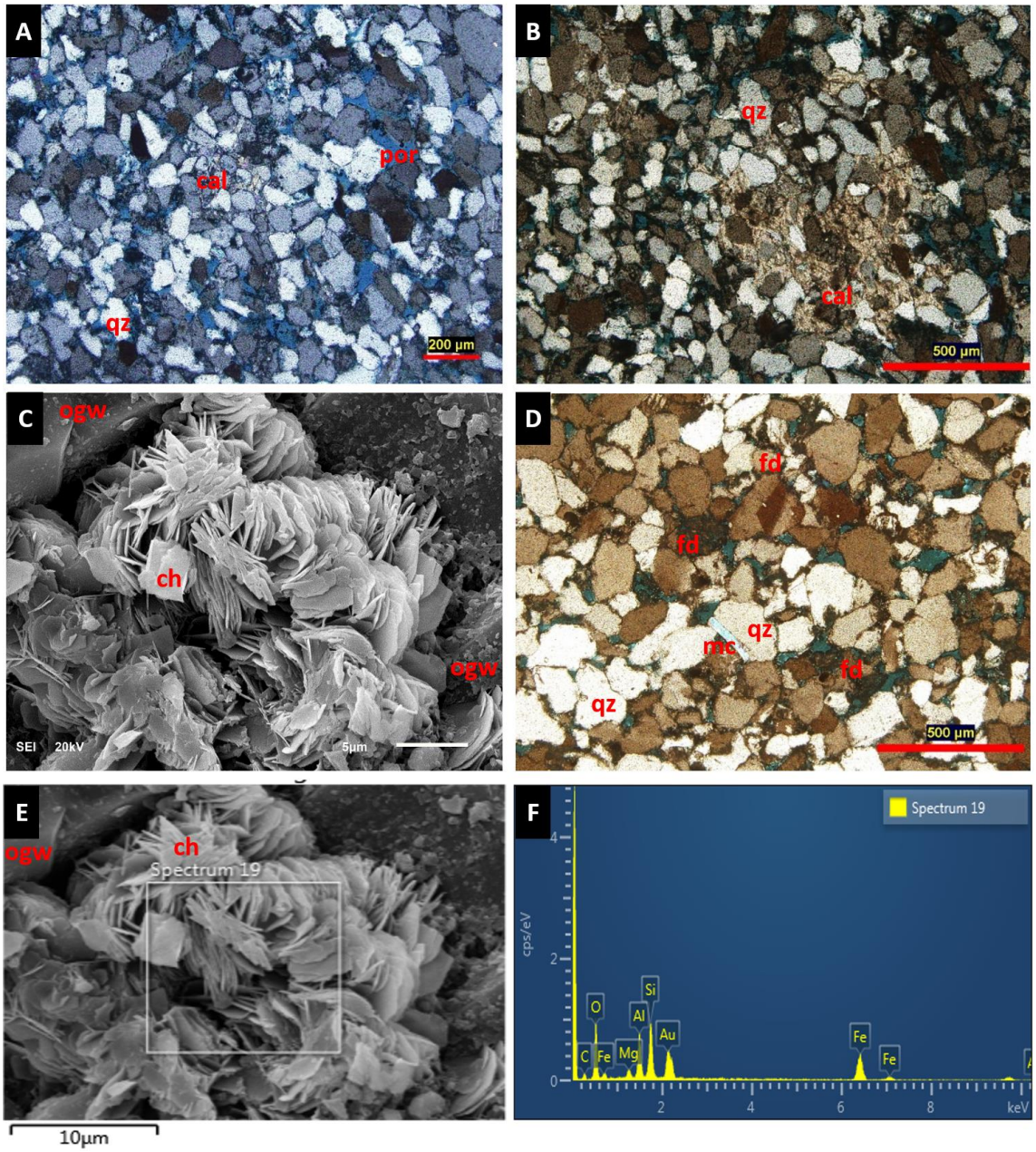

Figure 6-15: Examples of thin-section and SEM photomicrographs Note: ch: chlorite, qz: quartz, ogw: quartz overgrowth, fd: feldspar, mc: mica, Por: porosity. (A) Sub-feldspathic arenite sandstone (depth: 3449.68 m). (B) magnification photomicrographs of sandstones, showing calcite cement. (C) Diagenetic phase dominated by chlorite as pore filling (Chlorite grew on the surface of detrital grains) as well as authigenic quartz overgrowth. (D) magnification photomicrographs of sandstones, showing quartz, feldspars, felspar dissolution, mica, and porosity. Grain contact are mainly long, concavo-convex, and sutured. (E) Chlorite clay, showing the spectrum of the EDX. (F) Energy Dispersive X-Ray Spectrum (EDX), Chlorite $(Mg, Al, Fe)_{12}$ $[(Si, Al)_8 O_{20}]$ $(OH)_{16}$.

Table 6-1: Petrographic results (point-count) of the studied well-1. WS: well sorted; MS: moderately sorted; PS: poorly sorted; SR-R: sub-rounded to rounded; SR SA: sub-rounded- sub-angular.

Depth (m)	Textural Data			Rock name	Detrital Mineralogy								Authigenic Minerals					Porosity	
	Grain sorting	Grain roundness	AV. Pore connectivity		Poly crystalline Qtz. %	Monocrysta-lline Qtz. %	Lithic fragment. %	K-feldspar %	Plagioclase %	Micas %	Opaque %	Clay matrix %	Calcite cement %	Siderite cement %	Qtz over growth %	Pyrite cement %	Iron oxide cement %	Primary %	Secondary %
2965.4	MS-WS	SR-SA	Fair-good	Sub-Feldspathic Arenite	15.4	36	0	11.8	3.4	1.8	0.4	10.8	0	0	1.8	0	1.4	14.8	2.4
2967.3	MS-WS	SR-SA	Good	Sub-Feldspathic Arenite	12.4	34	0	10.4	3.8	0	1.8	9.8	0	1.4	1.8	0	3.4	18.4	2.8
2990.1	WS	SR-SA	Fair	Sub-Feldspathic Arenite	8.4	42.4	0	8.8	3.8	1.4	0.8	10.9	5	0.8	1.5	0	2.4	11.4	2.4
3317.3	MS	SR-SA	Fair-Poor	Sub-Feldspathic Arenite	24.8	29.4	0	13.8	0.8	0	1.2	11.6	1.4	0	3.4	0	0	11.8	1.8
3317.7	MS-PS	SR-SA	Fair-Poor	Sub-Feldspathic Arenite	27.8	23.8	0.4	14.4	0.8	2.4	0.4	14	0	0	2.4	0	0.4	10.8	2.4
3318	MS-PS	SR-SA	Fair-Poor	Sub-Feldspathic Arenite	23.8	32.8	0	11.8	0	0.8	0	14.6	0	0	2.8	0	0.8	10.8	1.8
3318.5	MS-WS	SR-SA	Fair	Sub-Feldspathic Arenite	19.4	35.8	0	10.8	0.8	0.8	0	13	0	0	3.4	0	0.8	13.8	1.4
3324.2	MS	A-SR	Fair -good	Sub-Feldspathic Arenite	28.4	17.4	0	13.8	0.8	0	0.4	13.2	0	0	6.4	0	1.8	15.4	2.4
3401.9	MS	SR-SA	Poor	Sub-Feldspathic Arenite	7.8	62.8	0	3.8	0.4	0	0.4	14.4	2	0.4	1	0	1.4	4.8	0.8
3403.5	MS-WS	SR-SA	Poor	Quartz Arenite	12	54.8	0	1.4	0.4	0.4	0.8	11.4	6.8	0.4	3.8	0	0.4	6	1.4

The presence of significant quantities of the clay matrix and precipitation of iron oxides and quartz overgrowths minerals in some of the studied reservoir sand beds contribute towards a decrease of the reservoir porosity at well-1.

Partial or total dissolution of feldspars during the diagenesis produces fair to fair-good reservoir porosity beds at well-1. Chlorite rims prevent precipitation of more quartz overgrowth and illite minerals during the diagenesis. Hence, chlorite clay mineral contributes enhancement of the reservoir porosity in studied intervals. The studied sandstones are poorly to moderately compacted and this indicated by the concavo-convex, tangential, long, and suture grain contact (Figure 6-15). Thin-section and SEM analysis show euhedral, smooth-faced, pyramidal quartz overgrowths. Kaolinite and chlorite are the main clay mineral identified in both X-ray diffractions and SEM-EDX analysis (Figure 6-14, Figure 6-15, Figure 6-16). Compaction of grains such as biotite (Figure 6-15) and fracturing of quartz was also observed.

6.7 Reservoir quality

6.7.1 Porosity and reservoir quality from thin-sections

Fair to good reservoir quality

The rock type of this reservoir is mainly sub-feldspathic arenite; granules to fine-grained, moderately sorted, angular to subrounded grains. Well cemented and highly compacted with long, concavo-convex, few point and minimum suture grains contact.

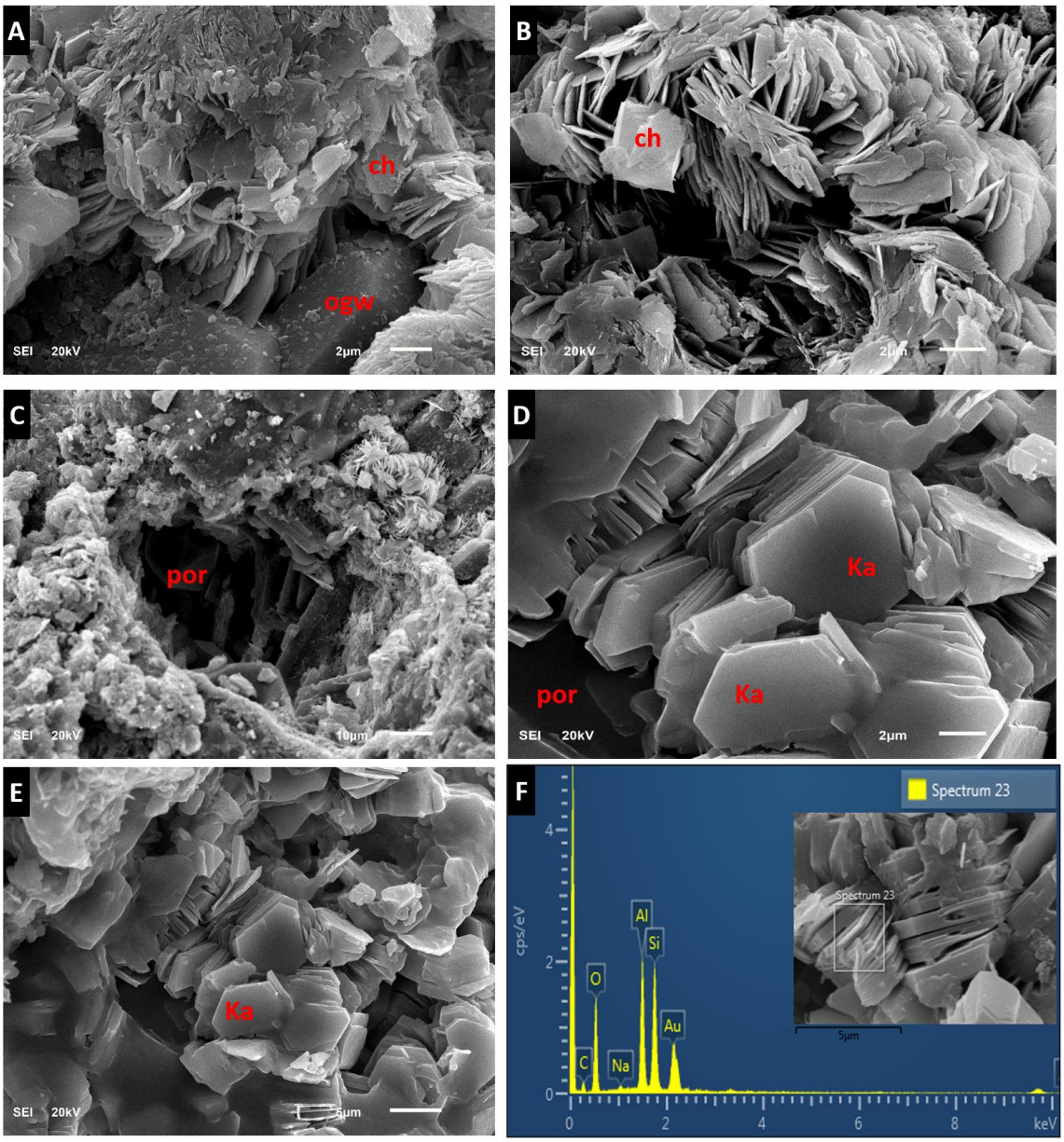

Figure 6-16: Examples of SEM photomicrographs Note: ch: chlorite, kn: kaolinite, gow: quartz overgrowth, and Por: porosity. (A) Quartz overgrowth coated by chlorite. (B) Diagenetic phase dominated by chlorite as pore filling. (C) Chlorite around the Pore-spaces. (D and E) Diagenetic phase dominated by booklet kaolinite as pore filling as well as authigenic quartz overgrowth. (D) Kaolinite clay, showing the spectrum of the Energy Dispersive X-Ray Spectrum (EDX), Kaolinite, $Al_4[Si_4O_{10}] (OH)_8$.

The detrital grains are commonly polycrystalline quartz with considerable amounts of monocrystalline quartz, some quantities of K-feldspar and minor quantities of plagioclase, traces of mica and minor heavy minerals, which occur as free grains such as pyroxene and others are enclosed inside the quartz grains were recorded.

The authigenic cement are mainly substantial quantities of quartz overgrowths and few iron oxides cement occur as pore filling were detected. The pore network mainly primary interparticle pores (14.8%) (Table 6-1), secondary interparticle porosity (2.4%) mainly through the partial to near dissolution of K-feldspar were detected (Figure 6-17A). Pore interconnectivity shows as fair-good.

Fair to poor reservoir quality

The rock type of this reservoir is mainly sub-feldspathic arenite (Figure 6-14); granules to medium-grained, moderate to poorly sorted, subrounded to subangular grains. Patchy cemented and moderately compacted with concavo-convex; long, point and minor suture grain contacts. The detrital grains are mainly composed of polycrystalline quartz with some amounts of monocrystalline quartz with fewer quantities of K-feldspar as well as minor plagioclase were detected. Few quantities of mica (Figure 6-15), minor opaques, as well as minors amount of heavy minerals, were found. Few quantities of quartz overgrowths and minor amounts of iron oxides were recognized as authigenic cement. The primary interparticle pores (10.8%), few secondary interparticle porosity and secondary intraparticle pore (2.4%) (Figure 6-17A) (Table 6-1) were found. Pore interconnectivity indicates as fair-poor.

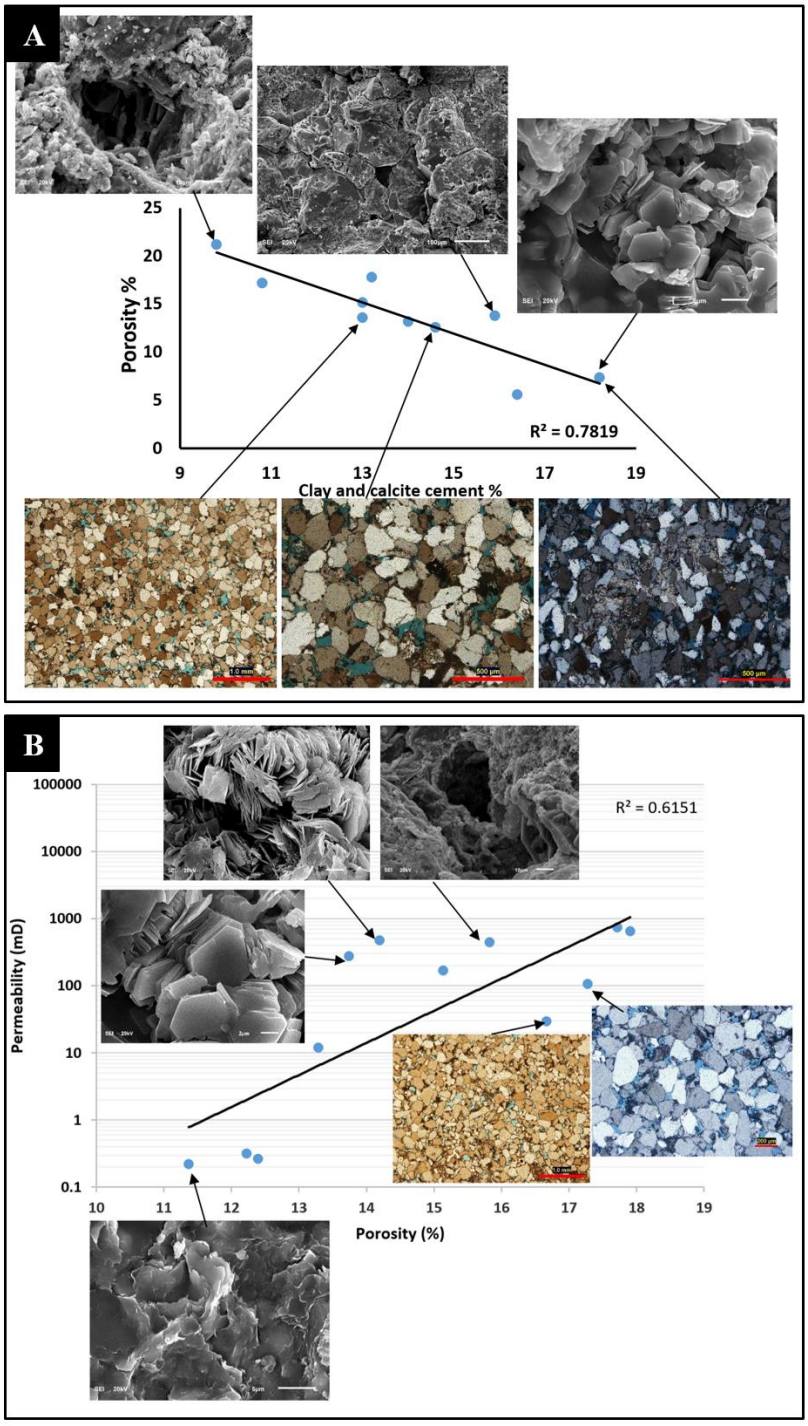

Figure 6-17: Reservoir properties data of the Abu Gabra sandstones and the related reservoir quality; (A) Intergranular porosity versus calcite cement and clay of well- 1 in the Sufyan oilfield (B) core plug horizontal permeability versus porosity.

Poor reservoir quality

The rock type of this reservoir is mainly quartz arenite, fine to medium-grained, moderately to well sorted, subrounded to subangular grains, well cemented and moderately compacted with concavo-convex, suture grains contact, float grains, long and minimum point.

The detrital grains are mainly monocrystalline quartz with some amounts of polycrystalline quartz were found. Few quantities of K-feldspar and plagioclase were detected.

Traces of mica and heavy minerals i.e. tourmaline, which occur as free grains and others are enclosed inside the quartz grains were observed. Considerable quantities of calcite and siderite cement occur as pore filling. Few patches of iron oxides and quartz overgrowths were recognized as authigenic cement. The interconnectivity is poor which are isolated primary interparticle pores (6%) (locked) spaced, traces and secondary interparticle porosity (1.4%) (Figure 6-17A) (Table 6-1) mainly through the partial to near dissolution of K-feldspar. Pore interconnectivity is poor.

6.7.2 Porosity and permeability from core plug analysis

Porosity and permeability were measured for the sandstones of diverse facies (Table 6-2). The sandstones that were deposited in the distributary channel during the HST have an average porosity of 17.6 % and average permeability of 494.33 mD. The average porosities and permeabilities of the underwater distributary channel sandstones are ranges between 15.4 % and 279.6 mD, respectively (Figure 6-17B), and those of mouth bar are 13.5 % and 144.3 mD, respectively, within the transgression system tracts (Table 6-2). The average porosities and permeabilities of the distal mouth bar sandstones are ranging from 12.23 %

and 0.31 mD, respectively (Figure 6-17B), and those of sheet sands (prodelta) are ranging from 11.88 % and 0.24 mD, respectively, within the transgression system tracts (Table 6-2).

6.8 Impact of depositional facies and diagenesis on reservoir quality

Facies analysis indicated that Abu Gabra Sandstone varies spatially and temporally (Figure 6-6 and Figure 6-7). Abu Gabra Formation deposited within a complex fluvio-deltaic and lacustrine systems and show a high degree of reservoir heterogeneity in a different scale from basin to micro-scale. This depositional facies heterogeneity is encountered as one of the main factors controlling the reservoir porosity and permeability.

Diagenetic processes such as cementation and dissolution are also main factors controlling the reservoir quality. For example, the presence of the clay matrix, pore filling, and kaolinite precipitation are the main factors considerably influence the reservoir quality (Bloch, 1991).

Generally, the basin and macro-scale heterogeneity seem to be controlled by the depositional facies, geometry, and architecture (Miall, 2010). The micro-scale heterogeneity mainly controlled by grain size and diagenetic processes (Aigner et al., 1990). Facies analysis from core and wireline logs revealed that the depositional systems of Abu Gabra Formation are mainly fan delta, braided delta, lacustrine system, and sublacustrine fan deposits. The understanding of the depositional reservoir heterogeneities might help for better prediction and assessment of reservoir quality and architecture (Slatt, 2006).

6.8.1 Depositional facies and sequence stratigraphic control

Depositional facies is a significant aspect that controlling the porosity and permeability of Abu Gabra Formation. In the study area, the late HST sandstones are interpreted to have been deposited in the delta plain environment, the early HST sandstone are interpreted to have been deposited in the delta front, and the TST sandstones are interpreted to have been deposited in the prodelta settings.

The late HST sandstones are more amalgamated than the early HST and the TST sandstones. The distributary channel sandstones have the maximum porosity and permeability within the late HST (Table 6-2). The porosity and permeability of the underwater distributary channel and the proximal mouth bar sandstone are greater than those deposited in the distal mouth bar within the early HST (Table 6-2). The sheet sands of the prodelta, show the minimum porosities and permeabilities within the TST (Table 6-2).

The Late HST distributary channel sandstones and the early HST underwater distributary channel and proximal mouth bar sandstones have the highest porosities and permeability, followed by the TST distal moth bar and sheet sand. The HST sandstones have a higher average secondary porosity than the TST sandstones (Table 6-2).

The TST sandstones have higher contents of calcite cements than the HST sandstones, which is controlled by the depositional settings of these sandstones. The Late HST distributary channel sandstones are less contact with Early Cretaceous thick shales of the lacustrine and distributed vertically and laterally, which makes the sandstones rarely being affected by the clay cement.

Table 6-2: The ranges of core porosities (%) and permeability es (mD) of the sandstones.

Nitrogen Permeability (Horizontal) mD	Helium Porosity (%)	Depositional facies	System tracts
644.99	17.91	Distributary channel	Late HST
732.07	17.72	Distributary channel	Late HST
105.03	17.28	Distributary channel	Late HST
29.54	16.67	Under-water distributary channel	Early HST
443.49	15.83	Under-water distributary channel	Early HST
168.24	15.14	Under-water distributary channel	Early HST
477.35	14.2	Under-water distributary channel	Early HST
276.99	13.74	Mouth bar	Early HST
11.77	13.29	Mouth bar	Early HST
0.31	12.23	Distal mouth bar	TST
0.26	12.4	Sheet sand	TST
0.22	11.37	Sheet sand	TST

6.8.2 Diagenetic control

Diagenetic processes are not changed the primary detrital composition only, but also affected the porosities and permeabilities of the Abu Gabra Formation sandstones because of dissolution of feldspars and micas, partial dissolution of the calcite cement and clays, the presence of clay matrix and precipitation of iron oxides, and quartz overgrowths.

Plots of intergranular porosity versus calcite cement (Figure 6-17A) and core plug horizontal permeability versus porosity (Figure 6-17B) reveal that cementation in reducing the primary Intergranular porosity of the Abu Gabra sandstones and the lowest porosities and permeabilities values affected by clay cement.

CHAPTER 7

GEOSTATISTICAL MODELING

7.1 Introduction

The latest studies of Abu Gabra Formation in Muglad Basin have focused mainly on source rocks rock characterization and evaluation (Lirong et al., 2013; Makeen et al., 2015a,b,c), sedimentology and tectonostratigraphy (Wu et al., 2015), tectonostratigraphic evolution and structural analysis (Yassin et al., 2016) without carefully investigating the reservoir characterization and geostatistical modeling of the sandstone beds within the area.

The geostatistical methods are commonly used in the oil industry for facies and reservoir property modeling (Deutsch, 2002a). These methods considered to be among the best tools to integrate data and information from a different source; sedimentology, stratigraphy, geophysics and petrophysics. It provides possible accurate models for reservoir rocks in 3D spatial distribution and their associated petrophysical properties (i.e. porosity, permeability and water saturation). A mining engineer from South Africa named, Daniel Krige, set the initial concepts for gold grade estimation (Krige, 1952). The geostatistics became much more closely affiliated with the work of Georges Matheron in Fontainebleau, France (Matheron, 1965, 1962) and during that time the geostatistics focused toward the mining industry (Journel and Huijbregts, 1978a). In the 80s, geostatistics was essentially viewed as a method to describe the spatial distribution and interpolation (Krige and Magri, 1982; Matrices et al., 1984). In 1992 Deusch and Journel published the famous geostatistics

software library (GSLIB) followed by many geostatistical techniques (Deutsch, 2002b). The minimum estimation variance is provided by Kriging at the unknown location through a set of linear combination of the surrounding values. Kriging became not suitable for reservoir modeling as it is not observing the high reservoir heterogeneities due to smoothing. Therefore, the stochastic approach has been introduced to reproduce the spatial variability and to deliver models that show high spatial variations based on a specified variogram model (Journel et al., 1997; Matheron, 1973). This approach has become a standard tool in reservoir modeling to address the reservoir heterogeneity and the uncertainty analysis.

In this chapter, the lithofacies classification for Abu Gabra Formation, Sufyan Sub-basin was performed using the available wells based on core analysis and wireline logs. The petrophysical reservoir properties such as porosity and volume of shale were also calculated using wireline logs (i.e., GR, RHOB, and NPHI) and core data. Cutoffs for facies, porosity, and shale volume were assigned and used for facies classification. Geostatistical analysis was performed for facies and petrophysical reservoir properties, it includes multivariate geostatistical analysis, variogram modeling, and data trend analysis. Facies association modeling was produced using Sequential Indicator Simulation (SIS) algorithm. Facies modeling was produced (three facies) using Sequential Indicator Simulation (SIS) algorithm. The modeled facies include clean sand (medium to coarse grained sandstone), shaly sand (fine to silty sandstone), and shale (shale/claystone) facies. The porosity model was done using Sequential Gaussian Simulation (SGS) algorithm.

7.2 Lithofacies classification and facies associations

Based on the interpretation of seismic, core, and well log data, four types of the depositional system were interpreted (fan delta, braided delta, lacustrine system, and sublacustrine fan deposits) in Sufyan Sub-basin. In this 3D geostatistical modeling part, we will concentrate on two depositional systems (braided delta and lacustrine systems). Four sub-environment were interpreted in the braided delta; those are fluvial-dominated delta plain, delta plain, delta front, and prodelta. Lithofacies associations interpretation indicate that ten lithofacies associations. The fluvial-dominated delta includes floodplains (FP), crevasses splays (CS), and channel fills (CF); the delta plain includes distributary channels (DC) and floodplains (FP); the delta front includes underwater distributary channels (UW DC), mouth bars (MB), Interdistributary bay (IDB), and distal bars (DB). The prodelta includes lacustrine mudstone (LM) and sheet sand (SS) (Figure 7-1).

Seven lithofacies were recognized in Abu Gabra Formation were using core description. It is mainly composed of continental-derived clastics (sandy, silty, and shaly facies).

Formation	Depositional system	Sub-environment	Microfacies	Abbreviation	Gamma ray geometry		
					Curve Shape	Lithofacies	Curve Samples
Abu Gabra	Braided Delta	Fluvial dominated delta plain **(LfA-7)**	Floodplain	FP	Linear shaped	Lf6, Lf5	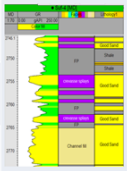
			Crevasse splays	CS	Funnel shaped	Lf6, Lf4, Lf2, Lf5	
			Channel fill	CF	Box or bell shaped	Lf6, Lf2, Lf3, Lf5	
		Delta plain **(LfA-6)**	Distributary channel	DC	Box or bell shaped	Lf2, Lf3, Lf6	

Formation	Depositional system	Sub-environment	Microfacies	Abbreviation	Gamma ray geometry		
					Curve Shape	Lithofacies	Curve Samples
Abu Gabra	Braided Delta	Proximal delta Front **(LfA-5)**	Underwater Distributary Channel	UW DC	Box or bell shaped	Lf3, Lf4, Lf6	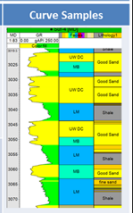
			Mouth Bar	MB	Funnel shaped	Lf5, Lf3	
		Distal delta Front **(LfA-4)**	Interdistributary Bay	IDB	Linear shaped	Lf5, Lf6	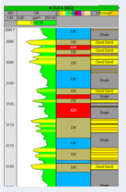
			Distal Bar	DB	Funnel shaped	Lf7, Lf5, Lf4	

Formation	Depositional system	Sub-environment	Microfacies	Abbreviation	Gamma ray geometry		
					Curve Shape	Lithofacies	Curve Samples
Abu Gabra	Lacustrine/ Prodelta	Prodelta/ Shallow Lacustrine **(LfA-3)**	Sheet Sand	SS	Interfinger	Lf5, Lf6, Lf4	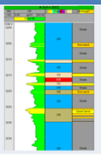
		Sub-lacustrine fan **(LFA-2)**	Sub-lacustrine distributary channel	SLDC	bell shaped	Lf3, Lf4, Lf6	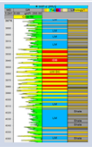
		Semi-Deep lacustrine **(LfA-1)**	Lacustrine mudstone	LM	Linear shaped	Lf7	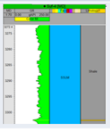

Figure 7-1: Four sub- environment were interpreted in the braided delta; those are fluvial-dominated delta plain, delta plain, delta front, and prodelta. Lithofacies associations interpretation indicate that ten lithofacies associations. The fluvial-dominated delta includes floodplains (FP), crevasses splays (CS), and channel fills (CF); the delta plain includes distributary channels (DC) and floodplains (FP); the delta front includes underwater distributary channels (UW DC), mouth bars (MB), Interdistributary bay (IDB), and distal bars (DB). The prodelta includes lacustrine mudstone (LM) and sheet sand (SS).

These include bedded conglomeratic sandstone (Lf1), planar cross-bedded sandstone (Lf2), trough cross-bedding sandstone (Lf3), massive sandstone (Lf4), ripples cross-laminated sandstone (Lf5), massive to blocky mudstone and siltstone (Lf6), and mudstone and shale (Lf7).

Based on the composition and vertical distribution, the identified facies can be grouped into three main facies groups. These are; the medium to coarse-grained sandstone group, fine to silty sandstone group, and shale to claystone group. Each facies group is described below in terms of its main characteristics, association, vertical distribution and depositional environment.

7.2.1 Medium to coarse-grained sandstones lithofacies group

Description: This lithofacies group consists of three lithofacies; bedded conglomerate (Lf1), planar (Lf2), and trough (Lf3) cross-bedded sandstone. It described as a light grey, medium to coarse-grained, unconsolidated to poorly consolidated, sub-rounded to sub-angular sandstones. The relatively coarse-grained sediments represent high energy and relatively high sediment supply exceeding the available accommodation space leading to high degree of amalgamation (sheet-like deposits).

This lithofacies is characterized by blocky shapes of low gamma rays (Figure 7-1). The corresponding lithological profile from the core and cutting description displays a medium to coarse grained sandstone and minor amounts of gravel with a grain size ranging from 60 to 75 mm. The Abu Gabra sandstones consist of Sub-feldspathic arenite to quartz arenite based on the sandstone classification of (Dott, 1964).

Table 7-1: The codes used to describe the Lithofacies. This table summarizes the facies grouping in the Abu Gabra Formation.

Facies Code	Lithofacies	Core Facies
1	Clean Sand Facies	Medium to coarse grained sandstones lithofacies group
2	Shaly Sand Facies	Fine to silty sandstone lithofacies group
3	Shale Facies	Shale/claystone lithofacies group

Detrital grains are dominated by quartz with an average of 54.94%, which is mostly monocrystalline quartz and polycrystalline quartz. The content of feldspars mostly potassium feldspar (K-feldspar) with average about 10.08% from the whole volume and the plagioclase is relatively low (generally less than 5%).

Few quantities of mica (0-2.4%) and minor opaque minerals (0-1.8%) were found. Feldspar is rarely found; it is less stable and alters to other minerals such as clays and micas during weathering and transportation. Detrital matrix clays have been recorded with much amount in all of the studies samples where their relative abundances vary between 9.8 and 4.6%.

Interpretation: The medium to coarse grained sandstone deposits indicated (delta plain) deltaic system. The bedded conglomerate sandstone facies (Lf1) represents a distributary channel deposits primary in fan delta front or braided delta plain. The planar cross-bedded sandstone facies (Lf2) is indicating transverse and linguoid bedforms (2-D dunes) in a fluvial channel (braided channel or point bar) or distributary channels deposited mainly in fluvial dominated part of the delta plain as well in crevasse splays. The trough cross-bedded sandstone facies (Lf3) is indicating for sinuous-crested and linguoid (3-D Dunes). Migrating 3-D dunes in a braided channel bar. Dunes (fluvial channel or delta distributary channel or delta mouth bar).

7.2.2 Fine to silty sandstone lithofacies group

Description: This lithofacies group consists of three lithofacies; massive sandstone (Lf4) and ripples cross-laminated sandstone (Lf5). The massive sandstone (Lf4) consist of very fine to coarse sandstone. Massive or faint lamination. It describes as a light grey massive

sandstone facies, with fine to coarse grain size. Long transportation distance was proposed based on the grain sorting results (well to moderately sorting).

The fine-grained sandstone is well sorted, suggesting the transport distances were great. The ripples cross-laminated sandstone (Lf5) consist of very fine to coarse sand. It describes as light grey ripples laminated sandstone facies, with very fine grain size. The grains vary from rounded to sub-rounded with moderately sorting with flaser bedding. Usually, they occupy the top part of coarser and sandy facies with an overall fining-up vertical trend.

This lithofacies is characterized by stacked funnel shapes of coarsening-upward cycles (Figure 7-1). The corresponding vertical profile from a cutting description shows mudstone interbedded with sandstone and siltstone.

Interpretation: The fine to silty grained sandstone deposits indicated (mainly delta front) deltaic system. The massive sandstone (Lf4) represents underwater distributary channels deposits primary in the braided delta. The ripples cross-laminated sandstone (Lf5) represents the ripples (top fluvial bar or delta mouth bar or levee or crevasse splay distal bar).

7.2.3 Shale/claystone lithofacies group

Description: This lithofacies group consists of two lithofacies; massive to blocky mudstone and siltstone (Lf6); mudstone, shale, and siltstone lithofacies (Lf7).

The massive to blocky mudstone and siltstone (Lf6) consist of mudstone and siltstone. It describes as a massive mudstone with desiccation cracks to blocky mudstone and siltstone. The mudstone is mainly dark grey moderately laminated to massive with some root casts. The mudstone and shale (Lf7) consist of mudstone, shale, very fine sandstone, and

siltstone. It describes as black shale, dark grey to greenish-grey mudstone, and horizontally laminated bedding siltstone and very fine sandstone. The very fine lithofacies deposits indicate that it is mainly deposited in Prodelta, semi-deep to deep lacustrine. This facies represents the low energy deposits. This lithofacies association is characterized by high gamma ray values (serrated linear shape of gamma ray) with a predominance of claystone in the lithology (Figure 7-1).

Interpretation: The shale/claystone lithofacies deposits indicated deltaic and lacustrine systems. The massive to blocky mudstone and siltstone (Lf6) represents overbank or flood deposits or prodelta deposits or interdistributary bay. The mudstone, shale, and siltstone lithofacies (Lf7) represent prodelta, shallow to deep lacustrine deposits or interdistributary bay.

7.3 Depositional systems

Braided delta deposits in Sufyan Sub-basin are developed mainly on the ramp slope side of the southern boundary fault. In Sufyan Sub-basin, braided delta deposits are characterized by vertical stacking of distal braided facies of distributary channels deposits in the delta plain and progradation of braided delta front deposits and prodelta that upgraded to lake setting. By combining the core data and logging curve, three, two, four, and two micro-facies were identified in the fluvial-dominated delta plain, delta plain, delta front, and prodelta (Figure 7-2) respectively.

In this study, the interpretation of the braided delta (Figure 7-2B) strongly enhanced by the integration of the high-resolution seismic attributes (Root Mean Square) (Figure 7-2A), spatially and the high-resolution wireline logs (Figure 7-2C), temporally.

7.4 Parasequence sets, Parasequences, and bed sets

Parasequence set is define as a succession of genetically related parasequences forming a distinctive stacking pattern and commonly bounded by major flooding surface and their correlative surfaces (Van Wagoner et al., 1990). Parasequence is defined as a relatively conformable succession of genetically related beds or bed-sets bounded by flooding surfaces and their correlative surfaces. Bed-sets is defined as a relatively conformable succession of genetically related beds bounded by surfaces (called bed-set surfaces) of erosion, non-deposition, or their correlative conformities (Van Wagoner et al., 1990).

In the study area, four parasequence sets interpreted in the 3rd order sequence (SQ-E) (Figure 7-2C). Each parasequence sets represent genetically related succession with distinctive stacking pattern and flooding surface as a boundary. Each parasequence set represents a depositional sequence.

Parasequence set-1: prodelta (with sand shale ratio 15 % and 85 % respectively) (Figure 7-3), Parasequence set-2: Delta front (with sand shale ratio 48 % and 52 % respectively), Parasequence set-3: Delta plain (with sand shale ratio 80 % and 20 % respectively), Parasequence set-4: Fluvial dominated delta plain (with sand shale ratio 75 % and 25 % respectively) (Figure 7-3). This subdivision mainly based on gamma ray well logs (GR) and described cores from Abu Gabra Formation.

Parasequence set-1 could be subdividing into three parasequences, parasequence set-2 could be subdividing into five parasequences (Figure 7-4C), parasequence set-3 could be subdividing into three parasequences, and parasequence set-4 could be subdividing into two parasequences (Figure 7-4C).

The stratigraphic zonation indicated that these parasequences sets and parasequences are completely present in the braided delta wells such as wells 1, 2, 4, and 5, which is located toward the northwest basin margin.

Parasequence set-2 divided into five parasequences (Figure 7-4), within each parasequence the sandstone bed-sets thickening upward, sandstone/claystone ratio increases upward, and grain size increases upwards. The parasequence boundary of each one characterized by an abrupt change in lithology from sandstone below the boundary to mudstone above the boundary and abrupt decrease in bed thickness. Parasequence set-2 characterized by progradational Parasequence set (Figure 7-4). Within this parasequence set, the rate of deposition increase upward and the rate of accommodation space decrease upward and overall the rate of deposition is greater than the rate of accommodation.

For wells 1, 2, 4, and 5; parasequence 2-1 could be subdividing into four bed-sets (Figure 7-4). Sandstone beds thickening upward, sandstone/claystone ratio increases upward, and grain size increases upwards. Well-1 shows increase in sandstones beds correlated with the other wells. Parasequence 2-4 could be subdividing into four bed-sets (Figure 7-4).

7.5 Petrophysical analysis

Wireline logs in Sufyan oilfield were used to characterize the petrophysical parameters of Abu Gabra Formation. The main objectives of the petrophysical analysis are the formation evaluation and the discrimination between reservoir (sand) rocks and non-reservoir (shale) zones in the available wells. The petrophysical characteristics were used to calculate the formation evaluation parameters such as shale volume (Vsh), effective and total porosity (Φ).

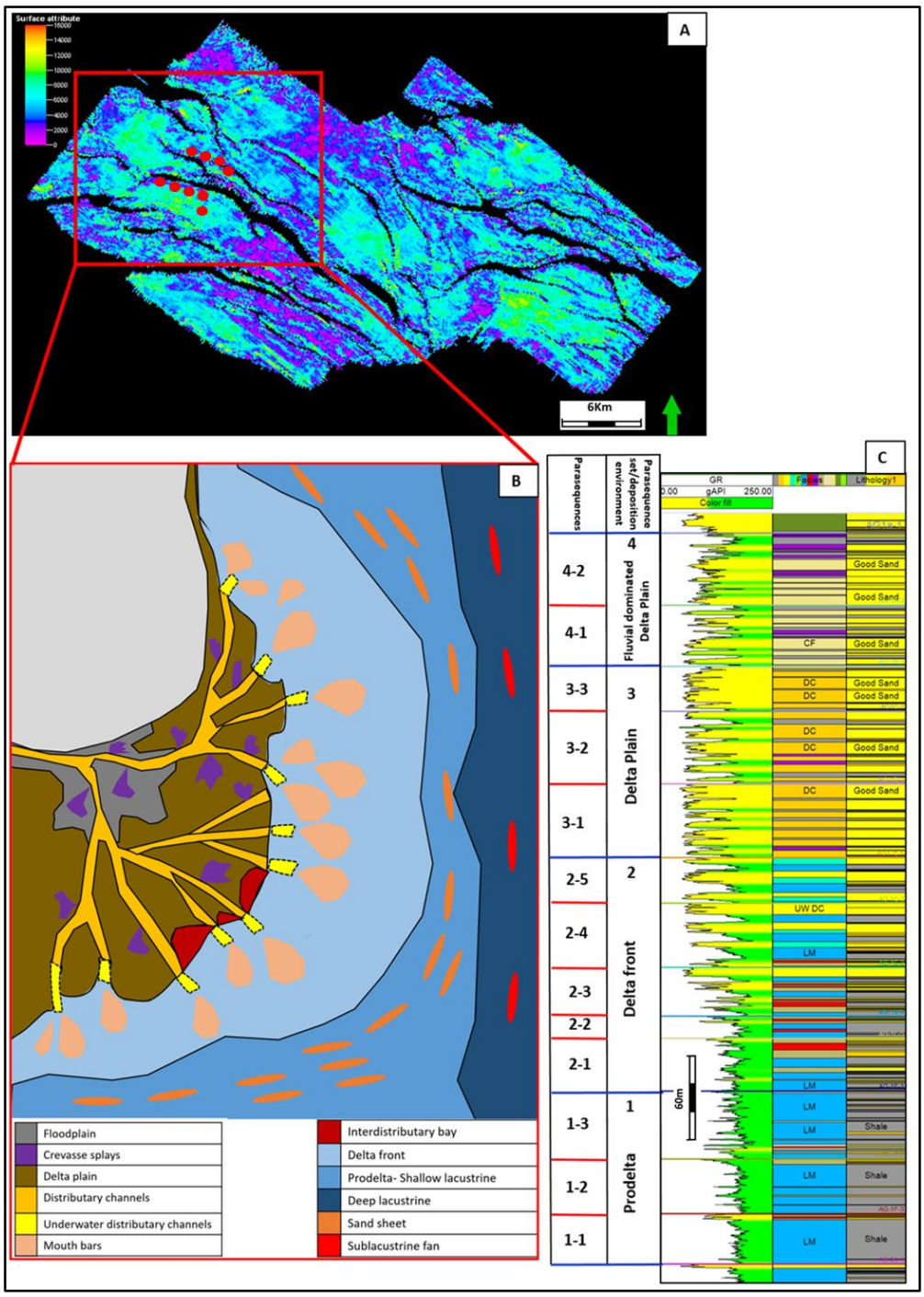

Figure 7-2: Conceptual model of braided delta interpreted in the study area. This diagram mainly based on well data, seismic facies, and seismic attributes (Root Mean Square =RMS) (A). Schematic diagram showing the depositional model in the late syn-rift-2 stage of Sufyan Sub-basin (B). Parasequence sets, parasequences, and facies associations interpreted using well logs (GR) and core data. The 3rd order sequence (SQ-E) composed of four parasequence sets, each one of them represent a depositional sequence. Parasequence set-1: prodelta, Parasequence set-2: Delta front, Parasequence set-3: Delta plain, Parasequence set-4: Fluvial dominated delta plain (C).

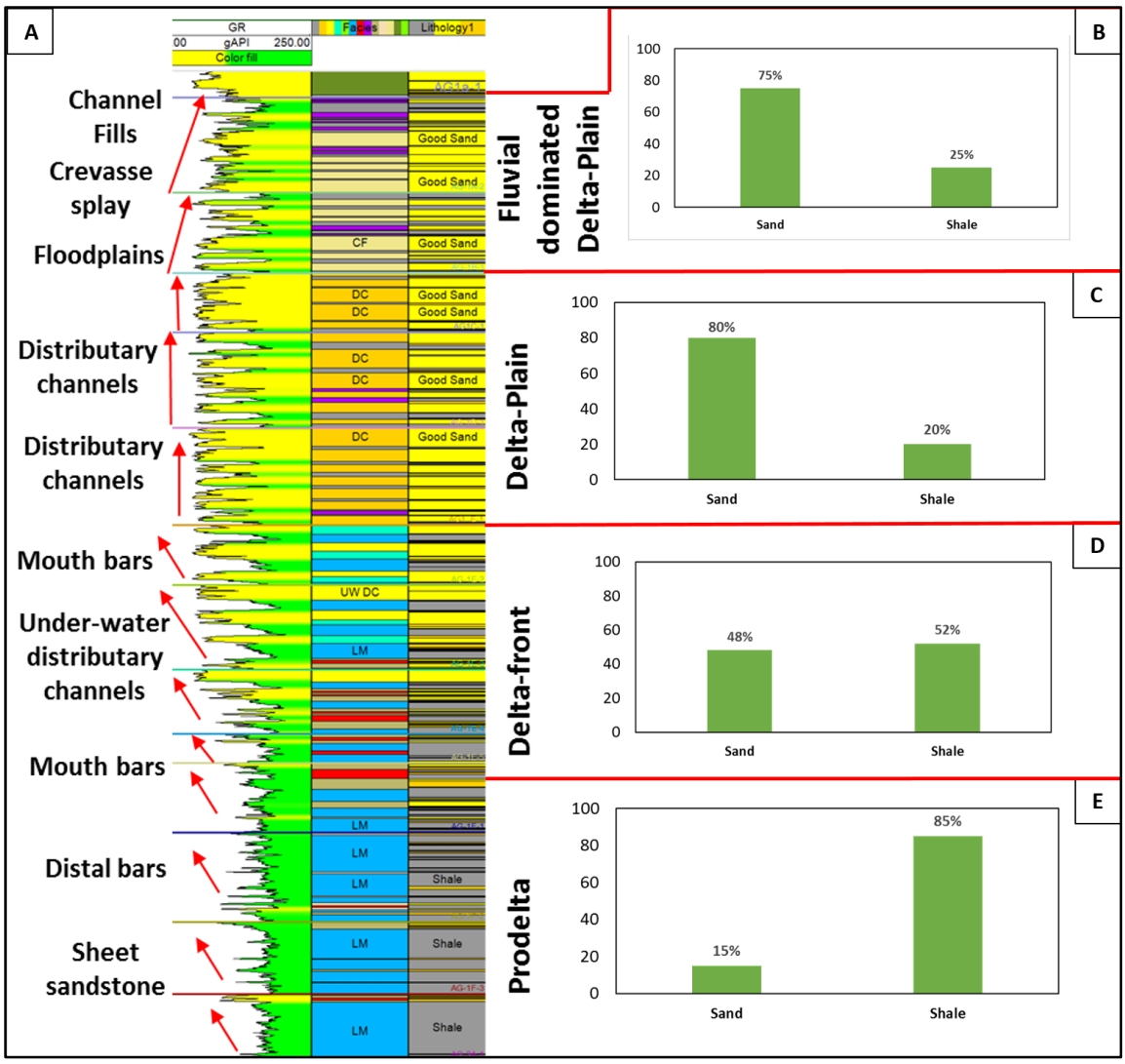

Figure 7-3: Vertical successions of the braided delta which were deposited in Sufyan Sub-basin (for well location, see Figs. 1C) (A). Well log is the gamma ray (GR). The yellow color is sandstone dominated and green is mudstone dominated. Sand and shale percentage in Abu Gabra Formation for different facies association calculated using well logs (B, C, D, and E).

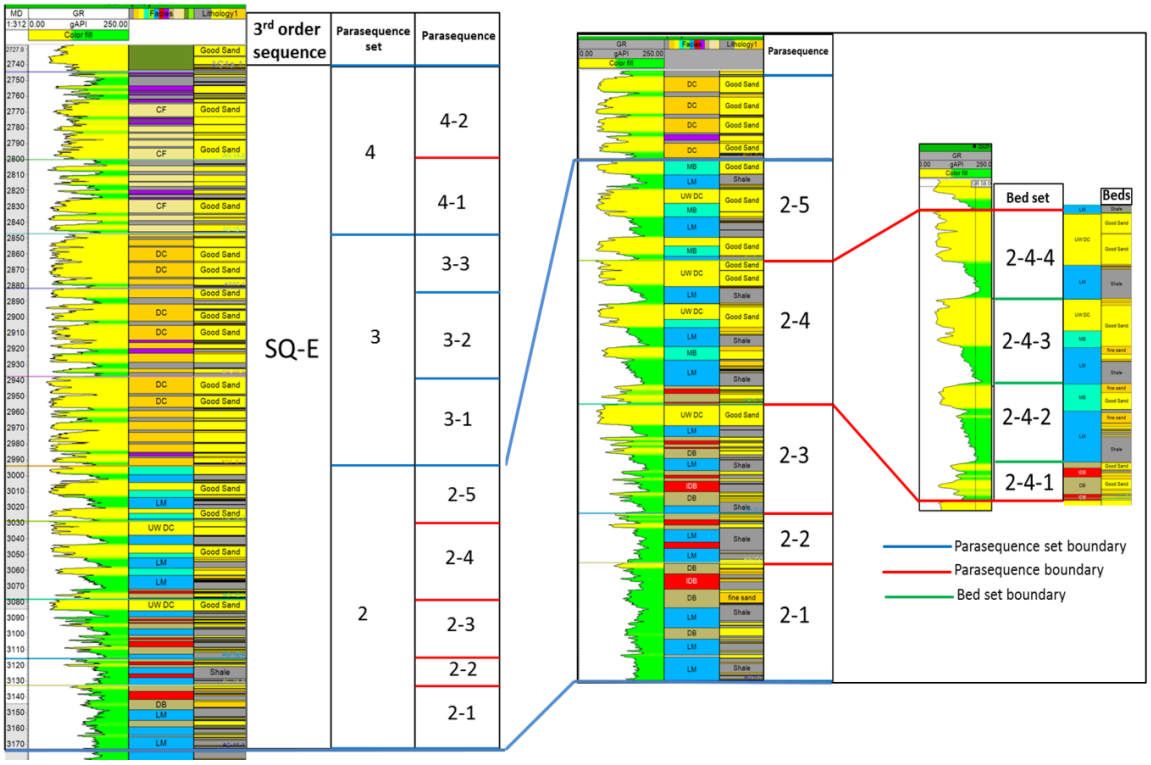

Figure 7-4: Well log (well-4) responses (GR) for a braided delta from the Early Cretaceous Abu Gabra Formation, Sufyan Sub-basin. Shows 3rd order sequence, parasequence sets, parasequences, bed set, and beds. The 3rd order sequence (SQ-E) composed of four parasequence sets, each one of them represent a depositional sequence. Parasequence set-1: prodelta, Parasequence set-2: Delta front, Parasequence set-3: Delta plain, Parasequence set-4: Fluvial dominated delta plain. Parasequence set-2, composed of five parasequences. Parasequence 2-4, composed of four-bed sets. Depth is in meter.

The selection of optimum petrophysical parameters is a critical factor for reservoir evaluation. Using well logs and available core data along with other geological information, the petrophysical properties (volume of shale and porosity) were estimated for Abu Gabra Formation. These properties are necessary input for populating the geocellular model described in the following chapter.

7.5.1 Sand/Shale discrimination

Combinations of wireline logs (mainly gamma ray (GR), density, and neutron) were used to identify the reservoir rocks from non-reservoir (shale) as discussed earlier. The character of density and neutron logs is significantly indicating sand when low density (density curve moving to the left) crossing over the neutron curve. In this case, greater cross over identifying better reservoir quality and vice versa. On the other hand, shale zones are identified by a high density (density curve moving to the right of neutron curve). Gamma ray (GR) log is a very useful log indicator for lithology identification. The gamma ray (GR) log identified sand by deflection to the left with decreased radiation for the gamma ray log. This deflection refers to the coarsening pattern in sandstone because increasing of the grain size generally associated with decreasing of matrix and shale contents.

For reliable lithological reconstruction, cross plots between well logs were used. The neutron–density cross plot is one of the useful methods for lithology identification. The values of this cross plot were used to identify the pure matrix and/or the related porosity from several wells in the study area. This cross plot uses a straight line relationship between two variables to quantify the desired characteristic and to identify lithology. The neutron

porosity log tends to respond to zones with high porosity (if the fluid is water or oil) and to zones with high clay content because of the bound water.

7.5.2 Shale volume (Vsh)

Many log combinations can be used to estimate the volume of shale because most log responses are influenced by the presence of shale in the formation such as resistivity, SP, gamma ray, density, neutron and compressional sonic. These logs are often called shale indicators (Poupon et al., 1970a). In this study, two popular methods of shale indicators were used; computing Vsh from GR log and computing Vsh from neutron-density logs.

Shale volume (Vsh) from gamma ray (GR)

This method is known as a single curve shale indicator. Gamma ray was used to evaluate the shale volume after correction of log responses for borehole effect, and when the rate of radioactivity of shale is constant. Quantitative evaluation of shale content using gamma ray logs ignores all radioactive minerals other than shale and clay (Poupon et al., 1970b). This method assumes a linear approximation of shale volume to index gamma ray ($V_{sh} = I_{GR}$). However, for more precise estimates of shale volume, the value of I_{GR} needs to be compared to the models provided by Steiber (1970), and Clavier et al. (1971). Calculation of gamma ray index (I_{GR}) is obtained from the following relationship (Poupon et al., 1970b) (Eq. 1.1).

The evaluation of the shale volume from the gamma ray log can be accomplished using one of the linear and nonlinear empirical equations (Eq. 1.1 to 1.5). The nonlinear equations

yield values lower than the linear one. The shale volume (Vsh) is expressed in either percentage or decimal fractions.

Linear equation

$I_{GR}=GR_{log}-GR_{min}/\ GR_{max}-GR_{min}$ (1.1)

GR_{log}: Gamma-ray value from log,

GR_{max}: Gamma-ray value from log at shale line,

GR_{min}: Gamma-ray value from the log at the sand line.

Nonlinear equations

Larionov (1969) for older rocks: Vsh =0.33 × ($2^{2IGR}-1$) (1.2)

Larionov (1969) for younger (Tertiary) rocks: Vsh = 0.083 ($2^{3.7\ I_{GR}}-1$) (1.3)

Steiber (1970): Vsh = $I_{GR}/(3-2\times I_{GR})$ (1.4)

Clavier (1971): Vsh = $1.7-[3.38-(IGR+0.7)^2]^{1/2}$ (1.5)

Shale volume (Vsh) from density-neutron logs

It is known as a two curve shale indicator method. In this method, two types of logs can be used in combination to obtain the volume of shale. The density neutron technique has been the preferred two curve shale indicator method to calculate shale volume, where radioactive sand occurs (Asquith and Gibson, 2007). Sand/shale models of density and neutron cross plots from all wells were used to determine the percentage of shale. From this plot, a clean sand line is typically established using the common sandstone parameters for density (2.65g/cm3) and neutron (-0.07 m^3/m^3).

A clay line is established from dry solid point (density= 2.3-2.85 g/cm^3, neutron range from 0.1to 0.4) to the 100% porosity fluid point. Density - neutron cross plot was used to estimate the shale volume for Abu Gabra Formation using the following relationship:

$Vsh= (\Phi_N- \Phi_D)/ (\Phi_{N\_Sh}- \Phi_{D\_sh})$

Where: Φ_N is the neutron porosity reading and Φ_D is the density porosity reading.

The shale parameters for the studied sandstone have been determined statistically using the cross plots and compared with the histograms for all wells.

7.5.3 Total and effective porosity

Porosity is an important parameter for formation evaluation and can be calculated from core data, density log, compressional sonic log, neutron log, or density-neutron cross plot (Serra and Abbot, 1980).

The density – neutron cross plot is the most accurate log analysis method for estimating porosity. The density log measurement is more sensitive to pore-space and the neutron measurement is more sensitive to lithology changes. For the shaly sand models, the following sets of equations were used as documented in log interpretation principles book by Schlumberger (1997):

RHOB = RHOB matrix + (RHOB shale - RHOB matrix) V_{sh} + (RHOB fluid – RHOB matrix) Φ effective and,

Φ_N = Φ neutron matrix + (Φ neutron shale - Φ neutron matrix) V shale + (1- Φ neutron matrix) Φ effective The total porosity is given by: ΦTotal = Φ effective + WCLP X V_{sh}

Where: RHOB is the density log, Φ_N is the neutron log and WCLP is the wet clay porosity from core analysis.

Applying this technique for porosity calculation, the porosity model has been constructed for Abu Gabra Formation. The accuracy of the calculated porosity logs was quality checked and validated with helium porosity measured from core samples. There is a very good match between porosity from core and porosity from logs.

7.5.4 Petrophysical properties cutoffs

The objectives of utilizing cutoff values are to eliminate the non-reservoir rocks (shale and silt) in reservoir modeling. Therefore, the intending to set the cutoff criteria needed to eliminate these non-reservoirs from the logged reservoir intervals. In order to achieve this objective, various cross plots between the calculated petrophysical properties were carried out for all wells.

The cross plot of effective porosity (PHIE) versus volume of shale (Vsh) was found more useful for lithology discrimination between sand/shale sequences in the study area (Figure 7-5). Detailed analysis was done using gamma ray color code as well as formation filters in order to understand the reliable cutoff values for modeling the porosity, shale volume and hence facies in the study area. Shale volume (Vsh) is used as a simple discriminator between sand and shale layers using the cut-offs criteria (if Vsh $\geq$ 50 % = shale). On the other hand, two types of sand facies were identified based on the porosity cutoffs (clean sand and shaly sand). Three facies have been identified based on the assigned petrophysical cutoff as shown in Table 7-2.

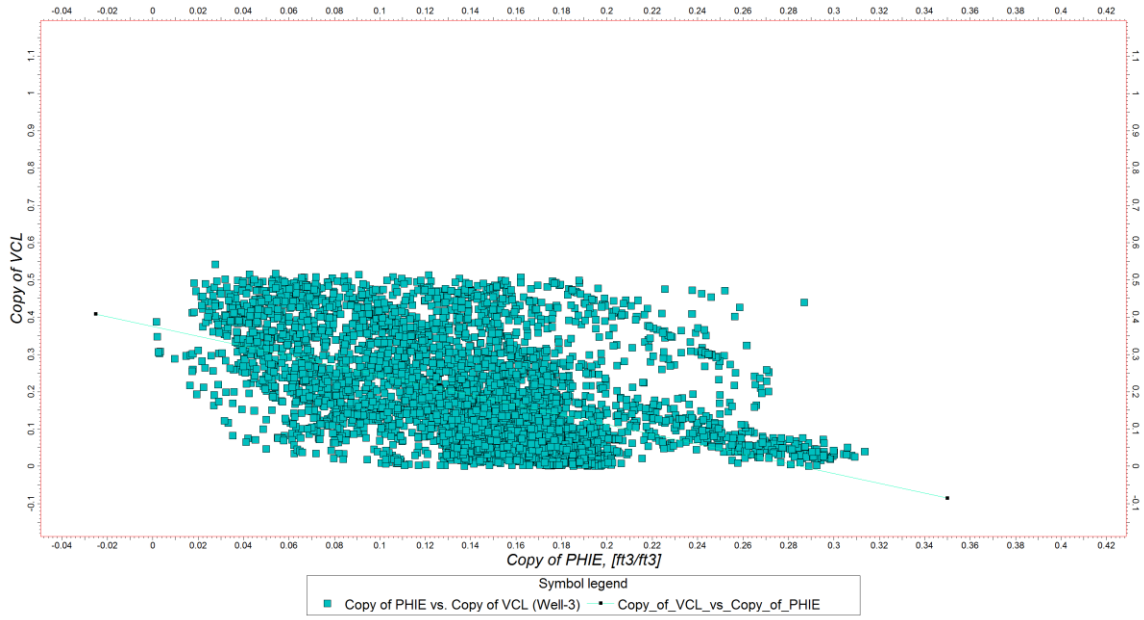

Figure 7-5: Petrophysical properties cut-offs defined from PHIE versus Vsh cross plots.

Table 7-2: Petrophysical properties cut-offs for facies modeling.

Code	Facies	Cutoff
0	Shale	Vsh >= 50%
1	Clean-sand	Vsh < 50% And PHIE >10%
2	Shaly-sand	Vsh < 50% And PHIE <= 10%

7.6 Structural modeling

The fluvio-lacustrine reservoirs of Muglad Basin are characterized by complex structure (Figure 7-6C), a high degree of lithofacies and petrophysical heterogeneity. For this reason, geostatistical approaches tied to the available well control is a useful approach for constructing three-dimensional models of reservoir properties.

In this study; the structural, depositional, stratigraphic and petrophysical data were all integrated to develop the 3D reservoir models for upper Abu Gabra Formation in Sufyan Sub-basin, Muglad Basin. These models were provided a better understanding of the structural and facies configuration in the study area. It is also produced a connectivity indicator for flow units between sand bodies constructed stochastically.

7.6.1 Structural Framework

In the study area, the 3D structural model was built for the selected area as shown in Figure 7-6B, C. The modeled section consists of one 3rd order sequence (sequence-E) (represents the most upper part of Abu Gabra Formation (thickness is about 563 meter) (Table 7-3).

The model integrated data from 9 wells in the study area. Well -5 was used as a blind test to validate the reservoir modeling results. The 3D structural model was built in depth domain using six seismic horizons. These horizons were interpreted in time domain then converted to depth domain using the velocity model obtained from check-shot data. The seismic horizons interpreted mainly based on the parasequence sets (four parasequence sets for Sequence-E) (Table 7-3).

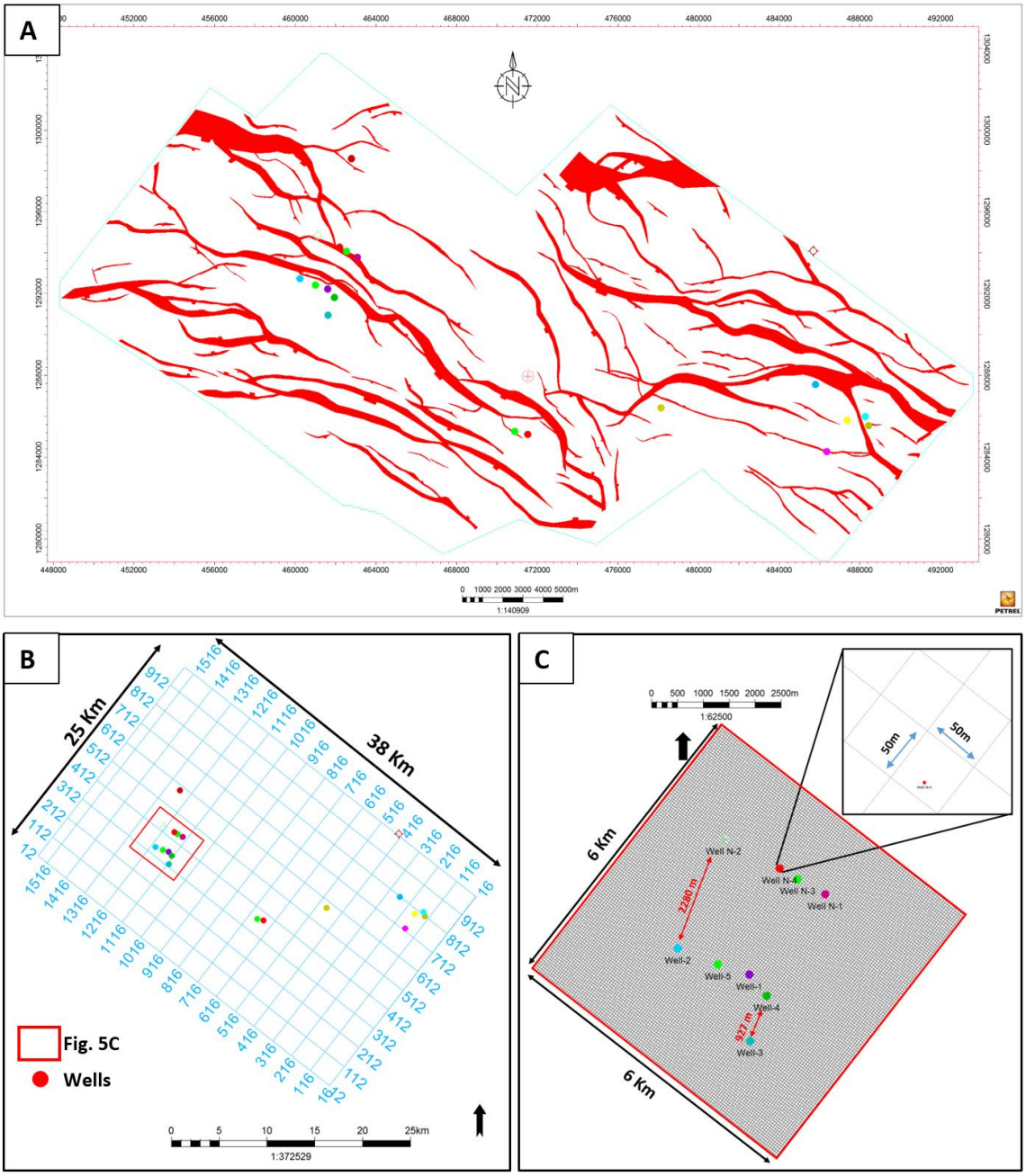

Figure 7-6: Structural map of top Abu Gabra Formation, interpreted from 3D seismic data shows faults and well locations (A). Base map showing well locations (22 wells) and 3D seismic survey in Sufyan field (B). Location map showing the selected area for 3D structural and property modeling including 9 wells (C).

Table 7-3: The interpreted 3rd order sequences (sequence-E), depositional environment, parasequence set, parasequences, and its thicknesses. These parameters were used to construct model zones.

3rd order sequence	Depositional Environment	Parasequence set	Parasequence set thickness (m)	Top/ Paraseq-uence	Parasequence Top (m)	Parasequence thickness (m)
SQ-E	Fluvial dominated delta plain	E-4	103	AG-1A-1 (4-2)	2743	57
				AG-1A-2 (4-1)	2800	46
	Delta plain	E-3	147	AG-1B-1 (3-3)	2846	35
				AG-1B-2 (3-2)	2881	57
				AG-1B-3 (3-1)	2938	55
	Delta front	E-2	179	AG-1E-1 (2-5)	2993	37
				AG-1E-2 (2-4)	3030	47
				AG-1E-3 (2-3)	3077	37
				AG-1E-4 (2-2)	3114	18
				AG-1E-5 (2-1)	3132	40
	Prodelta	E-1	134	AG-1F-1 (1-3)	3172	51
				AG-1F-2 (1-2)	3223	44
				AG-1F-3 (1-1)	3267	39

The interpreted faults from seismic data were also used as an input data into the software and formed the main vertical framework (Figure 7-7A). This fault system has introduced a complex structural model in geometry and connections between segments.

7.6.2 Fault Framework

Fault interpretation was done in the time domain. A time-depth conversion for these faults was performed using the velocity model before building the fault model. The main depth-converted faults (about 5 faults) were introduced to the fault model as shown in Figure 7-7A. The fault paths were quality checked to perform a necessary tie to the seismic data during fault modeling step. The faults were modeled in 3D space and tied to the seismic horizons and fault sticks, from which they were identified. The essential adjustment for fault model with the interpreted seismic horizons was carried out and quality checked to ensure the model consistency.

7.6.3 Pillar gridding

The basic skeleton of the top, middle and base was created in this process. The 3D grid was created with "I "and "J" increment 50x50 m includes the modeled faults (Figure 7-6C).

The grid boundary was created with reference to the selected area boundary. The "I" and "J" directions were assigned to the faults created in the fault model.

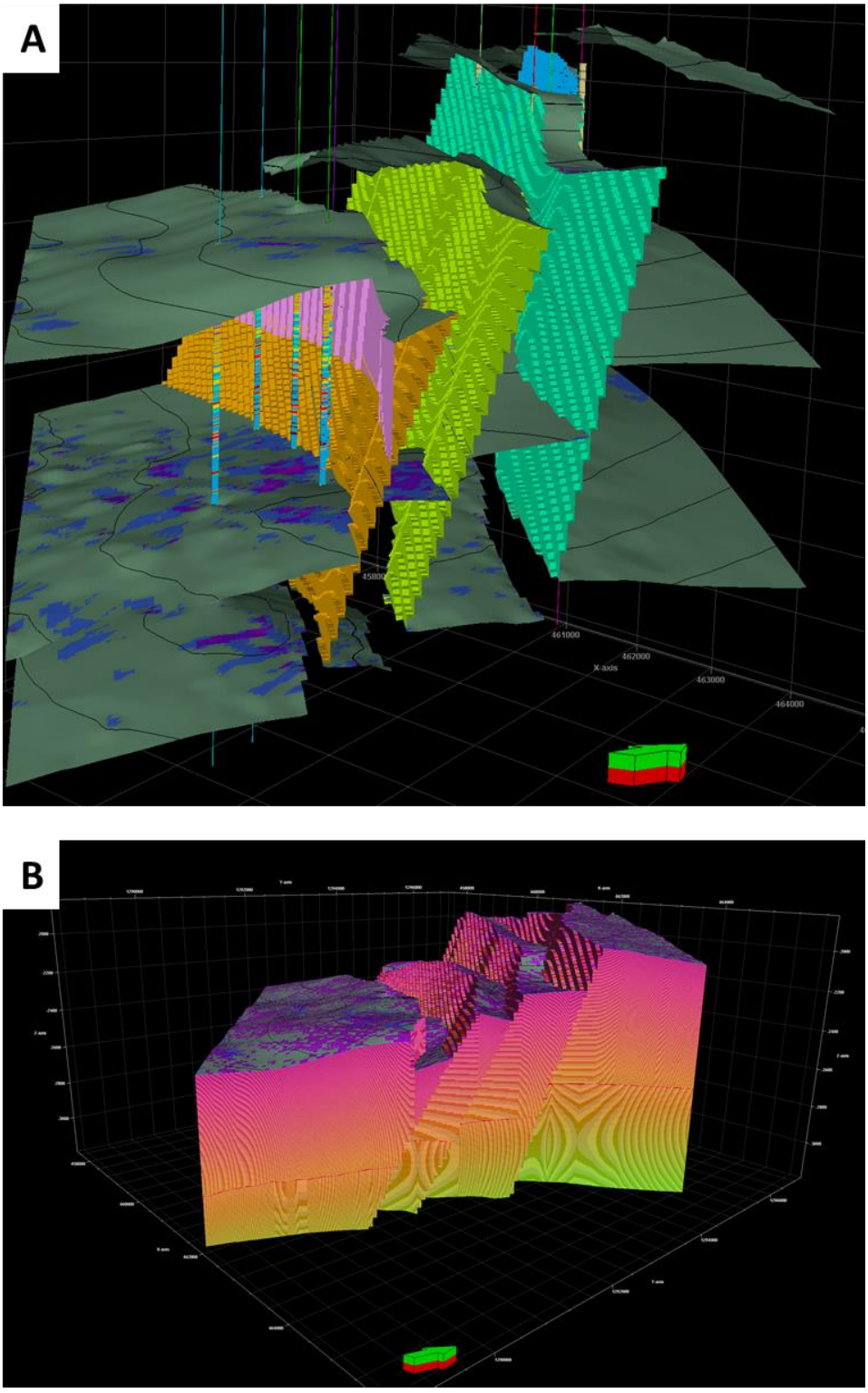

Figure 7-7: Three-dimensional (3D) view of the fault modeling, up-scaled well logs, horizons, and zones framework. Four zones were used for the model.

7.6.4 Horizons modeling and zones

Five seismic horizons were interpreted in the time domain and then converted to depth; grids were used for horizon modeling in this step. The required corrections for these horizons with reference to the well formation tops were applied. In the same way, the resulted horizons from this model were also quality checked with reference to the interpreted original seismic horizons. Four zones from the top model (zone-1) to bottom model (zone-4) were produced in the horizons modeling process with thicknesses of 103 m, 147m, 179m, and 134m respectively. These zones were created based on the sequence stratigraphic framework (uppermost part of Abu Gabra formation consist of one 3rd order sequence, this sequence could be subdividing into four parasequence sets) (Table 7-3).

7.6.5 Layering

Layering was performed for all zones with a different number of sub-layers based on the range of sand bodies' thickness using sequence stratigraphic framework (parasequence sets, parasequences, bed-sets, and beds). Based on core description and well logs analyses; the sub-layering process was completed for all zones. Higher resolution (1 meter) for layer thickness was used for the model due to thin sand bodies in this interval. A total of 563 layers characterizing SQ-E of Abu Gabra Formation have created the fine grid model (Table 7-4). The total grid cell number is 7,972,643.

Table 7-4: Distribution of cells in different zones in the three- dimensional grid with their corresponding deposition environment.

Zones	Depositional environment	Number of layers	Grid cells (nI X nJ X nK)	Number of cells
Zone-1	Fluvial dominated delta plain	103	119 X 119 X 103	1458583
Zone-2	Delta plain	147	119 X 119 X 147	2081667
Zone-3	Delta front	179	119 X 119 X 149	2534819
Zone-4	Prodelta/Shallow Lacustrine	134	119 X 119 X 134	1897574
Total		563		7972643

7.6.6 Upscaling

Upscaling of well log data to the geological grid scale was performed to capture the heterogeneity of well data using the arithmetic averaging method. This log upscaling was typically used for reservoir properties which were populated in the 3D grid. The upscaled logs include; Lithofacies associations, Lithofacies, and effective porosity, from all the nine wells except for well-5.

The quality check was performed on the results of log up-scaling to ensure proper capturing of the variability of the various units (Figure 7-8). It should be noted that the well-5 was excluded from this analysis and later was used as a blind test for model validation.

7.7 Facies association geostatistical modeling

Gamm ray (GR) log motives calibrated with core data was mainly used to interpret the facies association in target intervals. The interpreted facies associations for modeling are: Fluvial dominated delta plain and its includes channel fills sand and floodplain shale dominated (Figure 7-1). Delta plain and it includes distributary channel sand and floodplain dominated. Delta front and it includes lacustrine mudstone, underwater distributary channel sand, and mouth bar dominated with minor distal bars, and Interdistributary bay deposits. Prodelta and its includes lacustrine mudstone dominated with minor sheet sand (Figure 7-1).

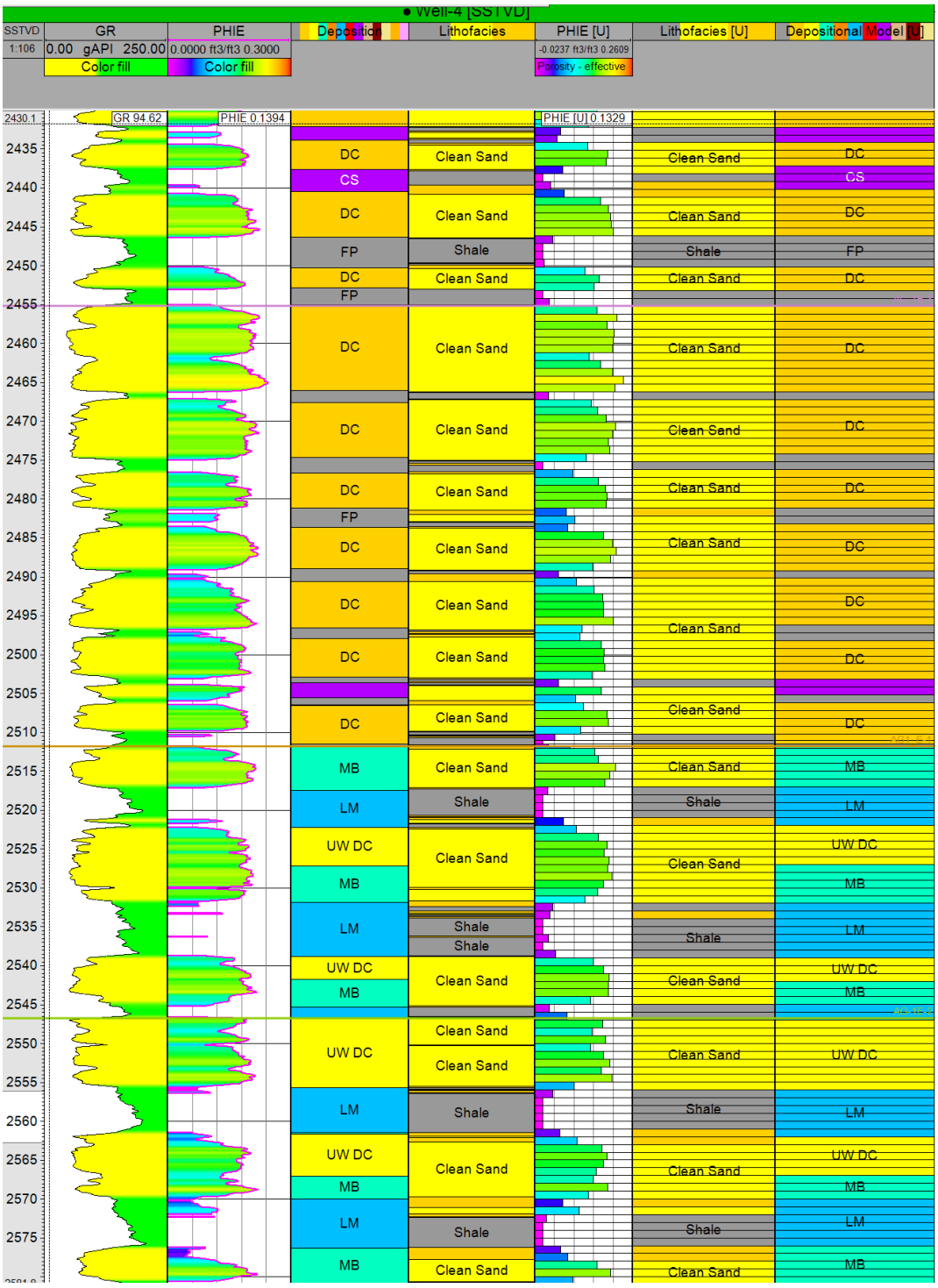

Figure 7-8: Well-4 showing the grid layering and comparison between up-scaled porosity logs (PHIE), depositional environment, and lithofacies against original input logs, there is a good match between original and up scaled logs.

7.7.1 Geostatistical data analysis

The primary factors affecting connectivity are thickness, width, aspect ratio, and amplitude. The variogram map (Figure 7-9) was constructed during this process to identify the major and minor directions of the property variability. The variogram map was constructed based on the structural map and it shows the anisotropy created mainly by the faults (Figure 7-6A). The major direction (125°) indicates the NW-SE faults trend (Figure 7-6A). The facies modeling is constrained by the following two inputs derived from the well data: vertical facies probability curve (Figure 7-10) and honoring facies at the wells. Therefore, the data analysis was performed to analyze the facies associations proportion and thickness.

Vertical proportion curve

The vertical proportion curves for all facies associations tell how the proportion of each facies varies vertically in the target zones. Figure 7-11 illustrate the probability curves for facies associations in four zones versus the number of layers. This analysis indicated a higher proportion of lacustrine mudstone and interdistributary bay deposits in zone-3 and 4 as shown in Figure 7-11. In zone-1 (Figure 7-11A), the proportion of channel fills and floodplain deposits are high (Figure 7-12A) and this is due to the sub-environment of the fluvial-dominated delta plain (Figure 7-3). In zone-2 (Figure 7-11B), the proportion of distributary channels and floodplains is high (Figure 7-12B) and this is due to the depositional setting of delta plain.

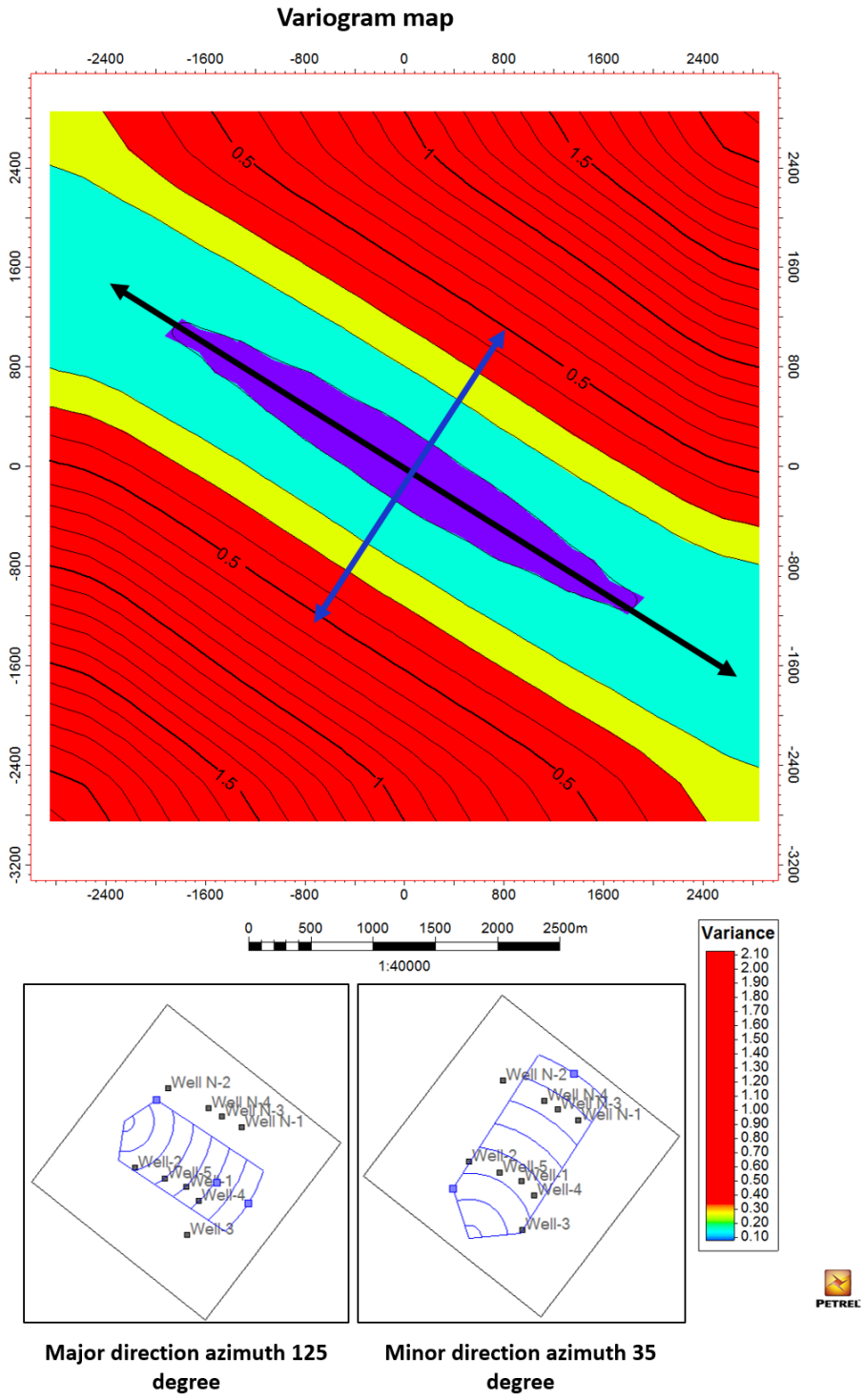

Figure 7-9: Variogram map for Abu Gabra Formation using the structural map of Sufyan field. The major direction (125°) indicates NW-SE trend.

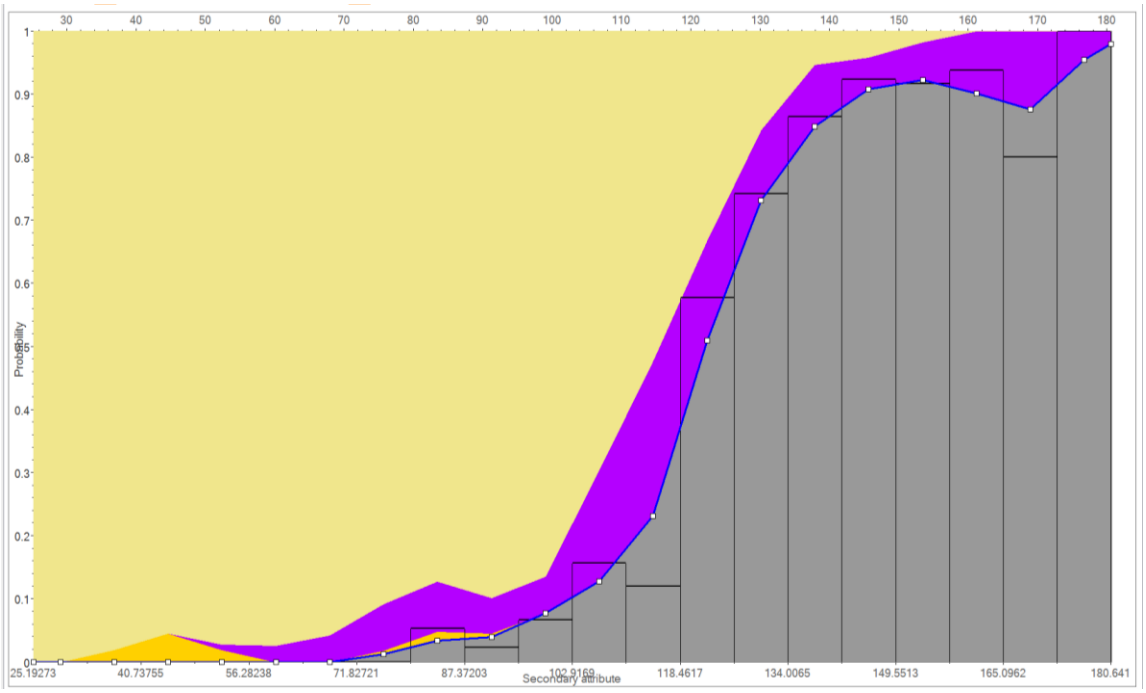

Figure 7-10: Facies association's probability analysis using Gamma-Ray (GR) as a secondary attribute in zone-1. Floodplain shale probability is high at high GR values, while channel fills sand probability is high at low GR values.

In zone-3 (Figure 7-11C), the proportion of underwater distributary channels, mouth bars, distal bars, interdistributary bay and lacustrine mud deposits are high (Figure 7-12C) and this is due to the depositional setting of delta front.

In zone-4 (Figure 7-11D), the proportion of the lacustrine mud, distal bars, and interdistributary bay deposits are high (Figure 7-12D) and this is due to the depositional setting of prodelta.

Facies associations thickness analysis

This analysis was performed to review the thickness distribution for each respective facies association. Statistical parameters, such as minimum, maximum, mean and standard deviations were calculated for all facies associations in each zone. The results of this analysis were used to estimate the required thickness of the facies associations in the modeling algorithm (Figure 7-13). The facies association thicknesses analysis and percentage in (A) zone-1, and (B) zone-2. In zones-1 and 2, the channel fills sand and crevasses splay and floodplain shale thicknesses are less than 10 m and represent more than 90% of the total depositional environment. (C) zone-3, and (D) zone-4. In zones-3 and 4 the lacustrine mud, distal bars, and Interdistributary bay deposits thicknesses are less than 10m and represent more than 90% of total modeled facies associations.

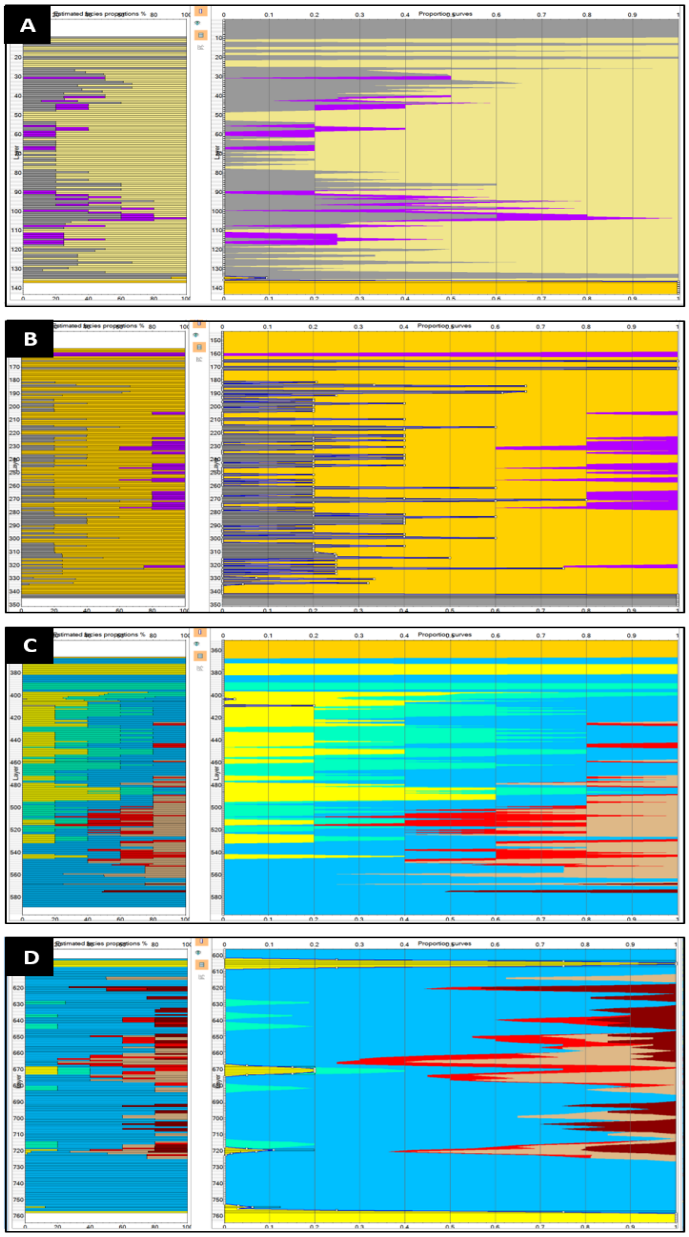

Figure 7-11: The left window displays the proportion of facies associations estimated from the selected input data in the four zones versus a number of layers used for the facies associations model. The right window displays the vertical proportion curves which quantify the vertical variability in the proportions of the different facies association based on model layers. (A) The proportion of the facies associations estimated from the selected input data in zone-1 (fluvial-dominated delta plain) (channel fills sand and floodplain shale dominated). (B) The proportion of the facies associations estimated from the selected input data in zone-2 (delta plain) (distributary channel sand and floodplain dominated, minor crevasse splay). (C) The proportion of the facies associations estimated from the selected input data in zone-3 (delta front) (lacustrine mud, underwater distributary channel sand, and mouth bar dominated). (D) The proportion of the facies associations estimated from the selected input data in zone-3 (prodelta) (lacustrine mud, distal bars, and Interdistributary bay deposits dominated).

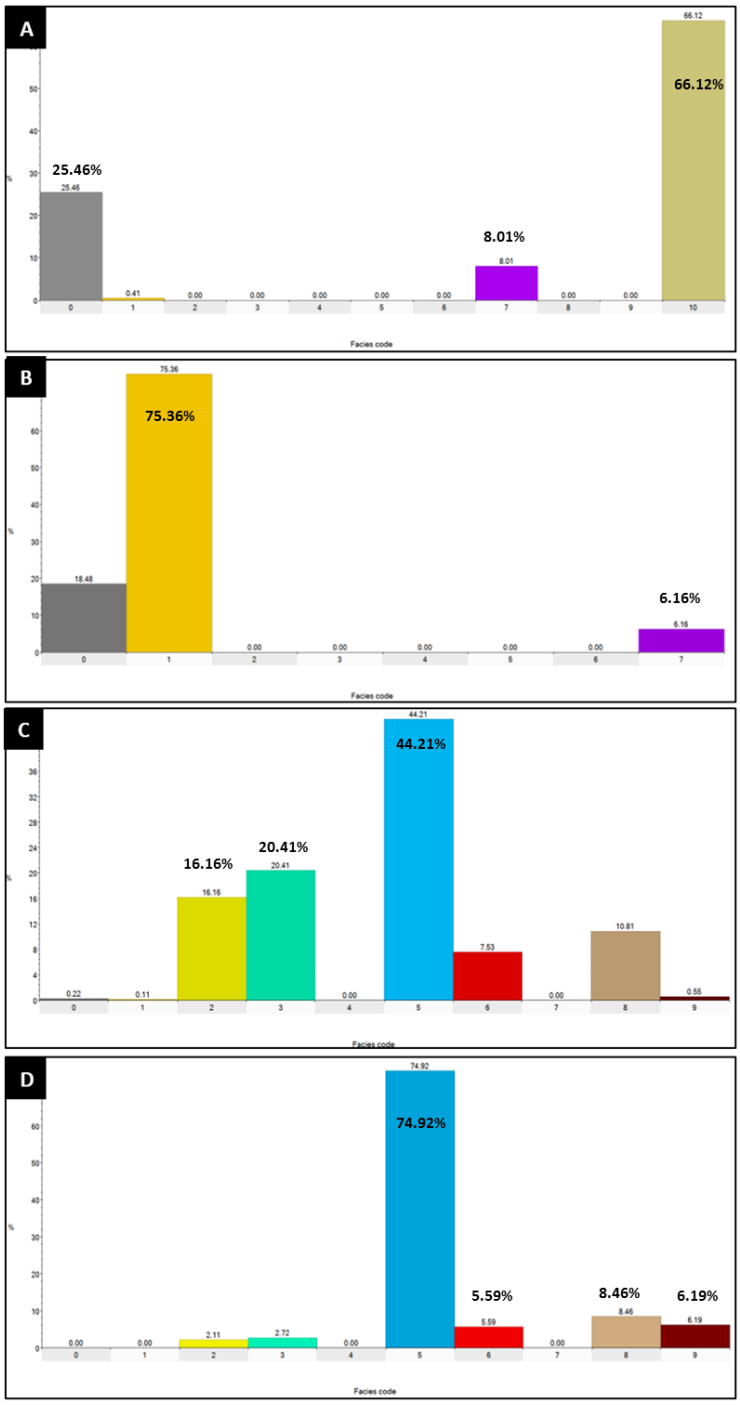

Figure 7-12: Facies associations distribution analysis in the four zones. (A) zone-1, dominated by channel fills sand deposits (66.12%) and floodplain shale (25.46%) (B) zone-2, dominated by distributary channels sand deposits (75.36%) and floodplain shale (18.48%). (C) zone-3, dominated by lacustrine mud deposits (44.21%), mouth bars deposits (20.41%) and underwater distributary channels sand (16.16%) with minor distal bar deposits (10.81%) and Interdistributary channels deposits (7.53%) (D) zone-4, dominated by lacustrine mud deposits (74.92%), with minor distal bar, Interdistributary channels, mouth bars, and underwater distributary channels deposits.

Variogram analysis

The variogram maps (Figure 7-9) were calculated for each zone in all possible azimuths. The structural maps of top zones-1, 2, 3, and 4 were used to calculate the variogram maps for each zone. These maps showed the direction of maximum continuity (major direction) and direction of minimum continuity (minor direction) as an orientation of the anisotropy. On the other hand, the indicator variograms were calculated for the discrete facies logs (upscaled logs) in each zone and for each facies separately. One of the variogram characteristics is the cyclicity pattern which is well-observed in zone-1 and zone-2 in these variograms. This cyclicity pattern indicates the deltaic system in Abu Gabra Formation. The vertical facies variability is also indicated from these variograms. This could be measured from high sill values (related to variance) in variograms. One of the variogram goals is to ensure that the proper grid resolution has been designed to enable the facies heterogeneity to be captured in the property grid. The layering process was based on this type of variogram analysis. The grid layering should be half of the vertical range to avoid the risk of over upscaling the log data and losing the ability to capture this vertical variation present in a given property. In these variograms, the average vertical range is 7 m and therefore, the layering thickness was used in the grid model is 3 – 4 m.

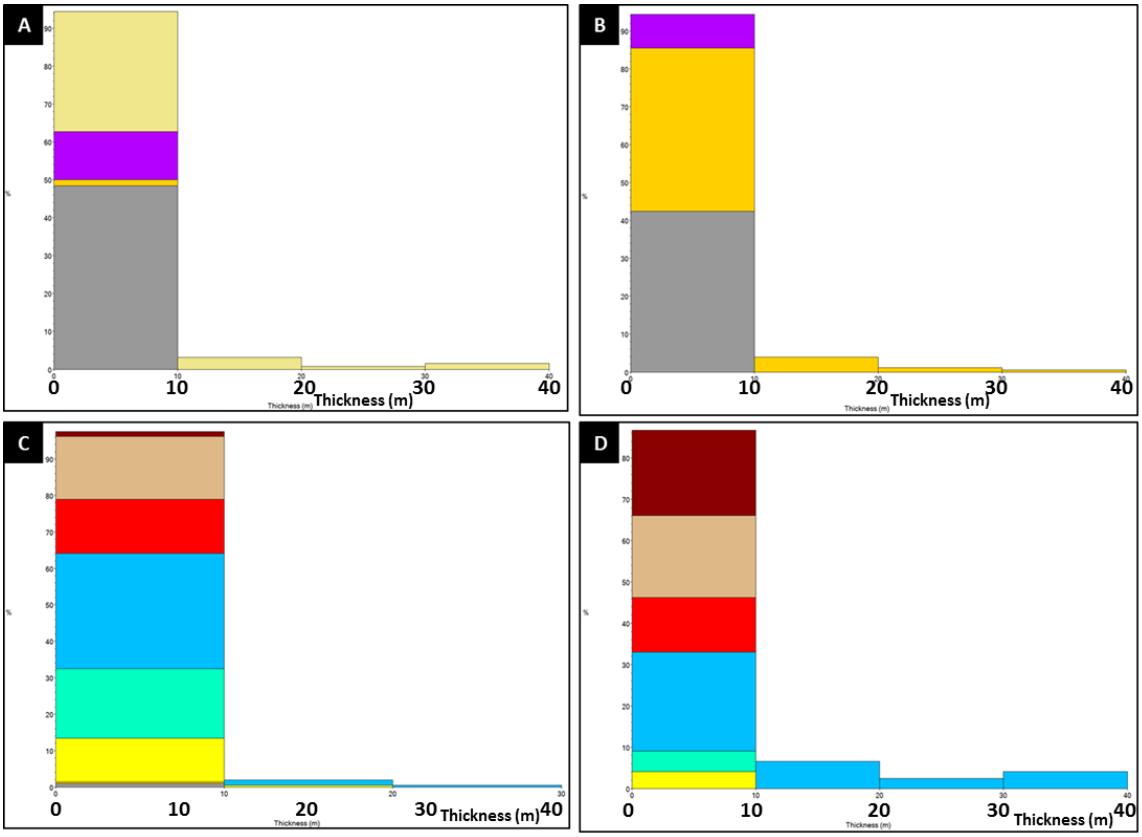

Figure 7-13: Facies association thicknesses analysis and percentage in (A) zone-1, and (B) zone-2. In zone- and zone-2, the channel fills sand and crevasses splay and floodplain shale thicknesses are less than 10 m and represent more than 90% of total depositional environment. (C) zone-3, and (D) zone-4. In zone-3 and zone-4 the lacustrine mud, distal bars, and Interdistributary bay deposits thicknesses are less than 10m and represent more than 90% of total modeled facies associations.

7.7.2 Construction of facies association model

Stochastic facies modeling allows for the large-scale heterogeneity at the facies level to be captured and therefore allows the critical flow units within the reservoir to be accurately modeled on the geological data. A geostatistical approach was initially used to distribute the facies model with reference to the constructed conceptual model. The applied methodology used for distributing the facies was the Sequential Indicator Simulation (SIS).

7.7.3 Facies associations distribution

The facies distribution in Sufyan Sub-basin, Muglad Basin is primarily controlled by faults and depositional environments (Yassin et al., 2016). The sand thickness is directly related to faulting and basin subsidence history.

The lateral and vertical facies association distribution within each zone is discussed based on fence diagrams, block diagrams, horizontal slice, and cross sections passing through many wells. Special emphasis is put on the reservoir versus non-reservoir facies distribution, channel pathways, and channel amalgamation.

Two fence diagrams (Figure 7-14), two block diagrams (Figure 7-15), six horizontal slices (Figure 7-16), and one cross-section (Figure 7-17A) were selected to display the facies distribution in the study area.

The horizontal slice (map view) (Figure 7-16A) indicate that the zone-1 of the model (uppermost) is dominant by floodplains and channel fills deposits. The amount of sand dominated facies decreases downward. In zone-2 (Figure 7-16B, C), the floodplains and distributary channels are dominated. In zone-3, underwater distributary channels, mouth

bars, distal bars, interdistributary bay and lacustrine mud deposits are dominated (Figure 7-16C, D). In zone-4 (Figure 7-16E), the proportion of the lacustrine mud is dominated.

In the fence diagrams (Figure 7-14A, B) and cross section (Figure 7-16A), successive channel belts show a pattern of lateral offset stacking in the upper zones, which is the product of vertical aggradation as well as lateral migration. There is an upward increase in channel dimensions, connectivity, and amalgamation from zone-3 to zone-2 to zone-1. The lowermost part SQ-E (Zones-4) shows a development of prodelta to shallow lacustrine mudstone with thin sandstone beds of underwater distributary channel, mouth bar, distal bar, and sheet sand facies. The facies maps (Figure 7-16A, B, C) reflect a common direction of flow and sediment supply trending toward SE direction as a general across the study area.

7.7.4 Model Validation

The blind test for facies model was performed using well-5 which hasn't been used for any process related to modeling. The facies association original log, up-scaled log, and modelled showed good match (Figure 7-18).

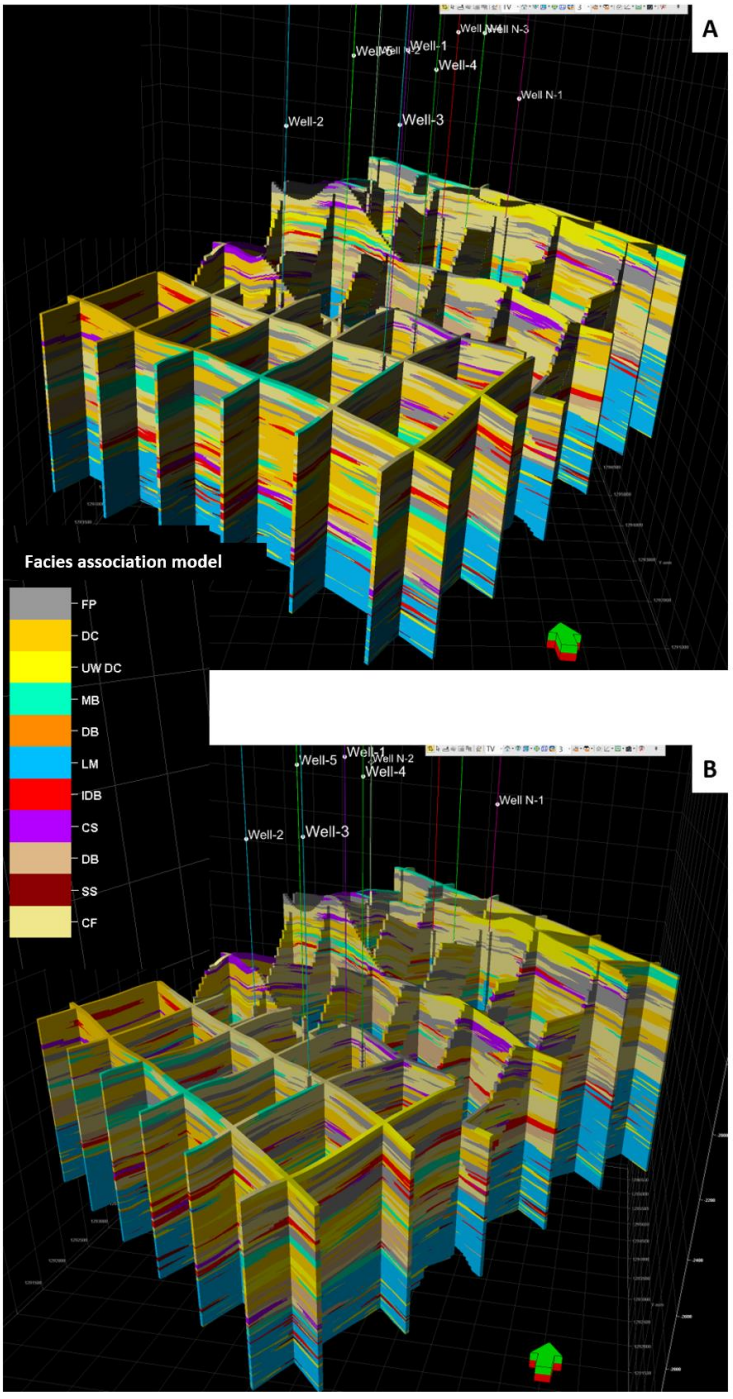

Figure 7-14: Fence diagram of the three dimensional (3D) model generated using sequential Indicator Simulation (SIS) algorithm, show the distribution of facies association in each zone (four zones). Channel fills (CF), floodplains (FP), and distributary channels (DC) are dominated in the upper zones. In the middle zones, mouth bars (MB), underwater distributary channels (UW DC), and lacustrine mud (LM) are dominated. In the lower zone, lacustrine mud (LM), Interdistributary bay (IDB), distal bars (DB), and sheet sand (SS) are dominated.

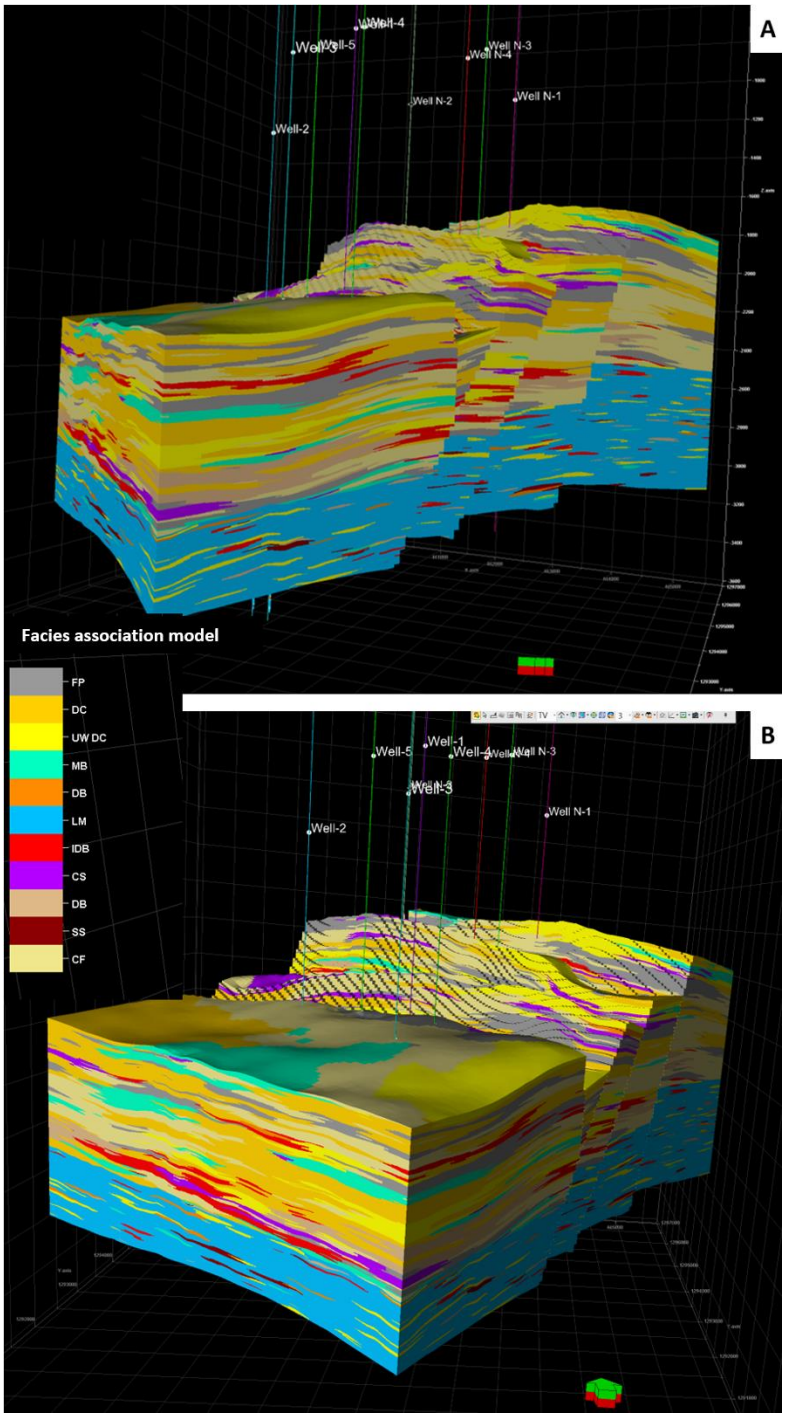

Figure 7-15: Block diagram of the three-dimensional (3D) model generated using sequential Indicator Simulation (SIS) algorithm, show the distribution of facies association in each zone (four zones). Channel fills (CF), floodplains (FP), and distributary channels (DC) are dominated in the upper zones. In the middle zones, mouth bars (MB), underwater distributary channels (UW DC), and lacustrine mud (LM) are dominated. In the lower zone, lacustrine mud (LM), Interdistributary bay (IDB), distal bars (DB), and sheet sand (SS) are dominated.

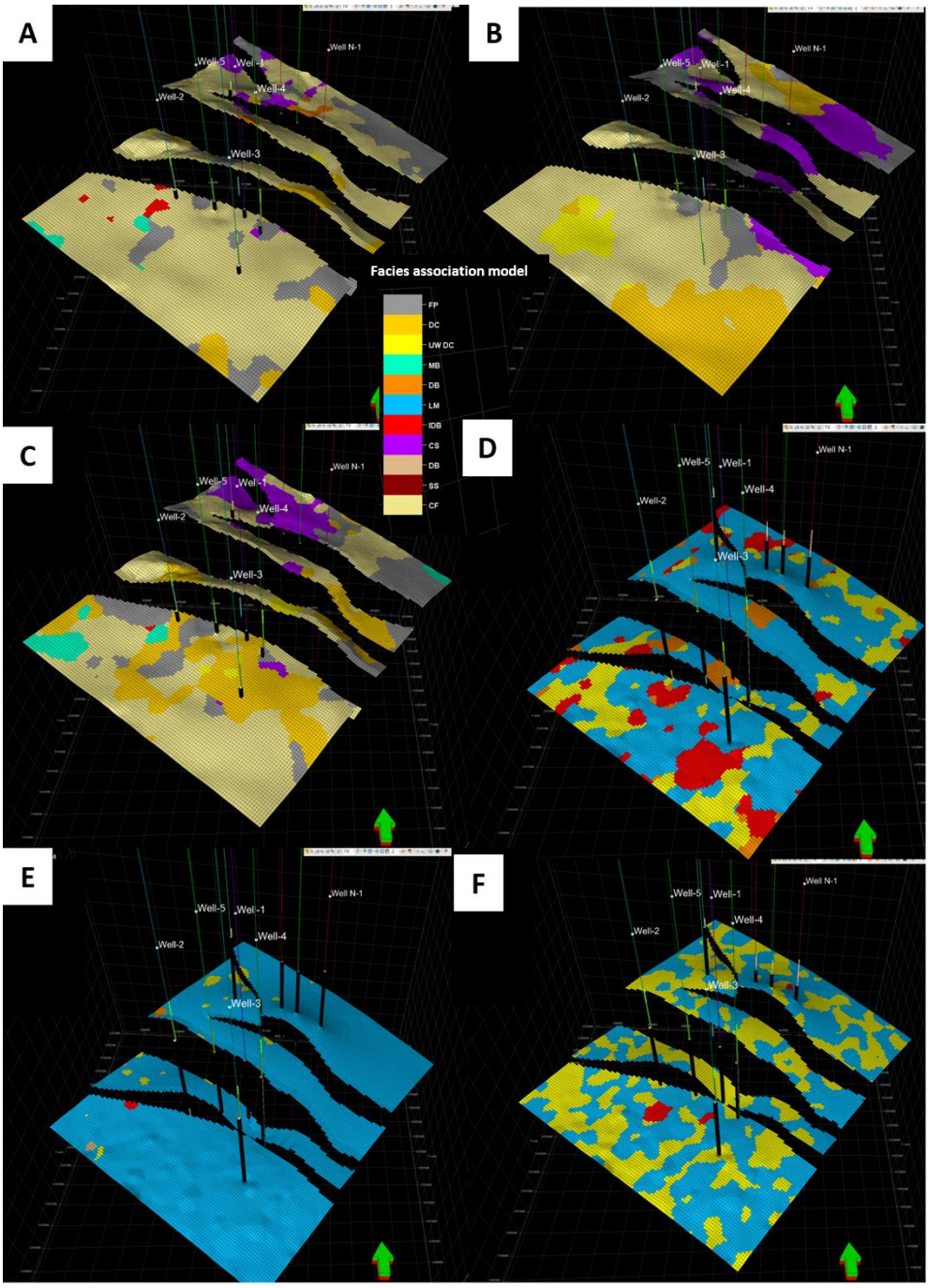

Figure 7-16: Horizontal slice (map view) showing the distribution of facies association in each zone (four zones). Channel fills (CF), floodplains (FP), and distributary channels (DC) are dominated in the upper zones. In the middle zones, mouth bars (MB), underwater distributary channels (UW DC), and lacustrine mud (LM) are dominated. In the lower zone, lacustrine mud (LM), Interdistributary bay (IDB), distal bars (DB), and sheet sand (SS) are dominated.

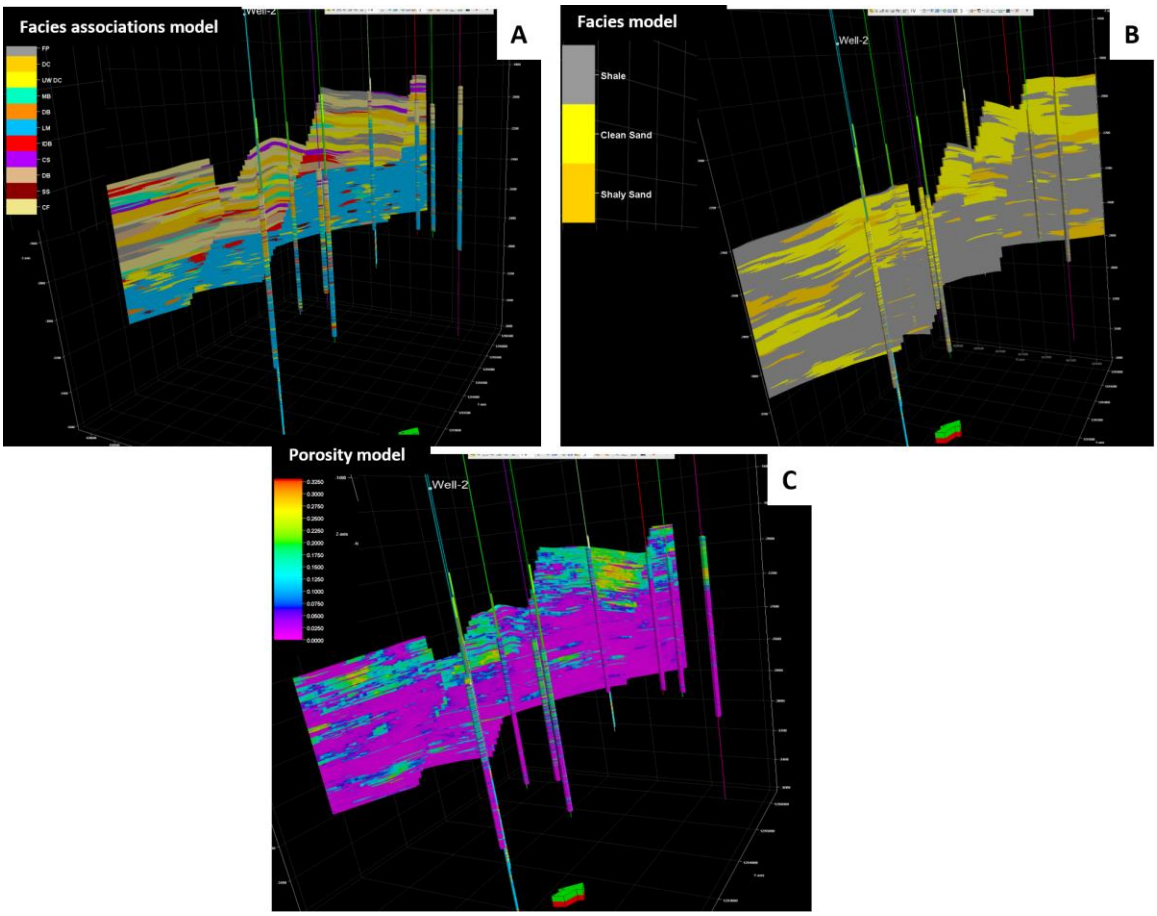

Figure 7-17: Different cross sections from the three-dimensional model for facies associations, facies, and porosity distribution passing through five wells.

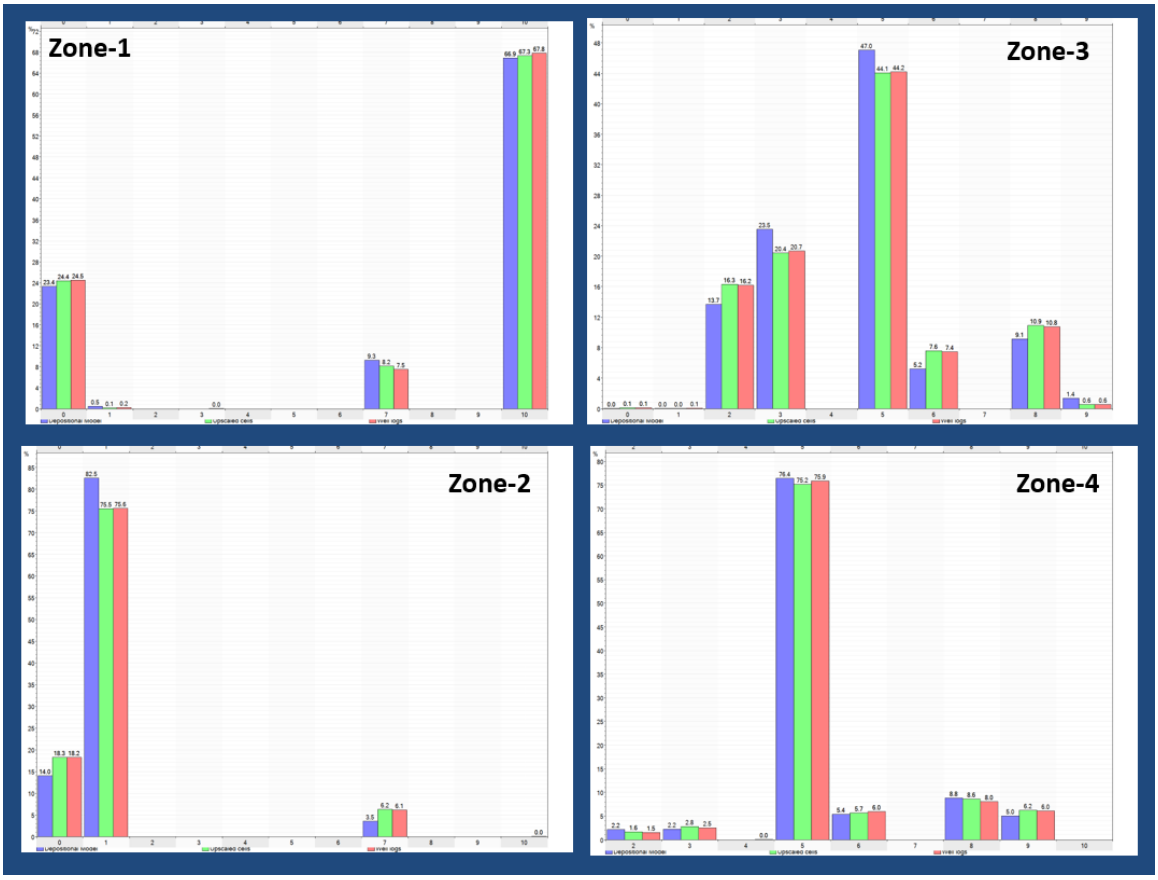

Figure 7-18: Facies association model validation using histograms showing a comparison between: original logs (red), up-scaled cells (green), and modeled (blue).

7.8 Facies geostatistical modeling

Discrete facies logs for each well were created using wireline log-based cut-off parameters as described in petrophysical analysis section. Porosity (Φ) and shale volume (V_{sh}) logs were mainly used along with gamma ray to classify the recognized facies in target intervals. The introduced facies for modeling are three including; shale, shaly sand, and clean sand.

Table 7-3 gives a description of the codes of the electro-facies along with their correlative core lithofacies.

7.8.1 Geostatistical data analysis

The facies modeling is constructed to address variations in sand body dimensions and connectivity. The primary factors affecting connectivity are thickness, width, aspect ratio, and amplitude. The facies modeling is constrained by the following two inputs derived from the well data: vertical facies probability curve and honoring facies at the wells. Therefore, the data analysis was performed to analyze the facies proportion and thickness. The variogram map was constructed during this process to identify the major and minor directions of the property variability.

Vertical proportion curve

The vertical proportion curves for all facies tell how the proportion of each facies varies vertically in the target zones. Figure 7-19 illustrate the probability curves for all facies in each zone versus the number of layers. This analysis indicated a higher proportion of shale

and shaly sand facies in zones-3 and 4 in comparison to zones-1 and 2 where sand facies is dominated as shown in Figure 7-19.

In zones-1 and 2, the proportion of clean sand facies is higher than in zones-3 and 4, this is due to the deposition of thick channel fills and distributary channels sandstone in the deltaic system (Figure 7-19A, B). In zone-4, the proportion of shale and shaly sand facies is high and this is due to the depositional setting of shallow to deep lacustrine systems. The shale percentage increase downward from zone-1 to zone-4.

Facies thickness analysis

This analysis was performed to review the thickness distribution for each respective facies (Figure 7-20). Statistical parameters, such as minimum, maximum, mean and standard deviations were calculated for all facies in each zone. The results of this analysis were used to estimate the required thickness of the facies in the modeling algorithm. In all zones; the clean sand, shaly sand, and shale thicknesses are less than 10 m and represent more than 90% of total facies.

Variogram analysis

The variogram maps (Figure 7-9) were calculated for each zone in all possible azimuths. The structural maps of zones 1, 2, 3, and 4 were used to calculate the variogram maps for each zone. These maps showed the direction of maximum continuity (major direction) and direction of minimum continuity (minor direction) as an orientation of the anisotropy.

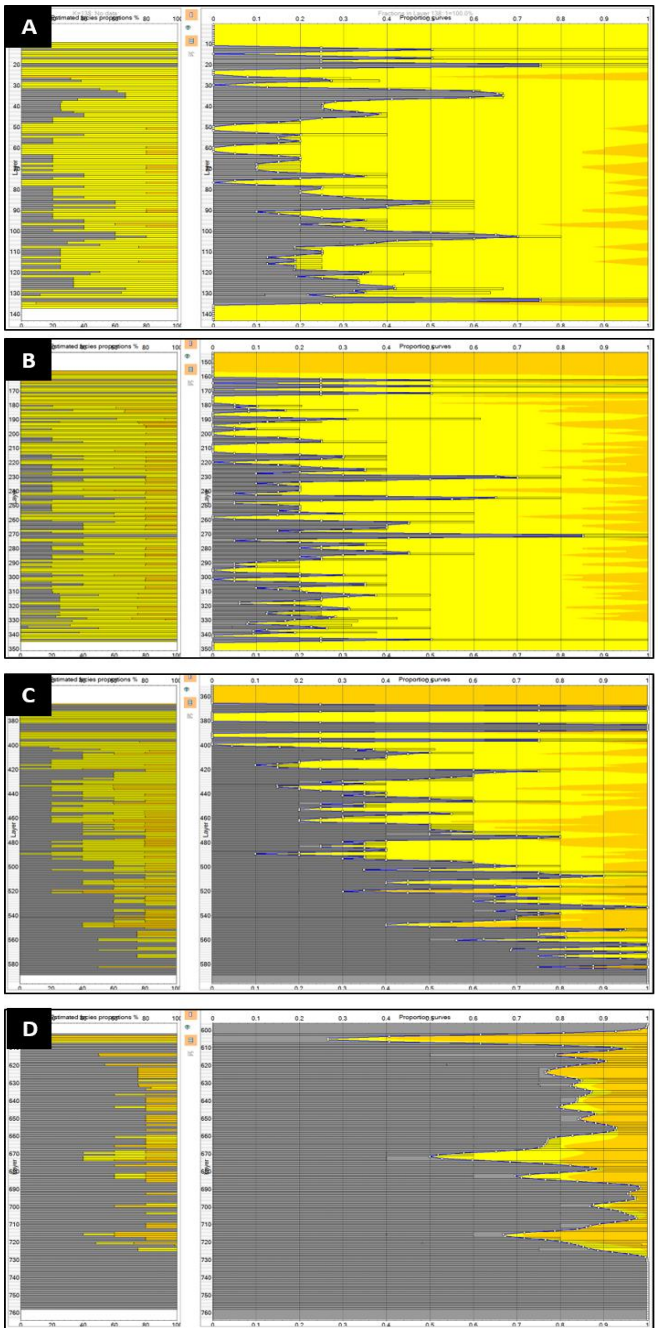

Figure 7-19: The left window displays the proportion of facies estimated from the selected input data in the four zones versus number of layers used for facies model. The right window displays the vertical proportion curves which quantify the vertical variability in the proportions of the different facies based on model layers. The shale percentage increase downward from zone-1 to zone-4. (A) The proportion of facies estimated from the selected input data in zone-1 (clean sand, shaly sand, and shale). (B) The proportion of deposition environment estimated from the selected input data in zone-2 (clean sand, shaly sand, and shale). (C) The proportion of deposition environment estimated from the selected input data in zone-3 (clean sand, shaly sand, and shale). (D) The proportion of deposition environment estimated from the selected input data in zone-3 (clean sand, shaly sand, and shale).

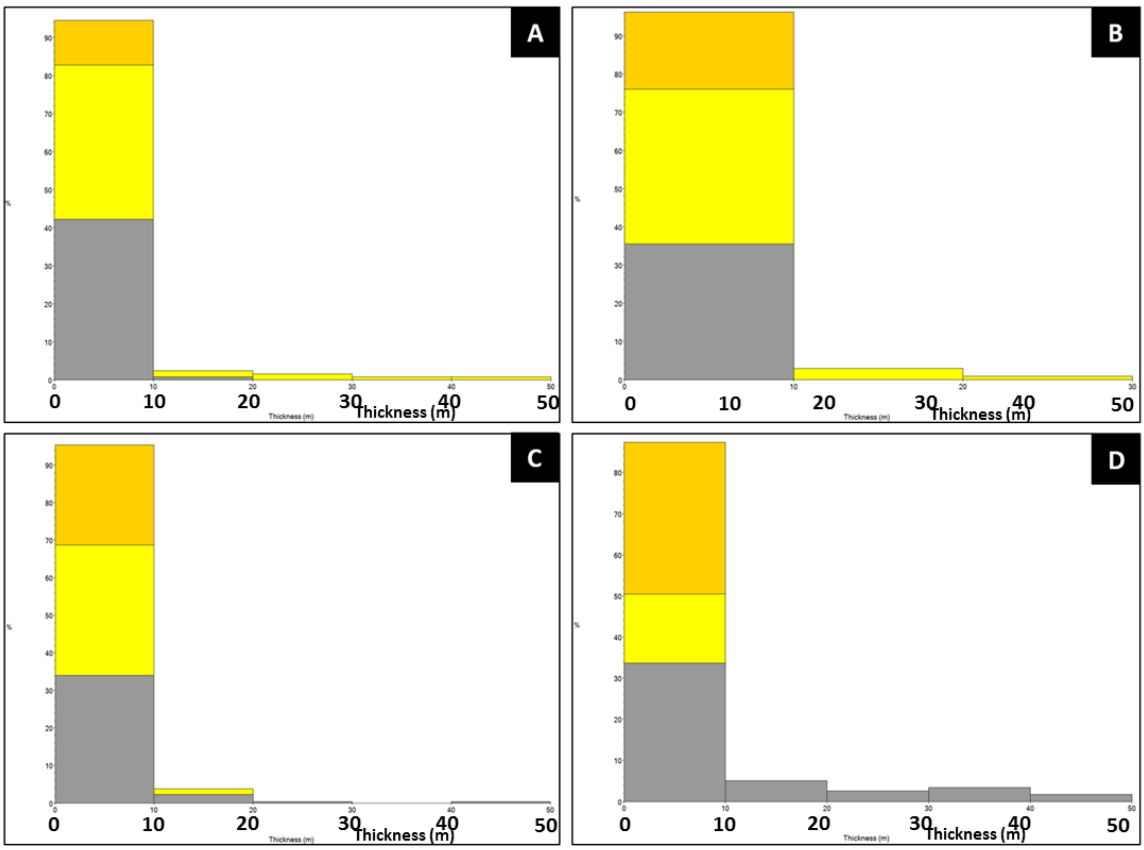

Figure 7-20: Vertical facies thickness analysis and percentage in (A) zone-1, and (B) zone-2. In zone- and zone-2, the shale, shaly sand, and clean sand thicknesses are less than 10 m and represent more than 90% of total facies thicknesses. (C) zone-3, and (D) zone-4. In zone-3 and zone-4 the shale, shaly sand, and clean sand thicknesses are less than 10m and represent more than 90% of total facies thicknesses.

On the other hand, the indicator variograms were calculated for the discrete facies logs (upscaled logs) in each zone and for each facies separately (Table 7-5). One of the variogram characteristics is the cyclicity pattern (Figure 7-21) which indicates for the deltaic system in Abu Gabra Formation. The vertical facies variability is also indicated from these variograms. This could be measured from high sill values (related to variance) in variograms. One of the variogram goals is to ensure that the proper grid resolution has been designed to enable the facies heterogeneity to be captured in the property grid. The layering process was based on this type of variogram analysis. The grid layering should be half of the vertical range to avoid the risk of over upscaling the log data and losing the ability to capture this vertical variation present in a given property. In these variograms, the average vertical range is 7 m and therefore, the layering thickness was used in the grid model is 3 – 4 m.

7.8.2 Construction of facies model

The facies modeling process is the population of the discrete data e.g. lithofacies, into the cells of the grid. The workflow for facies modeling construction includes distribution of the different facies inside the wells, interpretation of the facies stacking and depositional model. Populating the facies associations assigned at each well to cover inter-wells spaces by using different modeling algorithms. Stochastic facies modeling allows for the large-scale heterogeneity at the facies level to be captured and therefore allows the critical flow units within the reservoir to be accurately modeled on the geological data.

Table 7-5: The results of the variogram analysis used for facies modeling.

Zones	Lithofacies	Variogram range (m)			Model	Nugget
		Vertical	Major	Minor		
Zone-1	Shale	9	1100	930	Spherical	0.8
	Clean sand	8	900	840	Spherical	0
	Shaly sand	8	950	890	Spherical	0
Zone-2	Shale	10	1210	1130	Spherical	0.75
	Clean sand	7	860	800	Spherical	0
	Shaly sand	7	970	915	Spherical	0
Zone-3	Shale	10	1240	1020	Spherical	0.7
	Clean sand	8	825	775	Spherical	0
	Shaly sand	8	985	910	Spherical	0
Zone-4	Shale	9	1315	1115	Spherical	0.8
	Clean sand	6	750	690	Spherical	0
	Shaly sand	6	955	890	Spherical	0

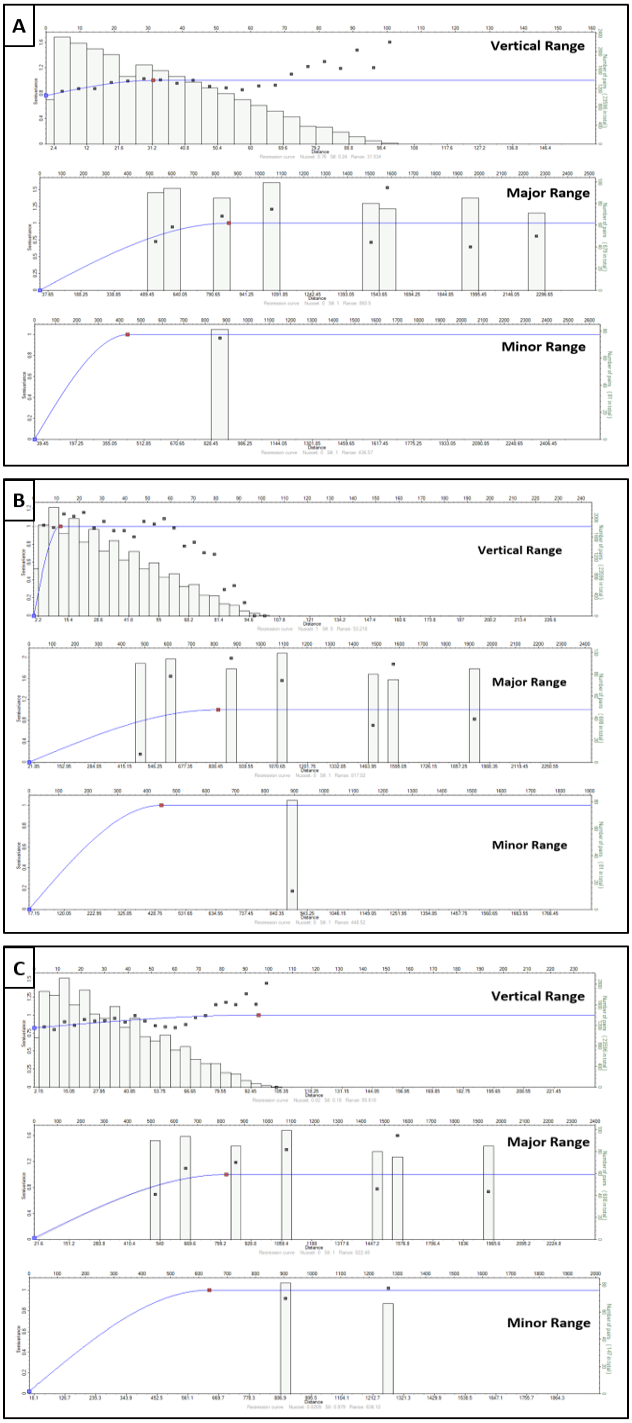

Figure 7-21: Variograms for Lithofacies. (A) Ranges for Shale lithofacies (B) Ranges for Clean-sand. (C) Ranges for Shaly-sand lithofacies.

A geostatistical approach was initially used to distribute the facies model with reference to the constructed conceptual model. The applied methodology used for distributing the facies was the Sequential Indicator Simulation (SIS).

7.8.3 Facies distribution

The facies distribution in Sufyan Sub-basin, Muglad Basin is primarily controlled by faults and depositional environments (Yassin et al., 2016). The sand thickness is directly related to faulting and basin subsidence.

The lateral and vertical facies distribution within each zone is discussed based on fence diagrams, block diagrams, horizontal slice, and cross sections passing through many wells. Special emphasis is put on the reservoir versus non-reservoir facies distribution, channel pathways, and channel amalgamation.

One block diagrams (Figure 7-22A), one fence diagrams (Figure 7-22B), three horizontal slices (Figure 7-23A, B, C), and one cross-section (Figure 7-17B) were selected to display the facies distribution in the study area.

These sections indicate that the zones-1 and 2 are dominant by clean sand facies with 70.43% and 70.77% respectively (Figure 7-24A, B). The amount of sand increases upward. In this zone; the sand facies is dominant in the uppermost, in the middle part the shaly sand facies is dominated, and in the lower part the shale facies is dominated. In zones-3 and 4, the shaly sand facies and shale facies are dominated with 52.51% and 85% respectively (Figure 7-24C, D).

7.8.4 Model Validation

The blind test for facies model was performed using well-5 which hasn't been used for any process related to modeling. The lithofacies logs from this well showed a good match with the constructed facies model (Figure 7-25). The lithofacies models were compared to the lithofacies models. Generally, the lateral and vertical facies variation depends on the large scale depositional environments for each zone.

In zone-1 and 2, the sand facies are dominated and this is because it deposited in the delta plain. In zone-3, the sand facies decreases downward where shaly facies of delta front are dominated. In zone-4, the proportion of the lacustrine mud is high and this is due to the depositional setting of prodelta.

7.9 Property modeling

The interpreted logs for effective porosity were used in the property modeling. Property modeling is the process of filling the cells of the grid with property values. The porosity logs were up-scaled to the fine-scale structural model using the simple arithmetic algorithm.

The properties were populated using the stochastic approach of Sequential Gaussian Simulation (SGS). This algorithm honors well data, any input distributions, variograms as well as data trends. The SGS also maintains the heterogeneity of the reservoir properties with reference to the horizontal and vertical variograms. Ten realizations for each zone were generated.

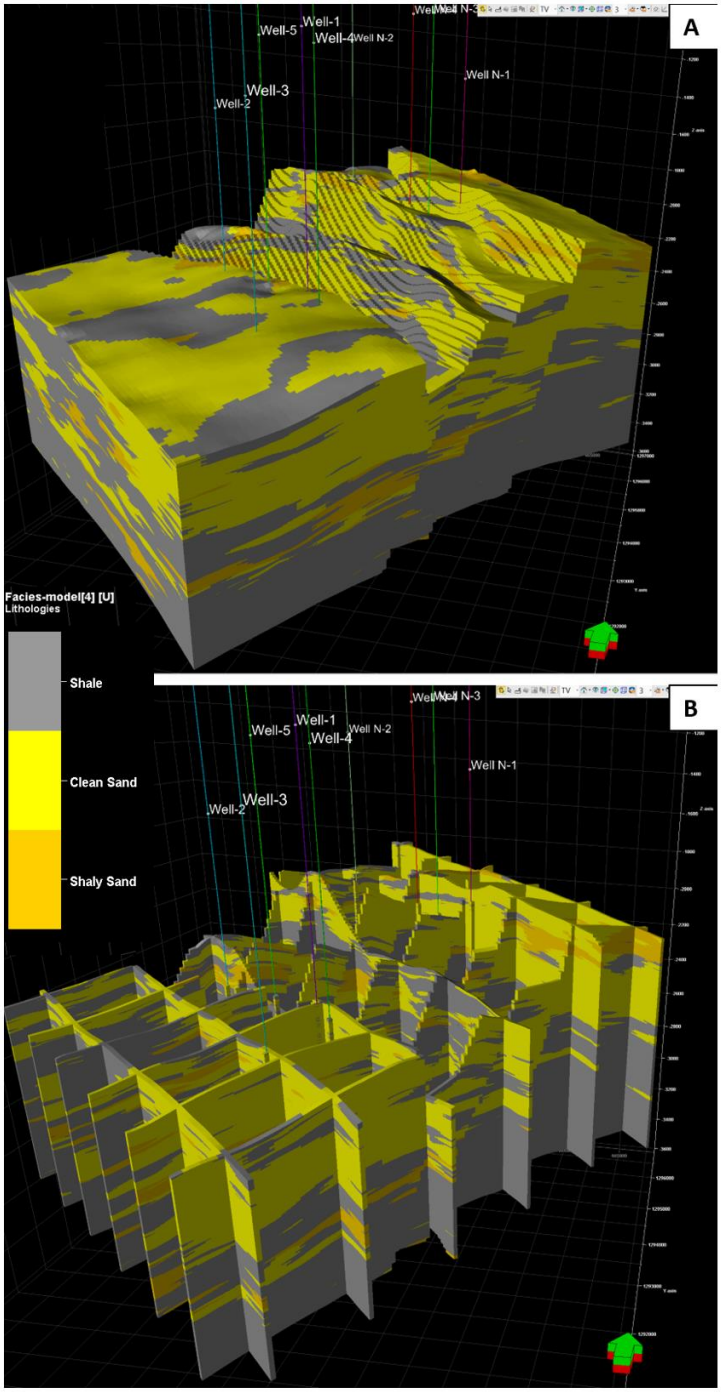

Figure 7-22: Three-dimensional (3D) model generated using sequential Indicator Simulation (SIS) algorithm, show the distribution of facies in each zone (four zones). Channel fills (CF), floodplains (FP), and distributary channels (DC) are dominated in the upper zones. In the middle zones, mouth bars (MB), underwater distributary channels (UW DC), and lacustrine mud (LM) are dominated. In the lower zone, lacustrine mud (LM), Interdistributary bay (IDB), distal bars (DB), and sheet sand (SS) are dominated.

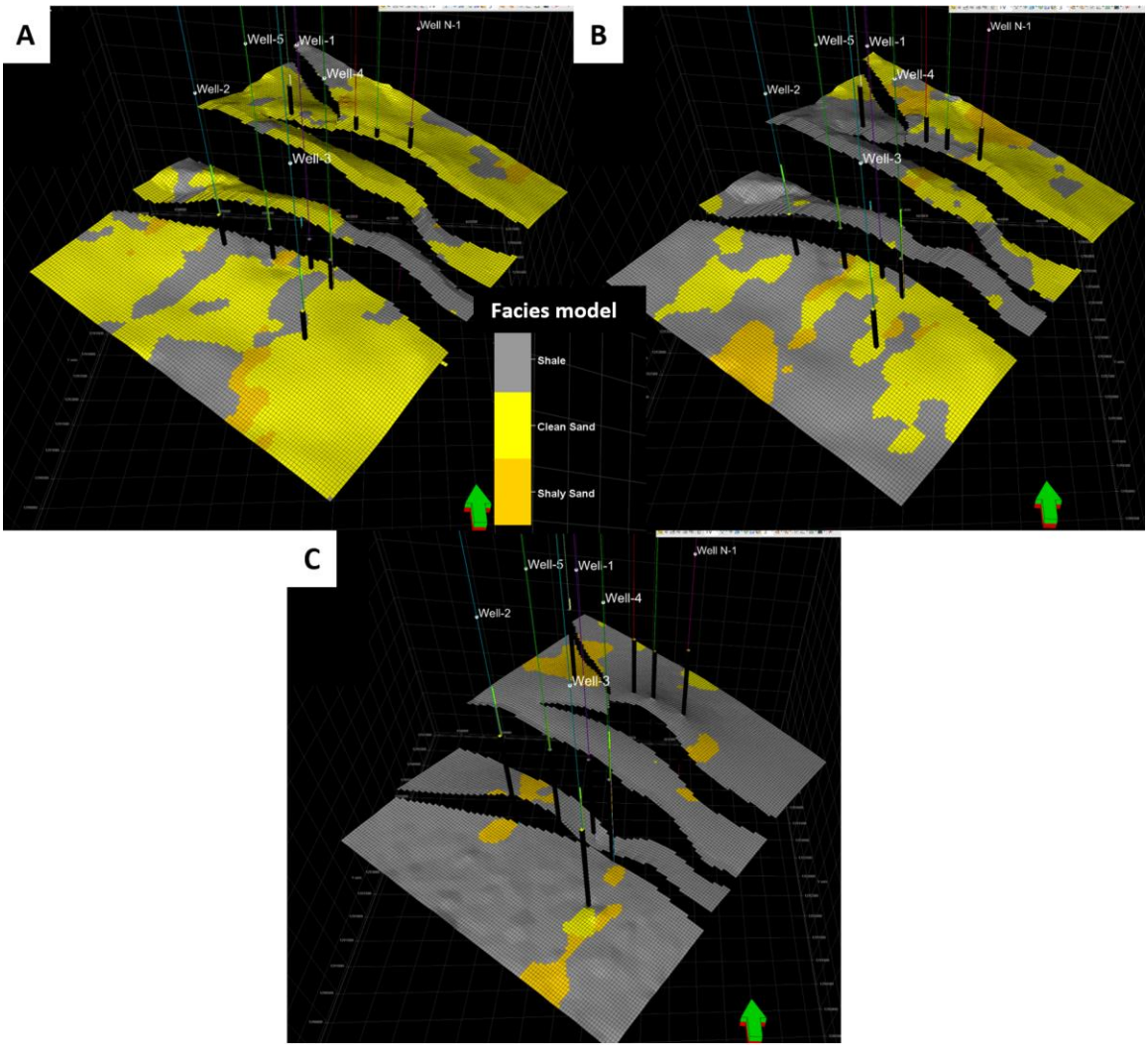

Figure 7-23: Facies distribution passing through five wells. Clean sand bodies dominated in the upper zone (A). The sand thickness decreases downward from A to C.

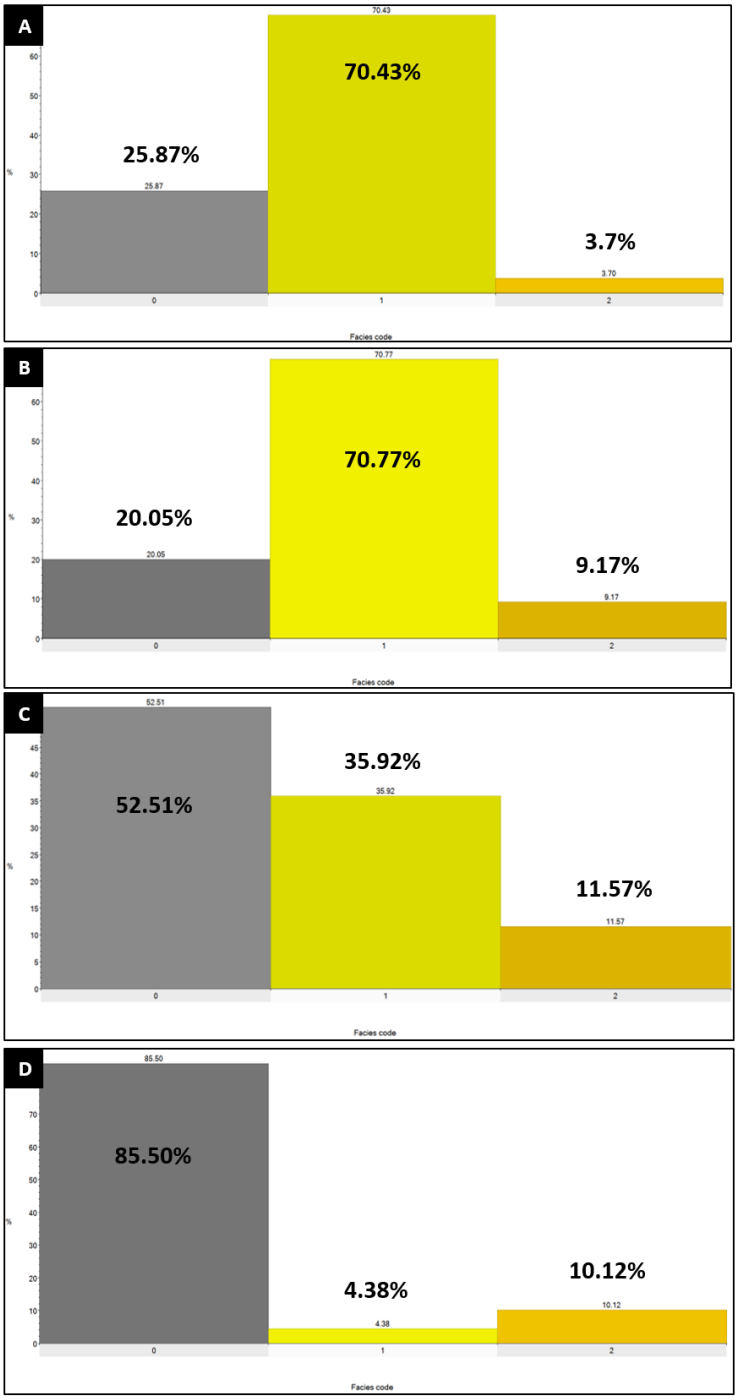

Figure 7-24: Lithofacies distribution analysis in the four zones. (A) zone-1, dominated by clean sand (70.43%) and shale (25.87%) with minor shaly sand (3.7%) (B) zone-2, dominated by shale (70.77%) and shale (20.25%) with minor shaly sand (9.17%). (C) zone-3, dominated by shale (52.51%) and clean sand (35.92%) with minor shaly sand (11.57%) (D) zone-4, dominated by shale (85.50%) and shaly sand (10.12%) with minor clean sand (4.38%).

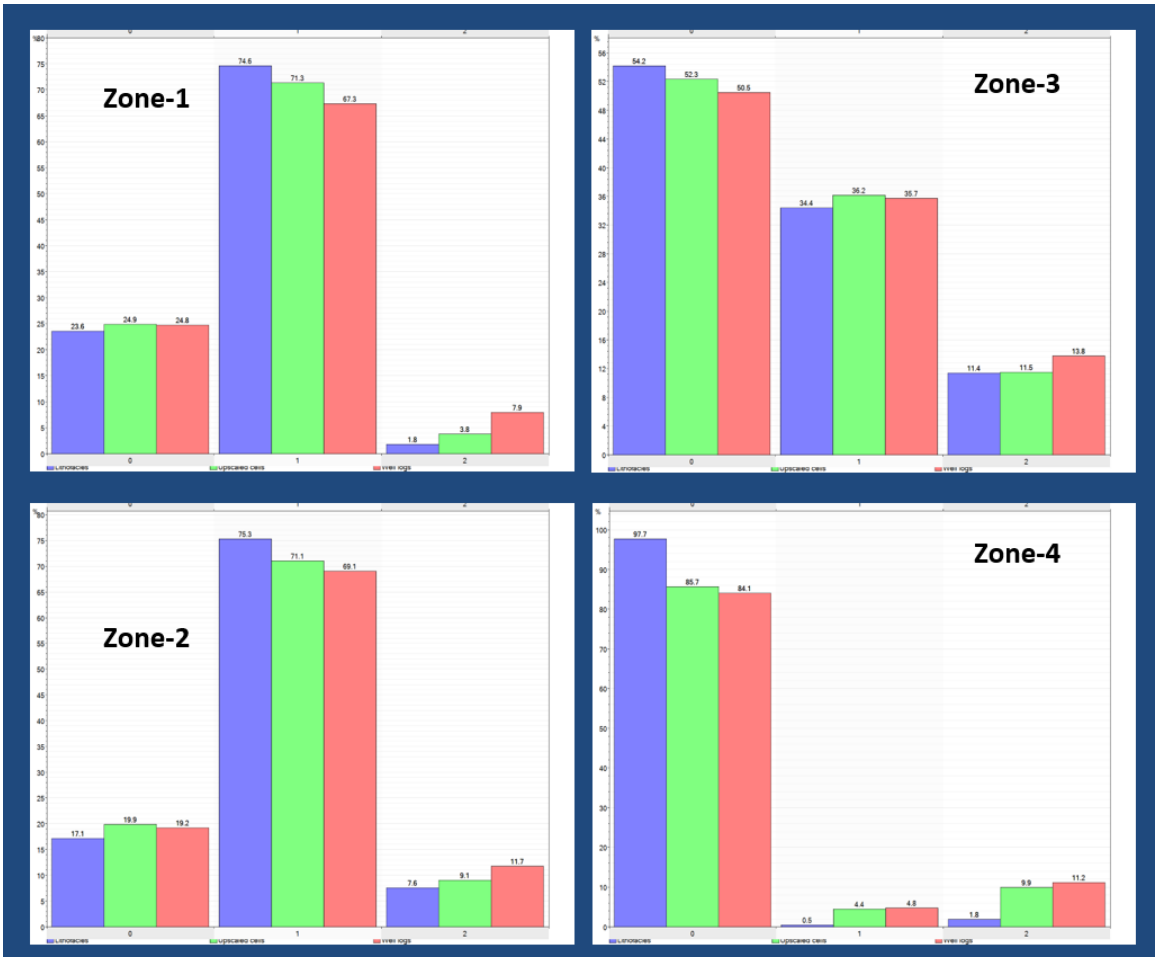

Figure 7-25: Facies model validation using histograms showing a comparison between original logs (red), up-scaled cells (green), and modeled (blue).

7.9.1 Geostatistical data analysis

Data analysis was carried out for the effective porosity and shale volume well logs. The data analysis was initiated by extracting a variogram map for each zone in the model in order to identify the direction of data variance. The directions of maximum and minimum variability (towards NE-SW and NW-SE, respectively) was used during variogram modeling. The input data fed to the geostatistical algorithms used in modeling should not have any trends i.e. it has to be stationary (Journel and Huijbregts, 1978b). In order to remove this non-stationary, certain data transformation has been performed. In order to ensure a normal distribution of the modeled data, the normal score transformation was performed for the data set used for analysis. The conditioned data were used in the subsequent analysis (for variogram analysis and also for modeling). This analysis of variogram modeling plays the key role in controlling the "texture" of the high-resolution details present in the output realizations. Experimental variograms were calculated in order to characterize the vertical and horizontal variations in their directions; vertical, major and minor directions based on the data trend identified from variogram maps.

The vertical experimental variograms were computed using the up-scaled logs (effective porosity) for each zone separately. The up-scaled facies logs were used as a secondary data in porosity variograms. The results of the variogram analysis are tabulated in Table 7-6. It is illustrating all variogram dimensions, as well as, direction and layering of the various model units.

7.9.2 Porosity modeling

The porosity was populated into the 3D model using the stochastic approach of Sequential Gaussian Simulation (SGS) algorithm. Ten realizations of porosity models have been produced using facies as secondary data for the model constraint.

The lateral and vertical porosity distribution within each zone is discussed based on fence diagrams, block diagrams, horizontal slice, and cross sections passing through many wells.

One block diagrams (Figure 7-26A), one fence diagrams (Figure 7-26B), four horizontal slices (Figure 7-27A, B, C, D), and one cross-section (Figure 7-17C) were selected to display the facies distribution in the study area.

The porosity model indicates good reservoir quality in the upper part of zone-1 related to the medium to coarse sandstone of the channel fills and distributary channels facies in this zone. In the lower part of zone-1, the porosity drastically decreases with depth and fine grain sandstone, muddier, and shaly facies are observed with relation to the delta front depositional environment (underwater distributary channel sandstone, mouth bar, interdistributary bay, and distal bar deposits). On the other hand, the non-reservoir rocks, mainly shale, with low porosity (< 0.05) are dominant in zones-3 and 4 are related to the shallow and deep lacustrine deposits.

Table 7-6: The results of the variogram analysis used for porosity modeling.

Zones	Model	Porosity Variogram range (m)		
		Vertical	Major	Minor
Zone-1	Spherical	8	1220	1130
Zone-2	Spherical	9	1115	1065
Zone-3	Spherical	7	1030	970
Zone-4	Spherical	9	980	935

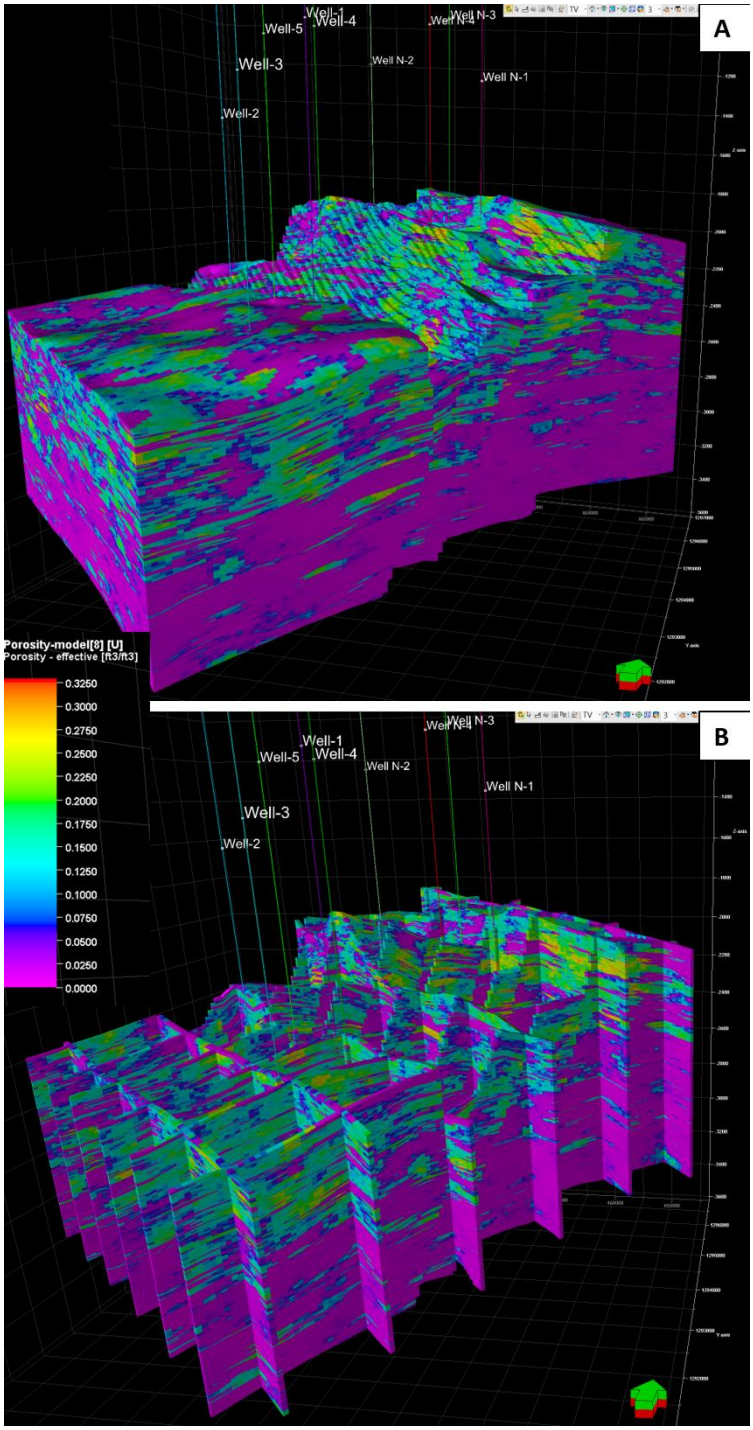

Figure 7-26: Porosity model in Abu Gabra Formation zones using Sequential Gaussian Simulation algorithm, this model populating porosity logs guided by facies. Red and yellow colors indicate good porosity (up to 0.32). The porosity variations can be related to facies in each zone and hence the for reservoir quality prediction will be more reliable.

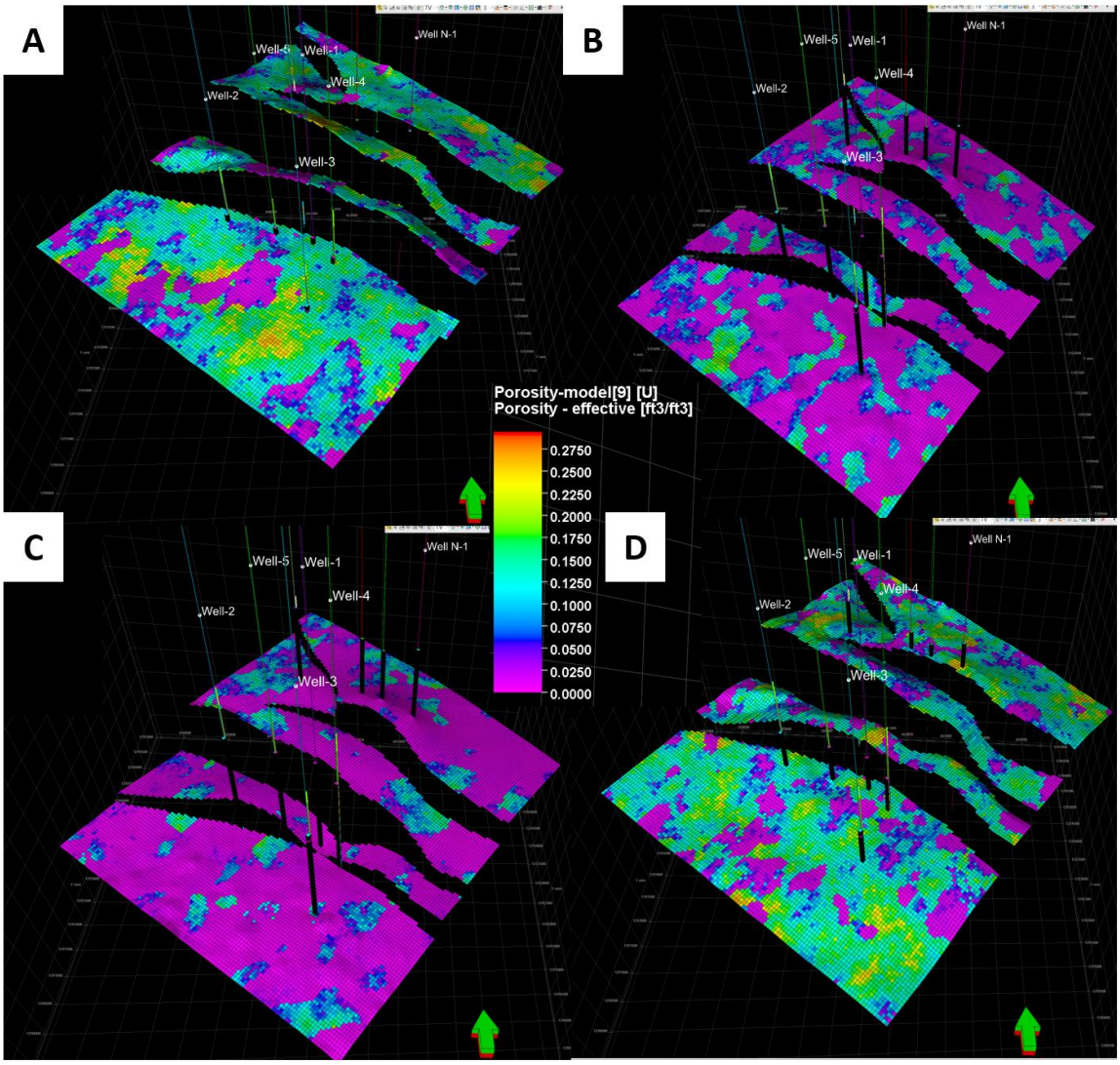

Figure 7-27: Porosity model in Abu Gabra Formation zones using Sequential Gaussian Simulation algorithm, this model populating porosity logs guided by facies. Red and yellow colors indicate good porosity (up to 0.32). The porosity variations can be related to facies in each zone and hence the for reservoir quality prediction will be more reliable.

CHAPTER 8

CONCLUSIONS AND RECOMMENDATIONS

8.1 Conclusions

Sufyan Sub-basin is an E-W trending Sub-basin located in the northwestern part of the Muglad Basin and in the eastern extension of the West and Central Africa Rift System (WCARS). It is bounded by three faults; two of those faults expose dextral strike-slip movement, with two depocenters at the western and eastern segments of the southern boundary fault. The Sub-basin is characterized by rhombic geometry and presence of negative flower structures, and en-echelon parallel normal faults, which indicate a pull-apart system.

Integration of the different scales of geological observations (from basin to reservoir scale) using subsurface data, produced a reliable geological model of the Cretaceous clastic sedimentary rocks of the Sufyan Sub-basin basin. The constructed model links the tectonic evolution of Sufyan Sub-basin with structural and sequence stratigraphy. A detailed study has conducted in Sufyan Sub-basin integrating the kinematic structural models that generated from the structural restoration with the depositional systems, stratigraphic sequences, and sand-body distribution in Sufyan sub-basin. The study indicated that faults initiation and reactivation along with the tectonic subsidence are responsible for the complexity of the Petroleum systems in the sub-basin. Specific conclusions are:

Structure and tectonic evolution

- Sufyan Sub-basin is believed to be highly affected by the Central African Shear Zone (CASZ). Structural analysis of the Sufyan Sub-basin revealed that it was mainly formed by dextral oblique shear movement. The Sub-basin origin is due to the transtensional movement and the Sub-basin type is pull-apart (rhombic graben). Sufyan Sub-basin is a pull-apart basin affected by both CASZ (transtensional) and Muglad Basin (extension).
- The lateral movement of the south boundary fault released the compressional stress during the late Santonian period and hence no big four-way dip closure trap has developed.
- The highly prospective areas identified in Sufyan Sub-basin based on this study are the areas of flower structure (but they are relatively small prospects) and the areas that near the two depocenters that controlled by F1-B and F1-D segments of the southern boundary fault (F1) in between the major transtensional (oblique) faults.
- The idea and approach for exploring Abu Gabra Formation targets (active rift phase) is different from the case of Bentiu Formation targets (non-active rift phase). The sedimentary facies, reservoir property, and structural setting are key controlling factors for Abu Gabra oil pools, and these three elements are suggested to be analyzed by any drilling candidate targeting of Abu Gabra Formation.

Depositional systems, sequence stratigraphic pattern, and their controls

- Data integration allow us to establish a tectono-sequence stratigraphic model for Sufyan Sub-basin.
- Based on tectonic evolution analysis, biostratigraphy, seismic, well logs and core data, Abu Gabra Formation divided further into two 2nd order sequences, each one deposited during sub-rift phases (syn-rift-1 and syn-rift-2). The vertical variation in the depositional sequences, seismic amplitudes (Low and high), and tectonic subsidence of Abu Gabra Formation support this subdivision. The sequence filling and evolution processes are controlled by the tectonic movements in the study area, and different sequence filling in Abu Gabra Formation have been caused by the rifting stages.
- Abu Gabra formation was filled during the syn-rifting phase of the first rifting cycle, which corresponded to the development of 3rd order sequences from SQ-A to SQ-E.
- Those five 3rd order sequences were developed during five stages of basin evolution (early syn-rift/rift initiation stage, rift climax-1 stage, late syn-rift-1stage, rift climax-2 stage, and late syn-rift-2 stage).
- Rift initiation/early syn-rift of Abu Gabra formation composed mainly of fan, fan-delta, and shallow lacustrine deposits. This sequence contains two system tracts, transgressive system tract (TST) and highstand system tract (HST).
- Rift climax stage in Abu Gabra Formation is characterized by high tectonic subsidence and therefore the considerable expansion of the lake and the maximum flooding occurred. At the sub-basin center, deep lacustrine mud deposits were developed while braided deltas and fan deltas occurred in the sub-basin margin. Sublacustrine fan deposits were recognized in this sequence near to the intra-basinal fault zones. This

sequence comprises two system tracts, transgressive system tract (TST) and highstand system tract (HST). The transgressive system tract (TST) is dominant and characterized by very thick claystone. This claystone is deposited in a deep lacustrine as a result of the increase of the accommodation space associated with the high subsidence.

- The Late syn-rift stage is characterized by low or no tectonic subsidence and therefore the lake level was dropped. At the sub-basin center, deep lacustrine mud deposits were developed while braided deltas and fan deltas occurred in the sub-basin margin. In Sufyan Sub-basin, fan delta mainly develops in the steep slope fault zone in the southern area while delta develops in the gentle slope fault zone (northern and northwestern areas). Fluvial environment and braided delta environment deposited at the ramp side of the major southern boundary fault and fan delta deposited at the cliff side of the major southern boundary fault, those environments are immediately followed by small shallow lakes in the middle. This sequence comprises two system tracts, transgressive system tract (TST) and highstand system tract (HST). The highstand system tract (HST) is dominant and characterized by thick sandstone. This sandstone is deposited in braided and Fan deltas as a result of the decrease of the accommodation space.

Sedimentology and reservoir characteristics

- Seven lithofacies were recognized in Abu Gabra Formation based on core description. It is mainly composed of continental-derived clastics. These include bedded conglomeratic sandstone, planar cross-bedded sandstone, trough cross-bedding

sandstone, massive sandstone, ripples cross-laminated sandstone, massive to blocky mudstone and siltstone, and mudstone and shale.

- On the basin scale, the Abu Gabra Formation showed difference depositional systems, sandstone bodies thickness, geometry, and architecture. Abu Gabra formation was filled during the syn-rifting phase of the first rifting cycle and could be subdividing into two 2nd order sequences.
- Abu Gabra Formation could be subdividing into five 3rd order sequences from SQ-A to SQ-E.
- For each sequence, at the sub-basin center, deep lacustrine mud deposits were developed while braided deltas and fan deltas occurred in the sub-basin margin. Fan-delta mainly develops in the steep slope fault zone in the southern area while delta develops in the gentle slope fault zone northern areas.
- In this study, the quantification of the inner-well scale heterogeneities are strongly enhanced by the integration of the high-resolution seismic attributes, spatially and high-resolution wireline logs, temporally.
- The results of this study might contribute to better understanding of reservoir heterogeneities and help in reservoir quality prediction, therefore enhancing the hydrocarbon productivity.

Geostatistical integration and reservoir modeling

- Multidisciplinary reservoir modeling approach is integrated to reveal reservoir architecture and heterogeneity in different scales.

- Detailed analysis and interpretation were carried out including: sedimentological facies analysis from conventional core and well logs, reconstruction of depositional models, stratigraphic analysis and well correlation, petrophysical reservoir property and cutoffs (i.e., porosity and volume of shale), reservoir architecture (i.e., channel bodies) from seismic attributes (RMS), 3D facies and property modeling.
- The 3D facies models showed a heterogeneous facies distribution in the study area supporting the interpretation drawn by sedimentologic and sequence stratigraphic analysis. The facies logs were produced using cutoffs of porosity and volume of shale. Three facies have been used in these models; clean sand, shaly sand, and shale. It is worth to mention that the sand facies has been classified into two types of sands (based on porosity cutoffs) in this study.
- In zones-1 and 2, thick sand bodies are common with quite good lateral extension and less shaly facies. Thick shale and claystone with thin sand bodies are observed in zones-3, and 4. This pattern of facies distribution suggests lower reservoir quality in zones-3, and 4 in comparison to zones-1 and 2.
- The porosity model has been conducted in the study area. This model was controlled by facies to enable data integration and interpretation.
- The porosity distribution has supported the interpretation mentioned above with regards to different reservoir quality and heterogeneity.

8.2 Recommendations

- Apply 3D structural restoration in the study area.
- Acquire conventional core in other reservoir sections such as in sublacustrine fan deposits.
- Acquire high-resolution 3D seismic.
- Reprocess the available 3D seismic data (pre-stack time/depth migration).
- Construct 3D geological model in another area after drilling more wells, to quantify the reservoir properties.
- Use seismic inversion (acoustic impedance) as a guide for porosity distribution.

References

Aigner, T., Brandenburg, A., van Vliet, A., Doyle, M., Lawrence, D., Westrich, J., 1990. Stratigraphic modelling of epicontinental basins: two applications. Sediment. Geol. 69, 167–190.

Al-Ramadan, K., Morad, S., Proust, J.N., Al-Aasm, I.S., 2005. Distribution of Diagenetic Alterations in Siliciclastic Shoreface Deposits within a Sequence Stratigraphic Framework: Evidence from the Upper Jurassic, Boulonnais, NW France. J. Sediment. Res. 75, 943–959.

Alejandro, E., Paul, M., 2006. Sequence-stratigraphic analysis of Eocene clastic foreland basin deposits in central Lake Maracaibo using high-resolution well correlation and 3-D seismic data. Am. Assoc. Pet. Geol. Bull. 90, 581–623.

Allen, P.A., Allen, J.R., 2013. Basin Analysis: Principles and Application to Petroleum Play Assessment, Journal of Chemical Information and Modeling. Wiley-Blackwell.

Asquith, G.B., Gibson, C.R., 2007. Basic Well Log Analysis. (Vol. 16). Tulsa: American association of petroleum geologists.

Ayhan, I., Nemec, W., 2005. Early Miocene lacustrine deposits and sequence stratigraphy of the Ermenek Basin, Central Taurides, Turkey. Sediment. Geol.

Binks, R.M., Fairhead, J.D., 1992. A plate tectonic setting for Mesozoic rifts of West and Central Africa. Tectonophysics 213, 141–151.

Bloch, S., 1991. Empirical predicition of porosity and permeability in sandstones. Am. Assoc. Pet. Geol. Bull. 75, 1145–1160.

Bosworth, W., 1992. Mesozoic and early Tertiary rift tectonics in East Africa. Tectonophysics 209, 115–137.

Caby, R., 2003. Terrane assembly and geodynamic evolution of central–western Hoggar: a synthesis. J. African Earth Sci.

Carroll, A.R., Bohacs, K.M., 1999. Stratigraphic classification of ancient lakes: Balancing tectonic and climatic controls. Geology 27, 99–102.

Catuneanu, O., 2006. Principles of Sequence Stratigraphy. Elsevier.

Catuneanu, O., 2002. Sequence stratigraphy of clastic systems: concepts, merits, and pitfalls. J. African Earth Sci. 35, 1–43.

Catuneanu, O., Abreu, V., Bhattacharya, J.P.P., Blum, M.D.D., Dalrymple, R.W.W., Eriksson, P.G.G., Fielding, C.R.R., Fisher, W.L.L., Galloway, W.E.E., Gibling, M.R.R., Giles, K. a. a, Holbrook, J.M.M., Jordan, R., Kendall, C.G.S.C.G.S.C., Macurda, B., Martinsen, O.J.J., Miall, a. D.D., Neal, J.E.E., Nummedal, D., Pomar, L., Posamentier, H.W.W., Pratt, B.R.R., Sarg, J.F.F., Shanley, K.W.W., Steel, R.J.J., Strasser, A., Tucker, M.E.E., Winker, C., 2009. Towards the standardization of sequence stratigraphy - Reply. Earth Sci. Rev. 94, 98–100.

Catuneanu, O., Galloway, W.E., Kendall, C.G.S.C., Miall, A.D., Posamentier, H.W., Strasser, A., Tucker, M.E., 2011. Sequence Stratigraphy: Methodology and Nomenclature. Newsletters Stratigr. 44, 173–245.

Catuneanu, O., Martins-Neto, M.A., Eriksson, P.G., 2005. Precambrian sequence stratigraphy. Sediment. Geol. 176.

Clavier, C., Hoyle, W., Meunier, D., 1971. Quantitative Interpretation of Thermal Neutron Decay Time Logs: Part I - Fundamentals and Techniques. J. Pet. Technol. 23, 756–763.

Daly, M., Chorowicz, J., Fairhead, J., 1989. Rift basin evolution in Africa: the influence of

reactivated steep basement shear zones. Geol. Soc. London Spec. Publ. 44, 309–334.

Davison, I., 1986. Listric normal fault profiles: calculation using bed-length balance and fault displacement. J. Struct. Geol. 8, 209–210.

Deusch, C. V, Journel, A.G., 1992. Geostatistical Software Library and User's Guide, New York. 119, 147.

Deutsch, C., 2002a. Geostatistical reservoir modeling: Oxford University Press, New York, 376 p. Google Sch. Doctoral Thesis. Masson, Paris.

Deutsch, C., 2002b. Geostatistical reservoir modeling: Oxford University Press, New York, 376 p. Google Sch. Doctoral Thesis. Masson, Paris.

Dixon, T., Stern, R., Hussein, I., 1987. Control of Red Sea rift geometry by Precambrian structures. Tectonics 6, 551–571.

Dong, W., Lin, C., Eriksson, K.A., Zhou, X., Liu, J., Teng, Y., 2011. Depositional systems and sequence architecture of the Oligocene Dongying Formation, Liaozhong depression, Bohai Bay Basin, Northeast China. Am. Assoc. Pet. Geol. Bull. 95, 1475–1493.

Dooley, T., McClay, K., 1997. Analog modeling of pull-apart Basins. Am. Assoc. Pet. Geol. Bull. 81, 1804–1826.

Dott, R.H., 1964. Wacke, Graywacke and Matrix--What Approach to Immature Sandstone Classification? SEPM J. Sediment. Res. Vol. 34, 625–632.

Douglas, J.C., 1995. Sequence stratigraphic analysis of individual depositional successions: effects of marine/nonmarine sediment partitioning and longitudinal sediment transport, Mannville Group, Alberta foreland basin, Canada. Am. Assoc. Pet. Geol. Bull. 79, 749–762.

Dula, W.F., 1991. Geometric Models of Listric Normal Faults and Rollover Folds. Am. Assoc. Pet. Geol. Bull. 75, 1609–1625.

Dunne, L., McPherson, J.G., Shanmugam, G., Moiola, R.J., 1988. Fan-Deltas and Braid Deltas: Varieties of Coarse-Grained Deltas: Discussion and Reply. Bull. Geol. Soc. Am. 99, 1987–1989.

Dutton, S.P., Loucks, R.G., 2010. Reprint of: Diagenetic controls on evolution of porosity and permeability in lower Tertiary Wilcox sandstones from shallow to ultradeep (200-6700m) burial, Gulf of Mexico Basin, U.S.A. Mar. Pet. Geol. 27, 1775–1787.

El-ghali, M.A.K., Mansurbeg, H., Morad, S., Al-Aasm, I., Ajdanlisky, G., 2006. Distribution of diagenetic alterations in fluvial and paralic deposits within sequence stratigraphic framework: Evidence from the Petrohan Terrigenous Group and the Svidol Formation, Lower Triassic, NW Bulgaria. Sediment. Geol. 190, 299–321.

El-Ghali, M.A.K., Morad, S., Mansurbeg, H., Caja, M.A., Ajdanlijsky, G., Ogle, N., Al-Aasm, I., Sirat, M., 2009. Distribution of diagenetic alterations within depositional facies and sequence stratigraphic framework of fluvial sandstones: Evidence from the Petrohan Terrigenous Group, Lower Triassic, NW Bulgaria. Mar. Pet. Geol. 26, 1212–1227.

El Hassan, W.M., El Nadi, A.H.H., 2015. Impact of inversion tectonics on hydrocarbon entrapment in the Baggara Basin, western Sudan. Mar. Pet. Geol. 68, 492–497.

Emery, D., K.J. Myers, 1996. Sequence Stratigraphy. John Wiley & Sons.

Fairhead, J., 1988. Mesozoic plate tectonic reconstructions of the central South Atlantic Ocean: the role of the West and Central African rift system. Tectonophysics 155, 181–191.

Fairhead, J., Binks, R., 1991. Differential opening of the Central and South Atlantic Oceans and the opening of the West African rift system. Tectonophysics 187, 191–203.

Fairhead, J., Green, C., Masterton, S., Guiraud, R., 2013. The role that plate tectonics, inferred stress changes and stratigraphic unconformities have on the evolution of the West and Central African rift system and the Atlantic. Tectonophysics 594, 118–127.

Feng, J., Cao, J., Hu, K., Peng, X., Chen, Y., Wang, Y., Wang, M., 2013. Dissolution and its impacts on reservoir formation in moderately to deeply buried strata of mixed siliciclastic-carbonate sediments, northwestern Qaidam Basin, northwest China. Mar. Pet. Geol. 39, 124–137.

Galloway, W.E., 1989. Genetic Stratigraphic Sequences in Basin Analysis II: Application to Northwest Gulf of Mexico Cenozoic Basin. Am. Assoc. Pet. Geol. Bull. 73, 143–154.

Gawthorpe, R.L., Leeder, M.R., 2000. Tectono-sedimentary evolution of active extensional basins. Basin Res. 12, 195–218.

Genik, G.J., 1993. Petroleum geology of Cretaceous-Tertiary rift basins in Niger, Chad, and Central African Republic. Am. Assoc. Pet. Geol. Bull. 77, 1405–1434.

Gibbs, A.D., 1983. Balanced cross-section construction from seismic sections in areas of extensional tectonics. J. Struct. Geol. Struct. Geol. 5, 153–160.

Gier, S., Worden, R.H., Johns, W.D., Kurzweil, H., 2008. Diagenesis and reservoir quality of Miocene sandstones in the Vienna Basin, Austria. Mar. Pet. Geol. 25, 681–695.

GRAS, 2005. Geological map of the Sudan, scale 1:2000, 000.

Guiraud, R., Bosworth, W., 1997. Senonian basin inversion and rejuvenation of rifting in Africa and Arabia: synthesis and implications to plate-scale tectonics. Tectonophysics

282, 39–82.

Guiraud, R., Bosworth, W., Thierry, J., Delplanque, A., 2005. Phanerozoic geological evolution of Northern and Central Africa: An overview. J. African Earth Sci. 43, 83–143.

Guiraud, R., Maurin, J.C., 1992. Early Cretaceous rifts of Western and Central Africa: an overview. Tectonophysics 213, 153–168.

Hongwen, D., Ruiju, W., Yi, X., Jianyu, G.U.O., Xiaojun, X.I.E., 2008. Tectono-Sequence Stratigraphic Analysis in Continental Faulted Basins. Earth Sci. Front. 15, 1–7.

Hou, Y., He, S., Ni, J., Wang, B., 2012. Tectono-sequence stratigraphic analysis on Paleogene Shahejie Formation in the Banqiao sub-basin, Eastern China. Mar. Pet. Geol. 36, 100–117.

Journel, A., Baafi, E., Schofield, N., 1997. The abuse of principles in model building and the quest for objectivity. Geostatistics Wollongong 96, pp.3-14.

Journel, A.G., Huijbregts, C.J., 1978a. Mining geostatistics. Academic Press, London, 600 p.

Journel, A.G., Huijbregts, C.J., 1978b. Mining geostatistics. Academic Press, London, 600 p.

Juhász, E., L.Ó. Kovács, P., Müller, Á., Tóth-Makk, L., Phillips, Lantos, M., 1997. Climatically driven sedimentary cycles in the late Miocene sediments of the Pannonian Basin, Hungary. Tectonophysics 82, 157–176.

Ketzer, J.M., Holz, M., Morad, S., Al-Aasm, I.S., 2003. Sequence stratigraphic distribution of diagenetic alterations in coal-bearing, paralic sandstones: evidence from the Rio Bonito Formation (early Permian), southern Brazil. Sedimentology 50, 855–877.

Kneller, B.C., Branney, M.J., 1995. Sustained high-density turbidity currents and the deposition of thick massive sands. Sedimentology 42, 607–616.

Krige, D.G., 1952. A Statistical Approach to Some Basic Mine Valuation Problems on the Witwatersrand. J. Chem. Metall. Min. Soc. South Africa.

Leeder, M.R., Gawthorpe, R.L., 1987. Sedimentary models for extensional tilt-block/ half-graben basins. In: Tectonics and Seismic Sequence Stratigraphy. Geol. Soc. London, Spec. Publ. 28, 139–152.

Lima, R.D., Ros, L.F. De, 2003. The role of depositional setting and diagenesis on the reservoir quality of Late Devonian sandstones from the Solimoes Basin, Brazilian Amazonia. Mar. Pet. Geol. 19, 1047–1071.

Lin, C., Eriksson, K., Li, S., Wan, Y., Ren, J., Zhang, Y., 2001. Sequence architecture, depositional systems, and controls on development of lacustrine basin fills in part of the Erlian basin, northeast China. Am. Assoc. Pet. Geol. Bull. 85, 2017–2043.

Lirong, D., Dingsheng, C., Zhi, L., Zhiwei, Z., 2013. Petroleum Geology of the Fula Sub-Basin, Muglad Basin, Sudan. J. Pet. 36, 43–59.

Luo, J.L., Morad, S., Salem, A., Ketzer, J.M., Lei, X.L., Guo, D.Y., Hlal, O., 2009. Impact of diagenesis on reservoir-quality evolution in fluvial and lacustrine-deltaic sandstones: Evidence from jurassic and triassic sandstones from the Ordos Basin, China. J. Pet. Geol. 32, 79–102.

Mahgoub, M.I., Padmanabhan, E., Abdullatif, O.M., 2016. Sedimentological reservoir characteristics of the Paleocene fluvial/lacustrine Yabus Sandstone, Melut Basin, Sudan. J. African Earth Sci. 123, 75–88.

Makeen, Y.M., Abdullah, W.H., Hakimi, M.H., 2013. Biological markers and organic

petrology study of organic matter in the Lower Cretaceous Abu Gabra sediments (Muglad Basin, Sudan): origin, type and palaeoenvironmental conditions. Arab. J. Geosci. 1–18.

Makeen, Y.M., Abdullah, W.H., Hakimi, M.H., Elhassan, O.M.A., 2015a. Organic geochemical characteristics of the Lower Cretaceous Abu Gabra Formation in the Great Moga oilfield, Muglad Basin, Sudan: Implications for depositional environment and oil-generation potential. J. African Earth Sci. 103, 102–112.

Makeen, Y.M., Abdullah, W.H., Hakimi, M.H., Hadad, Y.T., Elhassan, O.M.A., Mustapha, K.A., 2015b. Geochemical characteristics of crude oils, their asphaltene and related organic matter source inputs from Fula oilfields in the Muglad Basin, Sudan. Mar. Pet. Geol. 67, 816–828.

Makeen, Y.M., Abdullah, W.H., Hakimi, M.H., Mustapha, K.A., 2015c. Source rock characteristics of the Lower Cretaceous Abu Gabra Formation in the Muglad Basin, Sudan, and its relevance to oil generation studies. Mar. Pet. Geol. 59, 505–516.

Makeen, Y.M., Abdullah, W.H., Pearson, M.J., Hakimi, M.H., Ayinla, H.A., Elhassan, O.M.A., Abas, A.M., 2016. History of hydrocarbon generation, migration and accumulation in the Fula sub-basin, Muglad Basin, Sudan: Implications of a 2D basin modeling study. Mar. Pet. Geol. 77, 931–941.

Makeen, Y.M., Hakimi, M.H., Abdullah, W.H., 2015d. The origin, type and preservation of organic matter of the Barremian-Aptian organic-rich shales in the Muglad Basin, Southern Sudan, and their relation to paleoenvironmental and paleoclimate conditions. Mar. Pet. Geol. 65, 187–197.

Mann, D.C., 1989. Thick-skin and thin-skin detachment faults in continental Sudanese rift

basins. J. African Earth Sci. 8, 307–322.

Martins-Neto, M.A., Catuneanu, O., 2010. Rift sequence stratigraphy. Mar. Pet. Geol. 27, 247–253.

Matheron, G., 1973. The intrinsic random functions and their applications. Adv. Appl. Probab. 5, 439–468.

Matheron, G., 1965. Les variables regionalisées et leur estimation. Doctoral Thesis. Masson, Paris.

Matheron, G., 1962. Traité de géostatistique appliquée. Mémoires du Bureau de Recherches Géologiques et Minieres. Mémoires du Bur. Rech. Géologiques Minieres 14, 333.

Matrices, K., Diamond, P., Armstrong, M., 1984. Robustness of variograms and conditioning of kriging matrices. Math. Geol. 16.

McConnell, R.B., 1972. Geological development of the rift system of eastern Africa. Geol. Soc. Am. Bull. 83, 2549–2572.

McHargue, T.R., Heidrick, T.L., Livingston, J.E., 1992. Tectonostratigraphic development of the Interior Sudan rifts, Central Africa. Tectonophysics 213, 187–202.

McPherson, J.G., Shanmugam, G., Moiola, R.J., 1987. Fan-deltas and braid deltas : Varieties of coarse- grained deltas. Geol. Soc. Am. Bull., 331–340.

Miall, A.D., 2013. Principles of sedimentary basin analysis. Springer Science & Business Media.

Miall, A.D., 2010. The geology of stratigraphic sequences. second ed. Springer- Verlag, Berlin Heidelberg. 532pp.

Mohamed, A.Y., Ashcroft, W.A., Whiteman, A.J., 2001. Structural development and

crustal stretching in the Muglad Basin, southern Sudan. J. African Earth Sci. 32, 179–191.

Mohamed, A.Y., Pearson, M.J., Ashcroft, W.A., Iliffe, J.E., Whiteman, A.J., 1999. Modeling petroleum generation in the Southern Muglad rift basin, Sudan. Am. Assoc. Pet. Geol. Bull. 83, 1943–1964.

Morad, S., Al-Ramadan, K., Ketzer, J.M., De Ros, L.F., 2010. The impact of diagenesis on the heterogeneity of sandstone reservoirs: A review of the role of depositional fades and sequence stratigraphy. Am. Assoc. Pet. Geol. Bull.

Morley, C.K., 1995. Developments in the structural geology of rifts over the last decade and their impact on hydrocarbon exploration. Geol. Soc. London, Spec. Publ. 80, 1–32.

Morley, C.K., Haranya, C., Phoosongsee, W., Pongwapee, S., Kornsawan, A., Wonganan, N., 2004. Activation of rift oblique and rift parallel pre-existing fabrics during extension and their effect on deformation style : examples from the rifts of Thailand. J. Struct. Geol. 26, 1803–1829.

Morley, C.K., Nelson, R.A., Patton, T.L., Munn, S.G., 1990. Transfer zones in the East African rift system and their relevance to hydrocarbon exploration in rifts. Am. Assoc. Pet. Geol. Bull. 74, 1234–1253.

Mulder, T., Syvitski, J.P.M., 1995. Turbidity Currents Generated at River Mouths during Exceptional Discharges to the World Oceans. J. Geol. 103, 285–299.

Posamentier, H., Allen, G., 1999. Siliciclastic sequence stratigraphy: concepts and applications. Tulsa: SEPM Society for Sedimentary Geology Concepts in Sedimentology and Paleontology Series, 7, 210 pp.

Posamentier, H.W., Allen, G.P., 1993. Siliciclastic sequence stratigraphic patterns in foreland ramp-type basins. Geology.

Poupon, A., Clavier, C., Dumanoir, J., 1970a. Log Analysis of Sand-Shale Sequences: A Systematic Approach. J. Pet. Technol. 22, 867–881.

Poupon, A., Clavier, C., Dumanoir, J., 1970b. Log Analysis of Sand-Shale Sequences: A Systematic Approach. J. Pet. Technol. 22, 867–881.

Prosser, S., 1993. Rift-related linked depositional systems and their seismic expression. Geol. Soc. London, Spec. Publ. 71, 35–66.

Qiao, J., Liu, L., An, F., Xiao, F., Wang, Y., Wu, K., Zhao, Y., 2016. Hydrocarbon potential evaluation of the source rocks from the Abu Gabra Formation in the Sufyan Sag, Muglad Basin, Sudan. J. African Earth Sci. 118, 301–312.

Ravnås, R., Nøttvedt, A., Steel, R.J., Windelstad, J., 2000. Syn-rift sedimentary architectures in the Northern North Sea. Geol. Soc. London, Spec. Publ. 167, 133–177.

Rouby, D., Cobbold, P., Szatmari, P., Demercian, S., 1993. Restoration in plan view of faulted Upper Cretaceous and Oligocene horizons and its bearing on the history of salt tectonics in the Campos Basin (Brazil). Tectonophysics 228, 435–445.

Sanderson, D., Marchini, W., 1984. Transpression. J. Struct. Geol. 6, 449–458.

Sangree, J.B., Widmier, J.M., 1979. Interpretation of depositional facies from seismic data. Geophysics 44, 131–160.

Schlische, R.W., Olsen, P.E., 1990. Quantitative Filling Model for Continental Extensional Basins with Applications to Early Mesozoic Rifts of Eastern North America. J. Geol. 98, 135–155.

Schlumberger, 1997. Log Interpretation Principle/ Application, New York.

Schmid, S., Worden, R.H., Fisher, Q.J., 2004. Diagenesis and reservoir quality of the Sherwood Sandstone (Triassic), Corrib Field, Slyne Basin, west of Ireland. Mar. Pet. Geol. 21, 299–315.

Schull, T.J., 1988. Rift basins of interior Sudan: petroleum exploration and discovery. Am. Assoc. Pet. Geol. Bull. 72, 1128–1142.

Schwertmann, U., Niederbudde, E., 1993. Tonminerale in boden. In: lagaly, G. (Ed.), Tonminerale und Tone. 490 p., Steinkopff Verlag, Darmstadt.

Serra, O., Abbot, H.T., 1980. The contribution of logging data to sedimentology and stratigraphy. Am. Inst. Mining, Metall., and Petrol. Eng., Inc., SPE 9270, 19.

Shanley, K.W., McCabe, P.J., 1994. Perspectives on the sequence stratigraphy of continental strata. Am. Assoc. Pet. Geol. Bull. 78, 544–568.

Slatt, R.M., 2006. Stratigraphic Reservoir Characterization for Petroleum Geologists, Geophysicists, and Engineers - Origin, Recognition, Initiation, and Reservoir Quality, Developments in Petroleum Science.

Smith, M., Mosley, P., 1993. Crustal heterogeneity and basement influence on the development of the Kenya Rift, East Africa. Tectonics 12, 591–606.

Steiber, S.J., 1970. Pulsed neutron capture log evaluation. Fall Meet. Soc. Pet. Eng.

Taylor, K., Gawthorpe, R., Curtis, C., Marshall, J., 2000. Carbonate cementation in a sequence-stratigraphic framework: Upper Cretaceous sandstones, Book Cliffs, Utah-Colorado. J. Sediment. 70, 360–372.

Vail, P.R., Mitchum, J. r., R.M., Todd, R.G., Widmier, J.M., Thompson III, S. Sangree, J.B., Bubb, J.N., Hatlelid, W.G., 1977. Seismic Stratigraphy and Global Changes of

Sea-level. Payton, C.E. (Ed.), Seism. Stratigr. to Hydrocarb. Explor. AAPG Mem. 26, 49–212.

Van Wagoner, J.C., Mitchum, R.M., Campion, K.M., Rahmanian, V.D., 1990. Siliciclastic sequence stratigraphy in well logs, cores, and outcrops: concepts for high-resolution correlation of time and facies. AAPG Methods Explor. Ser., 7, 1–55.

Weimer, P., Posamentier, H.W., 1993. Siliciclastic Sequence Stratigraphy. AAPG Mem. 8, 292.

White, N.J., Jackson, J.A., McKenzie, D.P., 1986. The relationship between the geometry of normal faults and that of the sedimentary layers in their hanging walls. J. Struct. Geol. 8, 897–909.

Williams, G., 1993. Tectonics and seismic sequence stratigraphy: an introduction. Geol. Soc. London, Spec. 71, 1–13.

WILLIAMS, G.D., 1993. Tectonics and Seismic Sequence Stratigraphy.

Wu, D., Zhu, X., Su, Y., Li, Y., Li, Z., Zhou, Y., Zhang, M., 2015. Tectono-sequence stratigraphic analysis of the Lower Cretaceous Abu Gabra Formation in the Fula Sub-basin, Muglad Basin, southern Sudan. Mar. Pet. Geol. 67, 286–306.

Wu, J.E., Mcclay, K., Whitehouse, P., Dooley, T., 2009. 4D analogue modelling of transtensional pull-apart basins. Mar. Pet. Geol. 26, 1608–1623.

Yassin, M.A., Hariri, M.M., Abdullatif, O.M., Korvin, G., Makkawi, M., 2016. Evolution history of transtensional pull-apart, oblique rift basin and its implication on hydrocarbon exploration: A case study from Sufyan Sub-basin, Muglad Basin, Sudan. Mar. Pet. Geol. 79, 282–299.

Zhang, J., Qin, L., Zhang, Z., 2008. Depositional facies, diagenesis and their impact on the

reservoir quality of Silurian sandstones from Tazhong area in central Tarim Basin, western China. J. Asian Earth Sci. 33, 42–60.

Zhou, Y., Ji, Y., Pigott, J.D., Meng, Q., Wan, L., 2014. Tectono-stratigraphy of lower cretaceous tanan sub-basin, tamtsag basin, mongolia: Sequence architecture, depositional systems and controls on sediment infill. Mar. Pet. Geol. 49, 176–202.

VITA

Name: : Mohamed Abdelgader Ahmed Yassin

Nationality : Sudanese

Email : mohamedgadir@gmail.com

Mobile : 00249 912205757

Address : Sudapet Company Khartoum, Sudan

Academic Background : MSc Geology

CORE COMPETENCY

13+ years of petroleum industry and research experience in a variety of multidisciplinary Exploration & Development activities including Seismic interpretation; Seismic Inversion, Seismic attributes analysis; structural analysis; with vast experience in Discrete Fractures Network (DFN) modeling.

WORK EXPERIENCE

Staff Geoscientist

Sudapet Company-Sudan (Exploration & Production Dept.) (July, 2014 – Up to date)

Senior Geophysicist - Seismic Interpreter

Sudapet Company-Sudan (Exploration & Production Dept.) (Sep, 2009 – July, 2014)

- 2D and 3D seismic interpretation.
- Seismic attributes analysis including seismic inversion.
- Generate TWT maps.
- Build velocity model and conduct depth conversion.
- Generate structural maps.
- Conduct structural restoration to identify time of structuration and validate the interpretation.
- Natural Fracture Modeling (DFN model).
- Tectono-stratigraphic analysis (Rift basins analysis) using gravity, seismic, and well data.
- Manage technical geoscience projects.
- Mentor and support junior level geoscientists.

Senior Structural Geologist

FrogTech Company - Canberra, Australia (Feb, 2009 – Sep, 2009)

- Interpretation of terranes, basement composition, tectonic event-response mapping, basin timing, fill patterns and revision of reconstructions.
- Georeferencing all Sudan available data and load it in the Arc Map software.
- Lineaments (Faults) interpretation from gravity and magnetic data in all Sudan.

Geophysicist - Seismic Interpreter

Sudapet Company- Sudan (E & P Department) (Jan, 2007 – Feb, 2009)

- 2D and 3D seismic interpretation.
- Seismic attributes analysis.
- Generate TWT maps.
- Build velocity model and conduct depth conversion.
- Generate structural maps.
- Structural restoration to identify time of structuration and validate the interpretation.

Structural Geologist

China National Petroleum Company (CNPC), Research Institute of Petroleum, International Research Center (IRC) Beijing, China (Feb, 2006 – Jan, 2007)

- 2D seismic interpretation.
- Structural Restoration and balancing.
- Tectonic evolution history and structural style analysis.
- Data preparation for the petroleum system modeling such as grids, seismic facies maps, isopach maps, faults movement history, heat flow, TOC maps and timing of structuration.
- Traps validation as a part of dry hole analysis.

On the Job Training

Petrodar Operating Company (PDOC) - Sudan, (consortium between Petronas, CNPC, and ONGC) (Feb, 2005 – Jan, 2006)

- Seismic interpretation.
- Petrophysical evaluation.
- Wellsite geology.

Junior Geoscientist

Sudapet Company- Sudan (E&P Dept.) (Sep, 2004 – Feb, 2005)

- Follow up the geological and geophysical operation.

Research Assistant

Sudan University of Science and Technology- Sudan (Feb, 2003 – Sep, 2004)

- Practical laboratories of geology, physics and geophysics and field trips.
- Groundwater exploration using resistivity (SAS-3000).

SELECTED PROJECT

Structural and Tectono-Sequence stratigraphic Analysis: A case study from Sufyan Sub-Basin, Muglad Rift Basin, Sudan

(Sep, 2012 Up to date)

The main focus of this study is structural analysis, basin analysis, sedimentology, and sequence stratigraphy.

- Analyze the tectonic evolution and structural style of Sufyan sub-basin.
- Identify the possible causes of the unique trend of Sufyan Sub-basin, and the possible relationship with the Central African Shear Zone (CASZ).
- Characterize the sedimentary facies associations, depositional environment and establish sequence stratigraphic model.
- Establish the Tectono-Sequence stratigraphic model.

Characterization and Modeling of Fractured Basement Reservoir, Melut Rift Basin, Sudan

(May, 2011 Up to May, 2012)

Data Integration of different scale fractures, from cm to Km scales (3D Seismic, FMI, Satellite images, Gravity, Field work).

- Major faults (large scale) were interpreted using 3D seismic data, then medium scale faults were interpreted using seismic attributes (mainly coherency, 3D curvature, ant-track); finally the small scale fractures were interpreted using FMI data (well data).
- Discrete Fracture Network (DFN) model were generated, including large and medium scale fractures deterministically (from seismic data). Small scale fractures were modeled stochastically using fractures interpreted from FMI data.
- Origin model of those fractures were proposed.

Eltoor Field Development Plan Study (FDP), Muglad Rift Basin, Sudan

(March, 2008 Up to September, 2008)

Diffra/Balome Field Development Plan (FDP), Muglad Rift Basin, Sudan

(January, 2007 Up to October, 2007)

As Seismic Interpreter

- TWT maps generation.
- Velocity analysis, Time to Depth conversion, and mapping.
- Export grid maps, fault polygons, fault sticks for geological model.
- Structural Geomodel preparation (using Petrel software).
- Work QC by the clients at the workstation many times (Peers review).
- Final reporting preparation.
- Trained and coaching the junior staff.

SELECTED PUBLISHED WORKS

Articles:

- Evolution history of transtensional pull-apart, oblique rift basin and its implication on hydrocarbon exploration: A case study from Sufyan Sub-basin, Muglad Basin, Sudan. Article. **Jan, 2017**. Marine and Petroleum Geology.
- Chemostratigraphic and sedimentologic evolution of Wajid Group (Wajid Sandstone): An outcrop analog study from the Cambrian to Permian, SW Saudi Arabia. **Jan, 2017**. Elsevier/Journal of African Earth Sciences.

Conferences:

- Sedimentology and Reservoir Characteristics of Early Cretaceous Fluvio-Deltaic and Lacustrine Deposits, Upper Abu Gabra Formation, Sufyan Sub-basin, Muglad Basin, Sudan. European Geosciences Union (EGU) to be held in Vienna, Austria, 23–28 April **2017.**
- Structural and Tectonic Evolution of Abu Sufyan Sub-Basin, Muglad Rift Basin, Sudan. Geo**2016**/AAPG, Bahrain.
- Depositional systems, Sequence Stratigraphic Pattern, and their Controls: A case study from Fluvio-Deltaic and Lacustrine systems in Sufyan Sub-Basin, Muglad Rift Basin, Sudan. Vienna, Austria, Vol. 18, EGU2016-7107, **2016.**
- Hydrocarbon Potentials of Fractured Basement in Red Sea Region, Saudi Arabia. Geo**2014**/AAPG, Bahrain.
- Geochemistry of the Lower Paleozoic Wajid Formation in Saudi Arabia - Implications for Tectonic Setting and Provenance. June, **2014** EAGE conference, Amsterdam, Netherland.

- Outcrop Analog Model of Natural Fractured Carbonate Reservoir: A case Study from Khuff Formation, Central Saudi Arabia. Geo**2014** conference, Bahrain.
- Modeling Naturally Fractured Basement Reservoir: A case Study from Melut Rift Basin, Southeast Sudan. *AAPG International Conference & Exhibition in Istanbul,* Turkey*, 14-17 September **2014.***
- Geological Modeling of Fractured Carbonate reservoirs: Outcrop Analog from Khuff Carbonate Rocks in Saudi Arabia. 30th IAS Meeting of Sedimentology, Manchester, UK **2013**.
- Characterization of Fractured Basement Reservoir, Melut Basin, Southeast Sudan. AAPG **2013** Annual Convention and Exhibition, Pittsburgh, Pennsylvania, USA.
- Fracture Modeling using outcrop scale measurements for Rus Formation (EOCENE), Dammam Dome, Eastern Saudi Arabia. Poster presentation at the AAPG **2012** International Conference & Exhibition in Singapore.
- Petroleum System Modeling as a Useful Tool for Exploration Stage: A Case Study from Muglad Basin – Sudan. Geo**2010**/AAPG.
- Structural Restoration as an Effective Tool for Detecting the Evolution and Timing of Structural Development: A case study from the Muglad Basin, Sudan. Geo**2008**/AAPG.

EDUCATION

- **PhD, Geology** King Fahd University of Petroleum & Minerals (KFUPM), Dhahran, Saudi Arabia (2012 - 2017).
- **M.Sc., Petroleum Geosciences** (GPA 3.813/4.0), King Fahd University of Petroleum & Minerals (KFUPM), Dhahran, Saudi Arabia (2010 - 2012).
- **B.Sc., Geology & Geophysics** (Honors degree - Second Class Division One), University of Khartoum- Sudan (1997 - 2002).